Geology of the Apollo 14 Landing Site in the Fra Mauro Highlands

GEOLOGICAL SURVEY PROFESSIONAL PAPER 880

Prepared on behalf of the National Aeronautics and Space Administration

GEOLOGY OF THE APOLLO 14 LANDING SITE IN THE FRA MAURO HIGHLANDS

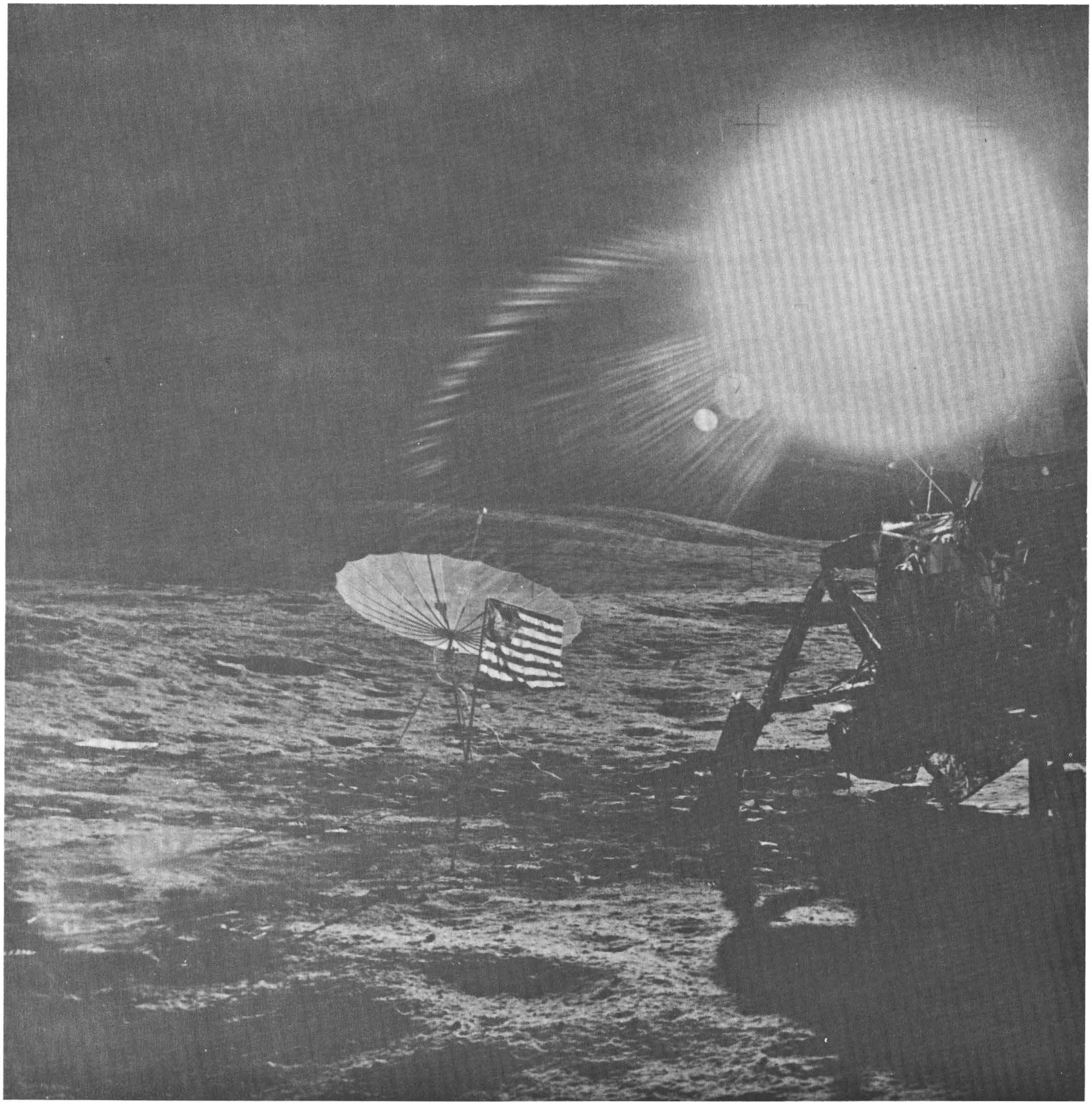

View east past Lunar Module toward Cone crater ridge. Umbrella-shaped object just beyond American flag is transmission antenna. Glow in upper right is the sun. (NASA photograph AS14-66-9304.)

Geology of the Apollo 14 Landing Site in the Fra Mauro Highlands

By G. A. SWANN, N. G. BAILEY, R. M. BATSON, R. E. EGGLETON, M. H. HAIT, H. E. HOLT, K. B. LARSON, V. S. REED, G. G. SCHABER, R. L. SUTTON, N. J. TRASK, G. E. ULRICH, *and* H. G. WILSHIRE

GEOLOGICAL SURVEY PROFESSIONAL PAPER 880

Prepared on behalf of the National Aeronautics and Space Administration

UNITED STATES GOVERNMENT PRINTING OFFICE, WASHINGTON : 1977

UNITED STATES DEPARTMENT OF THE INTERIOR

THOMAS S. KLEPPE, *Secretary*

GEOLOGICAL SURVEY

V. E. McKelvey, *Director*

Library of Congress Cataloging in Publication Data

Swann, Gordon Alfred, 1931–
Geology of the Apollo 14 landing site in the Fra Mauro highlands.

(Geological Survey Professional Paper 880)
Bibliography: p. 101–103
Supt. of Docs. no.: I 19.16:880
1. Lunar geology. I. Swann, Gordon Alfred, 1931– II. United States National Aeronautics and Space Administration.
III. Series: United States Geological Survey Professional Paper 880.
QB592.G46 559.9'1 74-26964

For sale by the Superintendent of Documents, U.S. Government Printing Office
Washington, D.C. 20402
Stock Number 024-001-02922-7

CONTENTS

ILLUSTRATIONS

[Plates are in pocket]

TABLES

GEOLOGY OF THE APOLLO 14 LANDING SITE IN THE FRA MAURO HIGHLANDS

By G. A. Swann, N. G. Bailey, R. M. Batson, R. E. Eggleton, M. H. Hait, H. E. Holt, K. B. Larson, V. S. Reed, G. G. Schaber, R. L. Sutton, N. J. Trask, G. E. Ulrich, and H. G. Wilshire

ABSTRACT

Apollo 14 landed in the Fra Mauro highlands on February 5, 1971, at latitude 3°40′24″ S., longitude 17°27′55″ W. The materials of the area are interpreted to be part of the large deposit of ejecta from the Imbrium basin and appear to be older than the materials of the maria. Because of its relatively old age, the regolith is thicker than on the typical mare, and the ages of the various surfaces within the landing site are reflected in the size-frequency distribution of rock fragments. Since lunar materials generally darken with age, their albedos serve as a general indication of the relative length of time that they have been exposed at the surface. Polarimetric properties and albedo appear to be useful signatures for comparative studies of lunar materials.

The Fra Mauro Formation at the Apollo 14 site comprises breccias that were formed by the Imbrium event and possibly other, earlier impact events. One type of breccia consists of mostly dark clasts in a lighter matrix; the other type, a mixture of light- and medium-gray clasts in a dark matrix. The origin of the breccias and the effects of exposure on the lunar surface are suggested by structures and textures of boulders photographed along the astronauts' traverse line.

INTRODUCTION

The Apollo 14 *Lunar Module* (*LM*)[1] landed on the lunar surface February 5, 1971, at lat 3°40′24″ S., long 17°27′55″ W., in the Fra Mauro region (figs. 1, 2). The landing site, 1,230 km south of the center of the Imbrium basin and 550 km south of the southern rim crest of the basin, was selected in order to study the Fra Mauro Formation, which covers large areas of the near side of the moon. This formation forms a broad belt surrounding Mare Imbrium and is believed to be material that was excavated by a large impact that formed the Imbrium basin.

The mission commander (CDR) was Adm. Alan B. Shepard, the first American astronaut, on Mercury 1, to fly into space. The LM pilot (LMP) was Capt. Edgar D. Mitchell, and the *Command Module* pilot (CMP) was Lt. Col. Stuart A. Roosa. Apollo was their first space flight. Shepard and Mitchell descended to the lunar surface, while Roosa remained in lunar orbit. In this report, the "astronaut crew" refers only to Shepard and Mitchell. Fred Haise, the Capsule Communicator (Capcom) during the periods of *Extravehicular Activity* (*EVA*), is referred to as "Fred" by the astronaut crew in the voice transcript excerpts in table 5.

All the astronauts had a period of training in basic geology before the Apollo missions. Beginning with Apollo 11, each astronaut crew received increasingly more training, not only in the fundamentals of geology but also in lunar geology and the detailed geology of the landing sites.

During the Apollo missions, an advisory team of scientists worked in the Mission Control Center at Houston in the *Science Operations Room* (*SOR*). By the time of Apollo 14 an interaction system had developed to the point where questions and suggestions from the science team could be sent to the crew at almost any time during EVA periods.

Many informal names used throughout the report were assigned to local landmarks before the missions, for ease of discussing landmarks and other features. Still others were named, usually by the astronaut crew, during the mission. For example, "Weird crater" (pl. 1) was named before the Apollo 14 mission because of the odd shape of three coalescing craters. A large boulder near Weird crater examined during the second EVA was referred to, therefore, as "Weird rock," although there appears to be nothing particularly "weird" about the rock.

The Apollo 14 LM landed about 1,100 m west of Cone crater, which is located on a ridge of the ridgy unit of the Fra Mauro Formation (pl. 1). Cone crater is a sharp-rimmed, relatively young crater approximately 370 m in diameter from which blocks were ejected as large as 15 m across derived from beneath the regolith. Sampling and description of these blocks, which the

[1]Many of the terms and names in this report are not included in standard glossaries and dictionaries, partly because much of the jargon of space flight and space science is so new. Italicized terms are explained in the Glossary.

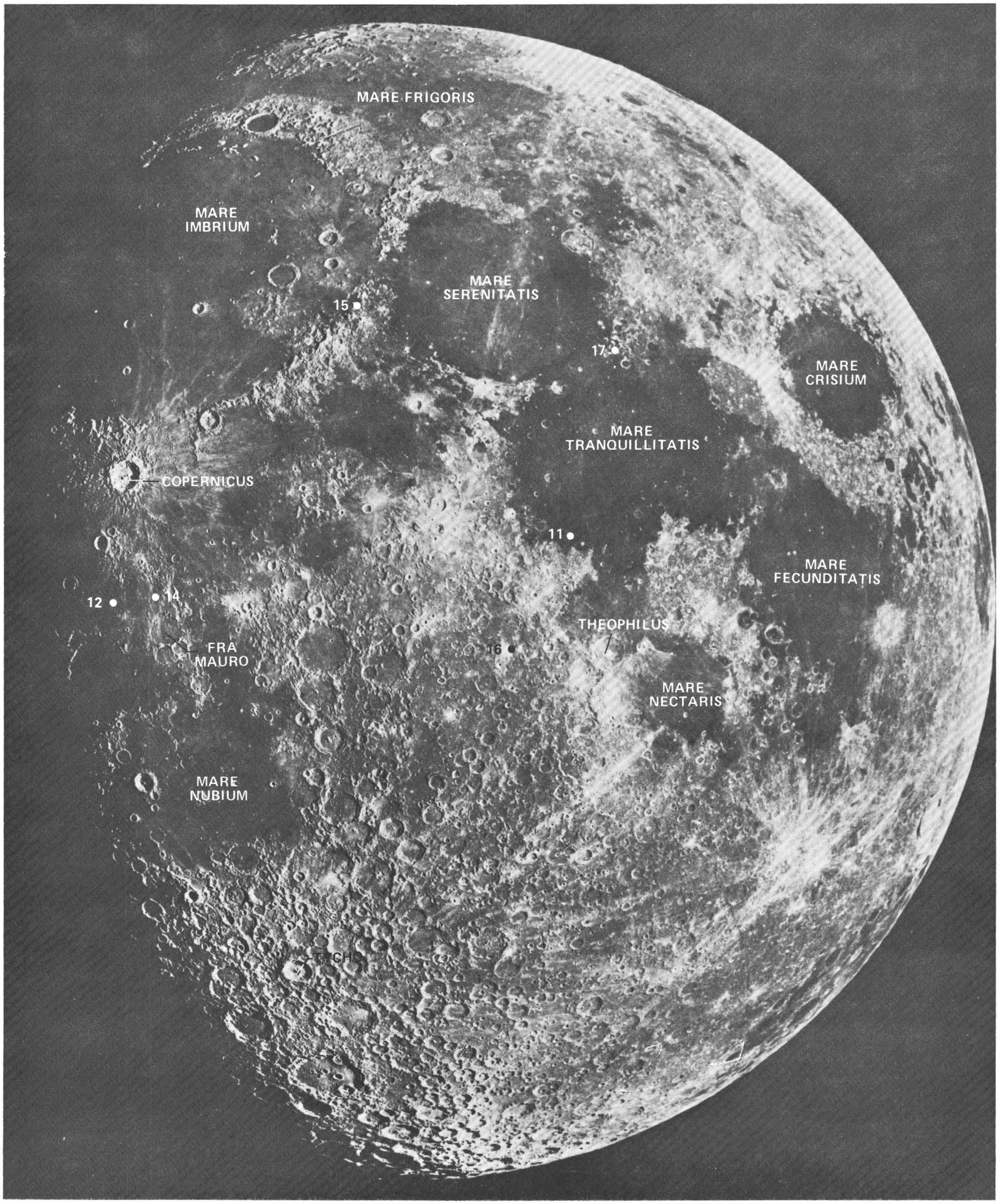

FIGURE 1.—Telescopic photograph of 9-day Moon showing Apollo 11–17 landing sites. Photograph number 113C, August 12, 1940 by J. H. Moore and J. P. Chappell. Lick Observatory 36-inch telescope. North is at top.

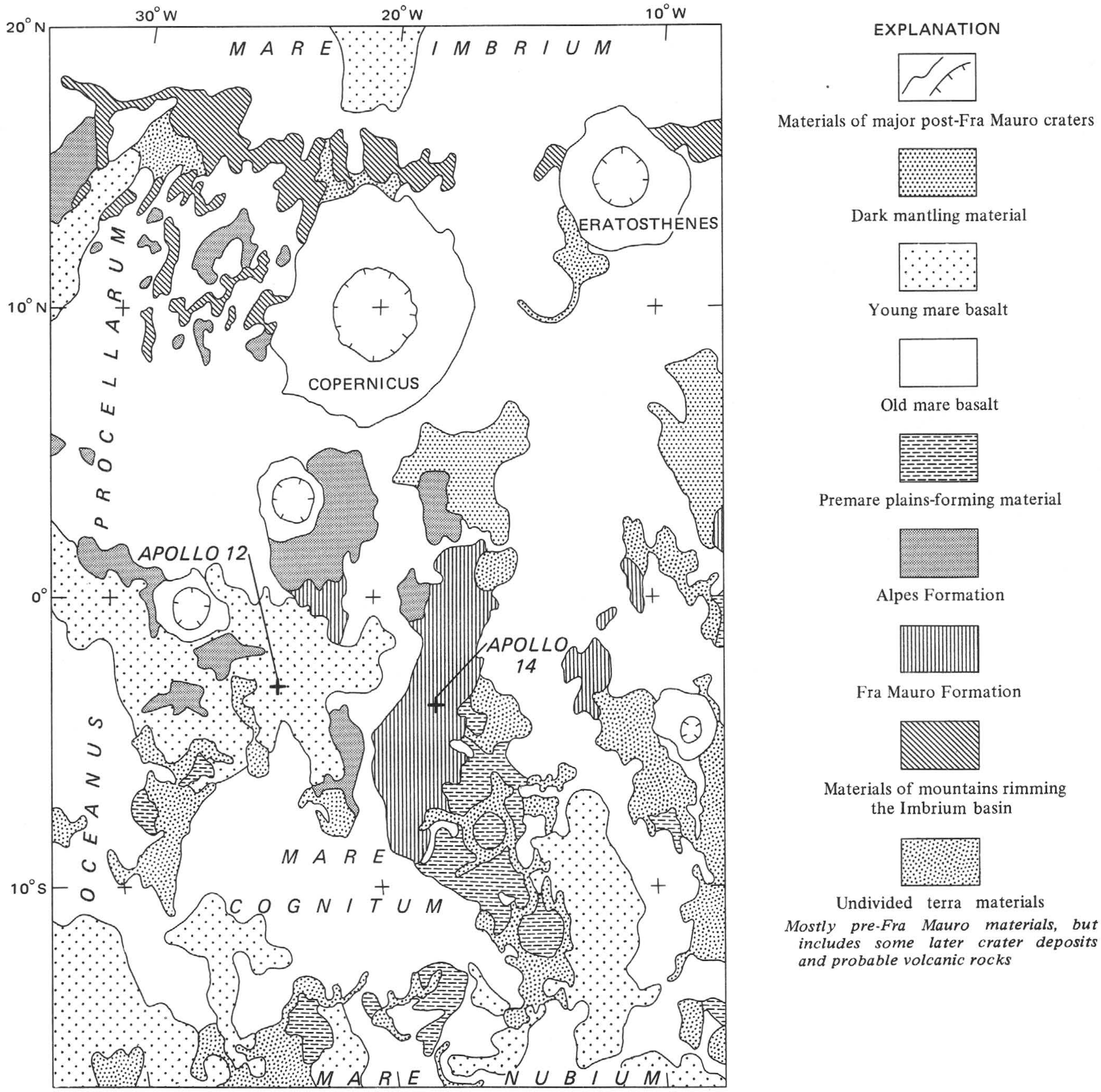

FIGURE 2.—Regional geologic map of the Apollo 12 and 14 landing sites. Adapted from Wilhelms and McCauley (1971).

pre-mission mapping (Eggleton and Offield, 1970) indicated would be unambiguous representatives of the Fra Mauro Formation, was a primary objective of the mission. The landing took place on a smooth terrain unit that was identified in pre-mission *Lunar Orbiter* and *Apollo orbital photographs*. Sampling and description of this unit was another major objective that was completed. The smooth unit, originally thought to be either highlands volcanic material or a smooth facies of the Fra Mauro Formation that was ponded in low areas between the ridges of the ridgy unit (Eggleton and Offield, 1970), was determined to be underlain by breccias similar to those of the ridgy unit.

Two EVA's, each about 5 hours long, were completed. Most of the first EVA was devoted to deploying the *Apollo Lunar Surface Experiments Package* (*ALSEP*). En route to deploying the ALSEP, the crew traveled westward over the smooth unit. The round-trip distance covered on this EVA was approximately 550 m (pl. 2). In addition to deploying the ALSEP, the

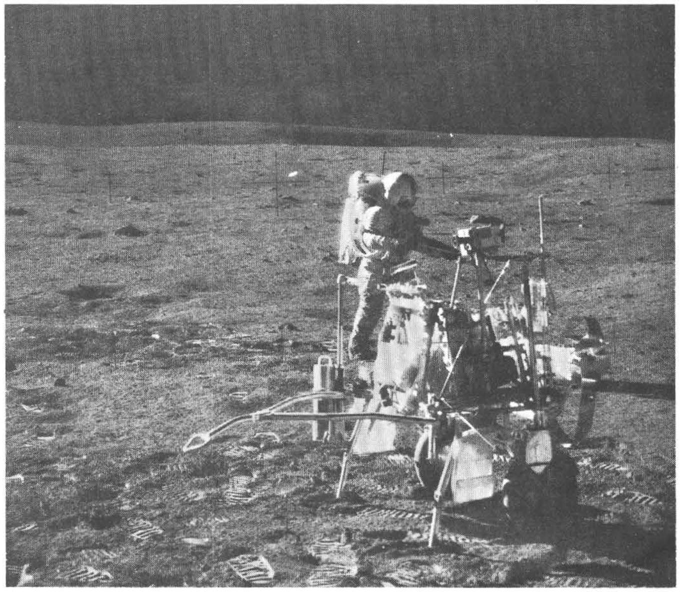

FIGURE 3.—Astronaut Shepard and the MET at station A. Old Nameless is crater on horizon. View southeast. (NASA photograph AS14-68-9404.)

crew collected 16 rock samples larger than 20 g for which locations have been determined (pl. 2): 14 in the *comprehensive sample* and 2 *football-size rocks*.

During the second EVA (pl. 2), the crew walked a round-trip distance of approximately 2,900 m. Heading eastward from the LM, they crossed the smooth and ridgy units (Ifs, Ifr), the apron unit (Ca), and the continuous ejecta blanket of Cone crater, and came within 20 m of the crater rim crest (pl. 1). They collected 30 rock samples larger than 20 g at points whose locations have been determined (pl. 2). One additional rock sample (14309) is from an unknown location. The *modularized equipment transporter* (MET) (Fig. 3) was used to transport the samples and collection tools.

The location of samples was established by relating returned samples to the *documented sample bags*, lunar-surface photographs, and Apollo 14 crew descriptions that pertain to the given samples. Lunar orientations of rock samples were also determined from lunar-surface photographs. Locations and orientations are established with various degrees of confidence; for some samples both are accurately known, for others neither.

A summary of sample documentation (table 5) cross-references all samples in sequence by traverse station, with lunar-surface documentary photographs, the status of determining sample location and orientation, brief megascopic sample descriptions, and comments by the astronaut crew at the time of sample collection.

Locations are known for all but 1 of the 47 rock samples that weigh more than 20 g, for all four *drive tubes*, and for all separately bagged soil samples. Fines and rock chips which represent residues from *weigh bags* are, for the most part, not tied to specific stations. Exceptions to this are the weigh bags used for the *bulk sample* (No. 1028), the comprehensive samples (Nos. 1027 and 1039), and samples from station H (No. 1038) (pl. 2).

Precise locations and orientations of 12 rock samples at the time of collection are known from lunar surface photographs (Nos. 14047, 14051, 14301, 14304, 14305, 14306, 14312, 14313, 14315, 14318, 14319, and 14321). The locations of other samples are known from the comments by the crew, but without photographs, the orientation of the samples when they were collected cannot be reconstructed. The approximate history of exposure of a rock sample can be determined from a study of rounding and pitting by micrometeorite bombardment, dust coatings, and glass coatings. Hörz, Morrison, and Hartung (1972) did this for samples 14053, 14055, 14066, 14073, 14301, 14303, 14305, 14306, 14307, 14310, 14311, 14318, and 14321. Rocks commonly are pitted on all sides, indicating that they have occupied more than one position on the lunar surface. This type of study has strengthened the evidence for "*gardening*" at the lunar surface and helps to define rates of turnover, or tumbling, of specific samples.

Photographic surveys taken during the Apollo 14 lunar stay were designed to (1) locate and illustrate topographic features at each major geologic station (pls. 2–6), (2) record the surface characteristics of each sample area and determine the orientation and location on the lunar surface of the samples at the time of collection, and (3) document geologic *targets of opportunity*.

Other photographic surveys were taken to document the deployment of the ALSEP and the *soil mechanics experiment*.

A total of 417 photographs were taken on the lunar surface with the *Hasselblad Electric Data Camera* (referred to as the Hasselblad camera throughout this paper). Fifteen panoramas, consisting of 275 photographs, were taken for major station location and general geologic documentation (pls. 3–6). Forty-nine pictures were taken for specific sample documentation, and 27 pictures were taken to document ALSEP deployment. The remaining pictures were of miscellaneous targets of opportunity. The major geologic stations were located on a rectified copy of Lunar Orbiter III frame H–133 by feature correlation between the Hasselblad and Lunar Orbiter photographs and by resection (pls. 2–6). Tables 6 through 9 are a log of the Hasselblad photographs taken on the lunar surface.

The nature of the lunar environment, and the limitations on doing conventional field geologic studies during Apollo missions, necessitate a somewhat different approach than is used in terrestrial geology to obtain field data. Much emphasis must be placed on detailed study of photographs taken on the lunar surface, and the application of interpretations from these photographs to interpretations of photographs taken from lunar orbit.

The primary sources of data for this report are photographs of the site and surrounding area taken before the Apollo 14 mission by Lunar Orbiters and Apollo 12, and photographs taken on the surface during the Apollo 14 mission. Other information is derived from preliminary examination of returned samples, published reports that discuss analyses of the samples, and oral descriptions by the astronaut crew.

The overall approach to this study included:

1. Pre-mission photogeologic mapping of the site.
2. Study of the astronaut crew's oral descriptions.
3. Preliminary study of returned samples, confined mostly to hand-sample and binocular microscope examination of rock samples larger then 20 g.
4. Detailed study of photographs taken on the lunar surface, including photometric and photogrammetric measurements.
5. Measurements of polarimetric and albedo characteristics of a limited number of samples.
6. Review of literature pertaining to analyzed samples.
7. Limited updating of the pre-mission geologic map (Eggleton and Offield, 1970) based on information gained from the mission.

GEOLOGY

Nearly all of the lunar surface is covered by a layer of comminuted rock debris, commonly several metres thick, formed by repeated meteorite impact. This layer, generally referred to as the lunar regolith, makes finding actual rock outcrops difficult. None were seen along the Apollo 14 traverse routes, and the local bedrock stratigraphy and structure must be inferred from a knowledge of cratering mechanics and from detailed study of boulders thought to represent local bedrock.

Craters that penetrate the regolith can provide much the same sort of information as drill holes. Cone crater at the Apollo 14 site is an example. Mixing of the regolith by cratering complicates the problem of determining what part of the local stratigraphic sequence a rock fragment from the regolith represents. This same process, however, transports materials over large distances so that at any one site, one can expect to obtain materials representative of other localities, some far away. Sampling regolith materials on the Moon is similar to sampling an alluvial fan, slide, or moraine at the foot of a mountain on Earth to obtain materials representative of the entire mountain. It is more complicated, however, because of the random character of cratering processes, to determine which materials are exotic and where they originally came from.

In general, we assume that the less time a fragment has been exposed at the lunar surface (as determined by geochemical exposure age techniques and by its state of erosion from micrometeorites), the less likely that it has had a complicated surface history. We also assume that a larger rock fragment is less likely to have had a history of multiple transport, and therefore it is more likely to be near its original source (see for example Shoemaker and others, 1970).

The original sources of many rock fragments can be inferred from the ejecta patterns observed around impact craters. Materials nearest the rim most commonly come from deepest within the crater, and those far out on the ejecta blanket come from nearest the surface of the *target materials* (Shoemaker, 1960). Boulders in the ejecta are presumed to be generally representative of local bedrock ejected from the crater, and ray patterns commonly indicate the sources of the ray materials. The source of any one fragment on an ejecta blanket or ray may, however, be different from that of the bulk of the ejecta. A qualitative evaluation can be made as to whether a fragment is part of the ejecta by comparing its appearance—rock type, degree of rounding, fillet buildup, exposure ages—with other rocks in the ejecta.

Because cratering erodes geologic features to form regolith, a relationship exists between ages of surfaces and thickness of regolith. This relationship can be determined if the rate of meteorite flux, which has been derived (Shoemaker and others, 1970; Shoemaker, 1971) is known. In order to determine the relative ages of surfaces at the Apollo 14 site, we have assumed that lunar materials darken with time upon exposure at the lunar surface (Adams and McCord, 1971), that crater rims erode with time (Soderblom, 1970; Soderblom and Lebofsky, 1972), that rock fragments erode with time so that the size-frequency distribution of rocks at the surface is an index of age of the surface (Shoemaker and others, 1970), and that the development of rock fillets (Shoemaker and others, 1968) on level surfaces increases with time.

All the boulders in the traverse area that were photographed and that show features that appear representative of the Fra Mauro rocks are discussed and illustrated. Where the photographs are suitable for stereoscopic models, they were set up on an AP/C analytical plotter, and contour maps were made at scales of 1:5 to 1:10 with contour intervals of 1 to 4 cm.

The scales, and therefore the contour intervals, were determined by visual estimate, because of a lack of precise photogrammetric control within the photographs.

OPTICAL PROPERTIES

Optical properties of lunar materials have long been used in lunar geologic mapping. The first lunar maps were made primarily from visual observations, which relied not only upon topography and surface textures but also on the apparent variations in reflectivities of materials. Quantitative measurements of the colors, reflectivities at zero *phase angle* (albedos), and polarimetric qualities of lunar surface materials have been derived from Earth-based telescopes integrating areas of several square kilometres and from *Surveyor* and Apollo photographs resolving surface features to centimetre scale.

The lunar surface exhibits a wide range in reflected surface brightness. The differences are considered indicative of different materials. Lunar surface processes produce a fine-grained reflective layer from materials of different compositions and albedos. The photometric function for the Moon indicates that the fine-scale microtexture controls the nature of the photometric function. The different composition of materials affects the brightness, and these brightness differences are greatest near zero phase angle (full Moon from Earth or downsun view on lunar surface).

The recognition that the photometric signatures of lunar materials might help put the samples and photographs into their broader regional geologic context led to preliminary photometric studies of lunar samples and of closeup lunar surface photographs. A total of nine samples (three from Apollo 11, two from Apollo 12, and four from Apollo 14) were allotted for this study. This is not enough for a comprehensive comparison of the different geologic units, but the results of the polarimetric measurements compare favorably with those from telescopic and Surveyor data.

The variation in amount of light reflected from the sample surfaces as the lighting angle is changed was measured in the laboratory. Each sample was mounted with its top surface level in the center of a goniometer. The goniometer has a movable light source and light-measuring detector, and angular positions are measurable to within 6 minutes of arc. The light source simulates sunlight in collimation and spectral variation. The detector is sensitive over the wavelengths (380–820 nanometres) of the lunar surface film spectral sensitivity. This measuring system simulates the geometry viewed on the Moon as well as the spectral range that the lunar surface film recorded. The photometric measurements of samples in the laboratory are directly correlated with measurements recorded in the returned lunar surface film.

In order to calculate the albedos of surface materials, scene luminances (intensities of reflected light) from the fine-grained surface materials and prominent rocks were measured from surface photographs taken during the EVA's. The measurements were made by microdensitometry, utilizing a 100-micrometre-diameter circular aperture, on second-generation film positives. The luminances were calculated from a sensitometric step wedge which is exposed on each magazine of processed film, and from the reported camera settings of iris and shutter speed used during lunar surface photography, with corrections applied for frame shading (lens vignetting). In photographs containing the *photometric chart* in the field of view, the sensitometric luminances of the gray steps on the chart were compared with luminances computed from the preflight calibration of the chart. The luminance data nominally agreed within 2 percent. Measurements of geologic materials were made at the lowest phase angles possible because lunar reflectance decreases rapidly with increasing phase angle, and the uncertainties in the local lunar photometric function at large phase angles tend to increase errors. All general comparisons between areas of measurements are made by projecting the measured luminance to the zero phase angle luminance (albedo) by means of the *photometric angles,* the lunar photometric function as determined by Willingham (1964), and an assumed solar irradiance of 13,000 lumens. Detailed comparisons of reflectance from lunar geologic materials are made at the same phase angle whenever possible. Comparisons of the optical properties of returned lunar samples with the in situ optical properties as determined from photographs provide a basis for delineation of similar materials in the photographs.

The polarimetric properties of the samples (the amount and orientation of polarized light reflected from the surfaces of the material) were also measured in the laboratory. Each sample was mounted with its top surface level in the center of a goniopolarimeter. The goniopolarimeter supports the light source and detector, which are moveable over 350° in azimuth and from horizontal to vertical, with their angular positions measurable to within 6 minutes of arc. The samples were illuminated by a xenon light source, which radiates a spectrum similar to the solar spectrum. The light is collimated to within ½°, which simulates the sun. The detector is sensitive to radiation from 380 to 820 nanometres, a bandwidth similar to the spectral sensitivity of the film used during the mission. A rotating polarizing filter, its angular position measurable to within 15 minutes of arc, was positioned in front of the detector. Measurements were made with the filter polarizing axis positioned 0° (vertical), 45°, and 90° (horizontal). The maximum and minimum polarizing orientations were also recorded. This measuring technique simulates the lunar surface polarimetric measurements that were planned for EVA 2, but were deleted because of time limitations.

BOULDERS

Detailed analysis of surface photographs of boulders ejected from Cone crater, and comparison of these photographs with returned samples, indicate that the Fra Mauro Formation is mainly composed of moderately coherent breccias in which dark lithic clasts, as large as 50 cm across, and less abundant light clasts are set in a light matrix. Subordinate rock types that may be part of the Fra Mauro Formation include coherent breccias with about equal amounts of light and dark clasts and breccias with irregular bands of very light clastic rock. Wilshire and Jackson (1972) classified the breccias according to their clast populations, color of matrix, and coherence, and have postulated a stratigraphic sequence for that part of the Fra Mauro Formation that was sampled by the Apollo 14 mission. We have adopted their classification and stratigraphic sequence for use in this report.

The lithologies of the boulders ejected from Cone crater reveal a complex history in which the youngest structures (several sets of intersecting fractures that cross clasts and matrices alike) may have resulted from the cratering event. Earlier events, presumably relating to the origin of the Fra Mauro Formation or older ejecta blankets, include lithologic layering, deformation, and induration of the breccias. Clasts of breccia within the breccias may in some cases represent pre-Imbrian cratering in the Imbrium basin region.

ACKNOWLEDGMENTS

We wish to thank the crew of Apollo 14 for the scientific data that they returned from the Moon. Much of the material presented here was drawn from the preliminary report by the Apollo Lunar Geology Investigation Team (Swann and others, 1971). A boulder-distribution map from which we derived the boulder-density map on plate 7 was compiled by J. P. Schafer, and Richard L. Tyner prepared the fragment distribution maps used on plate 7. Val L. Freeman and Eugene L. Boudette critically reviewed the manuscript. This report was prepared under NASA contract number T–5874A.

GEOLOGIC SETTING OF THE FRA MAURO SITE

The surface of the Moon is divided into relatively dark low-lying plains, or maria, and brighter, generally more rugged highlands or terrae (fig. 1). The highlands are texturally heterogeneous, consisting of level plains, gently rolling hills, mountains, scarps, and plateaus. In most parts of the highlands craters 20–100 km in diameter are abundant. On the near side of the Moon, the highlands are dominated by the great circular basins, each with several concentric rings. These basins are completely or partly filled by mare material and are interpreted to have been formed by impact of large meteorites or comets (Gilbert, 1893; Eggleton, 1964; Wilhelms and McCauley, 1971). Around several of the basins there are moderately to well-preserved tracts consisting of ridges that are radial to the basins. The surface materials in these tracts thus appear to be blanketing deposits of ejecta from the adjacent basin. Apollo 14 landed on a terrane of this type, previously mapped as ejecta from the Imbrium basin (fig. 2).

The areas mapped here as basin ejecta, as well as those elsewhere on the Moon, are characterized by a series of elongate hummocks and ridges generally radial to the center of the basin. Away from each basin, the ridges and hummocks grade into gently rolling terrain, the topographic grain of which remains radial to the basin. Hummocky topography that is concentric to the basins is present around some basins near the most prominent ring. Large, subdued craters, so conspicuous on the central part of the southern lunar highlands, are lacking in areas near the basins, where they appear to be covered by ejecta from the basins. Relatively far from the basins old subdued craters appear to be only partly buried by the blanketing material. One such partly buried, ancient crater, Fra Mauro (figs. 1, 4, 5), is covered by the blanketing material from the Imbrium basin on its northwest side but appears unburied on the southeast. Because the blanketing relations are so well displayed in the vicinity of this crater, the blanketing material around the Imbrium basin has been named the Fra Mauro Formation (Eggleton, 1964; Wilhelms, 1970).

Apollo 14 landed 40 km north of the north rim of the crater Fra Mauro in an area of linear to slightly sinuous ridges trending northward (fig. 4) (Eggleton and Offield, 1970). In this area, the Fra Mauro Formation grades southward from a deposit with well-defined ridges to a deposit of more gently rolling terrain with abundant craters in the size range 500 m to 5 km. The gently rolling terrain gives way to level plains material, part of the Cayley Formation (Morris and Wilhelms, 1967), 80 km south of the landing site. Results from the Apollo 15 and 16 missions have suggested that Imbrium basin ejecta may be more extensive over the near side of the Moon than previously thought (Swann and others, 1972; Muehlberger and others, 1972). It should be emphasized, however, that

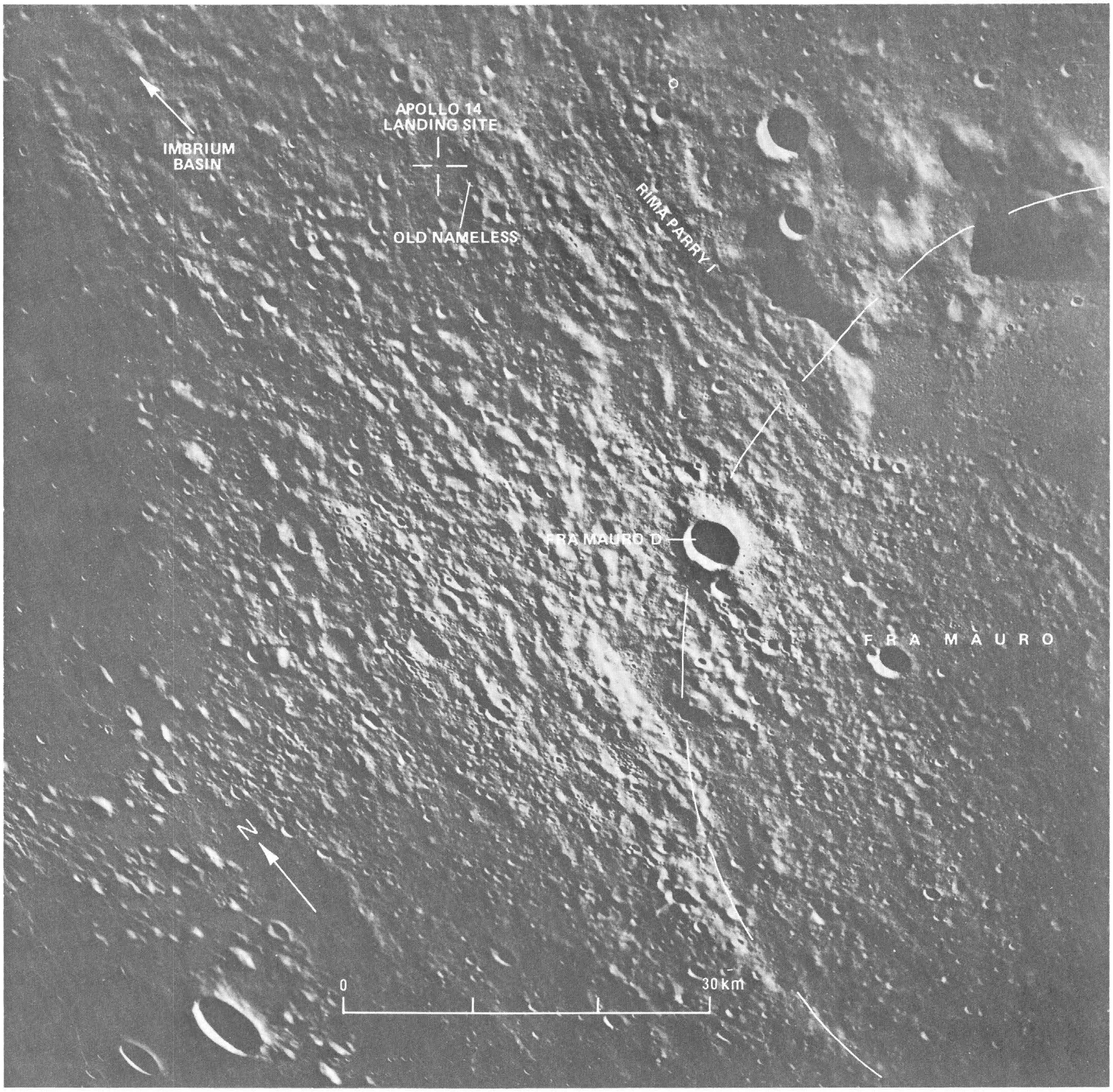

FIGURE 4.—View of the Apollo 14 landing site from the Apollo 12 Command Module, showing the ridgy nature of the Fra Mauro terrain. (NASA photograph AS12–52–7597.)

the Fra Mauro Formation, a mappable unit with well-defined limits, was established on the basis of objective criteria, and is not necessarily synonymous with Imbrium basin ejecta. Apollo 14 sampled a typical part of the formation, and as will be shown in this report, the returned samples very likely do represent Imbrium ejecta. Other formations and material on the Moon may also be composed of Imbrium ejecta, possibly with properties different from those found in the Fra Mauro Formation.

Stratigraphic relations around the margin of the Imbrium basin show that a number of significant geologic events occurred between the time that the basin formed and the time that it filled with mare material. Thus, the filling of mare basins may take place over long periods of time (Baldwin, 1963;

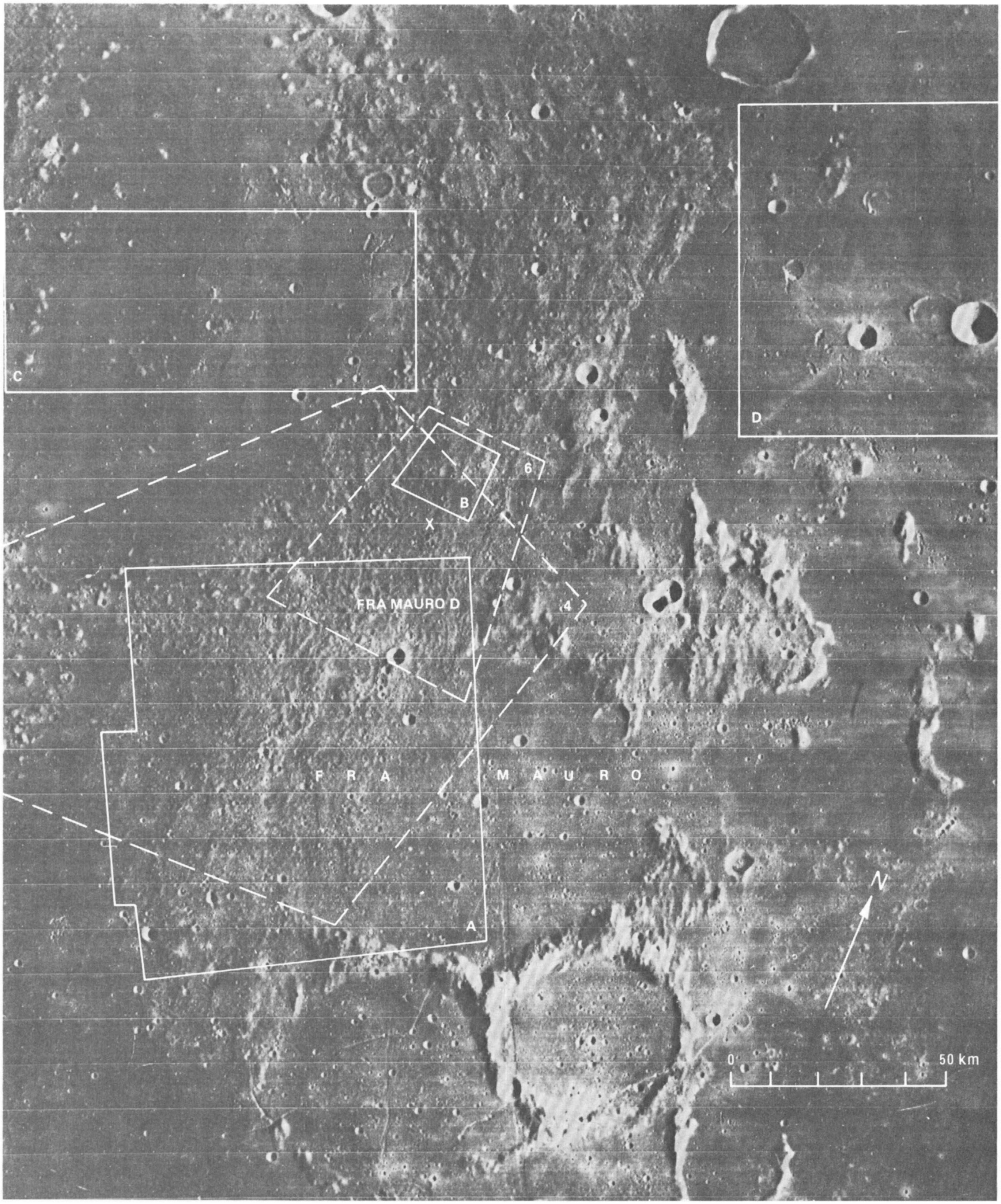

FIGURE 5.—Lunar Orbiter IV, Frame 120H3 showing areas in which craters were counted. Areas A and B are on the Fra Mauro Formation; areas C and D are on the adjacent mare. X is landing site; 4 and 6 show boundaries of figures 4 and 6. Note that area B was counted at two different scales.

Wilhelms, 1970). Events that occurred between the formation and filling of Imbrium included the formation of large craters such as Archimedes, emplacement of relatively light plains-forming highland (pre-mare) materials and, in the western part of the Moon, formation of the Orientale basin. On the basis of photographic evidence, the Fra Mauro Formation is older than the mare materials sampled by Apollos 11, 12, and 15. Another indication of its greater age is the fact that it has more superposed craters in the size range 500 m to 5 km than any mare surface (fig. 5).

The Fra Mauro Formation resembles the Hevelius Formation except for being more eroded and older than it. The Hevelius Formation surrounds the Orientale basin near the west limb of the Moon (McCauley, 1967a, b). The well-preserved ridges of the Hevelius Formation radial to the Orientale basin strongly suggest that the formation is composed of ejecta from the Orientale basin (fig. 6). A comparison of the Hevelius Formation with the Fra Mauro Formation supports the contention that the less well preserved, but otherwise similar, Fra Mauro Formation is composed of ejecta from the Ibrium basin. The ridges of the Fra Mauro Formation in the vicinity of the Apollo 14 landing site are mostly 1 to 4 km wide, a few to several tens of metres high, and on the order of 5 to 10 times as long as they are wide. They are slightly sinuous and roughly radial to the Imbrium basin. The radial ridges present in the Hevelius (McCauley, 1968) and Fra Mauro Formations appear to have formed largely by radial flow of material, probably fragmental rock debris, along the ground during excavation of the basins. Fracturing of the pre-Fra Mauro Formation rocks in a pattern radial to the Imbrium basin may also have contributed, at least locally, to the relief of the ridges. Flatter areas between the ridges have slightly lower albedo than the ridges themselves.

The regolith on the Fra Mauro Formation was expected to be thicker than that on the mare material because of its greater age and the greater abundance of craters from which regolith is formed. In order to sample bedrock beneath the regolith, the Apollo 14 mission was targeted to land close to Cone crater, a relatively fresh 370-m-diameter crater, at the crest of one of the north-south-trending ridges (pl. 1). Cone crater is surrounded by an extensive block field (pl. 7), presumably excavated from as deep as 65 m. The block field is interpreted to contain Imbrium ejecta excavated from beneath the local regolith.

Four map units of the Fra Mauro Formation were traversed by the Apollo 14 crew (pl. 1): (1) the smooth terrain unit (Ifs) on which the LM landed, (2) the apron unit (Ca) at the base of the ridge, (3) slopes of the ridgy unit (Ifr), and (4) the blocky rim deposit of

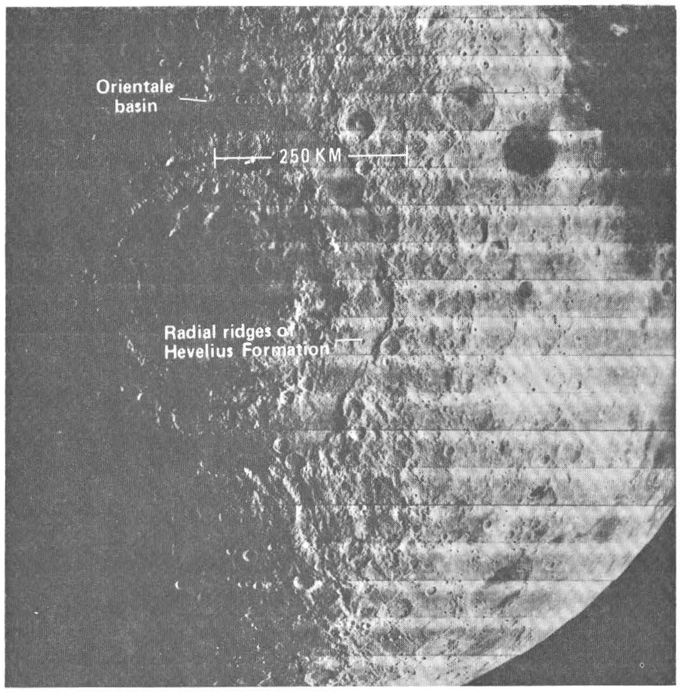

FIGURE 6.—Orientale basin showing radial ridges of Hevelius Formation (Lunar Orbiter IV mosaic.)

Cone crater. The smooth unit is relatively level over distances greater than a kilometre, but is densely populated with subdued crater forms a few hundred metres to a few tens of metres across and a few tens of metres to a few metres deep that give the surface an undulating form. The Fra Mauro ridge, which extends several kilometres north and south of Cone crater, has a slope of about 8° and is hummocky and ridgy at a scale of several metres. At least four moderately subdued craters of Eratosthenian age which are 200 to 1,000 m in diameter occur in the Fra Mauro ridge north, east, and south of Cone crater and within a few hundred metres of the rim crest of Cone crater (pl. 1). Their rim deposits cannot be identified on Lunar Orbiter photographs, but some unmodified crater remnants are probably buried in the regolith. The interiors of these craters have slopes between 10° and 15°, slightly greater than the slopes of the Fra Mauro ridge. The rim of Cone crater is moderately to abundantly strewn with 1- to 15-m blocks. The blocks form rather dense patches that extend as far as 125 m from the rim crest. In the remainder of the rim deposit, blocks 2 m across and larger are commonly spaced as much as a few tens of metres apart (pl. 7).

Craters ranging in size from 64 m to 8 km were counted on Lunar Orbiter III and IV frames that cover the Fra Mauro Formation and the mare areas adjacent to the Apollo 14 landing site (figs. 5, 7). The counting method consists of calculating the area of each parcel, A, B, C, and D, and counting all identifiable craters

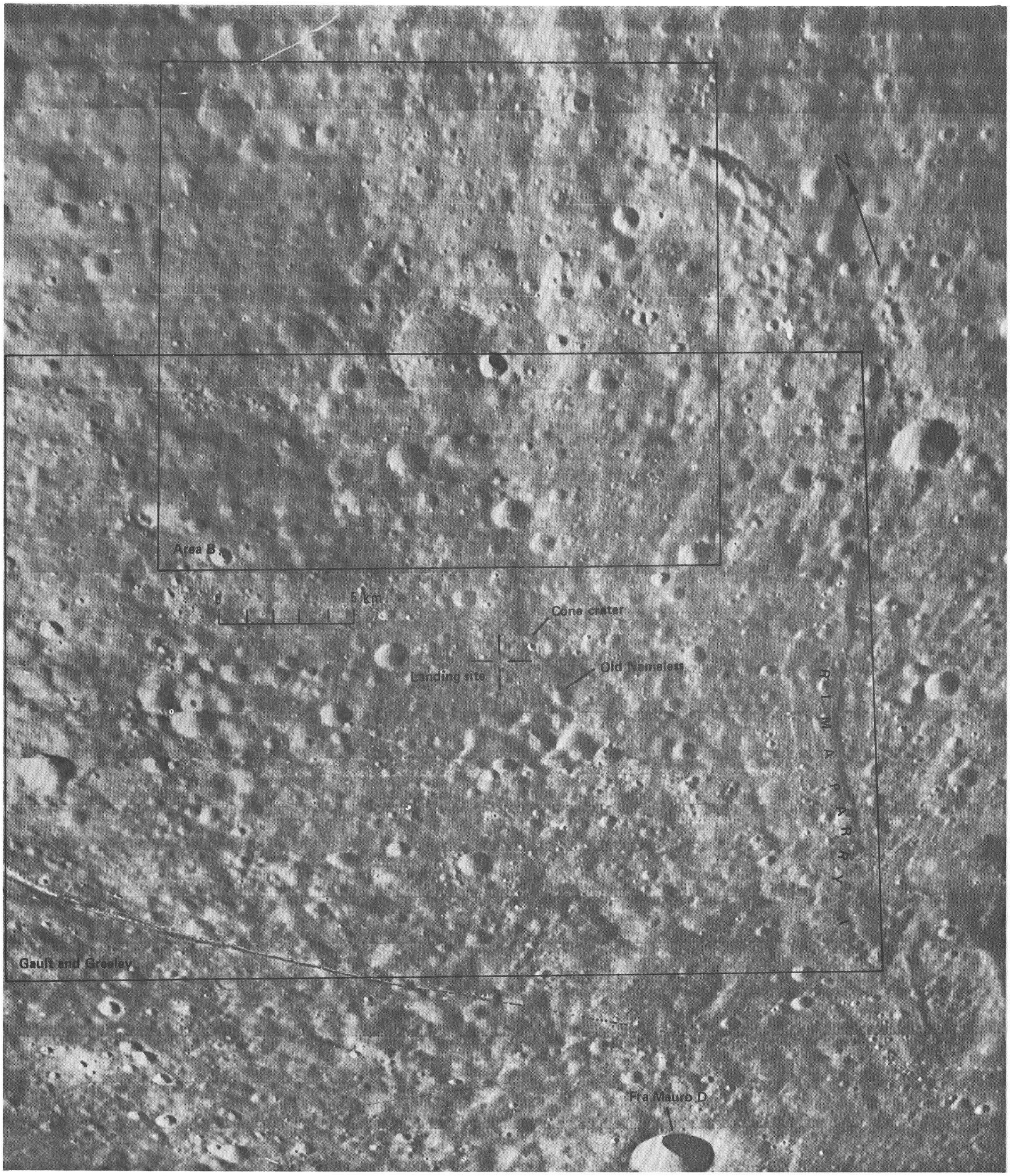

FIGURE 7.—Lunar Orbiter III, Frame 133M showing area B, which was also counted on Lunar Orbiter IV, Frame 120H3 of figure 5.

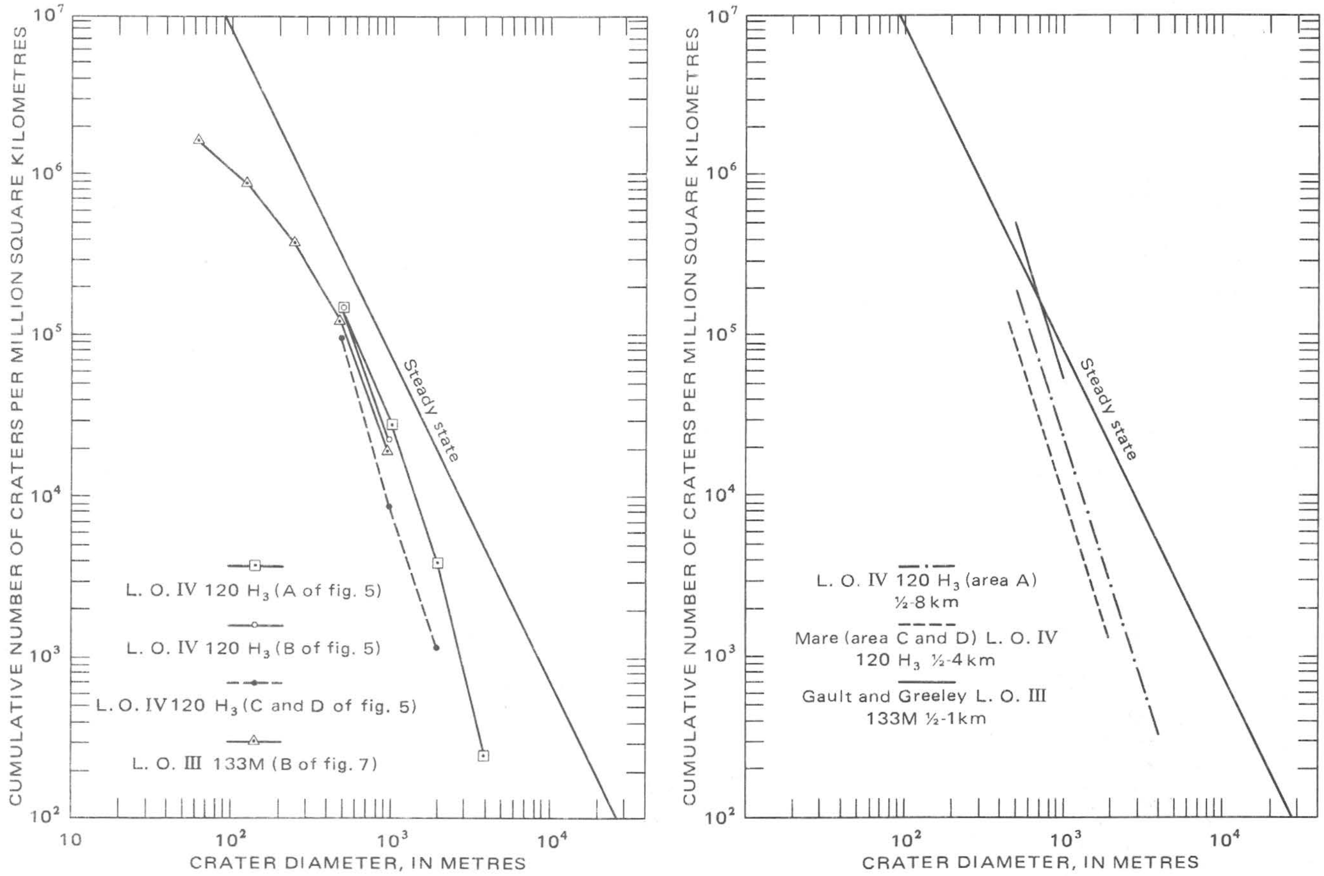

FIGURE 8.—Size frequency distribution of craters. *A*, Comparison of crater counts on the Fra Mauro Formation (areas A and B) and on the adjacent mare (areas C and D). (See figs. 5 and 7.) *B*, Comparison of production functions of craters for the Fra Mauro Formation determined from Lunar Orbiter III, Frame 133M (1,540 km^2) and from Lunar Orbiter IV, Frame 120H3 (8,172 km^2).

within the boundaries. The number of craters in each parcel is then normalized to an area of $10^6 km^2$. Cumulative numbers of craters are plotted on log-log coordinates (fig. 8*A*), and best-fit curves are calcualted by the least squares method for craters ½km or more in diameter. The theoretical steady-state function described by Trask (1966) is shown for comparison. Crater data are tabulated in table 1, which also gives the $\log_{10}$ cumulative numbers per $10^6 km^2$ and the derived crater ratio of Fra Mauro:mare.

The crater counts (fig. 8*A*) show that in the size range from ½ to 4 km, the Fra Mauro Formation has about 1.5 to 3.3 times as many craters as does the adjacent mare, which supports the inference that the Fra Mauro Formation is older. The mare in areas C and D has a crater density corresponding closely to that at the Apollo 11 site (Shoemaker and others, 1970; Gault and Greeley, oral commun., 1972).

We find only about half as many craters on the Fra Mauro Formation as do Gault and Greeley (oral commun., 1972) (fig. 8*B*), probably because of differences in crater recognition and in the sizes of the areas counted.

Craters smaller than 400 m are not as numerous on the Fra Mauro as on the adjacent mare (Trask, 1966), probably because the regolith is thicker and the slopes higher at the Fra Mauro site. Small craters in the lunar regolith are probably destroyed at a faster rate by downslope movement of loose debris on the rolling hills of the Fra Mauro area than on the more level mare surfaces (Soderblom, 1970). Also, soil at the Apollo 14 site apparently has a lower cohesion at shallow depths than that at earlier landing sites, which were on the maria (Mitchell and others, 1971).

On the basis of the diameters of the smallest craters that penetrate bedrock (Quaide and Oberbeck, 1968), the regolith in the Fra Mauro region is estimated to range from 5 to 12 m in thickness (Eggleton and Offield, 1970). Material with a seismic (P wave) velocity of 104 m/s was measured to a depth of 8.5 m at the site of the *Active Seismic Experiment* (*ASE*) (Watkins and Kovach, 1972). This velocity is appropriate for unconsolidated material, and it is reasonable to assume that this represents the total regolith thickness at the ASE site.

TABLE 1.—*Numbers of craters counted in each area, numbers of craters calculated per 10^6 km², and crater ratios between Fra Mauro Formation and adjacent mare surfaces in outer ring of Sinus Aestuum*

[Wilhelms and McCauley, 1971]

Cumulative number of craters counted

Diameter (metres)	Fra Mauro Formation: A (fig. 5) IV 120H3 (8,172 km²)	Fra Mauro Formation: B (fig. 5) IV120H3 (356 km²)	Fra Mauro Formation: B (fig. 5) III 133M (356 km²)	Mare: C and D (fig. 5) IV 120H3 (9,440 km²)
64– 128			265	
128– 256			186	
256– 512			95	
512–1,000	1,006	45	37	829
1,000–2,000	199	8	7	67
2,000–4,000	30			12
4,000–8,000	2			
Cumulative number of craters calculated per 10^6 km²				
512–1,000	151,409	148,877	123,596	96,475
1,000–2,000	28,274	22,472	19,663	8,683
2,000–4,000	3,917			1,588
Crater ratio, Fra Mauro:Mare				
512–1,000	1.58	1.54	1.28	
1,000–2,000	3.26	2.59	2.26	
2,000–4,000	2.47			

The variations in morphology of craters at the Apollo 14 site indicate a homologous series of craters of different ages. The age sequence of craters along the traverses from oldest to youngest is interpreted as follows (Eggleton and Offield, 1970) (pl. 1):

(1) Highly subdued craters expressed as very gentle depressions at the landing spot of the LM, west of the LM in the area of ALSEP deployment, and north of station A.

(2) The crater designated North Triplet, the moderately subdued 50-m crater east of station F, and the moderately subdued 10-m crater at station A.

(3) Cone crater and the sharp 45-m crater at station E.

(4) The sharp 30-m crater at station C′ and the small 10-m crater next to which a football-size rock was collected during the first EVA.

GEOLOGY OF THE FRA MAURO SITE

The geology of the site is divided into (1) the surficial geology or, more specifically, the character of the regolith, and morphologic features in, or reflected through, the regolith; and (2) the bedrock geology or, more specifically, the lithologic characteristics of local Fra Mauro Formation beneath the regolith. Because no exposures of bedrock were found during the mission, the nature of the Fra Mauro Formation must be inferred from rocks in the regolith that appear to have been derived from the underlying bedrock.

The geologic map (pl. 1) is derived from the study of photographs taken from lunar orbit and from the lunar surface. The map units therefore are based primarily on the morphologic characteristics of the surface and do not necessarily correspond directly to lithologic or structural units within bedrock.

SURFICIAL FEATURES

Lunar surface characteristics near Cone crater, such as grain-size distribution and surface morphology, are markedly different from those at stations more than a crater diameter away (pl. 5, 7). The distribution of rocks more than 1 m in diameter in the traverse area, and the distribution of rocks more than 20 cm in diameter at the panorama stations, are shown on plate 7. The LM landing point and station A are in areas where rock fragments larger than 2 or 3 cm in diameter are sparse (fig. 9A). Stations B, F, and G are in areas where rock fragments up to 20 cm in diameter are relatively common (fig. 9B), and stations B2, B3, and C′ are in areas where rock fragments more than 20 cm in diameter are abundant (figs. 9C, D). Station H has a moderate number of rock fragments more than 20 cm in diameter. Rock fragments up to large boulder size are fairly common east of station B1 and become increasingly abundant from east of station B1 to B2 to C′. The continuous ejecta blanket from Cone crater extends from the rim crest west to between stations B2 and B3 and is probably only patchy in the vicinity of station B1 (pl. 1; fig. 10). Farther west across the landing site, Cone crater ejecta occur only as isolated patches or along rays.

Surface material is noticeably finer grained at the LM and at stations A, B, B1, B2, F, G, and H than at stations B3 and C′ (see pl. 7). The topography where the surface material is finer is broadly undulating at wavelengths from tens to hundreds of metres and heights up to approximately 10 m. This topography characterizes old eroded craters, mostly of Eratosthenian and early Copernican ages. The topography at stations B3 and C′ is undulating at wavelengths from several metres up, and heights up to a metre or two. The undulatory surface topography in the vicinity of stations B3 and C′ reflects the original hummocky ejecta deposits from Cone crater.

The term regolith as used here refers generally to the debris layer that overlies the consolidated rock material of the lunar subsurface. The term can also be applied to a deposit that is developed on fragmental material such as the ejecta blanket of Cone crater; where it is used in this sense, it is specified. As previously stated, estimates of the thickness of the regolith at the Fra Mauro site range from 5 to 12 m. Seismic

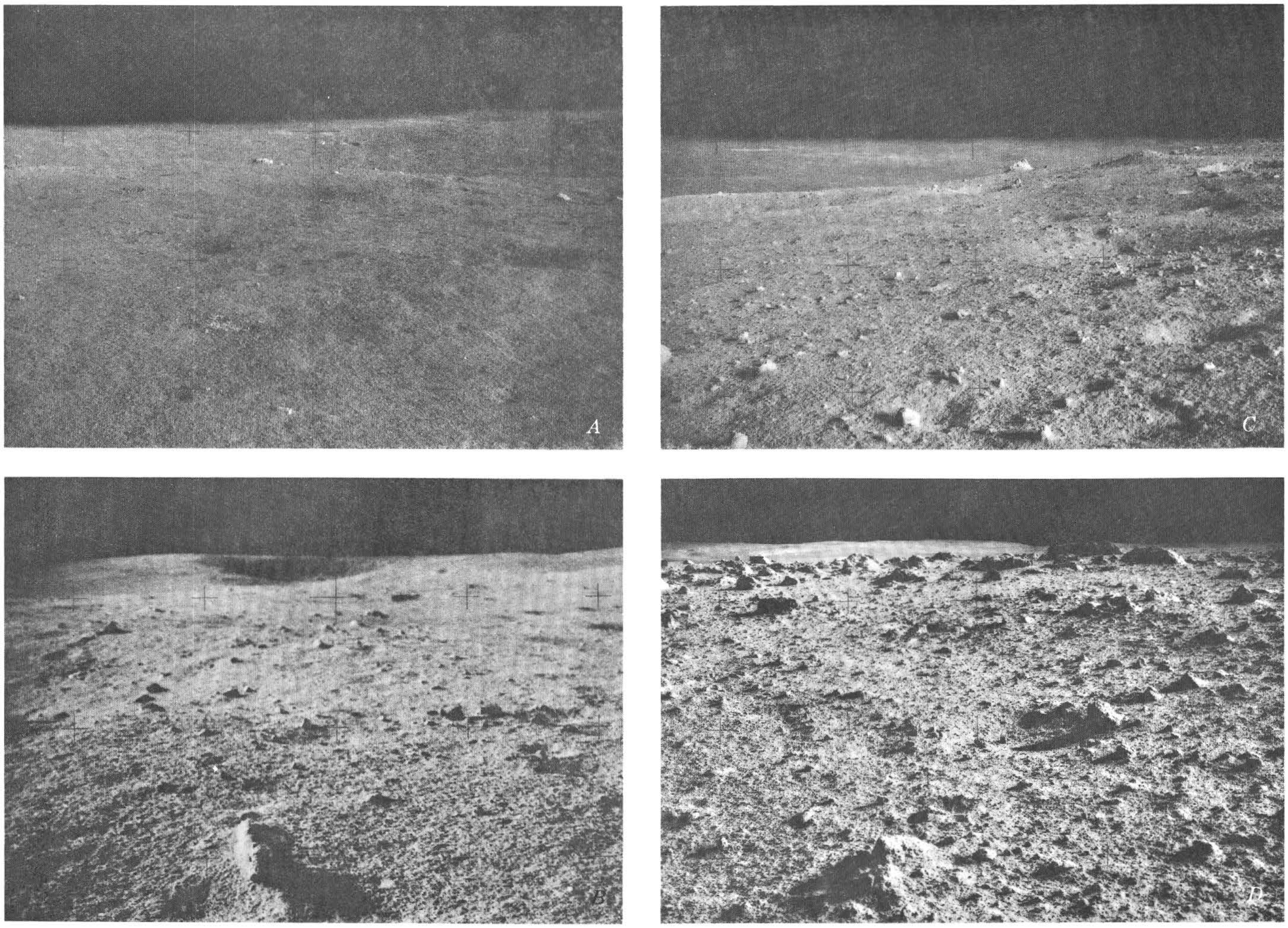

FIGURE 9.—Variation in abundance of rock fragments on surface in landing site area. *A*, View north from station A. Fragments in foreground are about 1 cm in diameter; boulder near center at middle ground is about ½ m in diameter. (NASA photograph AS14–68–9398.) *B*, View southeast from station F showing moderately abundant rock fragments. Old Nameless crater shows at horizon. Boulder in foreground is about 20 cm in diameter. (NASA photograph AS14–64–9152.) *C*, View north from station B3 showing abundance of rock fragments near the edge of the Cone crater ejecta blanket. The large boulder in the background is number 1005 on plate 6, pan 10. Fragments in foreground are 5–10 cm in diameter. (NASA photograph AS14–68–9432.) *D*, View northeast from the vicinity of station C′ showing abundance of rock fragments near Cone crater rim. Most fragments in foreground are 2–5 cm in diameter. (NASA photograph AS14–64–9106.)

data indicate a thickness of 8.5 m in the vicinity of the LM.

A rather continuous subdued ledge 9.5 m below the rim is visible in surface photographs of Old Nameless crater[2] located about 2.2 km south of station B2 (fig. 11). Below this ledge the walls of the crater are blocky. Just west of the rim crest of Old Nameless crater a small crater penetrates to slightly below the depth of the ledge and has blocky ejecta. This ledge is interpreted as the uppermost bedrock and suggests that the regolith is about 9.5 m thick in the vicinity of Old Nameless crater[3]. The actual thickness of the regolith in the Apollo 14 site probably varies because of the slopes of the ridges. In general, the regolith is probably somewhat thicker in the valleys and thinner on the ridge slopes and crests, largely because the trajectories of small crater ejecta are longer in the downslope direction than in the upslope (Soderblom, 1970).

[2]"Old Nameless" is the name applied to this crater by the crew of Apollo 13 for use in their landmark tracking during descent to the lunar surface. Apollo 13 did not land on the Moon owing to a spacecraft malfunction, and so the Apollo 14 mission was targeted for the Apollo 13 site. Apollo 14 was launched during a different time of year, so the ground track was not the same as that of Apollo 13, and Old Nameless crater was not used for a landmark. It therefore was not named on the Apollo 14 landing charts. The crew referred to it as Old Nameless, however, as they viewed it during the EVA's.

[3]A detailed study of Old Nameless crater on an AP/C analytical plotter showed that other features in the crater wall that appear as benches and possible layers are in reality the effect of light that is reflected from the upper surfaces of random hummocks.

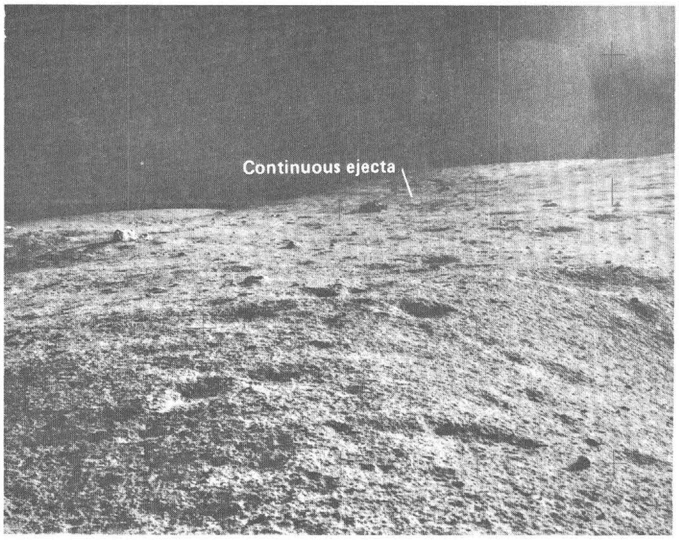

FIGURE 10.—View northeast from station B1 toward contact of Cone crater continuous ejecta about 175 m away. (NASA photograph AS14-64-9084.)

Although the rocks of the Apollo 14 and 16 sites are about the same age (Tatsumoto and others, 1972; Nyquist and others, 1972; Papanastassiou and Wasserberg, 1972; Kirsten, Horn, and Kiko, 1973), the regolith appears significantly thicker at the Apollo 16 site (fig. 12). The regolith is thick over old large craters which have been filled by erosion of their rims, and larger variations in regolith thickness are to be expected in the older areas of the Moon. During their early history, these areas were subjected to a high meteorite flux rate (Shoemaker, 1971, 1972), so that large craters were likelier to form. The regolith at the Apollo 17 site also appears to be thicker than at other sites. This could be explained by the presence of a large crater that has been destroyed by erosion, or by an addition of unconsolidated material such as volcanic ash and cinder, as was suggested by pre-Apollo 17 mapping (Scott and others, 1972).

The rate of regolith formation at the Apollo 14 and 16 sites, given a constant meteorite flux rate, should be somewhat higher than at the 11, 12, and 15 sites because the Apollo 14 and 16 breccias are somewhat more friable than are the basalts of the mare sites (fig. 13). However, the greater meteorite flux rate before flooding of the maria (Shoemaker, 1971, 1972) probably had a greater influence on this rate than did the difference in durability of materials.

The regolith that has developed on the Cone crater ejecta blanket appears to be thin. Small craters on the blanket have very blocky ejecta (fig. 14), which indicates that the ejecta of Cone crater has a higher internal abundance of rock fragments than is apparent at the surface and that overturning of the ejecta blanket by meteorite impact resulting in comminution of rocks has not extended to a significant depth. (See also sec-

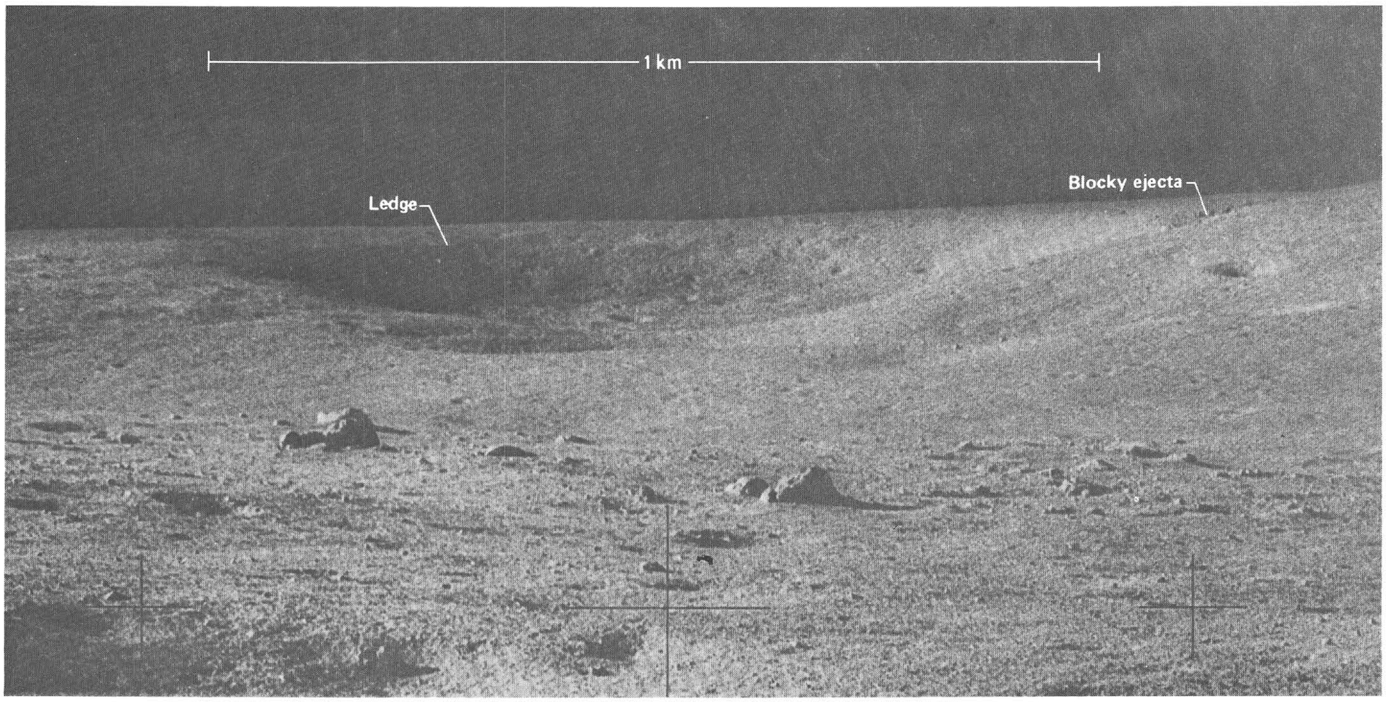

FIGURE 11.—Old Nameless crater, showing subdued ledge and blocky ejecta. View southeast from station B2. (Part of NASA photograph AS14-68-9425.)

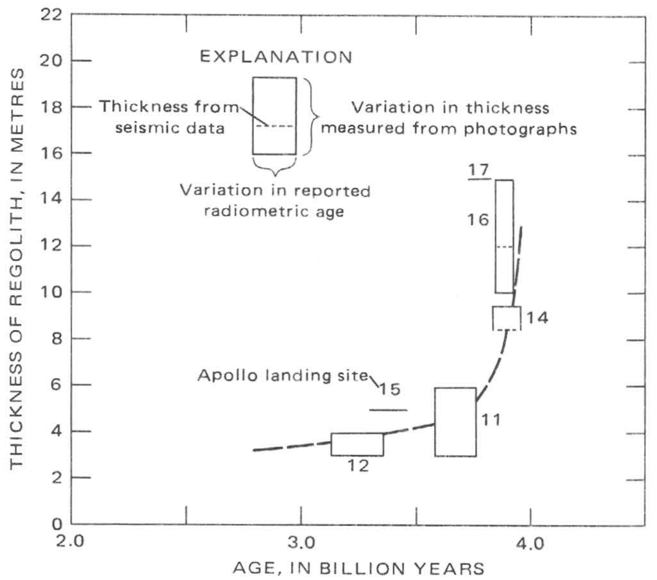

FIGURE 12.—Thickness of local regolith versus age of original surface as determined from radiometric ages of crystallization at Apollo landing sites 11–17.

tion entitled distribution of rock fragments.) The regolith on the Cone crater ejecta blanket is an immature, thin, and partial covering of fine-grained materials, some of which are probably original Cone crater ejecta, and some of which are products of erosion of rocks in the ejecta.

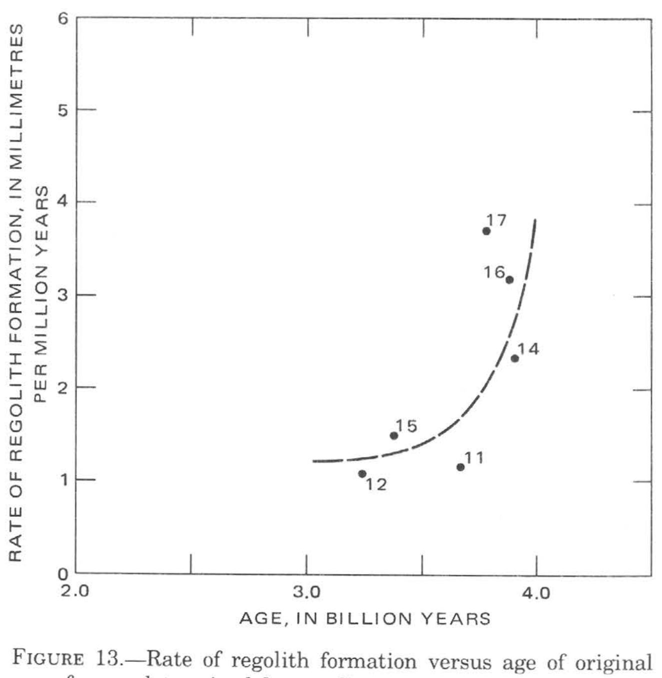

FIGURE 13.—Rate of regolith formation versus age of original surface as determined from radiometric ages of crystallization at Apollo landing sites 11, 12, 14–17. The values shown are median ages, and thicknesses from each landing site (numbered). The dashed curve was fitted by visual inspection.

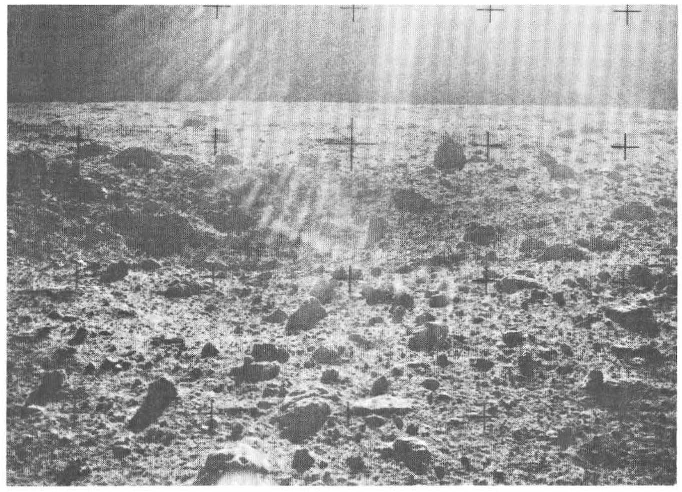

FIGURE 14.—Small crater in ejecta from Cone crater, with abundant blocks inside and on the rim of the crater. Fragments in foreground are 2–20 cm size. View east from station C′. NASA photograph AS14–64–9110.)

The smooth unit (Ifs, pl. 1) appears in Lunar Orbiter photographs to be a gently rolling terrane with a highly cratered surface. The ejecta blanket of Cone crater, however, is more hummocky and ridgy. These two types of surface morphologies extend down to centimetre scales. In order to evaluate the microrelief of the surfaces, detailed topographic maps with 1-cm contour intervals were constructed from two sample areas. Figure 15, an area west of the LM where sample 14304 was collected, shows that this surface is dominated by more or less equidimensional closed depressions. A similar map (fig. 16) at station C′, where a double core tube was driven, shows, in addition to the considerably higher abundance of rocks, that the surface is more hummocky and ridgy with a more complicated surface texture than that in the area west of the LM. Furthermore, at the location west of the LM, there are 27 craters between 10 and 50 cm in diameter in an 8 m^2 area; in the same location at station C′, there are only 6. It can therefore be concluded that a young surface created by ejecta from an impact crater tends to be ridgy and, as it grows older, tends to become one of coalescing closed depressions.

The Apollo 14 crew briefly described a "*raindrop pattern*" in the vicinity of station A similar to that previously described by the Apollo 12 crew. This pattern is readily seen in all of the panoramas, except at stations B3 and C′ (pl. 5), and in many of the sample documentation photographs (see figs. 50, 64, 66). It shows up best in photographs taken at low sun angle during EVA I (fig. 17). On fine-grained material the pattern appears to be formed by small craterlets up to 4 cm in diameter that saturate the surface. The raindrop pattern is interpreted to be formed by impact of small

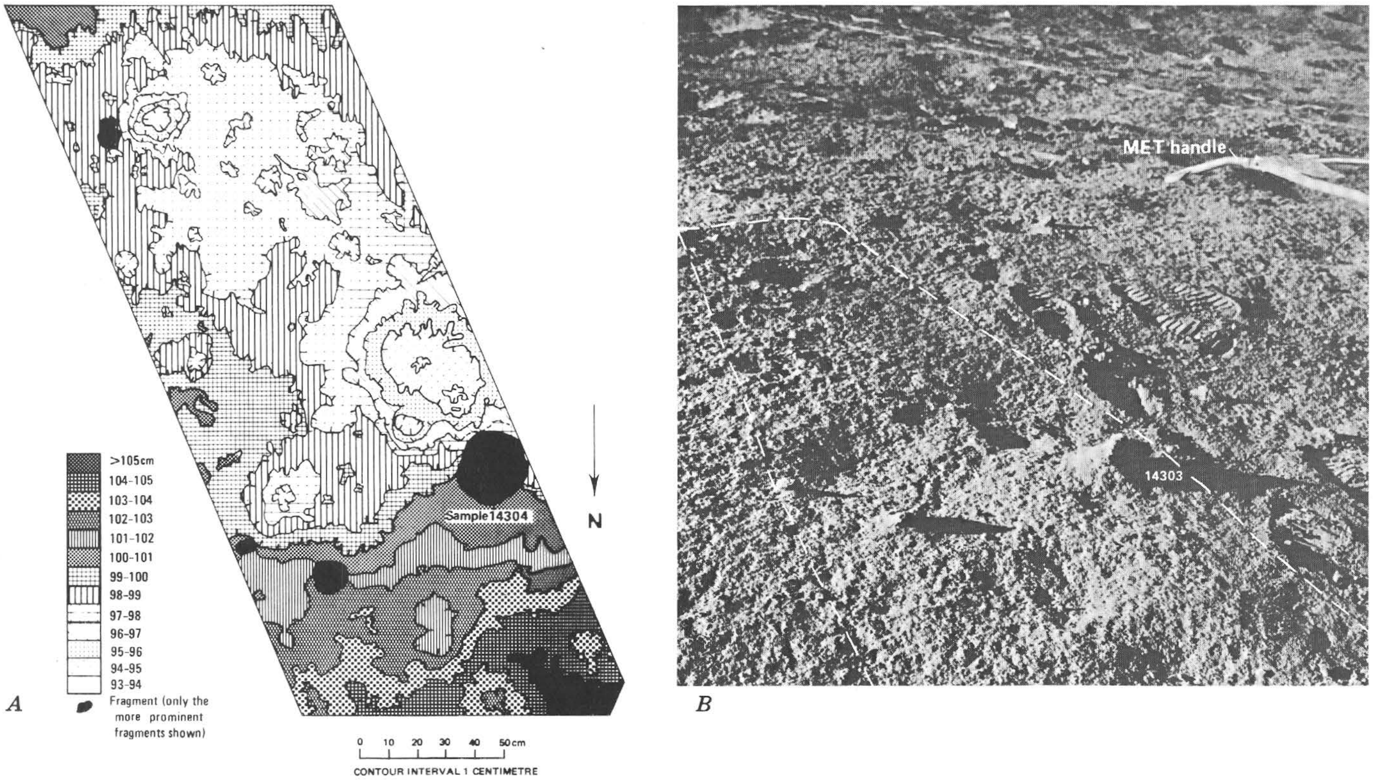

A *B*

FIGURE 15.—Surface morphology west of the LM. *A*, Hypsographic map of surface in the vicinity of sample 14304, which was collected northwest of the LM. *B*, Photograph showing the map area. (NASA photograph AS14–67–9391.) Map prepared by Raymond Jordan.

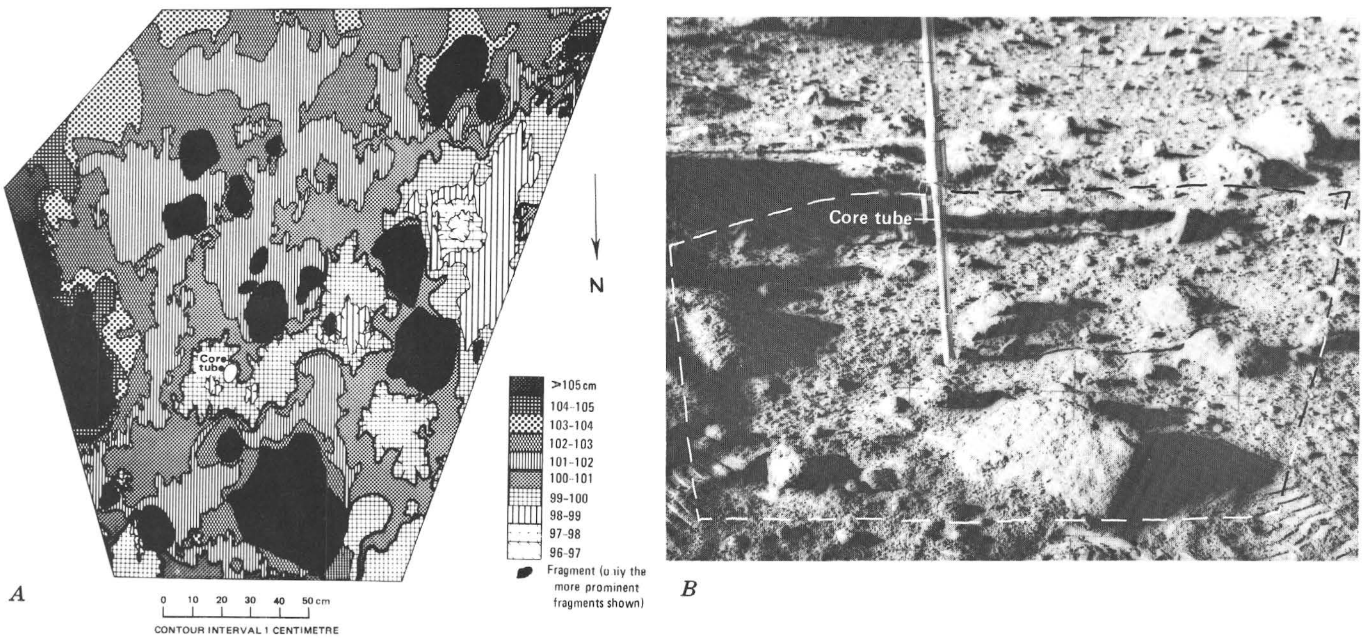

A *B*

FIGURE 16.—Surface morphology near Cone crater. *A*, Hypsographic map of area where double core tube was driven at station C′. *B*, Photograph showing the map area. (NASA photograph AS14–64–9125.) Map prepared by Raymond Jordan.

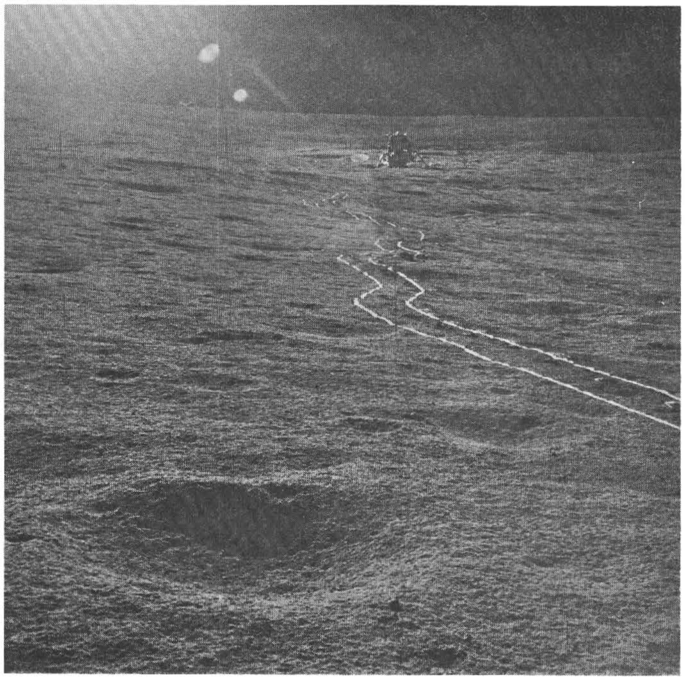

FIGURE 17.—"Raindrop" depressions on the surface of the smooth unit (pl. 1, unit Ifs) west of the LM. Bright lines are reflective tracks where the MET tires compressed the fine-grained material. View east. (NASA photograph AS14–67–9367.)

meteorites and by secondary particles from these impacts like those that form "*zap pits*" on rocks. A raindrop craterlet 1 cm deep is estimated to be destroyed by subsequent impacts in about 3 million years (Shoemaker and others, 1970), so that a fresh surface should become saturated by 4-cm craterlets in this time span.

Exposure ages of materials from Cone crater ejecta indicate that the crater was formed about 25–30 m.y. ago (Turner and others, 1971; Berdot and others, 1972; Crozaz and others, 1972). Where lighting is at a low incident angle to surfaces of boulders in Cone crater ejecta, zap pits are seen to cover the rock surfaces. This indicates that the surface of Cone crater ejecta should also be covered by a raindrop pattern, yet the pattern is much less evident in the ejecta blanket than in the western part of the area. Downslope movement of material, which would tend to destroy the craterlets, appears to have occurred on the steeper slopes on which the ejecta blanket was laid. Furthermore, the formation of craterlets would be impeded by the coarseness of the debris on the ejecta blanket. Small hummocks of fine-grained material a few centimetres in wavelength and height tend to obscure the craterlets. Also the sun angle was higher when the crew was on the ejecta blanket than it was during the first EVA, so the craterlets probably appeared less conspicuous.

DISTRIBUTION OF ROCK FRAGMENTS

Differences in the abundance of resolvable rock fragments at different stations along the traverse route are readily apparent on the panoramic photographs. It is also obvious that rock fragments are more abundant in the vicinity of Cone crater than elsewhere in the landing area. In order to help define the pattern and limits of Cone crater ejecta, boulders greater than 1 m across were plotted on the map of the landing site, and rock fragments more than 10 cm across were plotted on large-scale maps at each panorama station along the EVA II traverse route (pl. 7).

The areal distribution in the landing site of boulders more than 1 m across (approximate limit of resolution) was determined from Lunar Orbiter III photograph frame H–133. The densities of the boulder distributions were contoured at intervals of 1–2, 3–5, 6–10, 11–15, 16–20, and 21–25 boulders per 1,000 m^2, and the contours transferred to the rectified shaded-relief base. The lighting in much of the interior of Cone crater degrades the resolution, so that the densities shown in the regions of the map where the contours are dashed are probably lower than the actual densities. No boulders are visible in the totally shadowed region of Cone crater interior. Illumination of the remainder of the landing site favors identification of boulders, and therefore the counts are reasonably accurate.

Two bouldery ray patterns radiate from Cone crater, one to the north, and one to the southwest along the traverse area (pl. 7). Because the traverse route was along an identifiable ray, most if not all of the boulders along the traverse route, and probably many of the smaller fragments that were collected, are ejecta from Cone crater.

The area northeast of Cone crater is almost devoid of boulders, and so is the crater rim in this area. The variations in boulder abundances are probably due to differences in the physical characteristics of the Fra Mauro target materials before the Cone crater impact.

Much of the irregularity in ejecta patterns is probably the result of lithologic variations and fractures in the bedrock target materials of Cone crater. These must have been present from pre-Cone crater events, such as those that formed the Eratosthenian craters adjacent to Cone crater (pl. 1). A lens of friable material in the lower northeast part of Cone crater (pl. 1, geologic cross section) could explain the absence of boulders on the northeast rim.

In order to study areal distribution patterns of fragments too small to resolve on Lunar Orbiter photographs, fragments more than 10 cm across were plotted for 10 traverse stations on large-scale planimetric maps made from panoramic photographs taken with the Hasselblad cameras (pl. 7). The map areas are circles with 10-m radii; beyond 10 m, fragments up to 10 cm across are not accurately resolvable. The fragments are plotted to scale. The map distances and fragment sizes were determined from a perspective grid overlain on the panoramic photographs.

The maps show a general tendency toward an increase in the number of fragments greater than 10 cm toward Cone crater, which suggests an increase in the amount of Cone crater ejecta. The fragment population is slightly larger at station H than at the LM site and station A, which suggests an association of smaller fragments with the large rocks of station H (pl. 7).

The fragments within each map area are distributed somewhat nonuniformly. The fragment population is slightly larger in the southwest part of the station C′ map. Fragments are more abundant on the ejecta blanket of the small crater at C′ from which Cone crater ejecta was reexcavated than on the relatively undisturbed Cone crater ejecta (pl. 7).

Micrometeorite impact is generally considered to be the major cause of erosion on the lunar surface. (See for example Shoemaker and others, 1970.) Thus, on surfaces of similar materials, rock fragments larger than some minimal size should be less abundant on old surfaces than on younger surfaces, owing to longer exposure to erosion. The Apollo 14 site offers an excellent opportunity to test this hypothesis, in that surfaces of easily recognizable relative age differences along the traverse route were photographed in detail.

The surfaces in the traverse area are assigned relative ages on the basis of crater shapes and superposition (Eggleton and Offield, 1970). The ages of the surfaces of the areas in the station vicinities, from oldest to youngest, are: (1) station A in the relatively undisturbed Fra Mauro smooth unit; (2) station G approximately one-half crater diameter out on the ejecta of North Triplet crater; (3) stations B2 and C′ (looking northwest) on Cone crater ejecta; and (4) station C′ (looking southeast) on the ejecta of the 30-m crater at station C′.

In order to test the hypothesis that larger rock fragments are less abundant on older surfaces, the cumulative size-frequency distribution of resolvable rock fragments was determined for stations A, G, B2, and C′. Fragments 0.5 to 4 mm in size were counted on the *Apollo Lunar-Surface Closeup Camera* (*ALSCC*) photographs, fragments 4 mm to 1.6 cm in size were counted on the sample documentation photographs taken with the Hasselblad cameras, and fragments 1 m and larger were counted on the Lunar Orbiter photographs. No ALSCC photographs were taken at stations B2, C′, or G, so photographic information on fine particles at these stations is not available. Areas for which the counts were made or shown on plate 7, along with the cumulative size-frequencies of fragments, plotted on $\log_2 \times \log_{10}$ graphs. The approximation of the data points along straight lines, which have Pearson r correlations of $-.96$ to $-.99$ on the log-log plots, indicates that the fitted lines are statistically valid.

The cumulative size-frequency distribution curves show a decrease in the number of fragments larger than 1 cm with increasing age of the surfaces. The variations in the slopes of the size-frequency distribution curves are related to the ages of the surfaces; the older the surface, the greater the slope of the curve. Station B2 is an exception in that much of its surface is about the same age as that of the Cone crater ejecta at station C′. It is, however, more than a crater diameter away from Cone crater. Coarse particles were originally not as abundant at this distance from the impact point as they were near the crater rim. Also it is beyond the thin edge of the continuous ejecta blanket (pl. 1), so that the pre-Cone crater surface is partly exposed in the area. A problem arises in that no means have been devised with which to confidently distinguish in Hasselblad and ALSCC photographs small clods of regolith that are produced by impact from small coherent rock fragments. At the Apollo 14 site many of the small rock fragments are indurated matrix materials of the Fra Mauro rocks; thus, in photographs they resemble weakly indurated regolith breccias. No clods of boulder size can be identified in the photographs; all boulders that can be studied in detail appear to be well-indurated breccias. A total of five slightly coherent breccia samples were collected from stations A, B, and C′. Particles of agglutinates caused by shock lithification of fine regolith material by meteorite impact are common in the soil samples (McKay and others, 1972). Therefore, many of the small fragments that were counted were probably not eroded from larger rocks but are instead, small clods of local regolith indurated by impact processes. However, if even half of the smaller particles that were counted are soil breccias, the deviation from the curves shown would not be significant on this type of logarithmic plot.

A composite of the individual curves (fig. 18) shows that they converge at about 6×10^5 to 1×10^6 particles per 1,000 m^2 at a particle size of about 5 mm. The convergence point of the curves for fragments on surfaces of markedly different morphologic maturities suggests a steady-state size of particles smaller than about 5 mm, with the rate of production of 5 mm and smaller soil breccia particles approximately equalling the rate of destruction of 5 mm and smaller particles by erosion.

The increase in the slopes of the curves with increase in the age of the surface as shown in figure 18 indicates that small particles are formed by erosion of larger

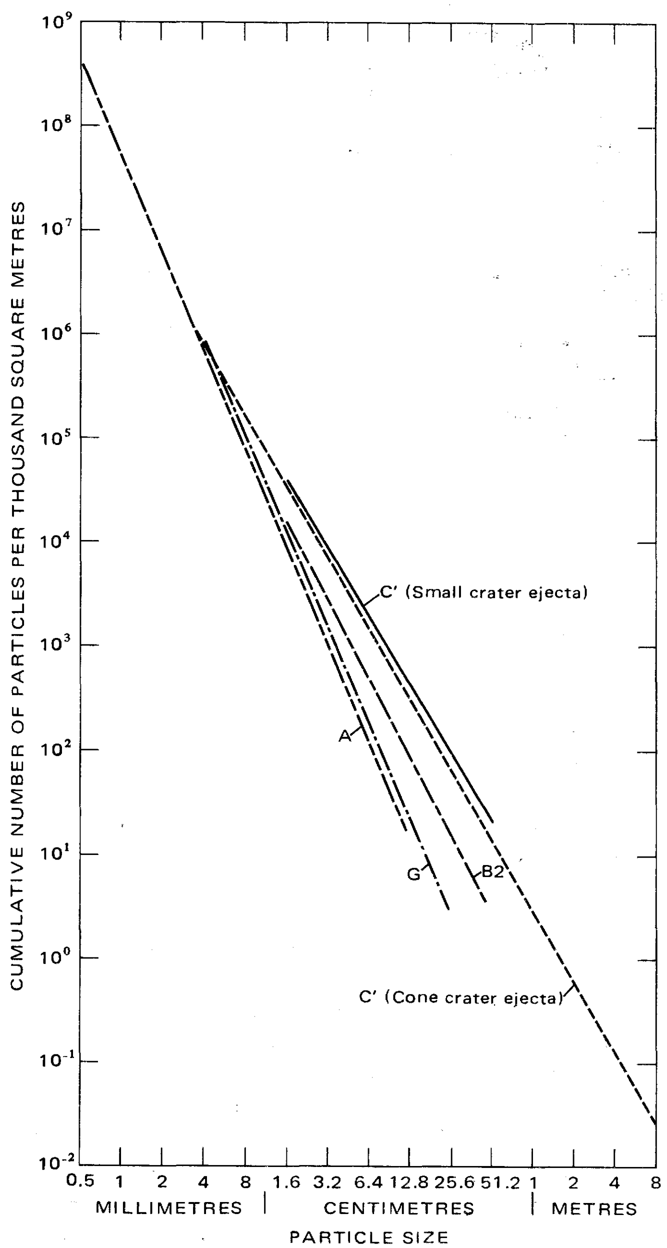

FIGURE 18.—Composite of fitted (least squares) size frequency curves for particles from 0.5 mm to 8 m. The curves and areas are shown individually on the graphs on the margins of the map on plate 7.

particles, and that, as the younger surfaces mature with time, the slopes of the curves will approach, and eventually exceed, that of the curve for station A by rotating around the convergence point. If no cratering events occur that are sufficiently large to excavate rocks from depth, a stage should be reached where the largest fragments are about 5 mm across, and all of these will be soil breccias. Continued stirring of the upper part of the regolith by small meteorites would both destroy and produce soil breccia particles that are about 5 mm across and smaller, and would continue to erode the remaining rock fragments, all of which would be smaller than 5 mm across. It is probable, however, that none of the lunar surface has been subjected to bombardment by small meteorites long enough for this stage of maturity to be reached, because occasional meteorite impacts with sufficient energy to excavate bedrock keep rejuvenating the rock fragment population on the surface.

FILLETS

Fillets have been defined as embankments of fine-grained material partly or entirely surrounding larger rock fragments (Shoemaker and others, 1968), and as accumulations of fine-grained material on uphill faces of rocks (Gault and others, 1967). They can be classified on the basis of shape into three groups: (1) concave, (2) low angle, and (3) convex (fig. 19). The shapes appear to be controlled largely by the attitude of the rock surface relative to the ground surface. Concave fillets are the most common and occur where the rock surface is steep. Low-angle fillets occur where the rock surface is also at a low angle and are generally shallow over the rock surface. Convex fillets are partly shielded by rock overhang and with time should develop into one of the other two types as the overhang volume is filled. The type that develops will depend on the shape of the rock surface above the overhang.

Mathematical models of fillet formation (Hait and Shoemaker, oral commun.) show that the common type concave fillet can be created from simple rebound of low-velocity, fine-grained particles striking the rock surface. The source for the fine particles is ejecta derived from small-scale impacts into the nearby regolith surface. The computer modeling simulated hemisphere (half-buried sphere), in a target area, on which particles were permitted to impact at varying incident angles and velocities. The preliminary results indicate that material eroding from the rock itself by spalling or micrometeorite erosion is not significant in fillet buildup, and that fillets are produced primarily by trapping of low-velocity materials ejected by cratering processes. A few rock fragments, however, are commonly seen on the fillet surface, and some are probably spalled from the rock.

This fillet model suggests that fillets grow with time and that their height might indicate the relative length of time that a rock has been in its present position on the lunar surface. However, variations in the heights of fillets on different boulders and smaller rocks that almost certainly were ejected from Cone crater, and thus have been at the surface for the same length of time, indicate that this is probably only a very qualitative indication of how long the rock has

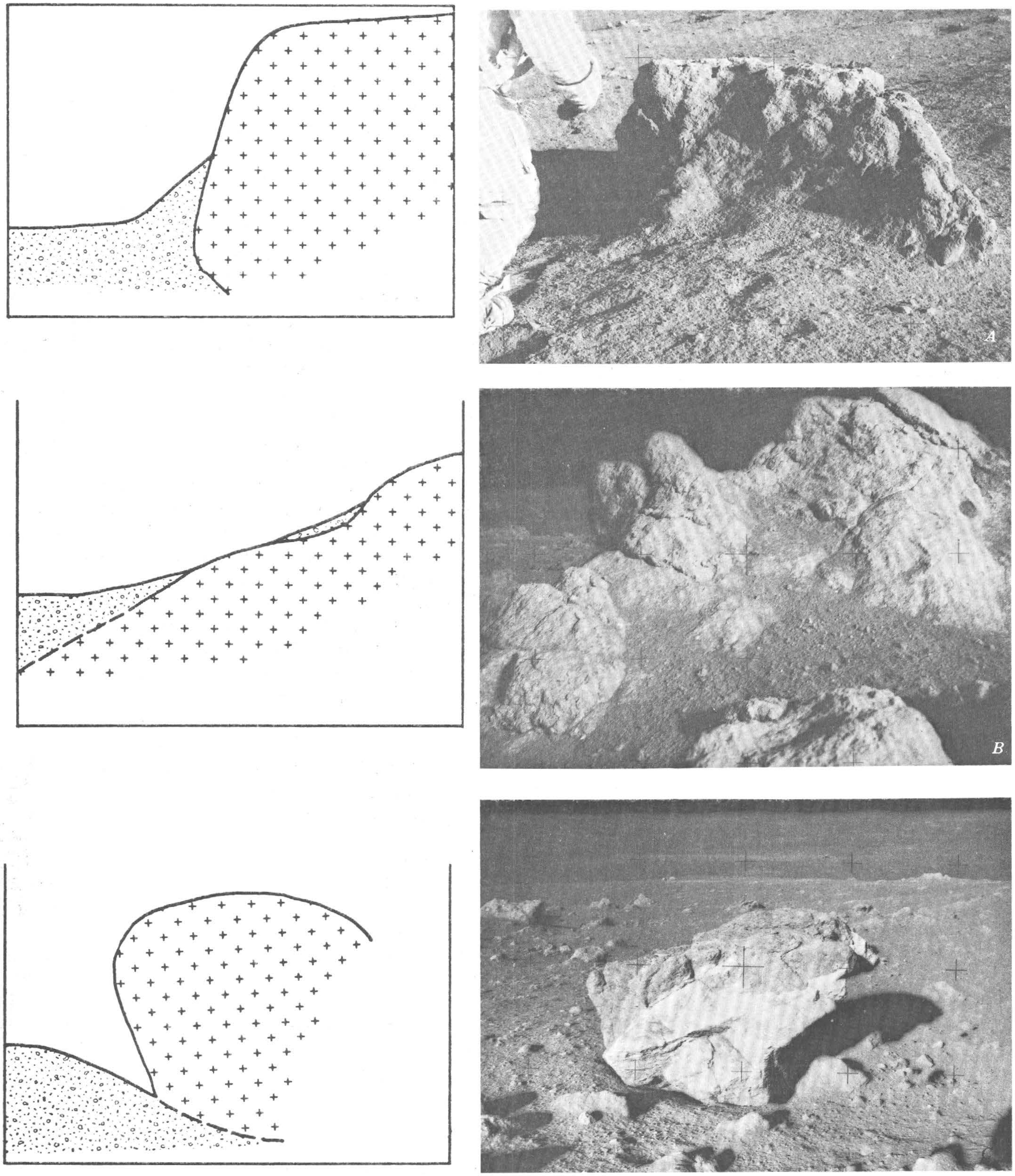

FIGURE 19.—Types of fillets. *A*, Concave with steep contact between rock and soil: example is Big rock at station B2 (part of NASA photograph AS14–68–9414). *B*, Low angle with low-dipping contact between rock and soil: example is Saddle rock at station C1 (NASA photograph AS14–68–9450). *C*, Convex under rock overhang: example is Contact rock at station C1 (NASA photograph AS14–68–9448).

been in place. Uncertainties arise because some cratering events are large enough to embank relatively large amounts of material against nearby rocks.

OPTICAL PROPERTIES

The polarizing characteristics of lunar materials were measured from earth-based telescopes prior to any of the lunar missions. These measurements are integrated over areas about 300 km2 and show the degree of polarization varies with phase angle, and that maximum polarization occurs at a phase angle of about 100°. The maximum polarization of incident light varies between about 5 and 20 percent. Although there is a continuum of values, with some overlap between mare and highland materials, the mare materials tend to have higher values of polarization (Dollfus, 1962; Wright and others, 1963; Wilhelms and Trask, 1965; Trask, 1966).

The television cameras flown on the Surveyor 6 and 7 missions had polarizing filters for measuring polarizing characteristics over areas of a few square centimetres to a square metre. Surveyor 6, which landed in Sinus Medii, indicated that the degree of polarization at a phase angle of 100° is about 16–19 percent. Surveyor 7, which landed on the ejecta blanket of the crater Tycho in the southern highlands, showed that the degree of polarization is about 7–9 percent at a phase angle of 100° (Shoemaker and others, 1968) (table 2).

TABLE 2.—*Albedo and polarimetric measurements from the Apollo 14, 11, and 12 sites and from the Surveyors 3, 5, 6, and 7 sites*

	Percent albedo		Percent polarization	
	Samples	Photos	Samples	Photos
Fra Mauro				
Smooth unit soil	13.1	8.2–9.4	9.5	------
Ridgy unit soil	----	9.0–14.4	----	------
Mare Tranquillitatis soil	----	9.0	20	------
Oceanus Procellarum (Surveyor 3; Apollo 12)		[1]8.5	18,15	------
Mare Tranquillitatis (Surveyor 5)		[1]7.9– 8.4	----	------
Sinus Medii (Surveyor 6)	----	[1]8.2	----	[1]16–19
Tycho rim (Surveyor 7)	----	------	----	[1]7–9

[1]Shoemaker and others, 1968.

Polarimetric measurements were made from four lunar soil samples: 19984,69 (Apollo 11, Mare Tranquillitatis), 12070,170 and a sample collected by Apollo 12 from the soil scoop of Surveyor 3 (Apollo 12, Oceanus Procellarum), and 14163,188 (Apollo 14, Fra Mauro). Only a few soil samples were collected by Apollo 14, and sample 14163,188 from near the LM was the only one made available for this study.

The polarization peaks of the samples are rather broad and occur at phase angles of about 100°–115° (fig. 20), slightly higher angles than the 100° peaks measured through the telescope and by the Surveyor 6 and 7 cameras. The polarization of light by the mare samples is noticeably higher than that of the Apollo 14 highlands sample. This is in general agreement with the telescopic and Surveyor measurements (table 2), and with measurements by Dollfus, Geake, and Titulaer (1971) on Apollo 12 lunar samples.

Polarization characteristics of three Fra Mauro breccias are compared with those of a mare basalt and of a *soil breccia* derived from mare basalt that is shown in figure 21. Although the curves for these rock samples do not have well-defined polarization peaks over phase angle ranges of 20° to 150°, and their measured maximums are widely spread with regard to their degree of polarization, the two mare samples have a considerably higher degree of polarization than the three Fra Mauro breccia samples.

Albedo measurements were taken from Apollo 14 surface photographs at traverse stations A, B, B1, B2, C′, C1, G, G1, and H (pl. 2). The luminance from undisturbed surface material was measured around the shadow of the astronaut's head and shoulders, where the phase angles were 3° to 6°. The measured luminance was then extrapolated to zero phase angle luminance (albedo) by means of the lunar photometric function compiled by Willingham (1964).

The albedos of the undisturbed fine-grained surface material at the intercrater areas along the geological traverse in the smooth unit range from 8.2 to 9.4 percent (table 2). The albedo variation does not reflect a pattern but appears to be randomly distributed, except at stations G and G1, which are located on the eroded ejecta of the 150-m diameter subdued North Triplet crater (pl. 1). The materials at these stations have albedos of 9.2 to 9.4 percent, which are in the higher part of the range of albedos for the smooth unit. Stations B1 and B2, at the lower part of the ridgy unit, also have slightly higher albedos, 9.1 and 9.6 percent, respectively, which probably indicates a measureable amount of Cone crater ejecta, with higher albedo, in the materials at these stations.

The fine-grained materials in Cone crater ejecta are crushed bedrock and represent newly generated regolith. The heterogeneous fine-grained mixture of crushed light and dark banded Fra Mauro rock has albedos ranging from 10.7 to 14.4 percent. This material shows slight to undetectable darkening where disturbed by astronaut activity, in contrast to the 5 to 11 percent darkening of the regolith on the plains at stations A, B, and G.

Pohn, Wildey, and Sutton (1970) report that the albedo of the Apollo 14 landing site area ranges from 10.8 to 11.4 percent, in an integrated area of about 65 km^2. The integration of small areas of bright rocks and craters probably increases the total reflectance in their

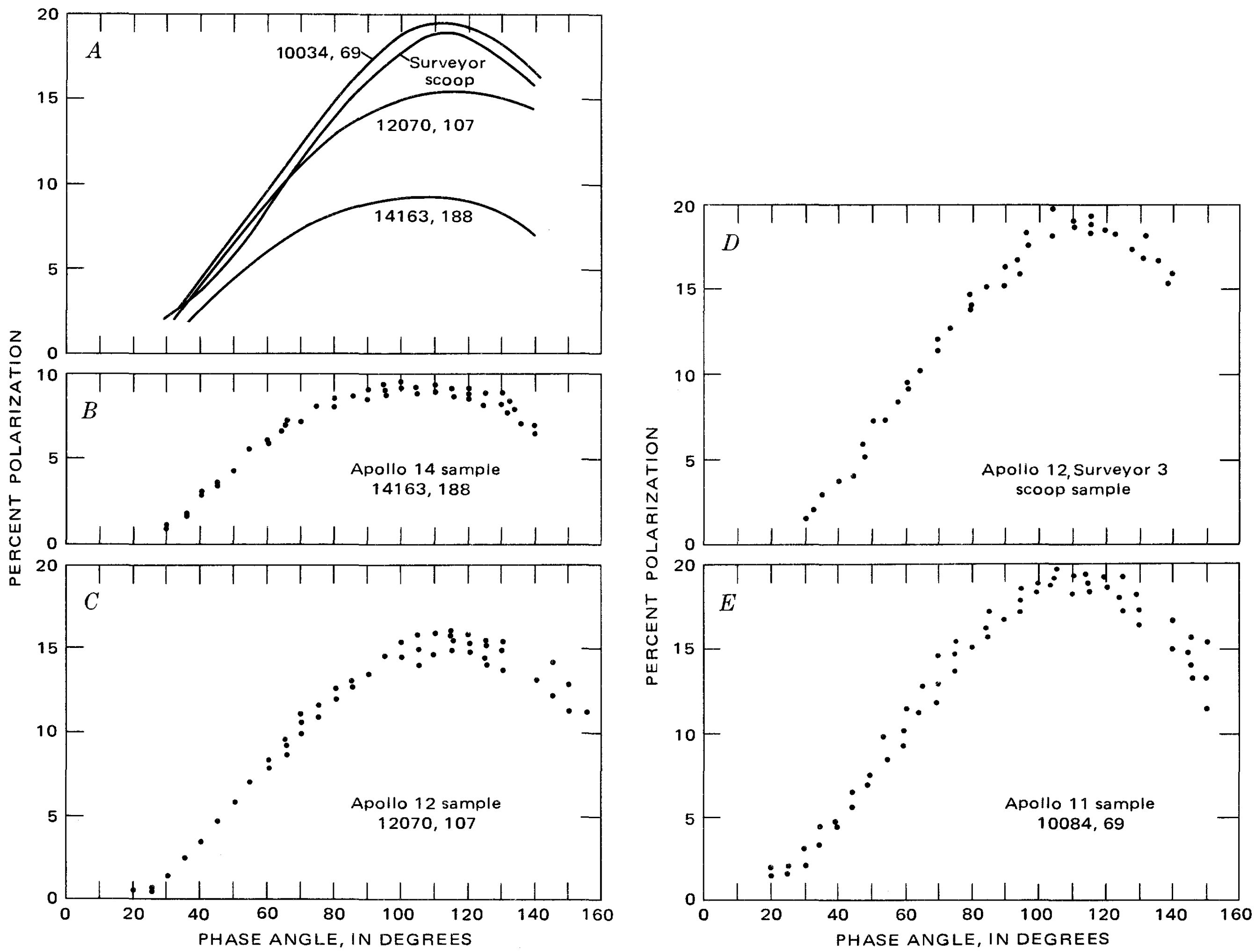

FIGURE 20.—Polarization scatter graphs of highland soil (Apollo 14) and mare soil (Apollos 11, 12, and Surveyor). *A*, Fit-by-eye curves comparing the scatter graph data. *B*, Apollo sample 14163,188. *C*, Apollo 12 sample 12070,107. *D*, Apollo 12, Surveyor 3 scoop sample. *E*, Apollo 11 sample 10084, 69.

measurements, compared with our spot measurements, in which bright rocks and craters were not included. The boulders of Fra Mauro material exposed on the rim of Cone crater have irregular concentrations of lighter and darker materials, which suggests that erosion of Fra Mauro rocks would initially produce a mottled regolith. The lunar regolith becomes darker with time than its parent material, probably because of increasing vitrification of regolith materials by high-energy impact (Adams and McCord, 1971). It also becomes more homogenized by mixing from repetitive impacts. The albedo of the Cone crater ejecta is representative of the broken bedrock material, and the uniformly darker material of the smooth unit represents cumulative darkening and homogenization since the Fra Mauro Formation was emplaced.

The ages derived by geochemical techniques for the Cone crater event, the North Triplet event, and the length of exposure of regolith near the LM correlate with the albedos of the associated materials. Cone crater ejecta, which has an albedo range of 10.7 to 14.4 percent, has probably darkened little if any since its formation. North Triplet crater had an original depth of about 30 m (judging from its 150 m diameter), compared to a regolith depth of about 8.5 m, so the cratering event must have ejected fresh Fra Mauro rocks, now on the crater rim. The albedo range of 9.2 to 9.4 percent at stations G and G1, compared with the albedo of Cone crater ejecta, indicates an average of about a 3 or 4 percent darkening of the uppermost layer since the North Triplet event.

The albedo of the regolith near the LM is 8.4 percent. The exposure age for surface materials from near the LM implies that that area has not been significantly churned by cratering during the past 600 m.y. (Turner and others, 1971), and the regolith in the LM area therefore is probably not homogenized to a uniform albedo with depth. The rather uniform 8.4 percent al-

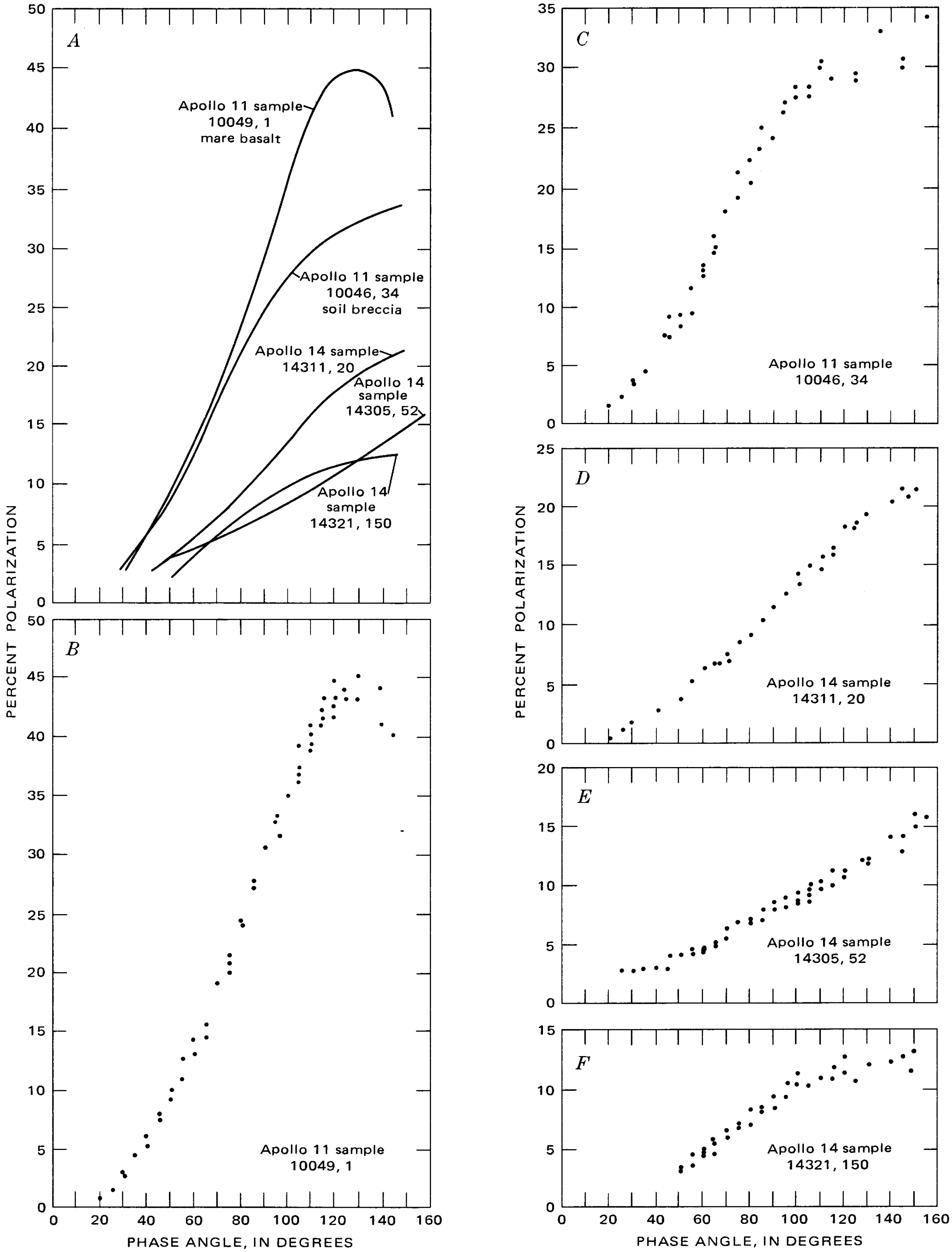

FIGURE 21.—Polarization scatter graphs of highland rocks (Apollo 14) and mare rocks (Apollo 11). *A*, Fit-by-eye curves comparing the scatter graph data. *B*, Apollo 11 sample 10049,1. *C*, Apollo 11 sample 10046,34. *D*, Apollo 14 sample 14311,20. *E*, Apollo 14 sample 14305,52. *F*, Apollo 14 sample 14321,150.

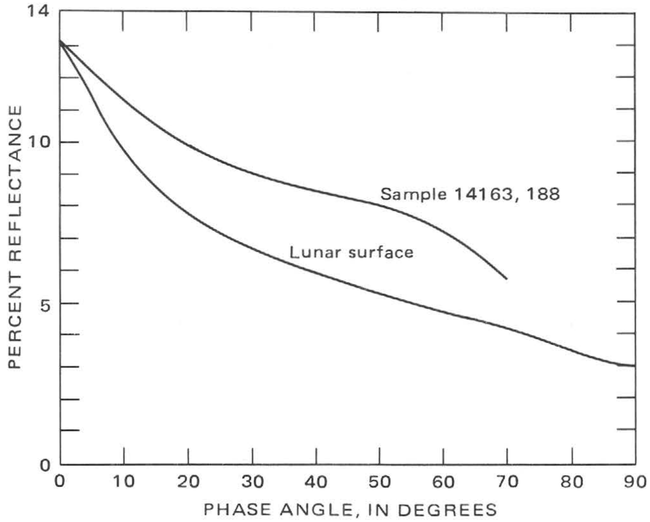

FIGURE 22.—Average reflectance of lunar surface compared with Apollo 14 soil sample 14163,188.

bedo on intercrater surface areas suggests that the additional 1 percent darkening is due to the 600-m.y. exposure age, as compared to the 100- to 260-m.y. age of North Triplet crater rim (Berdot and others, 1972). An approximation for the time required for surface layer darkening is provided by the sequential exposure ages of Apollo 14 samples. The rate of darkening appears to be initially rapid: 3 percent in about 200 m.y. with a slower rate of 1 percent in an additional 400 m.y. The heterogeneity in the albedos of Cone crater ejecta, and the relatively short exposure time of approximately 25 m.y., probably account for the inability to measure the degree of darkening of Cone crater ejecta.

The albedo of a small part of the Apollo 14 regolith bulk sample was measured in the laboratory and found to be 13.1 percent. When the sample holder was tapped, causing additional settling of the material, the albedo increased to 13.6 percent. Apparently the lunar material did not form its natural lunar microtexture in our atmosphere, and the albedo of the sample is greater than that of similar in-situ material. The regolith bulk sample was shoveled from the bottom of a 0.5-m crater reported by the astronaut crew to have a different colored layer, and it is possible that the albedo of sample 14163,188 is intrinsically higher than that of the surface, 8.4 percent. A comparison of the typical lunar photometric function with the measured function of the sample is shown in figure 22, where the lunar reflectance has a greater backscatter reflectance near zero phase angle.

The maximum albedo of 36 percent for the light parts of boulders at the Apollo 14 site is higher than any albedo that was measured on the lunar surface through the time of Apollo 14. (Muehlberger and others, 1972, report albedos as high as 55 percent for South Ray crater ejecta, Apollo 16.) Layered rock in the White rocks group at station C′ (fig. 23) contains dark clasts with an average albedo of 16 percent, gray matrix material with an average albedo of 20 percent, and a light-gray layer with an average albedo of 36 percent. Some light clasts such as those in Turtle rock (fig. 24) have albedos of 33 percent, about the same as that of the light layer in Layered rock. These comparable albedos imply that the light layers of the White rocks and the light clasts in some of the boulders have similar compositions.

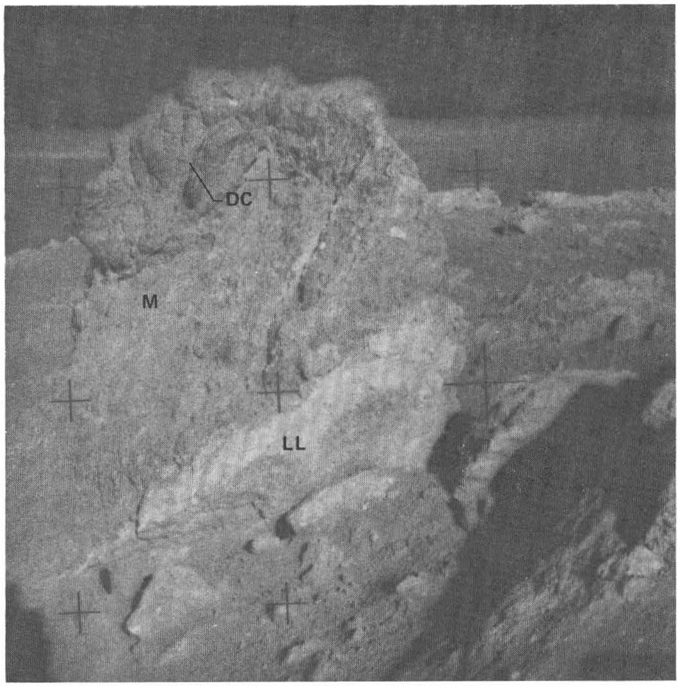

FIGURE 23.—Layered rock at station C1 showing albedo differences between dark clast (DC), matrix (M), and light layer (LL). Layered rock is about 2 m high. (NASA photograph AS14–68–9449.)

GEOLOGIC STRUCTURES

There is no direct evidence for tectonic features in the landing site. Old pre-Imbrian structures, unless reactivated after the Imbrium event, would be masked by the ejecta from the Imbrium and older basins. Fractures caused by craters certainly exist in the local bedrock, but they are visible only in boulders ejected from Cone crater. However, lineaments sparsely distributed over the landing site area suggest the existence of fractures in the local bedrock.

Lineaments on the lunar surface may be grouped on the basis of size into three categories: (1) lunar grid lineaments ranging from tens to hundreds of kilometres in length, which are related to straight rilles and scarps, linear mountain fronts, and sides of large polygonal craters (Strom, 1964; Elston and others,

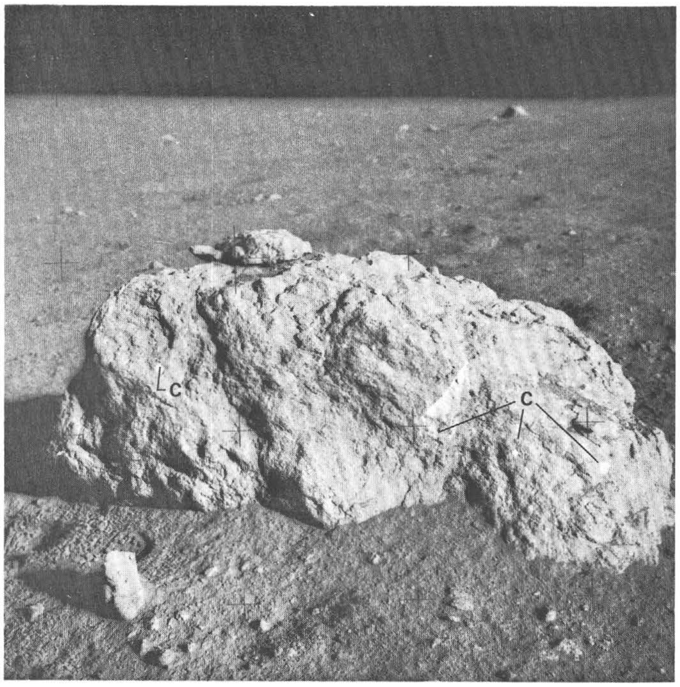

FIGURE 24.—Light clasts (C) in Turtle rock. (NASA photograph AS14-68-9476.)

1971); (2) regional-scale lineaments, ranging from tens to a few thousands of metres in length, which are elongate and commonly indistinct troughs and ridges expressed in the regolith (Carr, 1966; Schaber and Swann, 1971); and (3) small-scale lineaments ranging from a few centimetres to a few metres in length, which are also expressed as troughs and ridges in the regolith (Shoemaker and others, 1969; Schaber and Swann, 1971).

Small-scale lineaments at the Apollo 14 site that are visible in the Hasselblad photographs have two primary trends (northwest and northeast) and one secondary trend (north) (fig. 25). These features are poorly developed compared to those at the Apollo 11 and Apollo 12 sites (Schaber and Swann, 1971). The only well-defined linear features recognized on the Apollo 14 Hasselblad photographs are several features up to 100 m long that trend generally north in the vicinity of the LM (fig. 26). These unusually long lineaments, like the well-developed lineaments on the walls and rim crests of 200-m to 400-m subdued craters, may be surface reflections through the regolith of jointing in the bedrock (Schaber and Swann, 1971).

Regional-scale lineaments both at the Apollo 12 and 14 sites have northwest, northeast, north-northwest, and north-northeast trends. Apollo 12 features are about half again as abundant as those of the Apollo 14 site (fig. 27). Apollo 11 regional lineaments are about five times as abundant as those of the Apollo 14 site, but only the northwest and northeast systems are

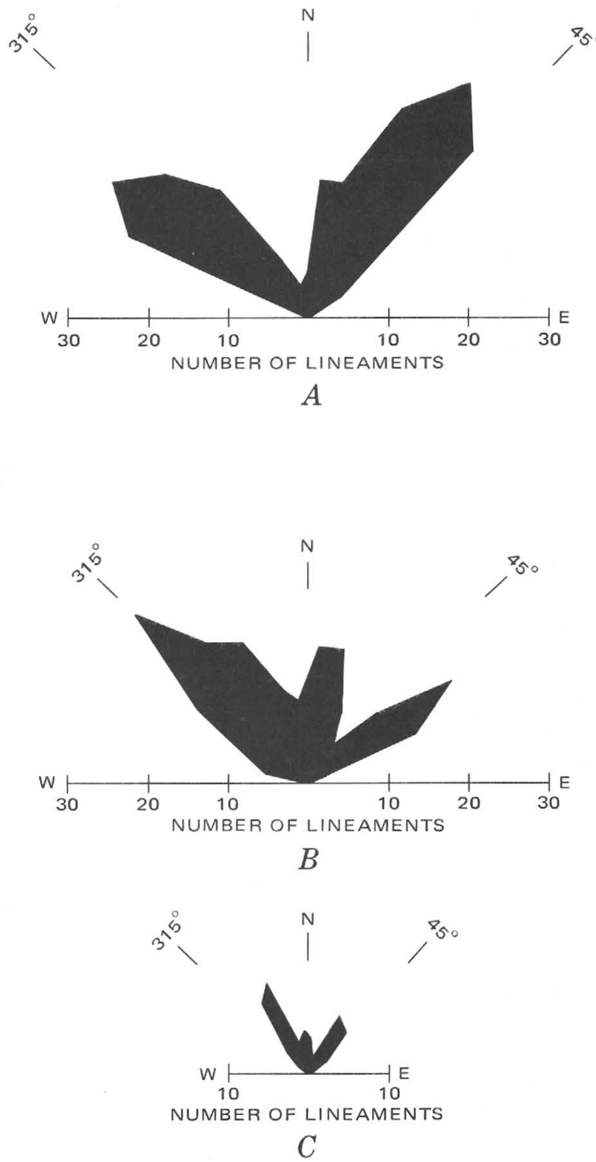

FIGURE 25.—Azimuth frequency diagrams of small-scale lineaments in the Apollo 11, 12, and 14 sites plotted from surface photographs. *A*, Apollo 11 (Schaber and Swann, 1971). *B*, Apollo 12 (Schaber and Swann, 1971). *C*, Apollo 14 (Swann and others, 1971).

strongly developed. A weak north-trending set is also present in the Apollo 11 regional data (fig. 27). The striking similarity of the Apollo 12 and Apollo 14 regional lineament systems may be due to the proximity of the two sites (approximately 200 km) and therefore may be a reflection of identical structural trends.

Earth-based telescopic observations of the Moon resulted in early recognition of the global system of lineaments that make up the lunar grid system. These lineaments are remarkably consistent and trend primarily northwest, northeast, and north, with less well developed north-northeast and north-northwest

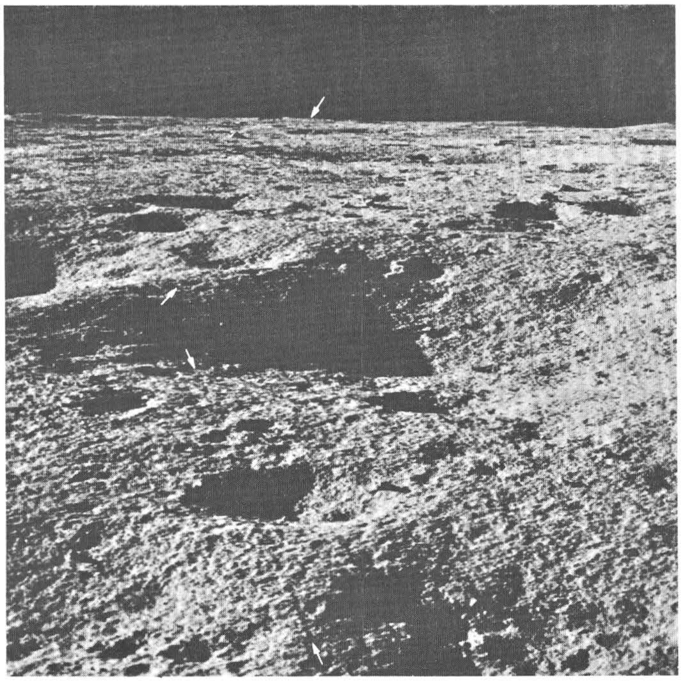

FIGURE 26.—Two long lineaments in the Apollo 14 landing site. View south. (NASA photograph AS14-66-9251.)

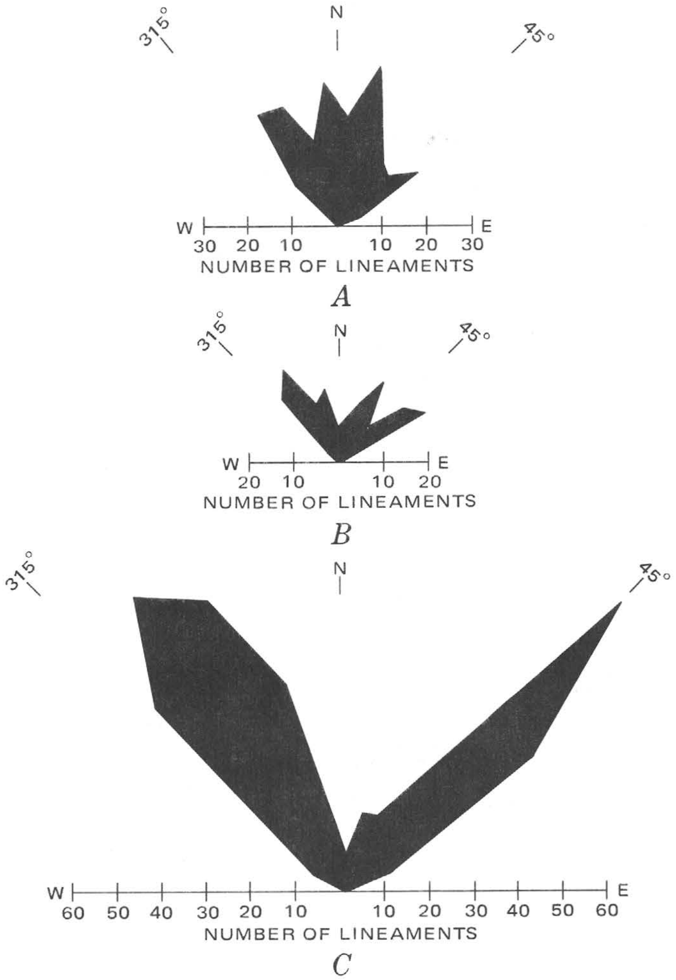

FIGURE 27.—Azimuth frequency diagrams of regional-scale lineaments in the Apollo 11, 12, and 14 landing sites. Plotted from Lunar Orbiter photographs (Schaber and Swann, 1971.)

trends (Strom, 1964; fig. 28). Television pictures transmitted from Ranger spacecraft indicated the existence of similar lunar grid lineaments at much smaller, or regional, scale. Azimuthal trends of the regional scale lineaments largely coincide with the lunar grid (Carr, 1966). The trends of small- and regional-scale lineaments in the Apollo 11, 12, and 14 sites are also in general agreement with those of the lunar grid and, as previously suggested, may therefore be related to ancient global structural systems (Carr, 1966; Schaber and Swann, 1971).

Howard and Larsen (1972), using cupric oxide and gypsum powders and simulated lunar lighting conditions, showed that apparent lineaments can be caused by lighting effects, and Wolfe and Bailey (1972) have shown that the acute angles of the two prominent lineament trends that were observed and photographed on the Apennine front by the Apollo 15 crew are bisected by the sun azimuth. The conclusions reached by Wolfe and Bailey agree with the laboratory work of Howard and Larsen in that at least some of the strongest lineament trends (especially the northwest and northeast systems) may be effects of lighting on rough surfaces and may not represent lunar structures.

There are, however, at least three sets of lineaments in the Apollo 11, 12, and 14 traverse areas, and as many as four or five in the Apollo 12 area, and only two strong trends appear on the Apennine front and on the laboratory models. This, and the agreement in azimuthal trends with those of the lunar grid, which is obviously not a lighting effect, suggests that at least some of the smaller lineaments may be related to structures and are not simply effects of lighting. It is therefore suggested that when three or more sets of distinct lineaments are observed, one or more of them are actual lineaments and are not the effects of lighting.

FRA MAURO FORMATION

Samples of Cone crater ejecta indicate that the Fra Mauro Formation includes complex fragmental rocks derived from the brecciation of older igneous and possibly in some cases clastic rocks that predate the Imbrium event (see for example Lunar Sample Preliminary Examination Team, 1971; Swann and others, 1971; Warner, 1972; Wilshire and Jackson, 1972). Wilshire and Jackson (1972) have classified the Apollo 14 rocks into the following types:

1. Homogeneous crystalline rocks, basaltic (type B).
2. Homogeneous crystalline rocks, metaclastic (type C).

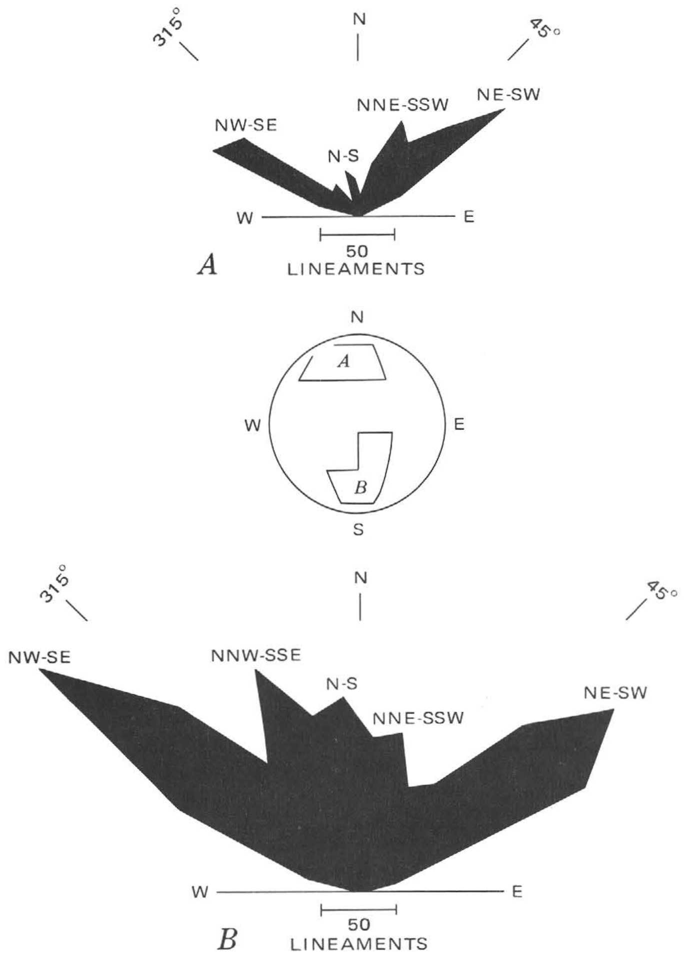

FIGURE 28.—Azimuth frequency diagram of lunar grid lineaments. *A*, Plots from northern hemisphere. *B*, Plots from southern hemisphere. The diagram represents the apparent azimuth as viewed in orthographic projection; 10,000 total plots (Strom, 1964).

3. Fragmental rocks, light clasts dominant, matrix friable (type F_1).
4. Fragmental rocks, light clasts dominant, matrix coherent to moderately coherent (type F_2).
5. Fragmental rocks, dark clasts dominant, matrix friable (type F_3).
6. Fragmental rocks, dark clasts dominant, matrix coherent to moderately coherent (type F_4).

Eggleton and Offield (1970) estimate the Fra Mauro to be about 200 m thick in the ridge areas. Kovach and Watkins (1972) interpret a 299-m/s seismic velocity layer that is estimated to range from 19 to 76 m in thickness to be the Fra Mauro Formation. We believe that variations in the degree of annealing and thus friability of Fra Mauro rocks and superposed brecciation and fracturing by post-Fra Mauro cratering events, render thickness estimates from seismic data alone unreliable. Cone crater is about 65 m deep and, therefore, if Eggleton and Offield's estimate of thickness is correct, only the upper third of the Fra Mauro Formation was exposed by the Cone crater event. It is unlikely that Cone crater penetrated completely through the Fra Mauro Formation, even if Eggleton and Offield's estimate of the thickness is greatly in error. The crater missed penetrating the base of the ridge by about 30 m, and if the ridge is a depositional feature of the Imbrium ejecta blanket, then the crater could not have penetrated to the average base of the ejecta. However, a 0.75-km-diameter Eratosthenian crater immediately south of Cone crater and a 1.5-km-diameter Imbrian crater adjacent to Cone crater on the east (Eggleton and Offield, 1970) probably did penetrate to depths greater than 200 m, and therefore material would have been ejected from below the base of the Fra Mauro Formation. This material might be found any place in the landing site, and some was probably reejected by the Cone crater event. Evidence in the samples of a fossil regolith that developed on the pre-Fra Mauro surface might be the best clue as to whether samples from below the Fra Mauro were collected.

Swann and others (1971) suggested that the boulders of the White rocks group, many of which are very light colored and were observed only near the rim crest of Cone crater, may have come from the deepest level to which the crater penetrates. The samples of the White rocks are described by Wilshire and Jackson (1972) and by Chao and others (1972) as friable, and we now believe that the White rocks materials extend in the subsurface toward the northeast of Cone crater and are more friable in that direction, which accounts for the lack of boulders on the northeast rim of Cone crater. The distribution of rock types in the ejecta of Cone crater led Wilshire and Jackson (1972) to suggest that the deepest units ejected from Cone crater are composed of dark-clast fragmental rocks with friable to moderately coherent matrix (type F_4 breccia; fig. 29), and that they are interlayered with light-colored, though dark-clast-dominant, fragmental rocks of the White rocks type (type F_3 breccias; fig. 30). Light-clast-dominant breccias with coherent to moderately coherent matrix (type F_2; fig. 31) are believed to have been derived from a higher part of the Fra Mauro Formation. The fragmental rocks with dominant light clasts and friable matrix (type F_1; fig. 32) are regolith breccias derived from the uppermost target materials of Cone crater and also are formed elsewhere by impact into the regolith. Thus it is reasonable to assume that the uppermost Fra Mauro unit, the light-clast or F_2-type breccia, provided most of the regolith from which the light-clast-dominant F_1-type breccias were derived. The igneous and metaclastic rocks are probably relatively hard clasts that were eroded from the softer

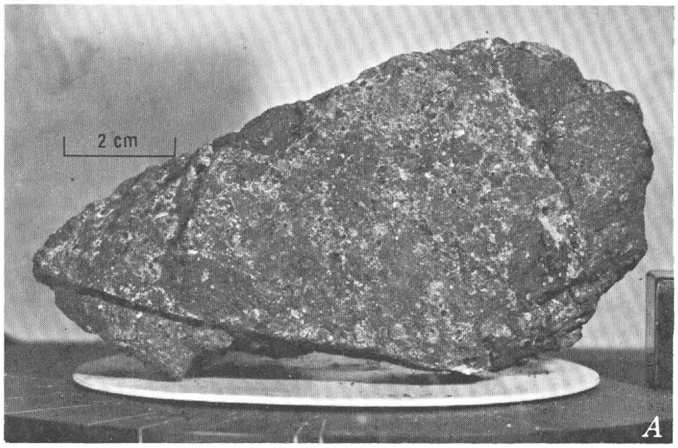

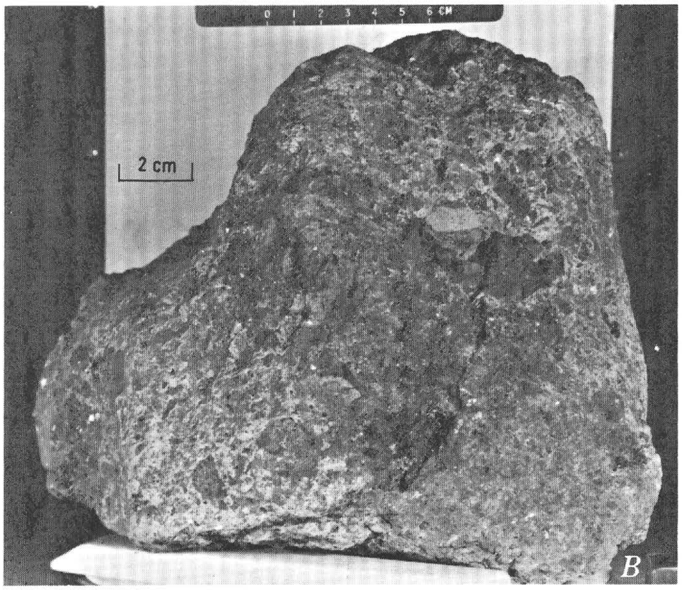

FIGURE 29.—F_4 breccia rock types. *A*, Sample 14306. Note prominent planar glass-lined fracture near bottom left. Compare with figures 68 and 69. (Part of NASA photograph S–71–22014.) *B*, Sample 14321, "Big Bertha." Compare with figures 76 and 77. (Part of NASA photograph S–71–22164.)

matrix breccias of the Fra Mauro Formation by micrometeorite impact.

Layering or bedding within the Fra Mauro fragmental rocks can be seen in photographs of several of the large boulders at the Apollo 14 site. In addition, many of the same kinds of structures, such as layering and fracturing, are found in the samples (fig. 29).

Samples 14053, taken from a boulder at station C2, and 14068, collected at station C′ (pl. 2), may be representative of materials from the base of the Fra Mauro Formation. Sample 14053 is a coarse-grained gabbroic rock with silicon- and potassium-rich glass in its interstices. It is somewhat similar in composition and texture to some of the crystalline rocks returned by Apollo 12, and may therefore be a mare-type basalt (Kushiro and others, 1972; Lovering and others, 1972; Chao and others, 1972). Schürmann and Hafner (1972) conclude that the rock was heated by impact events, probably at the Imbrium basin site, and was later quenched, probably in a cold regolith, at the Fra Mauro site. The large boulder does appear friable in the photographs (Schürmann and Hafner, 1972), but when Astronaut Mitchell failed to break a sample with the hammer, he exclaimed "No, man; that's hard, hard, hard." Shepard then picked a loose piece (sample 14053) off the opposite side of the rock. If Schürmann and Hafner's interpretation is correct, the boulder appears to be an unusually coarse and well-annealed regolith breccia.

Sample 14068, studied in detail by several investigators, is reported by Warner (1972) to be a high-grade metamorphic breccia with no, or only a trace of,

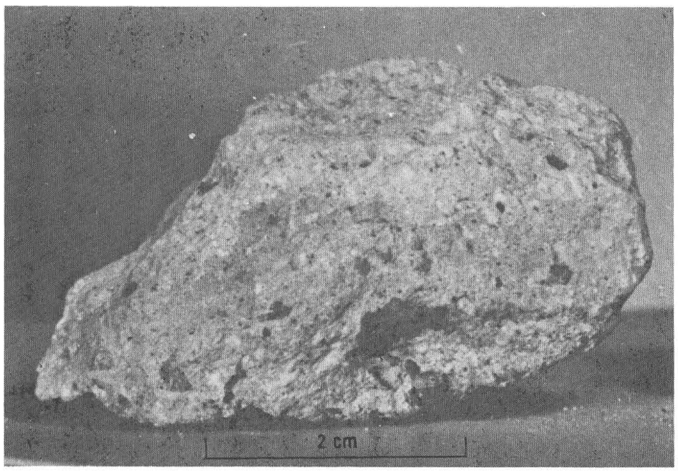

FIGURE 30.—F_3 breccia rock type. Sample 14082. Compare with figures 59 and 60. (Part of NASA photograph S–71–32443.)

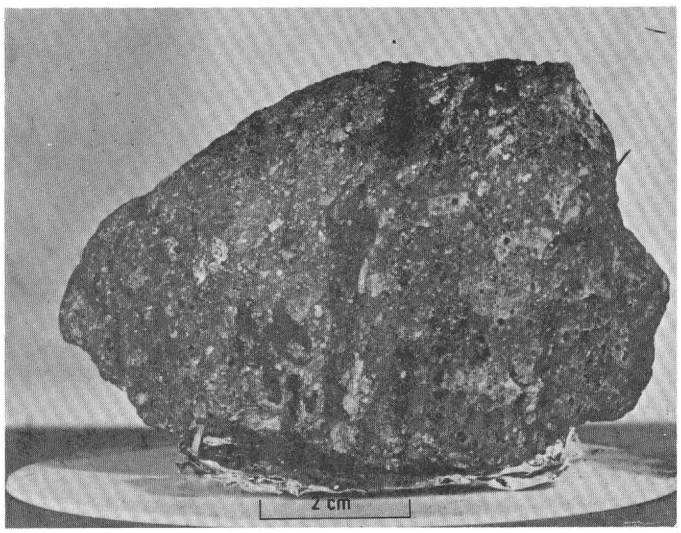

FIGURE 31.—F_2 breccia rock type. Sample 14318. Note zap pits (Z) on surface and dark glass coating (G) near lower center. Compare with figures 74 and 76. (Part of NASA photograph S–71–22016.)

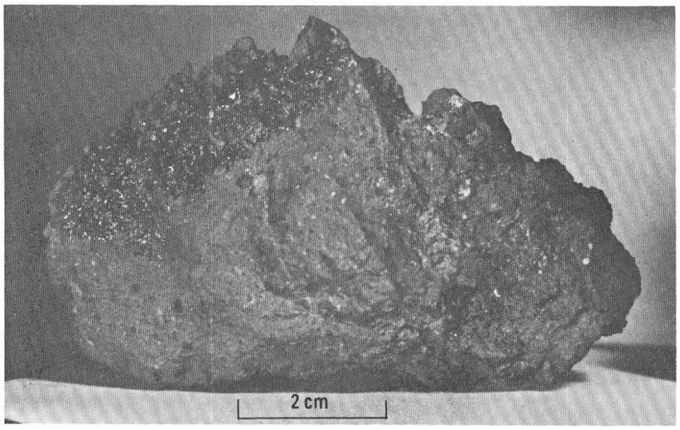

FIGURE 32.—F_1 breccia rock type. Sample 14047. Note glass coating on upper left. Compare with figures 51 and 52. (Part of NASA photograph S-71-21452.)

glass in the matrix and no glass clasts, that melted at a temperature greater than 1,000° C. Nelen, Noonan, and Fredriksson (1972) report that the rock has a fine-grained, quenched texture, and Helz (1972) reports a cooling regime similar to that of sample 14053. Helz's additional observation of dark microbreccia rimming parts of 14068, together with its similarities to 14053, suggests that if Schürmann and Hafner's interpretation is correct, sample 14068 may also have been quenched in a cold (presumably pre-Fra Mauro) regolith, part of which annealed to the rock to form the dark microbreccia. The chemical composition of the major elements of the microbreccia (Helz, 1972) is similar to the average composition of Apollo 14 fines (Compston and others, 1972a). This supports the hypothesis that 14068 may have been quenched in the pre-Fra Mauro regolith, but only if the pre-Fra Mauro regolith, probably formed from ejecta from other large basins, is similar in composition to the present regolith on the Fra Mauro.

If these two samples do represent material from the pre-Fra Mauro regolith, they probably were ejected from a crater large enough to penetrate to the base of the Fra Mauro Formation, and later ejected from Cone crater. An exposure age of up to 30 m.y. based on the $^{38}Ar/^{37}Ar$ ratio has been reported for sample 14053 (Turner and others, 1971). This is consistent with other ages reported for the Cone crater impact and suggests that if the rock were excavated by a pre-Cone crater event, then it was reburied, presumably by ejecta from the same event. No exposure age has been reported for sample 14068 that we know of.

Sample 14072, collected at station C′, was studied in detail by several investigators, and is reported by Bence and Papike (1972), Longhi, Walkder, and Hayes (1972, p. 131), and Steele and Smith (1972, p. 973) to be similar in texture and mineralogy to sample 14053 and to several Apollo 12 basalts.

The ^{40}Ar–^{39}Ar age given for sample 14053 (Turner and others, 1971) is 3.93 ±0.05 b.y., which is consistent with the age of formation of the Imbrium basin (see for example Nyquist and others, 1972). Compston and others (1972a), on the basis of a rubidium-strontium age suggest that sample 14072 could have a crystallization age as great as 4.06 b.y., and York, Kenyon, and Doyle (1972), on the basis of a ^{40}Ar–^{39}Ar age, suggest that 14072 may have crystallized 4.04±.05 b.y. ago. It is not clear, however, to what extent the radiogenic clocks were reset by the Imbrium event (see for example Compston and others, 1972a), and age variations of Fra Mauro materials that range from the age of the Imbrium event to some earlier period of time are to be expected. The composition and radiogenic ages of samples 14053 and 14072 are evidence of the existence of mare-type basalts in the Imbrium target materials before the basin formed.

Although there appears to be general agreement among various workers that the F_1 breccias of Wilshire and Jackson are regolith or soil breccias (Chao and others, 1972; Warner, 1972), there is some disagreement as to the origin of some following F_2 breccias. Chao, Minkin, and Best (1972), Quaide and Wrigley (1972), and Floran, Cameron, Bence, and Papike (1972) all interpret sample 14313 to be a soil breccia. Juan, Chen, Huang, Chen, and Wang Lee (1972), however, suggest that the presence of undeformed glass spherules in the sample indicates that it was not formed by shock lithification. Von Englehardt, Arndt, Stoffler, and Schneider (1972) and Quaide and Wrigley (1972) interpret sample 14318 to be a soil breccia.

This could shed some doubt as to the existence of the F_2 unit of Wilshire and Jackson by suggesting that what they interpret as F_2 breccias, as well as the F_1 breccia, are actually soil breccias formed in regolith that was derived from the Fra Mauro Formation. However, as Wilshire and Jackson point out, the clast population of the F_2 breccias is markedly different from that of the dominant F_4 breccias, which indicates that the F_2 breccias could not be derived from an F_4 breccia parent. The difficulty probably lies in distinguishing soil breccias derived from F_2 breccia from the parent F_2 breccia itself.

Sample 14305, an F_4 breccia, lies on the north edge of a small, sharp, irregular depression that appears to have been formed by impact of rock 14305, the lower southwest edge of the rock having formed the major part of the depression (fig. 33). The vertical southwest edge of the rock appears to have formed the northeast-trending, grooved part of the depression as the rock slid to the northeast. A small fillet approximately 1 cm deep lies against the southeast edge of the rock, as

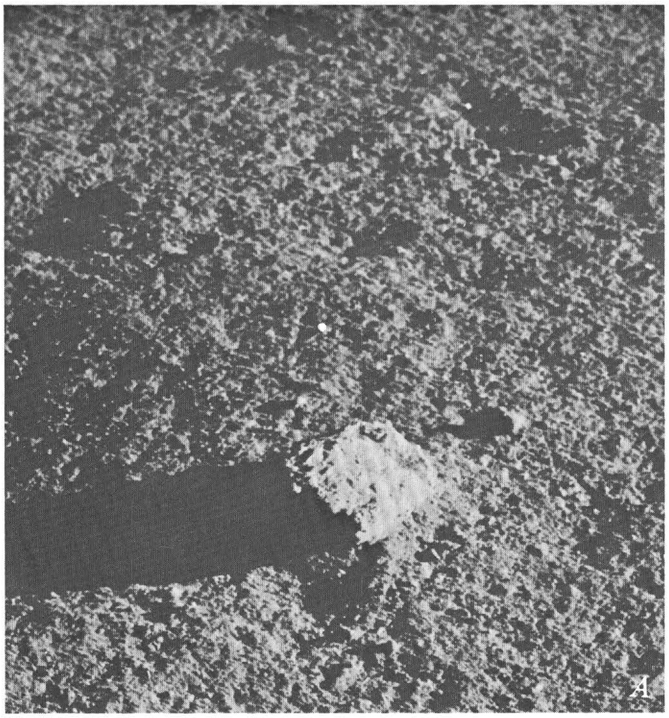

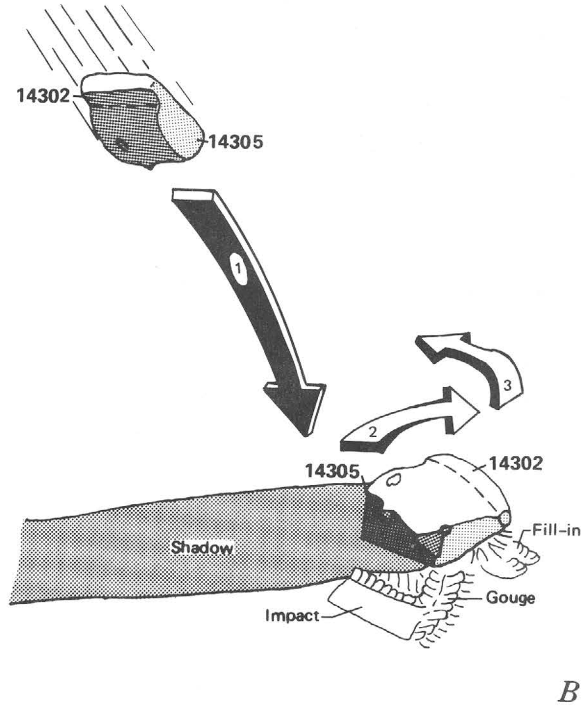

FIGURE 33.—Sample 14305. *A*, Shown before collection. Compare with figures 66 and 67. (Part of NASA photograph AS14–67–9393.) *B*, Diagram showing the possible route taken by the fragment to reach the position shown in *A* (Swann and others, 1971).

though the rock dug into the fine-grained surface material as it slid into the present position. The fillet partly fills the northwest side of two 3-cm raindrop depressions, which indicates that the fillet material moved away from the rock rather than toward it; such would be the case if the material were pushed out by impact of the rock rather than banked against the rock. The freshness of the crater formed by the rock and the angularity of the crater edges suggest that the rock has been in this position for a relatively short period of time. Features as small as the two raindrop depressions, which were formed before emplacement of 14305, should be destroyed in less than 10^6 yr (Shoemaker and others, 1970); yet they are still very sharp and fresh in appearance. Eldidge, O'Kelley, and Northcutt (1972) infer from exposure ages in the 10–20 m.y. range reported by Lunar Sample Preliminary Examination Team (1971) that the rock may have originated from Cone crater. If so, it probably has a complex history of transport and landed in its present position considerably more recently than the Cone crater event.

BOULDERS

Boulders at the Fra Mauro site provided the first opportunity to study the textures and fabrics of lunar bedrock. The fragmental nature of all of the boulders is evident in the photographs. Clasts from the limit of resolution (about 1 cm) up to 10 cm across are abundant, and the top of Layered rock near station C′ is interpreted to be a clast about 1.7 m across. Because the boulders are randomly oriented with respect to their original bedrock position, directional features mostly are referred to as left and right, top and bottom, with respect to the photograph; angles unless otherwise specified are with respect to the average ground surface.

In some of the boulders distinct lithologic layers are evident, whereas in others, evidence for lithologic differences between layers is subtle or absent. Parting planes that are interpreted as layers or bedding are referred to as S_a planes and are shown on the maps of the boulders as dashed lines. Some of the boulders have other moderately to well developed systematic sets of partings that are referred to as S_b, S_c, and S_d planes. No sequence of development is implied by the letter subscripts of the S-planes, except that S_a (bedding) is interpreted to be the oldest of the S-planes. A variety of less systematic, mostly curved fractures are also present in some of the boulders.

Most of the boulders are rounded and completely covered by zap pits as large as 1 cm across. Some of the boulders have knobby surfaces; others have subplanar surfaces. The relative size of boulders described below is shown in figure 34.

WEIRD ROCK

Weird rock (fig. 35), at station F, is about 2.5 m across at the base and protrudes about 1.5 m above the

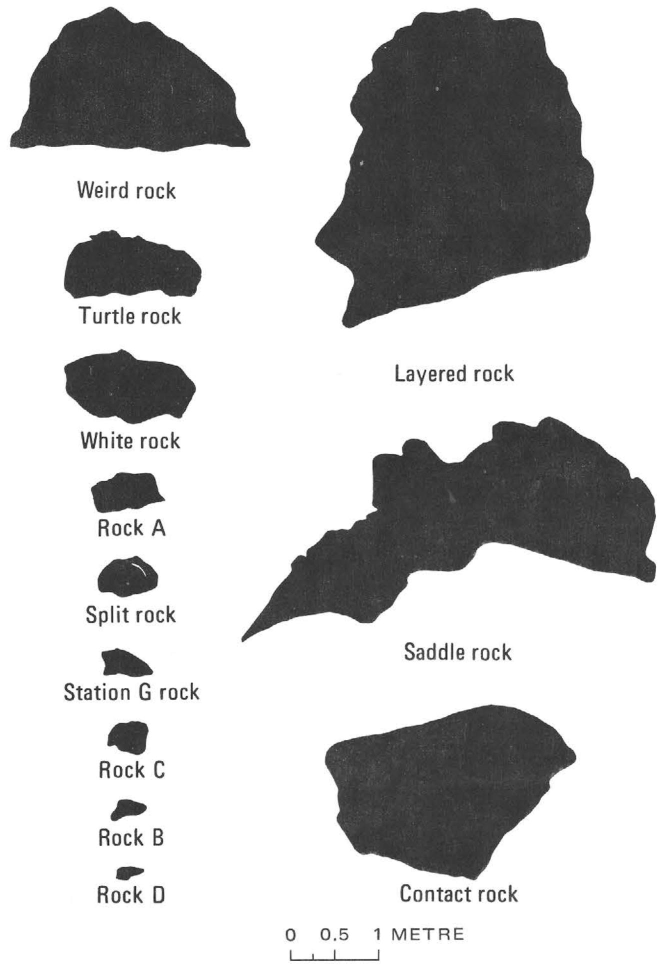

FIGURE 34.—Relative sizes of boulders.

ground surface. Its surface varies from subrounded to subangular and is hackly to knobby on a scale of about 10 cm.

The exposed lower 40 cm of the boulder has a pronounced set of approximately horizontal partings that is considered to be bedding (S_a). This set of partings is present, but weakly developed, in the upper part of the boulder. The lower part of the boulder, in the area of well-developed horizontal partings, contains two, and possibly three, relatively large clasts that are not crossed by the horizontal partings. A second set of partings (S_b) that dips to the right pervades the entire boulder, including the three clasts. A third set (S_c) that dips to the right is poorly developed in the upper part of the boulder.

The horizontal set is interpreted as partings along bedding planes developed in fine matrix material which was deposited simultaneously with the clasts in the lower part of the boulder. The matrix is not draped around the clasts, which indicates that differential compaction between the matrix and clasts has not taken place. Some of the clasts in the samples are crushed (Wilshire and Jackson, 1972), which suggests that the clasts in the boulder also may have been compacted along with the matrix material.

STATION H CLUSTER

A small blocky area photographed in the North Boulder Field contains four boulders with well-developed parting sets (fig. 36). Rocks A and B (figs. 37, 38) are subangular, with planar faces on their tops that appear to have been broken along the planes labeled S_a. Rocks C and D (figs. 39, 40) are subrounded and more knobby and irregular in shape. The differences in shape and rounding between A and B, and C and D, probably arise because the S_a planes are better developed in rocks A and B than in C and D. Three other parting sets are visible in rock A and are labeled S_b, S_c, and S_d in figure 37. Rock D has a second parting set labeled S_b in figure 40. Rocks B and C appear to have only one parting set; the other fractures appear to be randomly oriented (figs. 38, 39).

The S_a partings in rocks A and B are subhorizontal sets that are parallel to a well-developed alinement of light-colored tabular clasts (1–5 cm in long direction) (figs. 37 and 38). The tabular alinement of the clasts is interpreted as resulting from preferential orientation during deposition, and the partings therefore depict bedding planes. Rocks C and D have only a suggestion of tabular alinement of clasts. The alinement is parallel to fairly well-developed parting sets that also are interpreted as bedding planes.

The angle between the poles of the S_a and S_b planes of rocks A and D is approximately 60°. This suggests that the S_b planes of both rocks may have a common origin.

TURTLE ROCK

Turtle rock, approximately 1.5 m across (fig. 41), is the largest boulder in a field of rocks at station H. Two loose rocks (samples 14312 and 14319) were collected from the upper surface of Turtle rock and two chips (one identified as sample 14314) from the fillet adjacent to the boulder. The rock is subrounded, with a somewhat hackly surface. The discontinuous, subplanar surfaces on top of the rock are probably controlled by fractures.

Turtle rock contains abundant centimetre-size clasts; a few clasts are as large as 10 cm in an unresolvable matrix. The clasts are dark gray to white; most are approximately equant, but tabular, ellipsoidal, and contorted forms are common. Many of the white clasts are in depressions, which suggests that they may be softer and less resistant to erosion than the matrix. The surface of Turtle rock is covered with zap pits that generally range in diameter from a centimetre down to the limit of photographic resolution (about 2 mm). Several circular depressions as large as 4 cm in diameter may also be impact pits.

A moderately well developed but faint set of subparallel, discontinuous partings (S_a in fig. 41) are interpreted as bedding planes. Commonly they appear to abut against both sides of clasts along a line, but they do not cut across the clasts. There is some tendency toward convergence and divergence of the planes, and some planes are slightly curved, suggesting weakly developed crossbedding.

The other partings in the rock appear to be randomly oriented, and only one, a large fracture extending from the "turtle" to the ground, was mapped. Some of the fractures near the top of the rock appear to be spall fractures caused by micrometeorite bombardment, and their attitudes appear to be partly controlled by the bedding planes.

STATION G ROCK

An unnamed rock in the documentation photographs for sample 14306 (fig. 42) appears to be a medium-gray breccia with medium- to dark-gray clasts dominant and with sparse light clasts. The rock is subangular, with a knobby to hackly surface.

Two well-developed sets (S_a and S_b) and one poorly developed (S_c) set of partings are present (fig. 42). A planar face on the lower left part of the rock appears to be an S_a plane, and another, on the top left (not visible in the figure) appears to be an S_b plane. The S_a partings appear to be the most uniformly developed, and there is a faint suggestion of alinement of dark clasts parallel to these planes; it is upon these rather weak lines of evidence that this set is interpreted as bedding planes.

WHITE ROCKS

The White rocks at station C1 are the largest boulders examined by the astronaut crew. They exhibit a wide variety of structures and features. Four of the largest in the White rocks group were studied and named: White rock, Saddle rock, Layered rock, and Contact rock. Sample 14082 was chipped from White rock, the only rock in the group that was sampled. The rocks are categorized from photographs on the basis of light and dark rock types, as shown in figure 43.

Saddle rock is dominantly light with dark patches. Layered rock is the darkest of the group. Contact rock is approximately half light and half dark, and White rock (hidden in figure 43) is dominantly light. The major rock types within the light and dark groups are summarized in table 3.

The boulders contain a variety of planar surfaces including layering and closely spaced parting sets and large, well-defined fractures that appear to crosscut the layering. The general patterns of the traces of the partings on the rock surfaces are shown in figures 44 and 45.

White rock (figs. 45, 46) at the east side of White rocks boulder field, is about 1.25 m long in an east-west direction. It has a rather blocky shape and appears to be predominantly of one rock type, except for a prominent dark clast in its near end in figure 46. Two nearly orthogonal sets of widely spaced but well-developed planar surfaces are visible, but it is not apparent whether these surfaces represent layering or joints.

Saddle rock (figs. 44, 45), at the north end of the White rocks boulder field, is about 4.5 m long in its north-south direction. The rock has an irregular surface with dark hackly patches and resistant pinnacles. The crest line forms nearly a right angle toward the northwest, which may reflect internal structural control. Saddle rock shows evidence of at least three sets of planar surfaces. The most prominent surface, which is interpreted as layering, or S_a, is inclined to the right and is generally expressed as a series of parallel indentations and discontinuous ribs. The S_a-plane apparently controls the shape of the east face of the pinnacle that is immediately south of the saddle. The second most prominent set of S-planes, S_b, consists of subvertical fractures that are spaced a few centimetres apart with a north-northeast trend. These are expressed as closely spaced shadow lines inclined to the left crossing the short resistant ribs of the S_a planes. The S_c planes appear to be fine grooves that are traces of planes on the rock surfaces, the poles of which are oriented at about 70° to the poles of the S_b planes. Other fractures in Saddle rock appear to be curved and randomly oriented.

Layered rock (figs. 23, 44, 45), at the west end of White rocks boulder field, is approximately 3 m long and 2 m high. The upper three-fourths of the exposed part of the rock is composed of dark fragmental material, and the lower one-fourth is a layer of light material. The upper one-fourth of the rock has a knobby surface texture, and the lower three-fourths has an irregular, hackly surface texture. The light layer in the lower part appears similar in tone and texture to the light layer in White rock, and its composition may be represented by sample 14082 from White rock. The upper part of the rock is interpreted to be a clast about 1.7 m long, which in turn is dominated by clasts 30–40 cm long. Small light-colored spots are interpreted to be clasts within the 30–40 cm clasts. If this interpretation is correct, the 1.7-m clast is the largest recognized at the Fra Mauro site.

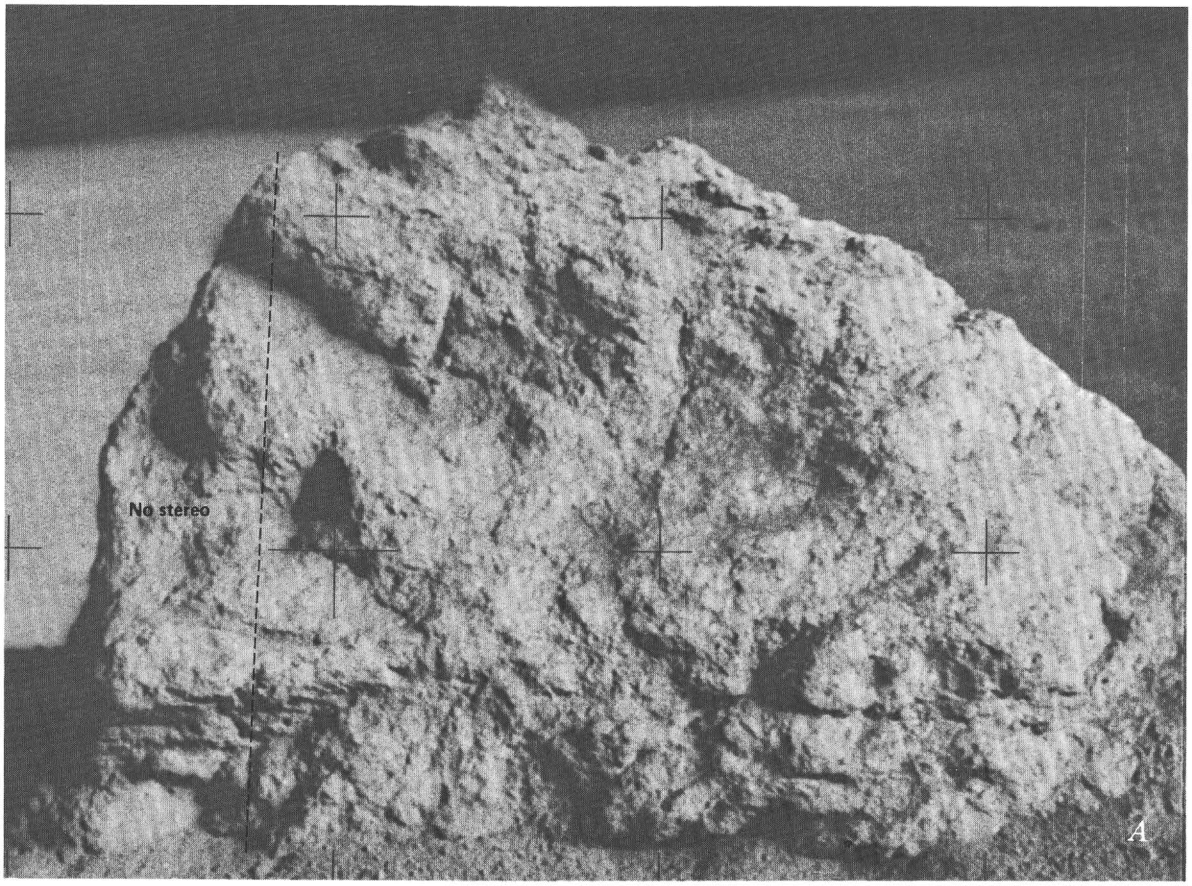

FIGURE 35.—Weird rock. *A*, View from the south. (NASA photograph AS14–64–9135.)

The rock may therefore represent three cycles of brecciation and deposition: (1) the formation and induration of fragmental debris that makes up the 20–30-cm clasts; (2) the formation and induration of fragmental debris that makes up the 1.7-m clast; and (3) the formation and induration of fragmental debris that makes up the entire rock and that gives it its layered appearance.

Contact rock at the south end of the field is approximately 3 m long in its north-south direction. The upper part of the rock is rounded and knobby, and the lower, lighter part is angular. The most striking feature is the irregular contact between the dark upper part and the lighter part below (figs. 19C, 44, 45). The light layer contains what appear to be fine fractures or possibly thin layers subparallel to the contact in the rock; these may represent parting planes along layering (S_a). Irregularities of the contact between the layers are similar in appearance and scale to layers within the ejecta blanket of Meteor Crater (fig. 47), as described by McCauley and Masursky (1969).

Contact rock is the only boulder of the four described that does not have a well-developed fillet. It rests in a depression with a slightly raised rim; the rim appears to have been made by impact of the rock with the surface. This suggests that the rock has not been in its present position for as long as the other boulders in the group, and that although the rock was originally ejected from Cone crater, it has been moved after the Cone crater event. The angularity of the lower part of the rock also suggests that this part of the rock has not been exposed to erosion for a long period of time. Contact rock is probably a large spall from a boulder that was struck by a meteorite and broken. It may have been broken from Layered or Saddle rock, and its original position may have been between Layered and Saddle rocks (figs. 44 and 45). The only other likely origin is that it was ejected from the 30-m crater at station C′. The rock is about two crater diameters away from this crater and appears rather large to have been ejected this far by such a small event.

SPLIT ROCK

At station C′, a boulder has broken into two large pieces (fig. 48). This well-rounded boulder, along with others in the strewn field, was probably ejected from Cone crater. The edges of the fracture that separates the boulder pieces are sharp. The rounding of the boul-

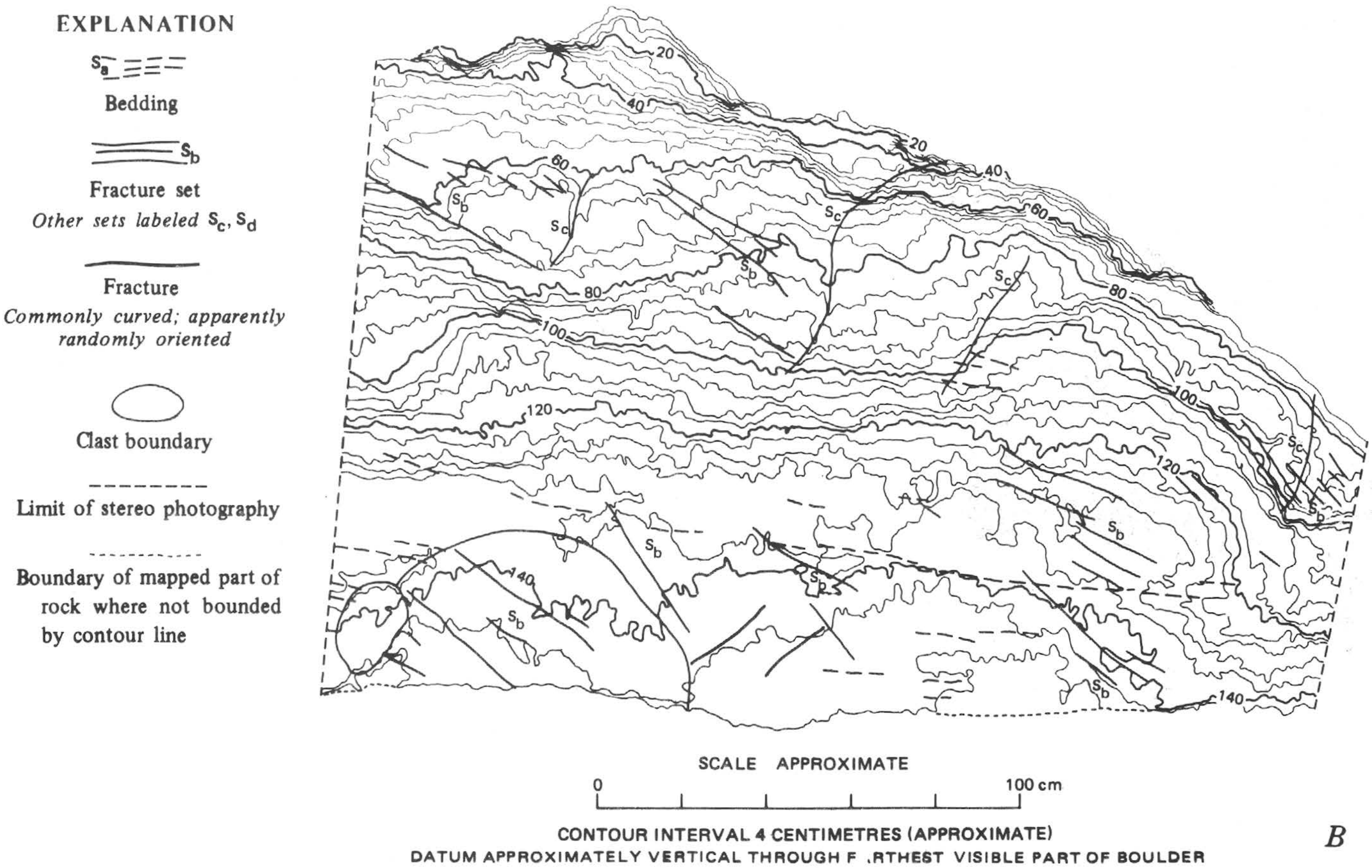

B, Topographic map showing fracture surfaces. Topography drawn by Raymond Jordan from NASA photographs AS14–64–9135, 9136.

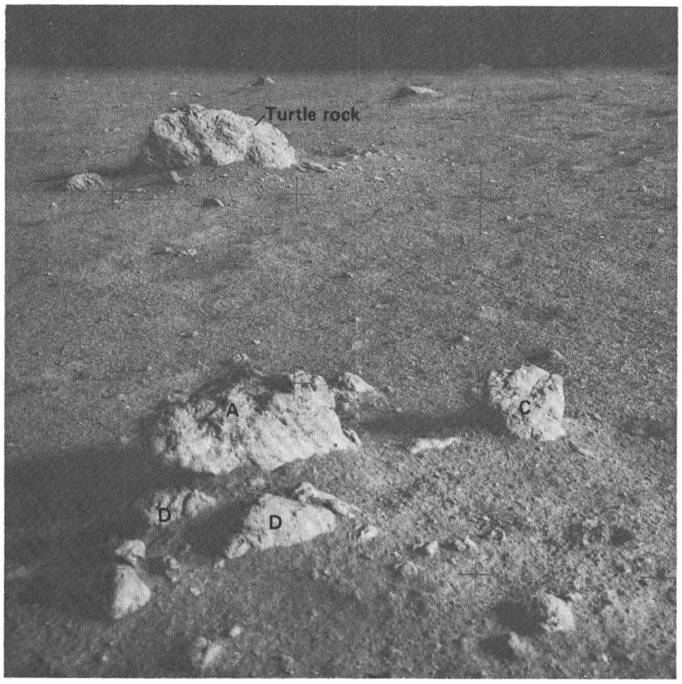

FIGURE 36.—North Boulder Field cluster (station H area). Letters refer to rocks in figures 37–40. (Part of NASA photograph AS14–68–9471.)

der is similar to that of most of the other boulders on the Cone crater ejecta blanket and probably occurred after the boulder was ejected from the crater. The sharpness of the fracture, however, suggests that the fracture is relatively recent and formed long after the boulder assumed its present rounded form. This type of fracture is probably caused by meteorite impact.

DISCUSSION

All the boulders whose surface textures and internal structures are visible in the photographs appear to be clastic rocks of impact origin. Layering, which is expressed as irregular compositional banding, alinement of tabular clasts, and regular fine-scale partings, is probably depositional layering and can be discerned on the photographs with varying degrees of certainty. Smaller scale layering in samples is reported by Wilshire and Jackson (1972) and is interpreted as primary layering from the Imbrium event. The layering therefore is the earliest structure recognizable in the boulders, and the other planar elements are interpreted as post-depositional fractures.

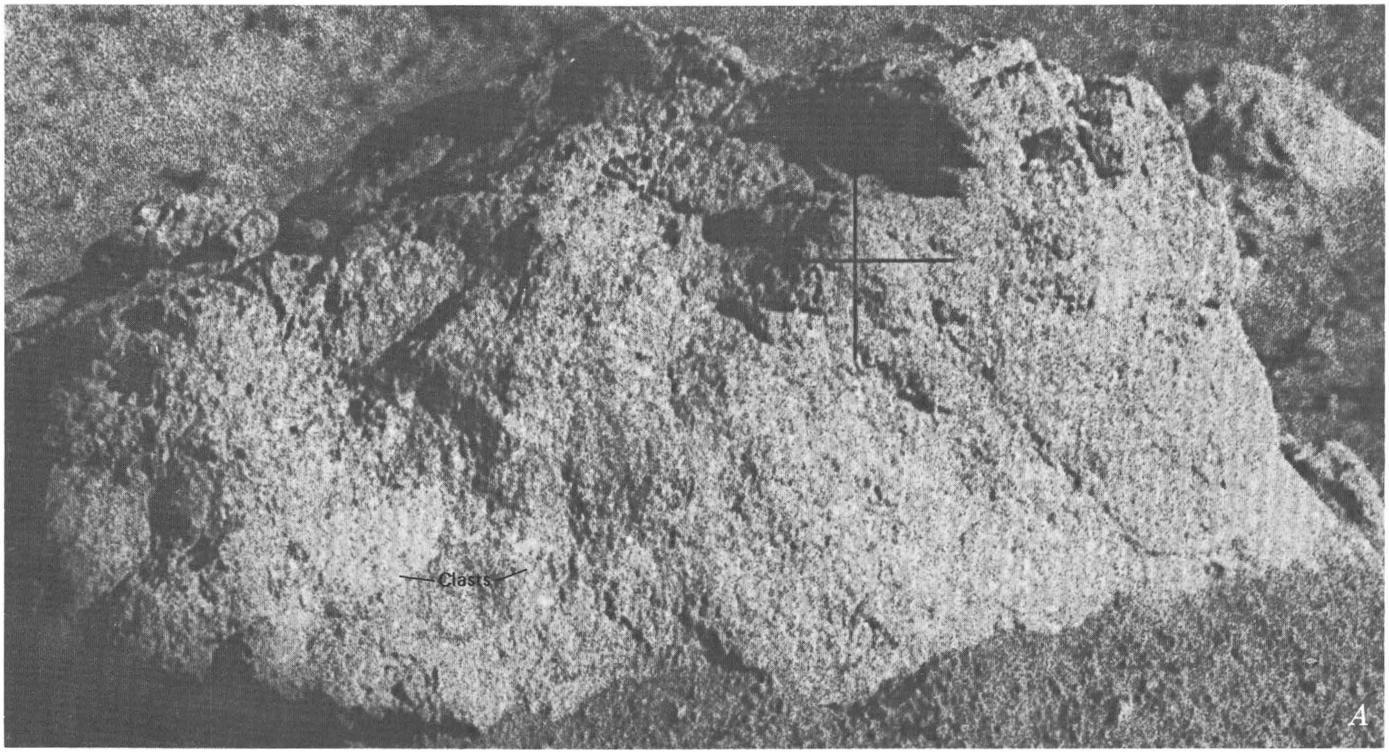

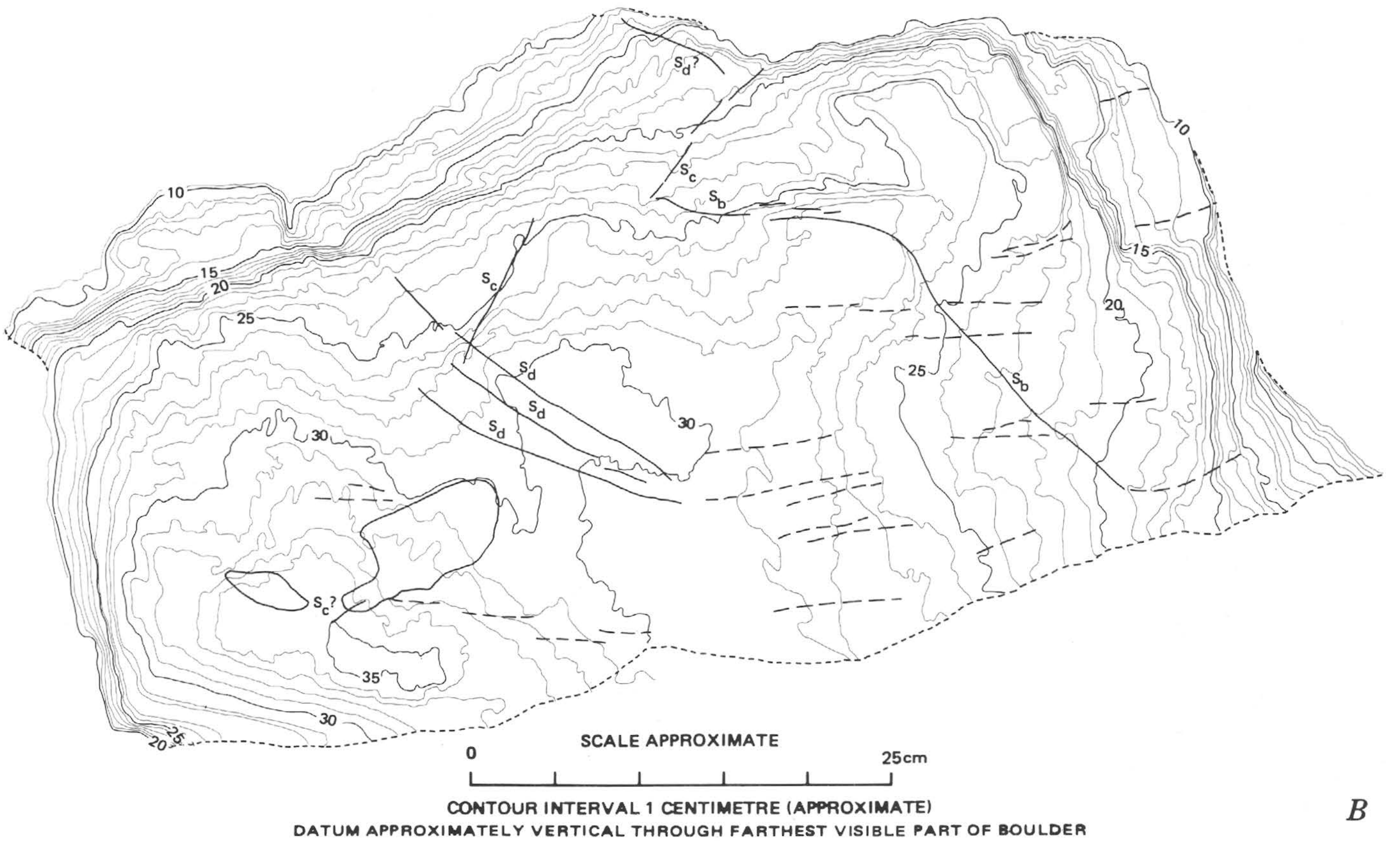

FIGURE 37.—Rock A in North Boulder Field cluster. *A*, View from south. Note alined light-colored tabular clasts. (Part of NASA photograph AS14–68–9468.) *B*, Topographic map showing relation of fractures and bedding. See figure 35 for explanation of symbols. Topography drawn by Raymond Jordan from NASA photographs AS14–68–9468, 9469.

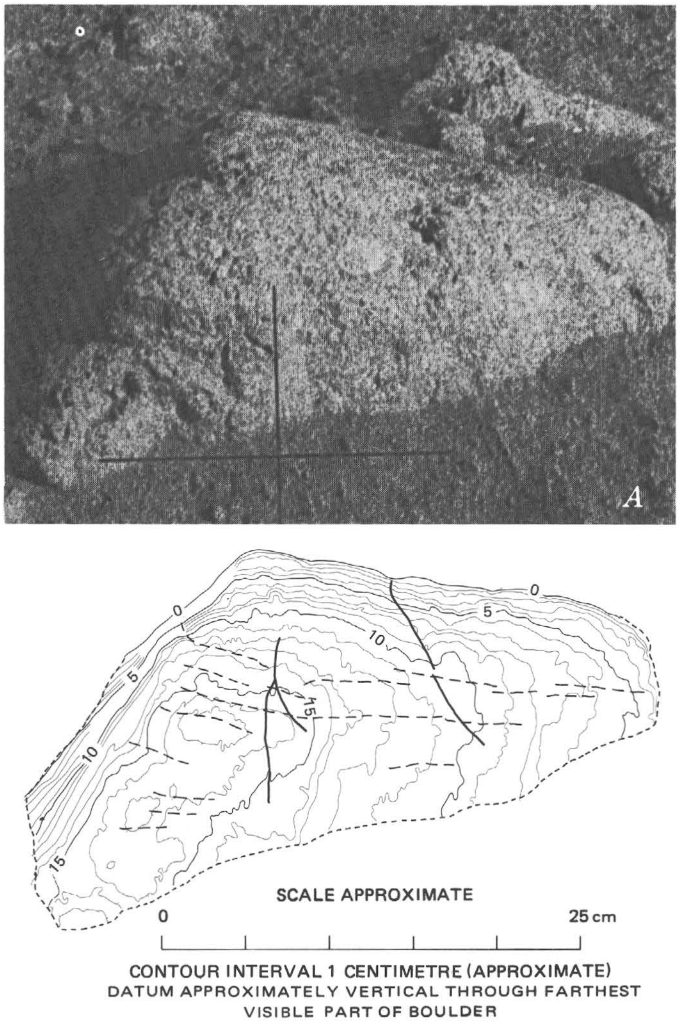

FIGURE 38.—Rock B in North Boulder Field cluster. *A*, View from south. Note alined light-colored tabular clasts. (Part of NASA photograph AS14–68–9468.) *B*, Topographic map showing relation of fractures. See figure 35 for explanation of symbols. Topography drawn by Raymond Jordan from NASA photographs AS14–68–9468, 9469.

These late fractures may be—

(1) Tensional joints formed by cooling after deposition of the ejecta from the Imbrium basin.

(2) Fractures that were formed in bedrock by Imbrian and Eratosthenian cratering events, especially from those Eratosthenian craters that occur near Cone crater (pl. 1).

(3) Fractures caused by the Cone crater event. It appears unlikely, however, that any one fracture or fracture set can be related with certainty to the Cone crater event from photographic evidence alone.

(4) The result of impacts that occurred after the rocks were brought to the surface by the Cone crater event. Several of the boulders such as Split rock, and possibly Layered and Contact rocks, appear to have been broken by meteorite impact long after being emplaced by the Cone crater event. Irregular fractures along the surfaces of rocks such as Turtle rock appear to be spall fractures caused by fatigue from repeated bombardment of micrometeorites, or possibly by diurnal thermal expansion and contraction. These spall fractures appear to be controlled to some extent by preexisting partings.

The fine matrix material of the boulders was probably produced by comminution caused by the Imbrium impact (Wilshire and Jackson, 1972). The largest probable clast is the 1.7-m one in the upper part of Layered rock. This indicates that the size of fragments that were ejected from the Imbrium basin at this distance from the impact ranged from below the limit of microscopic resolution to at least 1.7 m across.

SUMMARY OF CONCLUSIONS

At the Apollo 14 site, the Fra Mauro Formation consists of ejecta from the Imbrium basin. The upper 65 m is layered fragmental rock, some of which may have been derived from pre-Imbrian clastic rocks. Some of the pre-Imbrian cratering history therefore may be recorded in the multiple breccias of the Fra Mauro Formation. It also appears that some mare-type basalts existed in the area of the Imbrium basin before the basin formed.

The regolith in the Apollo 14 site is typically about 8.5 to 9.5 m thick, but on surfaces as old as that of the Fra Mauro Formation, areas with anomalously thick regolith are probably accumulations of fragmental debris that fill old craters. Comparison of regolith thicknesses at all Apollo landing sites shows that the rate of regolith formation fell off rapidly from about 3.7 to 3.4 b.y. ago. This agrees with other lines of evidence shown by other workers that the flux of meteorites decreased markedly during this time. After about 3.4 b.y. ago the growth rate of the Moon by accretion was probably insignificant.

The character of the regolith surface is an indicator of relative age, or maturity, of the surface. Young ejecta from craters tends to be ridgy, and as it matures it tends toward a morphology of coalescing closed depressions. Materials exposed at the lunar surface tend to darken with age, and variations in the albedos of surfaces of different ages are measureable at the Fra Mauro site. The albedos correlate with morphologic ages.

The slopes of cumulative size-frequency distribution curves for fragments increase with the age of the sur-

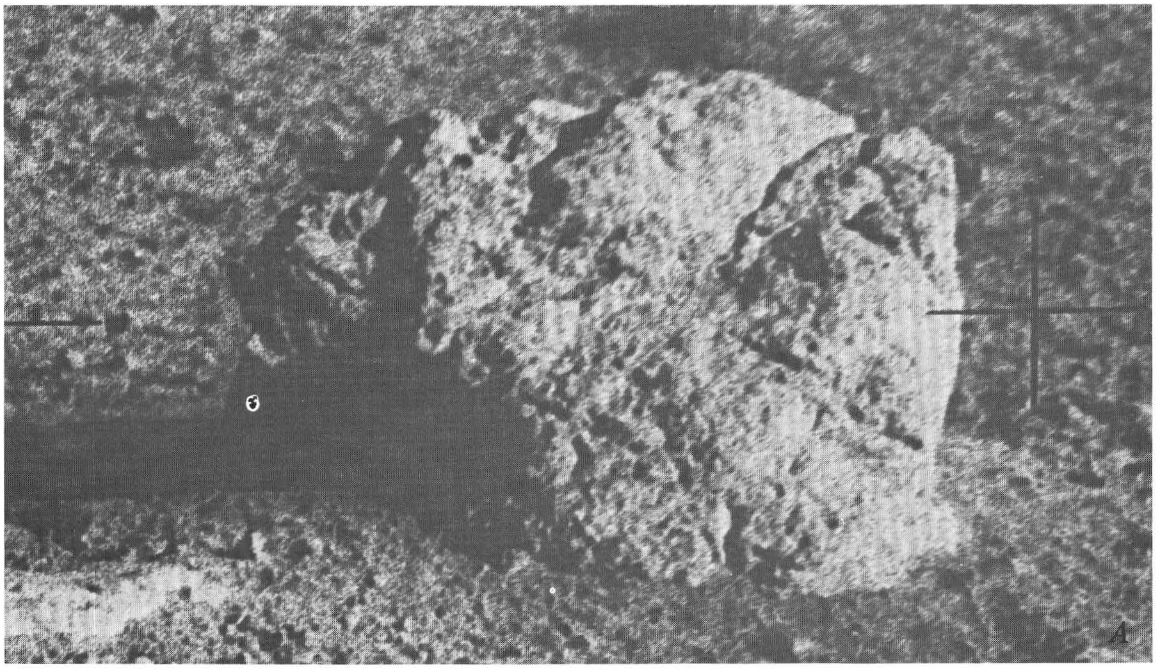

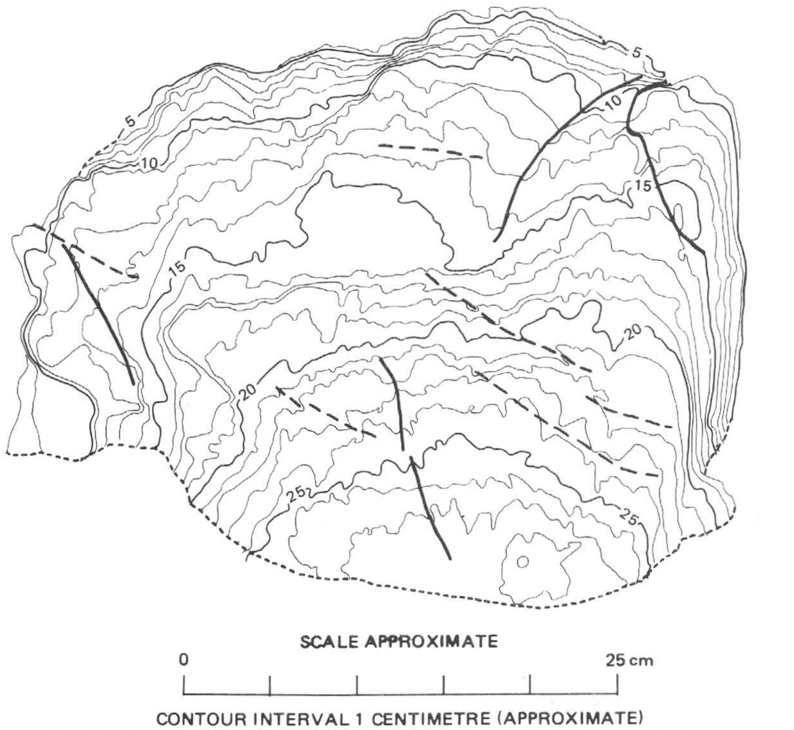

FIGURE 39.—Rock C in North Boulder Field cluster. *A*, View toward north. (Part of NASA photograph AS14–68–9468.) *B*, Topographic map showing fractures. See figure 35 for explanation of symbols. Topography drawn by Raymond Jordan from NASA photographs AS14–68–9468, 9469.

face. This is because large rocks are eroded by meteorite impact with a resulting increase in the number of smaller rocks. At about 6×10^5 to 1×10^6 fragments per 1000 m^2, a steady-state is reached at about a 1-cm fragment size, which indicates that fragments of this size are formed by shock-induration of fine regolith materials at about the same rate that the fragments are destroyed by meteorite impact.

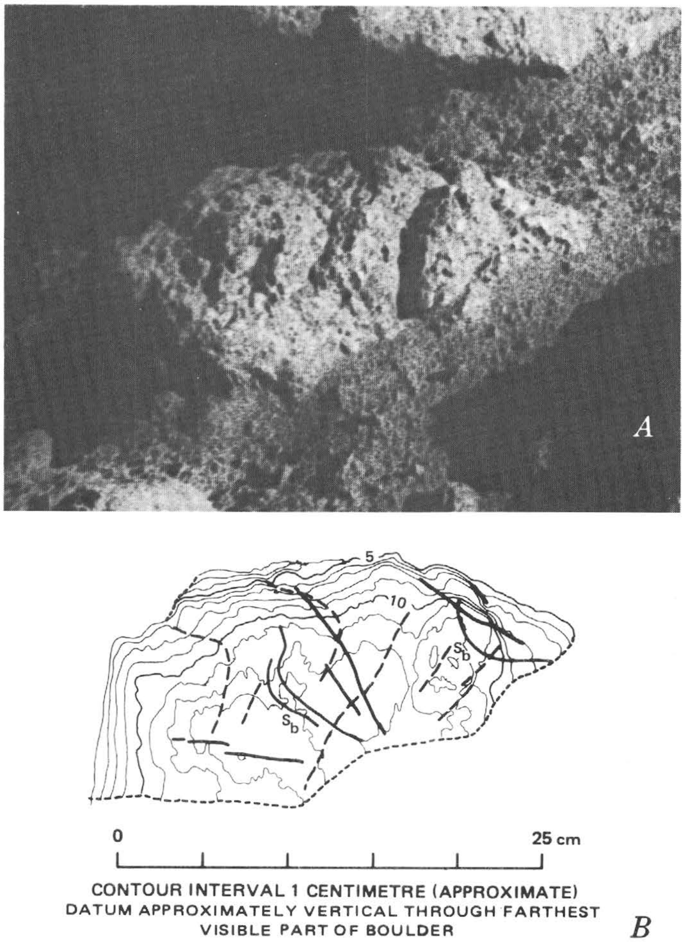

FIGURE 40.—Rock D in North Boulder Field cluster. *A*, View toward north. (Part of NASA photograph AS14–68–9468.) *B*, Topographic map showing fractures. See figure 35 for explanation of symbols. Topography drawn by Raymond Jordan from NASA photographs AS14–68–9468, 9469.

SAMPLE DOCUMENTATION AND ENVIRONMENTS

INTRODUCTION

Sample documentation includes all of the crew's observations and descriptions of samples and sample environments, as well as the lunar surface photographs that show the terrain of the landing site and which are used to determine sample distribution and lunar orientations. Documentation is required to help relate specific samples to the overall geology of the landing site.

This section is divided into two parts. The first includes illustrations of sample environments using selected lunar surface photographs. Samples are covered in sequence by ascending *Lunar Receiving Laboratory* (*LRL*) number. Where known, samples are identified, and insert photographs show the lunar orientation of certain rock samples as reconstructed by oblique lighting in the LRL. In several cases, model casts have been used instead of the actual samples. Orthogonal layouts show the lunar orientation and amount of burial of several samples, using selected photographs taken in the LRL. These photographs, commonly referred to as "mugshots," document the shapes of the samples from all sides.

The second part (tables 4, 5) summarizes all sample documentation, listing sample locations in sequence by traverse station, lunar surface documentary photographs, status of determining sample location and orientation, brief megascopic description of the samples, and comments by the astronaut crew at the time of sample collection (excerpted from the mission transcript). The sample descriptions are based on a very preliminary examination of the rock samples in the LRL, and should be considered analogous to a field description of the rocks that accompanies the crew's comments from the field.

We have tried to relate all the rock samples for which there are lunar surface documentary photographs to the specific and detailed geologic environments where those samples were collected (figs. 49 to 78). The purpose is to show the samples in their lunar settings—their orientations at the time of collection, their amount of burial, and their associations with other rock fragments in the immediate area, and the general charcter of the fine-grained regolith at the sample sites. All of these factors are important in reconstructing the history of any given sample on the lunar surface. It is clear, from samples returned by Apollo 14 and previous missions, that rocks are likely to be tumbled and broken from time to time during their exposure at the lunar surface. The rate of tumbling and regolith gardening may be further defined by studying samples.

Several terms are used in the sketches on the sample documentation photographs and in the tabulated data summarizing sample environments:

Area covered.—Perspective scales are included in most photographs to show distances and sizes of features. Most detail is, of course, seen within 3 m of the camera, and the environmental summaries are limited to the near field of view. The horizon on some photographs may be several kilometres away.

Rock burial and fillets.—Fillets are embankments of fine-grained material against rocks on the surface, and are discussed on pages 20–22 in this report. Burial refers to the amount of rock that is below the average ground surface, exclusive of the fillet.

Color.—Colors are interpreted from lunar surface photographs and from LRL sample photographs. They are subjective only and are mostly limited to relative

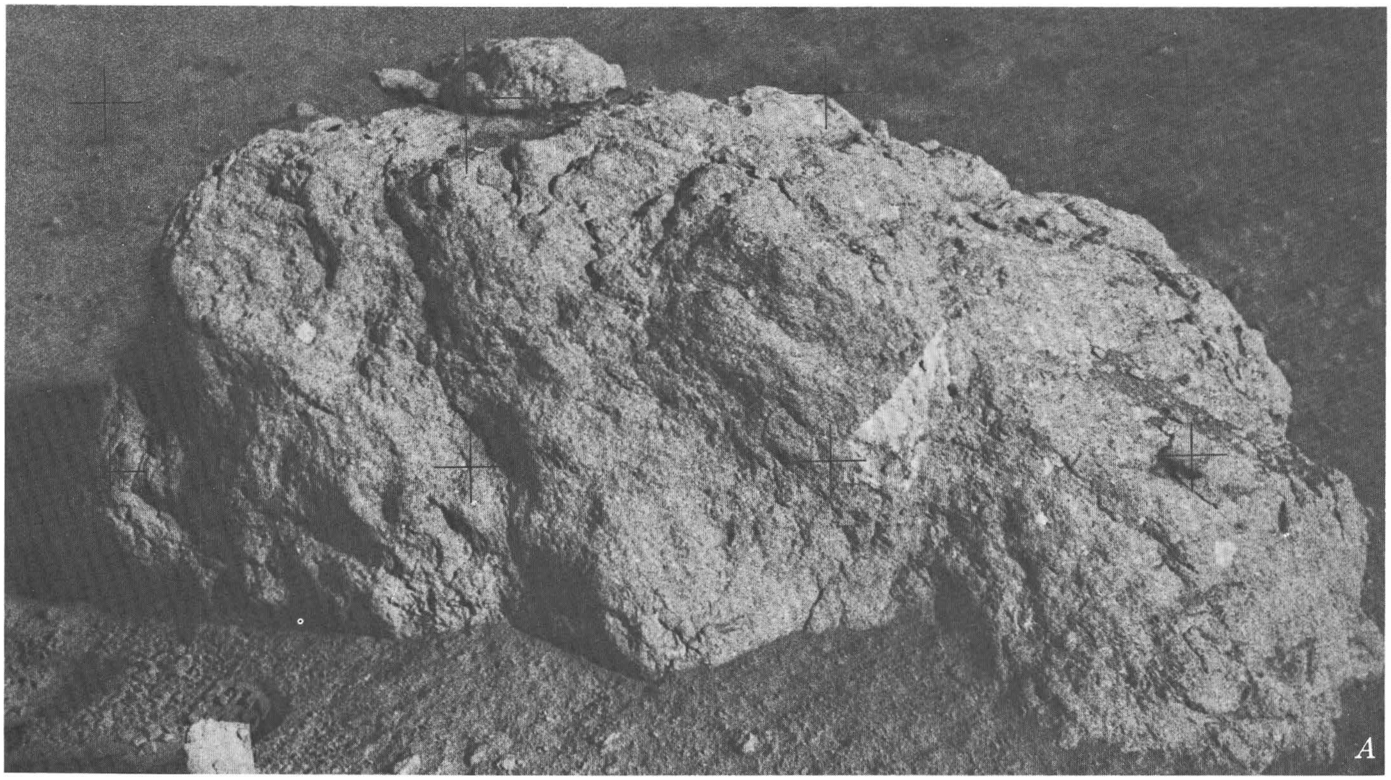

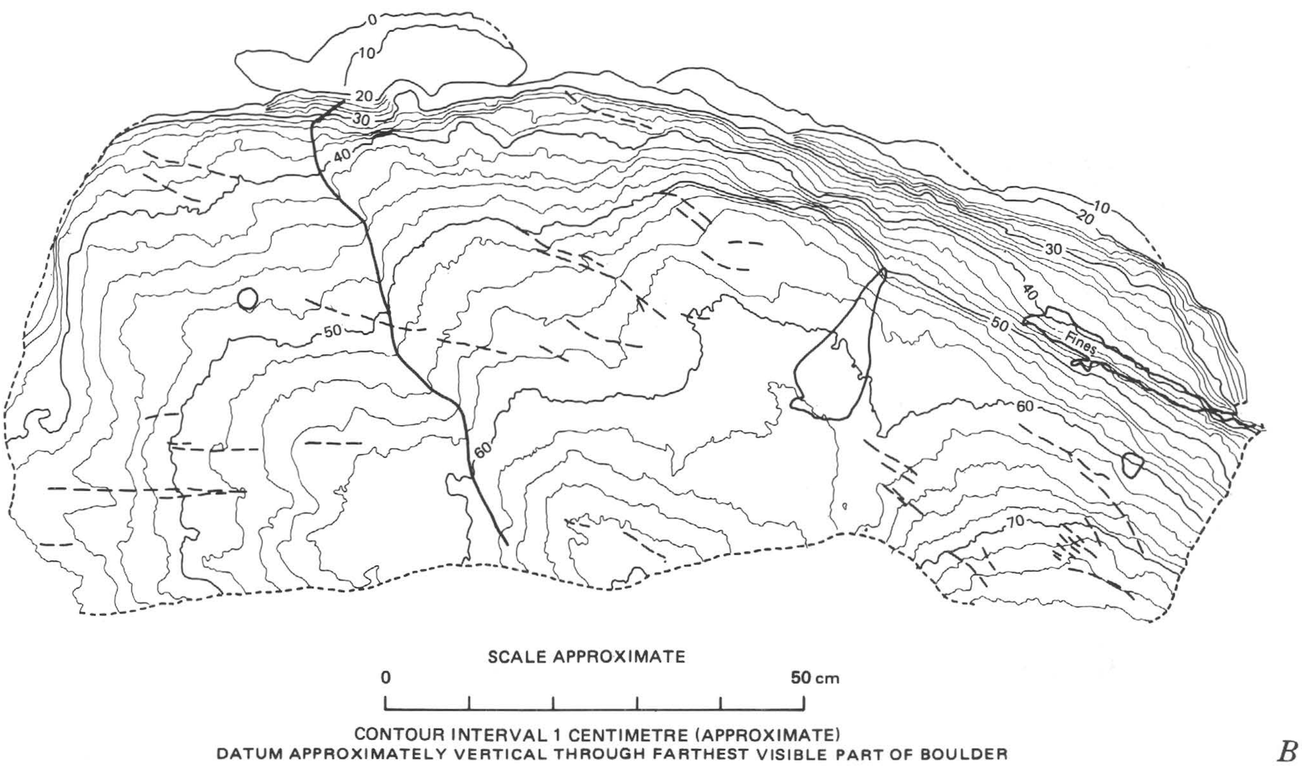

FIGURE 41.—Turtle rock. *A*, View toward north (note white clasts). (Part of NASA photograph AS14–68–9476.) *B*, Topographic map showing fractures and clasts. See figure 35 for explanation of symbols. Topography drawn by Raymond Jordan from NASA photographs AS14–68–9474, 9475.

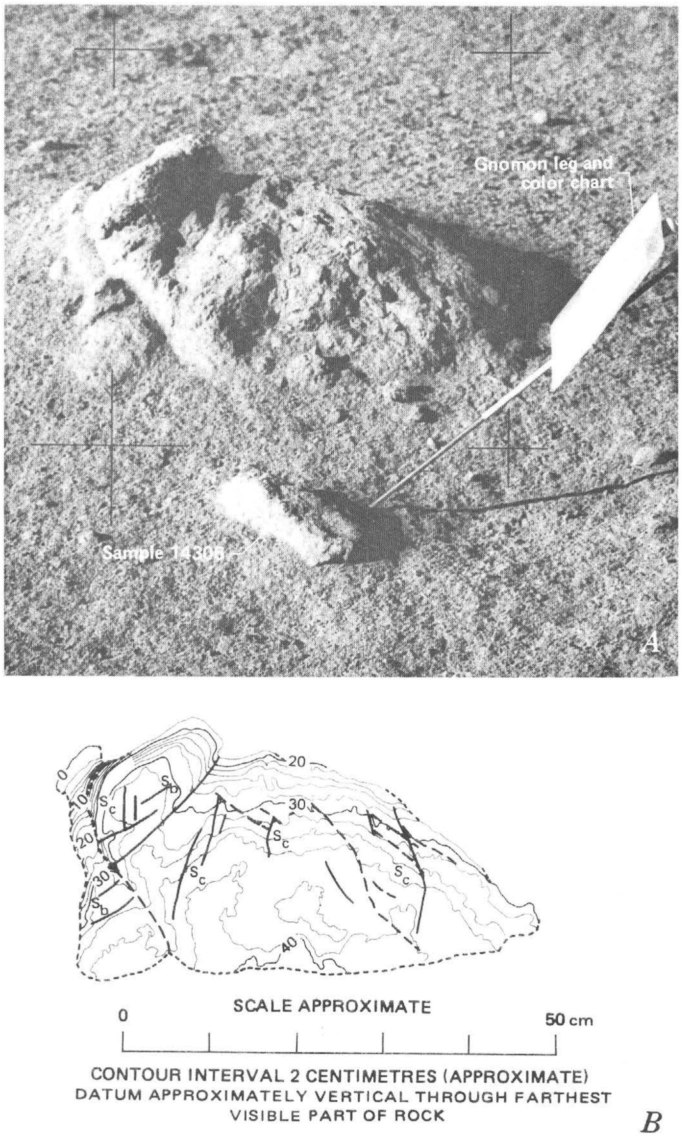

FIGURE 42.—Station G rock. *A*, View toward south. (Part of NASA photograph AS14–68–9461.) *B*, Topographic map showing fractures. See figure 35 for explanation of symbols. Topography drawn by Raymond Jordan from NASA photographs AS14–68–9460, 9461.

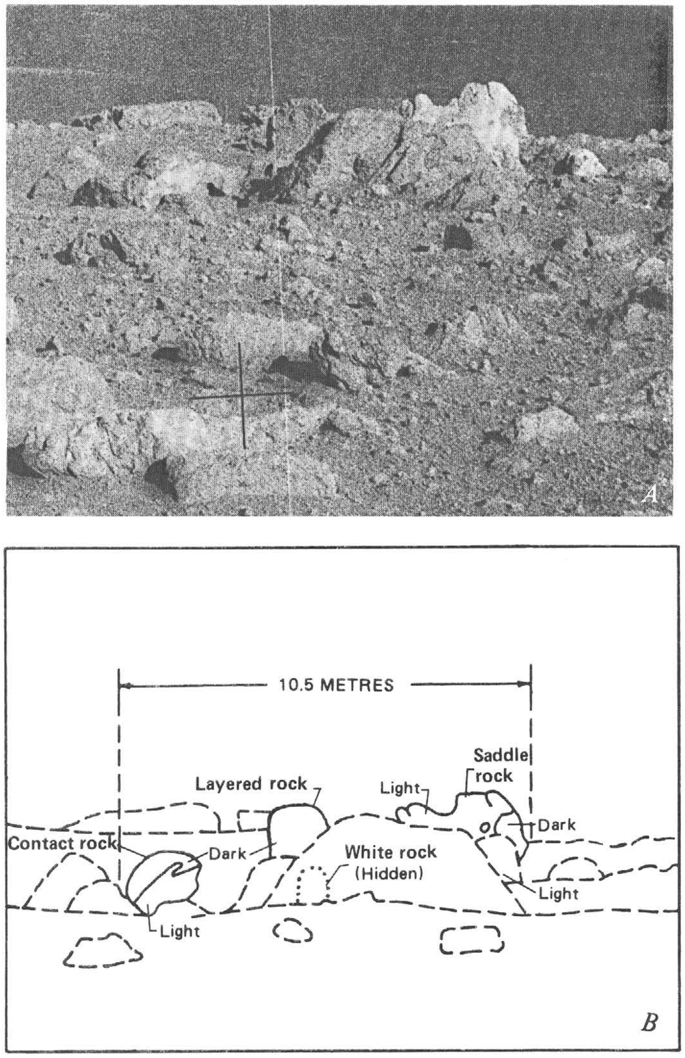

FIGURE 43.—White rocks area from station C′. *A*, West-northwest view showing the tonal contrasts between the major rock divisions. The lower part of the White rocks area is obscured by a large trapezoidal mass of gray rocks in the middleground. Enlargement of part of NASA photograph AS14–64–9099. *B*, Sketch showing tones and informal names.

shades of gray, although brown or olive is used occasionally as a modifier.

Size ranges of fragments.—Fragments range from minute particles below the resolution of the lunar surface photographs to boulders measured in metres. The largest boulders near Cone crater seen in Lunar Orbiter photographs are approximately 15 m across. The largest rock sample (14321) returned by Apollo 14 was 23 cm in diameter and weighed approximately 9 kg.

Fines: Assessment of compaction.—Variations in firmness of the lunar soil have been documented by descriptions and photographs and by soils mechanics measurements (Mitchell and others, 1971). No attempt is made here to be quantitative, but rather to give an indication of relative firmness by interpretation of photographs or by comments from the crew. The softest areas are typically rims and inner walls of fresh small craters.

Slopes.—In most cases slope angles are not given, although they can be determined from photographs and topographic contours. The slopes of the west side of the Cone crater ridge where traversed are generally less than 8°, although the crew traversed local grades up to 12° or 15°. Slopes associatied with documented sample areas may help to indicate possible directions of movement of fine-grained material.

TABLE 3.—*Summary of photogeologic rock-type characteristics*

Code	Location	Surface texture	Erosional resistance	Clasts (color and size)	Occurrence
			Light rocks		
L1	Layered rock	Smoothly undulating	High	Light; from <1 cm to several centimetres	Layer
L2	Saddle rock	Smooth	High	Light and dark; from <1 cm to several centimetres	Well to poorly layered
L3	Saddle rock	Knobby, lumpy	High	Light; a few centimetres	Layer
L4	Saddle rock	Moderately smooth	Moderate	Light; ~1 cm	Underlies a surface that slopes south
L5	Saddle rock	Moderately rough	Moderate	Dark; ~1 cm	Irregular clasts
L6	Contact rock	Finely rough	Moderate	Light; from <1 cm to a few centimetres	Irregular layer
L7	White rock	Granular	Moderate	Light; ~1 cm	Block
L8	All rocks	Too fine to tell	Moderate to high	Unknown	Clasts
			Dark Rocks		
D1	Layered rock	Smooth	High	Unknown	Clasts
D2	Contact rock	Finely rough	Moderate	Light and dark; ~1 cm	Layer
D3	Layered rock	Bumpy	Moderate	Light and dark (several centimetres)	Layer
D4	Saddle rock	Coarsely hackly	Low	Light; from ~1 cm to tens of centimetres	Irregular area

SAMPLES

14041–14046 (FRAGMENTS FROM SAME ROCK) (FIGS. 49, 50)

Station: A
Location: 150 m NWof LM and 90 m N of North Triplet crater
Rock type: Fractured fine-grained friable breccia

SAMPLE AREA CHARACTERISTICS

Slopes: Level
Fragment population:
- *Distribution and size range:* Sparse, from limit of resolution to 20 cm
- *Color:* Light gray
- *Shapes:* Knobby, irregular
- *Fillets:* Poorly developed
- *Apparent burial:* ⅛–¼
- *Dust cover:* Moderately high

Fines:
- *Color:* Light medium gray
- *Compaction:* Firm

Craters:
- *Distribution and size range:* Abundant 10- to 30-cm craters. Sample from south rim of a 6-to 8-m subdued crater
- *Shape:* Moderately sharp to subdued
- *Ejecta:* Small 20-cm fresh crater west of sample has cloddy ejecta

SAMPLE CHARACTERISTICS

Sample 14041
- *Size:* Originally about 10×8×6 cm; 346+g
- *Color:* Light olive gray
- *Shape:* Originally elongate, blocky
- *Fillet:* None
- *Apparent burial:* ⅛
- *Dust cover:* Moderately high
- *Comparison with other rocks in area:* Appears similar to other large fragments in sample area
- *Probable origin:* Soil breccia formed from a nearby impact

14047 (FIGS. 51, 52)

Station: B
Location: 330 m NE of LM and 65 m NNW of rim of Weird crater
Rock type: Fine-grained clastic breccia

SAMPLE AREA CHARACTERISTICS

Slopes: Locally slopes to the north but generally flat. In immediate sample vicinity slopes slightly steeper to north into floor of 40-cm crater
Fragment population:
- *Distribution and size range:* Sparse from limit of resolution up to 10 cm
- *Color:* Light brownish gray
- *Shapes:* Blocky, hackly with subangular edges; subrounded on exposed top surfaces
- *Fillets:* Moderately developed
- *Apparent burial:* ¼–⅓
- *Dust cover:* Moderate to heavy

Fines:
- *Color:* Light medium gray
- *Compaction:* Moderately firm to soft

Craters:
- *Distribution and size range:* Abundant 3- to 50-cm craters
- *Shape:* Subdued except for 50-cm crater with raised rim in upper center of documentary photographs AS14–64–9073 and 9074
- *Ejecta:* Mostly fines with a few fragments; two 10-cm fragments (including 14047) on rim crest of 40-cm crater

SAMPLE CHARACTERISTICS

Sample 14047
- *Size:* 5×5.5×10 cm; 242 g
- *Color:* Brownish gray
- *Shape:* Blocky with hackly surface, subangular corners; fractured; subrounded on top exposed surfaces
- *Fillet:* Moderately developed
- *Apparent burial:* ⅓
- *Dust cover:* Moderate to heavy
- *Comparison with other rocks in area:* Appears similar to two other large fragments in the panorama photographs taken at station B

Probable origin: Ejected from Center Triplet or Cone crater
Comments: Glass spatter covers buried edge of 14047. Rock very friable

14051 (FIGS. 53, 54)

Station: C′
Location: 1.29 km ENE of LM and approximately 95 m SE of rim of Cone crater
Rock type: Fine-grained, polymict breccia

SAMPLE AREA CHARACTERISTICS

Slopes: Gentle southward slope
Fragment population:
Distribution and size range: Abundant from limit of resolution to 1.5-m blocks
Color: Medium gray to very light gray (almost white); brownish gray
Shapes: Irregular; subrounded to rounded on exposed surfaces
Fillets: Moderately to well developed
Apparent burial: ½–⅔
Dust cover: Moderate to high
Fines:
Color: Brownish gray
Compaction: Firm
Craters:
Distribution and size range: Abundant 5- to 70-cm craters in and near sample area
Shape: Moderately subdued to subdued
Ejecta: Blocky ejecta around several of the 50-to 70-cm craters

SAMPLE CHARACTERISTICS

Sample 14051
Size: 3×3.5×6 cm; 191.51 g
Color: Pale brown
Shape: Blocky, subangular to subrounded
Fillet: None
Apparent burial: ¼
Dust cover: Moderate
Comparison with other rocks in area: Appears similar; slightly less buried than most of the fragments in the area
Probable origin: Ejected from Cone crater

14053 (FIGS. 55, 56)

Station: C2
Location: 1.21 km ENE of LM and approximately 130 m south of rim of Cone crater
Rock type: Crystalline plagioclase-rich basalt. (Assumed to be a clast from breccia boulder)

SAMPLE AREA CHARACTERISTICS

Slopes: 10°–15° south away from rim of Cone crater
Fragment population:
Distribution and size range: Moderately abundant, from limit of resolution to 2.5 m
Color: Medium gray to light gray
Shapes: Larger boulders rounded; smaller fragments angular to rounded. (Some may be clasts from coarser breccia)
Fillets: Well developed on large boulder; absent on smaller angular fragments
Apparent burial: ⅛–⅔
Dust cover: Heavy
Fines:
Color: Medium gray
Compaction: Firm
Craters:
Distribution and size range: Abundant small irregularities <10 cm. Very few distinct 15- to 30-cm craters
Shape: Irregular, subdued
Ejecta: Within the continuous ejecta blanket of Cone crater

SAMPLE CHARACTERISTICS

Sample 14053
Size: 8×6×3 cm; 251.3 g
Color: Salt and pepper gray
Shape: Slabby, rectangular with rounded corners; one side freshly broken, unweathered; the exposed surface displays rounding and micrometeorite pits
Fillet: Well developed on host boulder. Sample itself dusty, may have been partly covered by fillet material
Apparent burial: ⅓–½
Dust cover: Moderately heavy
Comparison with other rocks in area: Sample not identified, but presumably is a clast from the large breccia boulder and is not the only one of its kind, although crystalline rocks are relatively rare in the Apollo 14 samples
Probable origin: Ejected from Cone crater

14068–72 (FIGS. 57, 58)

Station: C′
Location: 1.28 km ENE of LM and 100 m SE of Cone crater rim
Rock types: Crystalline rocks; diabasic to feldspar-rich (with pyroxene, olivine, plagioclase)

SAMPLE AREA CHARACTERISTICS

Slopes: Locally flat; generally slight slope to south
Fragment population:
Distribution and size range: Abundant from limit of resolution to 75 cm. Mostly derived from Cone crater
Color: Light to medium gray
Shapes: Angular to subrounded
Fillets: Poorly to moderately well developed
Apparent burial: Less than 1/10–¼
Dust cover: Area too disturbed to differentiate original dust cover from man-made
Fines:
Color: Light gray to light brownish gray
Compaction: Moderate
Craters:
Distribution and size range: Entire area of photo documentation too disturbed to see any intact craters
Ejecta: Materials ejected from 30-m crater just south of station C′, which were originally ejected from Cone crater

SAMPLE CHARACTERISTICS

Sample 14068
Size: 4.2×3.2×2.7 cm; 35.47 g
Color: Medium dark gray
Shape: Blocky, angular, irregular
Fillet: Area too disturbed to discern
Apparent burial: Area too disturbed to discern
Dust cover: Area too disturbed to discern
Comparison with other rocks in area: Appears similar
Probable origin: Cone crater ejecta reejected from 30-m crater
Sample 14069
Size: 4×3×2.5 cm; 24.87 g
Color: Medium light gray

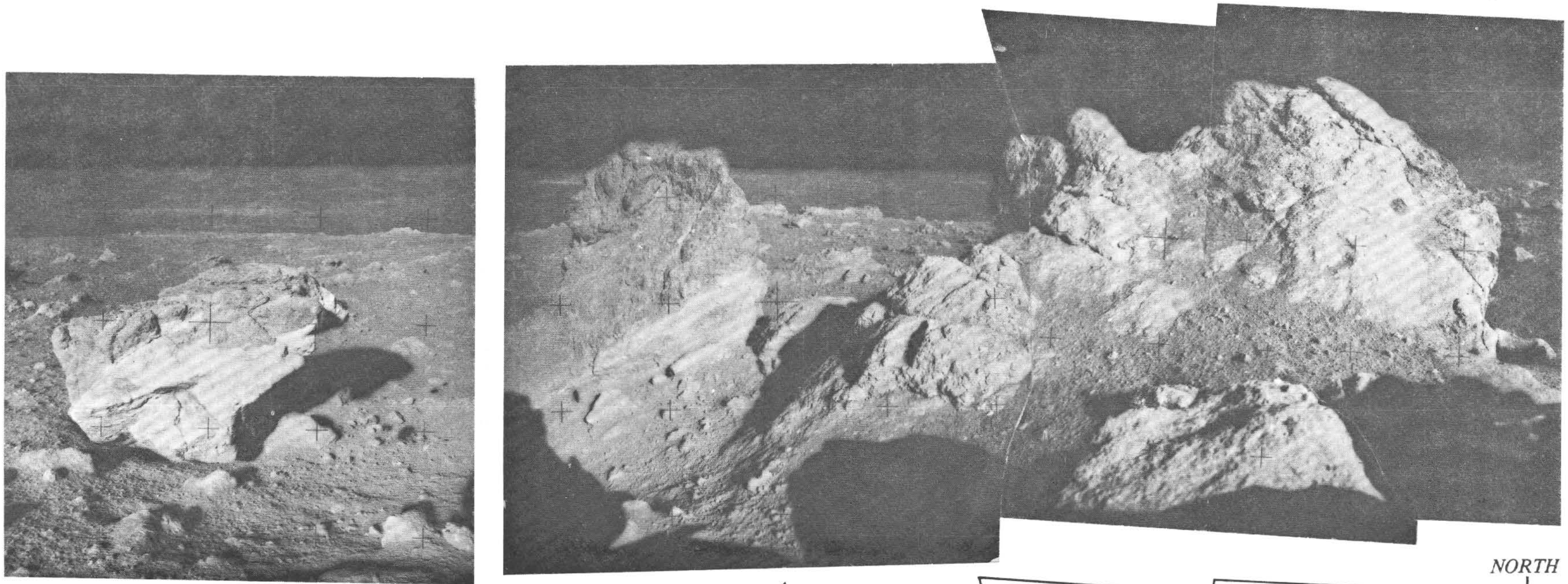

A

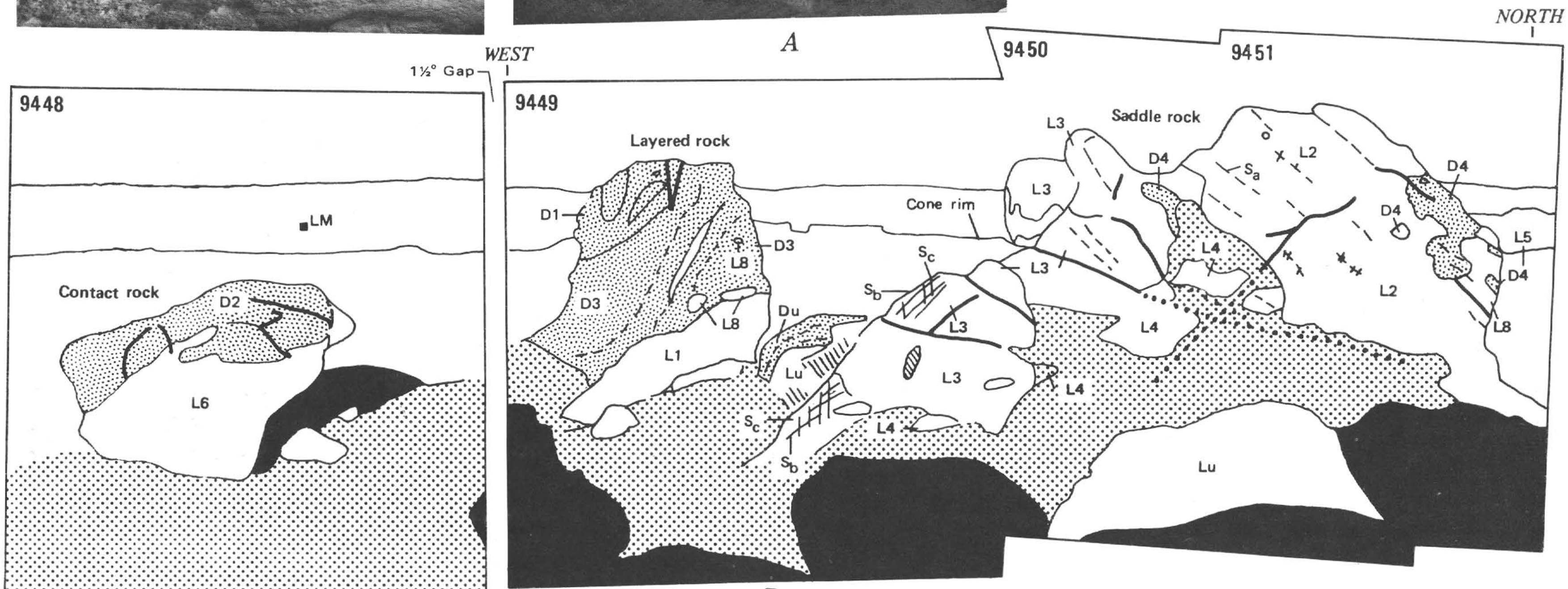
NORTH
9450
9451
WEST
1½° Gap
9448
9449
LM
Contact rock
D2
L6
Layered rock
D1
D3
L8
L1
Du
Lu
Cone rim
S_c
S_b
L3
L4
Saddle rock
D4
S_a
L2
L5

B

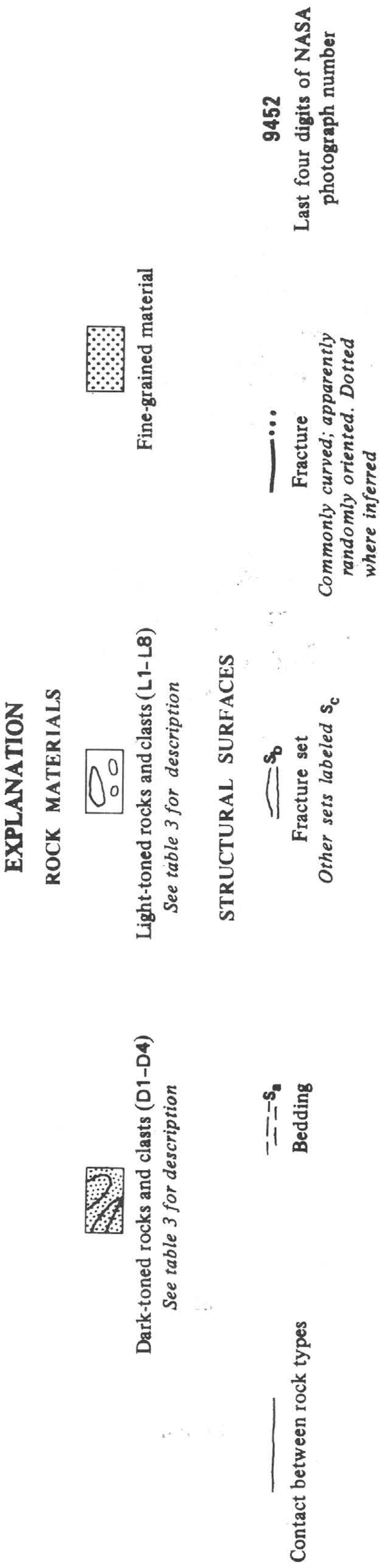

FIGURE 44.—White rocks group. *A*, Appearance of light and dark rock materials. (NASA photographs AS14-68-9448 to 9451.) *B*, Diagram showing distribution of rock types and structures (Swann and others, 1971).

Shape: Blocky, subrounded
Fillet: Area too disturbed to discern
Apparent burial: Area too disturbed to discern
Dust cover: Area too disturbed to discern
Comparison with other rocks in area: Appears similar
Probable origin: Cone crater ejecta reejected from 30-m crater

Sample 14070
Size: 4.2×3×2 cm; 36.46 g
Color: Medium light gray
Shape: Blocky, subangular
Fillet: Area too disturbed to discern
Apparent burial: Area too disturbed to discern
Dust cover: Area too disturbed to discern
Comparison with other rocks in area: Appears similar
Probable origin: Cone crater ejecta reejected from 30-m crater

Sample 14071
Size: 2×0.8×0.5 cm; 2.16 g
Color: Light gray?
Shape: Slabby, angular
Fillet: Area too disturbed to discern
Apparent burial: Area too disturbed to discern
Dust cover: Area too disturbed to discern
Comparison with other rocks in area: Appears similar
Probable origin: Cone crater ejecta reejected from 30-m crater

Sample 14072
Size: 4.1×3.4×2.1; 45.06 g
Color: Medium light gray
Shape: Blocky, subrounded
Fillet: Area too disturbed to discern
Apparent burial: Area too disturbed to discern
Dust cover: Area too disturbed to discern
Comparison with other rocks in area: Appears similar
Probable origin: Cone crater ejecta reejected from 30-m crater

14082, 14083 (SAME ROCK, BROKEN)
(FIGS. 59, 60)

Station: C1 (White Rocks area)
Location: 1.24 km ENE of LM and 17 m SE of Cone crater rim
Rock type: Felsic breccia

SAMPLE AREA CHARACTERISTICS

Slopes: Gentle slope to the south
Fragment population: Derived from Cone crater
Distribution and size range: Abundant from limit of resolution to 3 m
Color: Very light gray, almost white, to medium gray
Shapes: Irregular with subrounded to rounded edges, parallel fracture sets; knobby
Fillets: Generally well developed; a few poorly to moderately developed
Dust cover: Moderately heavy
Fines:
Color: Nearly white to brownish gray
Compaction: Moderately loose
Craters: None discernible
Ejecta: Essentially all of the materials are ejecta from Cone crater

SAMPLE CHARACTERISTICS

Samples 14082 and 14083
Size: Sample 14082: 6×3.6×2 cm; 61.16g
Sample 14083: 3.2×1.5×2.2 cm; 13.37 g
Color: Very light gray
Shape: Blocky, subangular
Fillet: Moderately well developed on boulder from which samples were taken

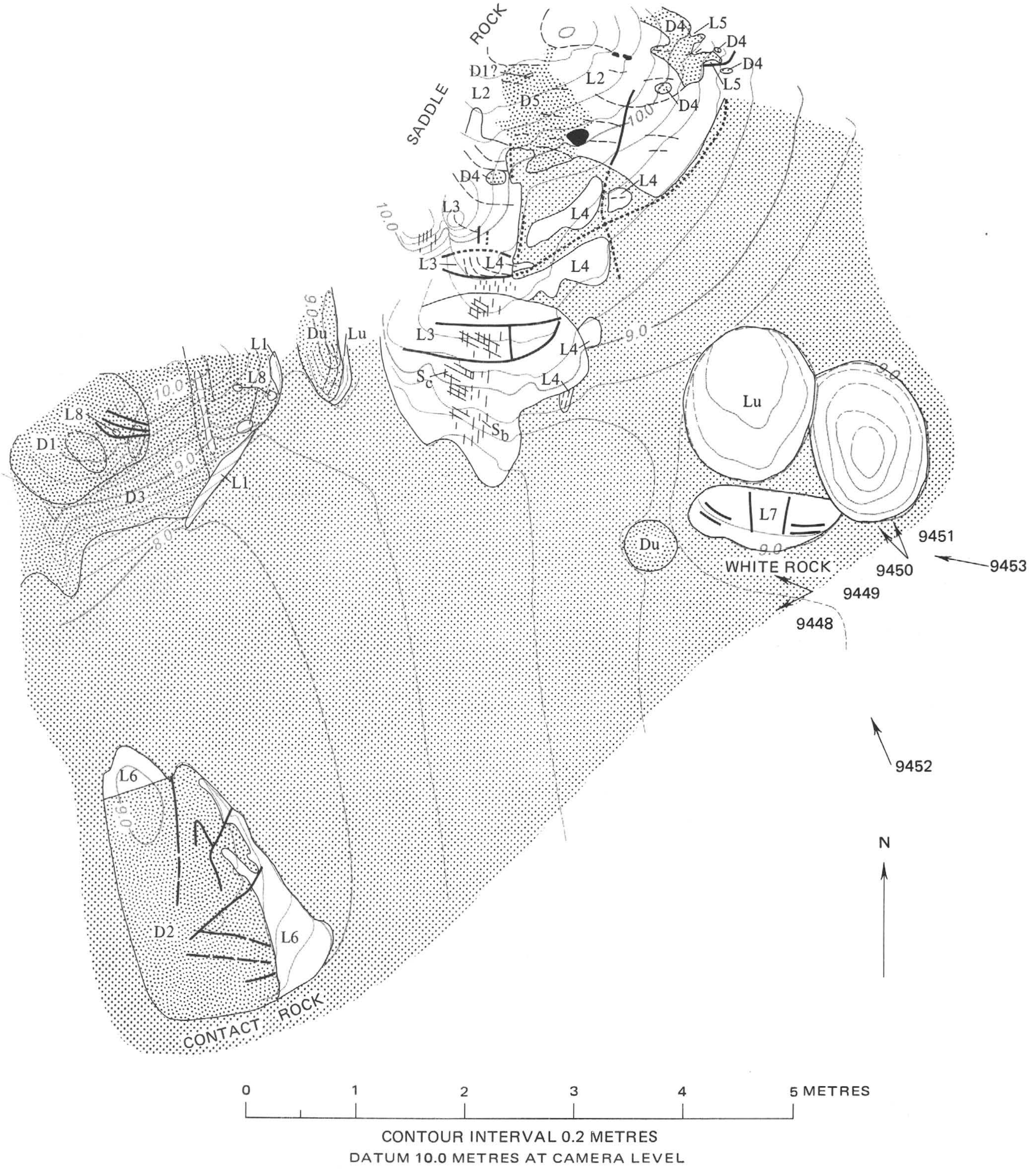

FIGURE 45.—Geologic map of the White rocks area. (Compiled from NASA photographs AS14–68–9448, 9449.) (Swann and others, 1971.) See table 3 for explanation of letter symbols. Explanation on opposite page.

EXPLANATION

ROCK MATERIALS

Dark-toned rocks and clasts (D1–D4)
See table 3 for description

Light-toned rocks and clasts (L1–L8)
See table 3 for description

Fine-grained material

Loose fragments

STRUCTURAL SURFACES

Contact between rock types

Bedding

S_c S_b
Fracture sets

Fracture
Commonly curved; apparently randomly oriented. Dotted where inferred

9452
Last four digits of NASA photograph number
Base of arrow shows camera position; arrow shows direction camera was pointed

Apparent burial: Boulder from which samples were taken buried approximately $\frac{1}{4}$
Dust cover: Slight
Comparison with other rocks in area: Appear representative of boulder from which they were taken. May be similar to white portions of other boulders
Probable origin: Cone crater ejecta from the Fra Mauro formation
Comments: Fines generally have lower albedo than the rocks in the sample area

14301, 14313 (FIGS. 61, 62, 63)

Station: G1
Location: 150 m east of LM on north rim crest of North Triplet Crater
Rock type: Coherent clastic breccia

SAMPLE AREA CHARACTERISTICS

Slopes: Level
Fragment population:
Distribution and size range: Moderately abundant from limit of resolution to 15 cm
Color: Medium gray

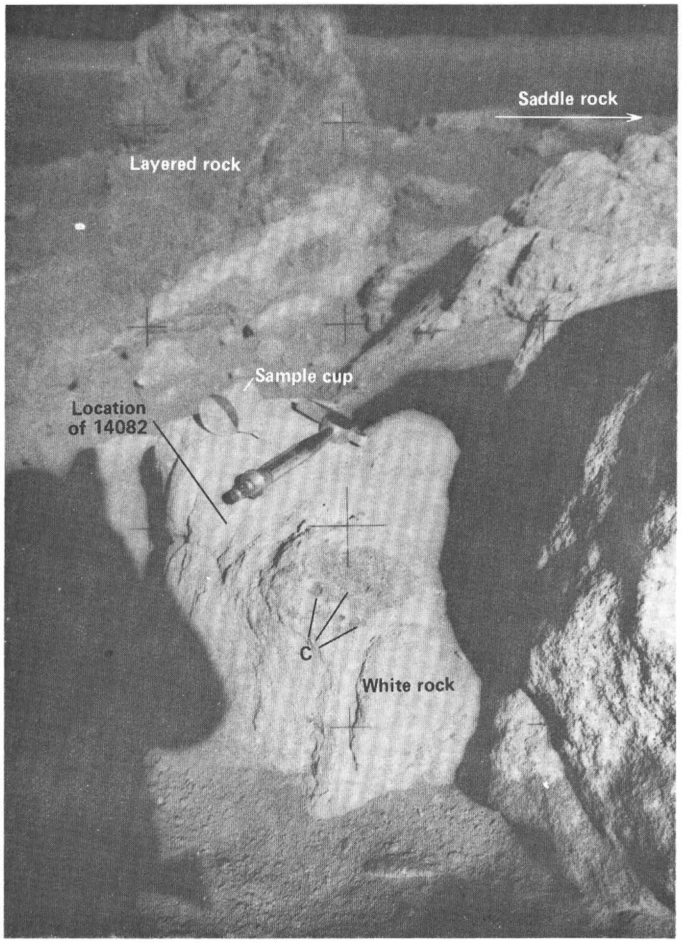

FIGURE 46.—White rock in the White rocks group. Sample 14082 was taken from just below the near end of hammer handle. Large dark clasts (C) in center of near end of White rock. Compare with figures 59 and 60. (NASA photograph AS14–68–9453.)

Shapes: Tabular; angular to rounded on exposed surfaces
Fillets: Moderately to well developed
Apparent burial: $\frac{1}{3}$–$\frac{3}{4}$
Dust cover: Heavy
Fines:
Color: Medium gray
Compaction: Moderately firm
Craters:
Distribution and size range: Abundant from 5–70 cm
Shape: Subdued
Ejecta: Many of the fragments are probably associated with the small craters that have reejected material from North Triplet crater

SAMPLE CHARACTERISTICS

Sample 14301
Size: 12.5×12×8 cm; 1360.6 g

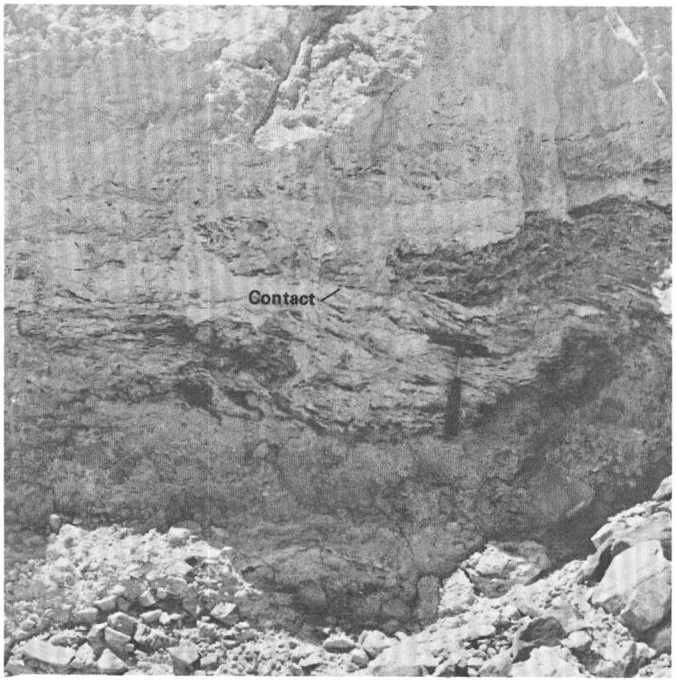

FIGURE 47.—Layering in uppermost parts of the ejecta sequence at Meteor Crater, Arizona. Photograph courtesy of J. F. McCauley.

Color: Medium to light gray
Shape: Subangular to subrounded; blocky equant; subrounded on exposed surfaces
Fillet: Moderately well developed
Apparent burial: ¾
Dust cover: Heavy
Comparison with other rocks in area: Similar
Probable origin: North Triplet crater

Comments: Excepting samples dug from trenches, 14301 is probably the most deeply buried rock sampled on this or previous missions

Sample 14313
Size: 6×6×4 cm; 144 g
Color: Medium light gray
Shape: Blocky; angular to subrounded; relatively flat on exposed top
Fillet: Poorly developed
Apparent burial: ½
Dust cover: Moderate to heavy
Comparison with other rocks in area: Appears similar to most surrounding fragments
Probable origin: North Triplet crater

14304 (FIGS. 64, 65)

Station: No station number; EVA 1
Location: 80 m NW of LM on SW rim of 10-m crater
Rock type: Moderately coherent clastic breccia

SAMPLE AREA CHARACTERISTICS

Slopes: Slight slope to south
Fragment population:
Distribution and size range: Sparse from limit of resolution to 20 cm
Color: Light gray
Shapes: Irregular, knobby, subrounded on exposed surfaces

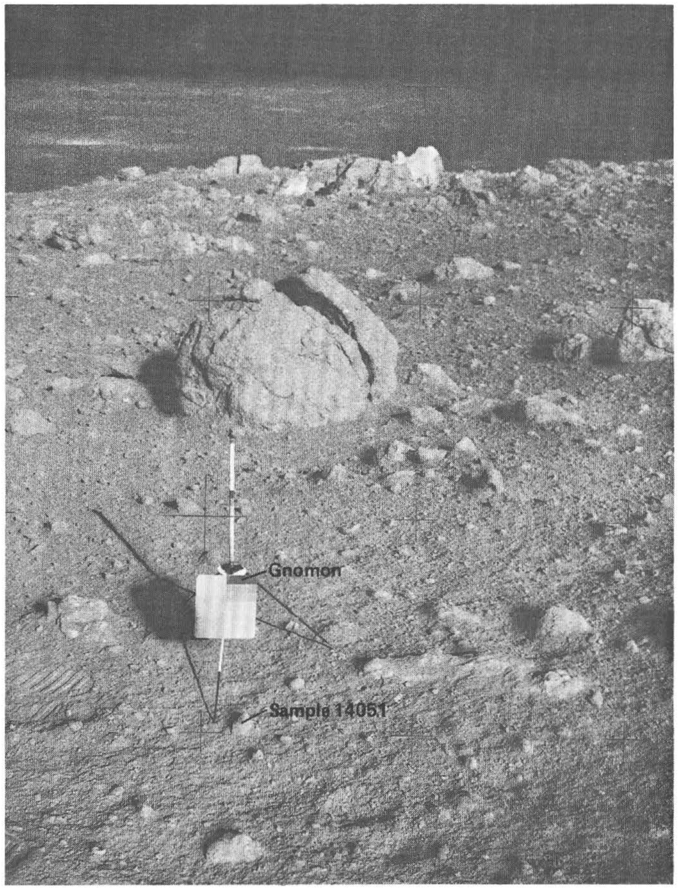

FIGURE 48.—Split rock at station C′ just beyond gnomon. The near horizon is the south rim of Cone crater. Note White rocks group near rim. (NASA photograph AS14–68–9445.)

Fillets: Poorly developed
Apparent burial: ⅛–¼
Dust cover: Moderate

Fines:
Color: Medium gray
Compaction: Moderate; upper 2 cm powdery

Craters:
Distribution and size range: Abundant from a few centimetres to 50 cm
Shape: Subdued
Ejecta: Larger fragments (including 14304) appear to be associated with 30- to 50-cm craters

According to Cdr. Shepard's comments, samples 14304 and 14305 were picked up near the southwest rim of a sharp 10-m crater which had been described earlier from the LM by Astronaut Mitchell. The 10-m crater is not shown in the sample documentation photographs and it is not clear that these rocks are part of the ejecta from that crater

SAMPLE CHARACTERISTICS

Sample 14304
Size: 20×11×10 cm; 2498.9 g
Color: Medium grayish brown
Shape: Blocky, subrounded
Fillet: Poorly developed
Apparent burial: ⅛–¼

TABLE 4.—*Sample locations and page references by sequential LRL number*

LRL Sample No.	Traverse station	Page reference
14001 to 14012	Contingency sample	50
14041 to 14046	A	42, 53
14047 and 14048	B	4, 42,
14049 and 14050	Bg	54
14051 and 14052	C′	4, 43, 54
14053 and 14054	C2	4, 29, 30, 43, 55
14055 to 14062	E	4, 56
14063 to 14065	Cl	55
14066 and 14067	F	4, 56
14068 to 14072	C′	29, 30, 43, 45, 54
14073 to 14079	G	4, 58
14080 and 14081	G	58
14082 to 14084	Cl	33, 45, 47, 55
14140 to 14143	C′	54
14144	C′	54
14145 to 14148	G	57
14149 to 14152	G	58
14153 to 14156	G	58
14160 to 14163	Bulk sample	22, 25, 52
14165 to 14189	Comprehensive sample collected on EVA–1.	50
14190 to 14204	Not known, residue from weigh bag 1031, EVA–2.	61
14210 and 14211	A	52
14220	G	56
14230	G	57
14240	G	58
14250 to 14289	Comprehensive sample	50
14290 to 14297	Probably station H residue from weigh bag 1038, EVA–2.	61
14301	Gl	4, 47, 48, 59
14302	Included with 14305, EVA–1	49
14303	Comprehensive sample?	4, 50, 51
14304	EVA–1	4, 48, 49, 51
14305	EVA–1	4, 30, 31, 49, 51
14306	G	4, 49, 59
14307	G	4, 59
14308	Dg, included with 14311	4, 61
14309	Not known, probably broken from EVA–2 grab sample.	
14310	G	4, 58
14311	Dg	4, 56
14312	H	4, 32, 60, 61
14313	Gl	4, 30, 47, 48, 59
14314	H	60, 65, 67
14315	H	4, 60, 75, 76
14316	H	60
14317	H	60
14318	H	4, 30, 60, 75, 76
14319	H	4, 32, 60, 61, 65
14320	H	60, 75, 77
14321	Cl	4, 55, 78, 79
14411	A, core bit	53
14414	G, core bit	56, 57
14421	Comprehensive sample	50
14422 to 14453	Bulk sample	52

Dust cover: Moderate

Comparison with other rocks in area: Appears similar in texture and albedo

Probable origin: Lack of fillet and association with two small fresh craters suggests it has been in its present position for very short time. If 14304 made the two craters as suggested in figure 64, its source was probably from the southeast

14305 (14302 FRAGMENT OF SAME ROCK) (FIGS. 66, 67)

Station: No station number; EVA 1
Location: 80 m NW of LM and 100 m ESE of ALSEP central station.
Rock type: Coherent clastic breccia

SAMPLE AREA CHARACTERISTICS

Slopes: Level regolith surface
Fragment population:
- *Distribution and size range:* Fairly abundant from limit of resolution up to 1 cm; sparse from 1 to 15 cm
- *Color:* Medium gray
- *Shapes:* Angular to subrounded, fractured
- *Fillets:* Poorly developed
- *Apparent burial:* ¼–⅓
- *Dust cover:* Moderate

Fines:
- *Color:* Medium gray
- *Compaction:* Medium

Craters:
- *Distribution and size range:* Abundant moderately fresh craters from 10 to 50 cm
- *Shape:* Sharp to subdued
- *Ejecta:* Fresh 20-cm crater is rimmed with clods
- See comment relating to sample 14304

SAMPLE CHARACTERISTICS

Sample 14305 (14302)
- *Size:* 14×15×10 cm; 2497.5 g
- *Color:* Medium gray
- *Shape:* Subrounded to angular; blocky; pyramidal
- *Fillet:* None
- *Apparent burial:* ⅓
- *Dust cover:* Moderate
- *Comparison with other rocks in area:* Largest fragment in photographs; shape and texture similar to smaller fragments
- *Probable origin:* Lack of fillet and freshness of secondary crater suggests it has been in its present position for very short time. Direction of sliding after making secondary (fig. 33) suggests its source was from the southwest

14306 (FIGS. 68, 69)

Station: G
Location: 230 m ESE of LM and 50 m E of North Triplet rim crest
Rock type: Coherent clastic breccia

SAMPLE AREA CHARACTERISTICS

Slopes: Level regolith surface
Fragment population:
- *Distribution and size range:* Sparse from limit of resolution to 60 cm
- *Color:* Medium light gray
- *Shapes:* Irregular to sub-tabular
- *Fillets:* Moderately well developed
- *Apparent burial:* ⅛–⅓
- *Dust cover:* Moderate on smaller fragments; heavier on 60-cm boulder

Fines:
- *Color:* Medium light gray
- *Compaction:* Moderate to high

Craters:
- *Distribution and size range:* Moderate abundance of 20- to 50-cm craters
- *Shape:* Subdued
- *Ejecta:* Not discernable

SAMPLE CHARACTERISTICS

Sample 14306
- *Size:* 5×7.5×6 cm; 584.5 g
- *Color:* Light gray with white clasts
- *Shape:* Blocky, subangular
- *Fillet:* None
- *Apparent burial:* ¼–⅓
- *Dust cover:* Low to moderate
- *Comparison with other rocks in area:* Appears somewhat more tabular and less irregular than 60-cm boulder but similar in color and albedo. Planar structures and flat near face similar to boulder

TABLE 5.—*Cross-reference of lunar samples with locations, lunar-surface photographs, status of determining sample location and orientation, megascopic sample description, and comments by the astronaut crew during sample collection*

Sample Number	Weight (g)	Lunar-surface Photographs:[1,2]	Location Status	Orien-tation[3]	Sample description[4]	Crew comments[5]
EVA 1—Station: LM Area Toward ALSEP Site:						
		65–9206 LM Pan B 66–9325 LM Pan A 66–9339 LM Pan A	Approx.	NA	Contingency sample	LMP: Houston. While Al's getting that television, I'll go ahead and get my contingency sample out of the way. The contingency sample is being taken about 25 feet to the 0100 position of the LM, adjacent to about a 5-foot crater. I'll identify it for you later. *** CDR: The soil is very fine here. Very fine grain, and as we mentioned before there are very few samples that are of any size at all. Mostly hand-sample size and rocks of generally 1 or 2 inches or less. *** LMP: We couldn't get them all in *** the SRC. We got the contingency sample here. And it so happens that the material cracked on the contingency sample bag, and it's leaking. So we're putting it in the weigh bag [No. 1039] with these other rocks. [The small rocks from the comprehensive sample area] And the weight of that total combination is 5 pounds.
14001	31.8				2–4 mm fines	
14002	42.1				1–2 mm fines	
14003	947.9				<1 mm fines	
14004	33.0				4–10 mm fines	
14006	12.13				rock	
14007	3.67				rock chip	
14008	4.35				rock chip	
14009	1.09				rock chip	
14010	1.00				rock chip	
14011	0.68				rock chip	
14012	0.103				residue from weigh bag 1039	
		67–9388 USB 67–9389 DSB	Approx.	NA	Comprehensive sample	CDR: Okay, Houston, on this comprehensive sample we're about a third of the way back to the LM. I've not found an area exactly what I want, so I have drawn a circle which is approximately 2 metres in radius, and I'm going to pick the surface rocks from that, and sample the surface fines from that area. CDR: I've documented this location with a locator shot back to the LM and to the ALSEP. (AS14–67–9388, 9389) LMP: Okay, Al. Need some help there? CDR: Yes, I wanted to pick up all the walnut-size rocks in your tongs. And we'll get the surface fines, here. *** CDR: Why don't you work that side of it, and I'll work this side. LMP: Okay. CDR: You have to be careful you don't put them in the ground. If you make consecutive passes up the whole circle we can tell. *** CDR: For this amount of time, we can really only get the ones that are essentially there. LMP: Yes, let me grab another weigh bag, because you're too far away for me to— CDR: An inch in diameter. *** LMP: Can't help you very well this way. *** CDR: I think I've got them, Ed. LMP: Okay. I'll get one for the fines. CDR: Get one for the fines and we'll start. I'd just say, just grab an undisturbed site out of reach quadrant, we didn't hit with our feet. Cut it down to about a centimetre level and fill the bag that way. LMP: Okay. You want the medium-size scoop or the big scoop for this? CDR: No, the medium-size scoop is the best. All you've got to do is cut the surface to the depth of about a centimetre in an undistrubed area here where we haven't picked up the rocks. Okay? LMP: Okay. I'm bringing the stuff over right now. CC: Al and Ed this is Houston. We show about 8 minutes remaining until you should be at the MESA [Modularized Equipment Storage Assembly, a storage area of the exterior of the Lunar Module] to start closeout. CDR: Okay, we will be able to bring the comprehensive sample at that time. *** LMP: Hey, don't close it, here's one in here for that. [larger rock?] LMP: Here's one in here I picked up. CDR: Oh, okay. Dump it in here, then. [possibly refers to sample 14303?] LMP: Okay, I'll start over here in this undisturbed area. CDR: Yes, just get that area and then right here in this area. And fill up the bag to the line. Now I'll head on back a little farther, get a football-size rock. *** LMP: All right, let me get about three more scoops, Al. I can get there before long. *** LMP: Boy, my sample's packing down. It was more than that when I left the site. *** LMP: Oh, There went my sample bag.
14165	9.10				<1 mm fines residue	
14166	20.50				1–2 mm fines from	
14167	26.50				2–4 mm fines weigh bag	
14168	43.90				4–10 mm fines 1027	
14169	78.66				rock	
14170	26.34				rock	
14171	37.79				rock	
14172	32.10				rock	
14173	19.59				rock	
14174	11.62				rock chip	
14175	7.48				rock chip	
14176	4.12				rock chip	
14177	2.32				rock chip	
14178	2.88				rock chip	
14179	3.03				rock chip	
14180	4.75				rock chip	
14181	2.48				rock chip	
14182	2.29				rock chip	
14183	1.40				rock chip	
14184	1.48				rock chip	
14185	1.52				rock chip	
14186	1.26				rock chip	
14187	1.09				rock chip	
14188	1.60				rock chip	
14189	0.36				residue, weigh bag 1027	
					comprehensive sample (weigh bag 1039)	
14250	4.06				rock chip	
14251	1.51				rock chip	
14252	0.86				rock chip	
14253	1.23				rock chip	
14254	1.01				rock chip	
14255	22.15				rock	
14256	13.71				4–10 mm fines	
14257	30.48				2-4 mm fines	
14258	64.33				1–2 mm fines	
14259	2694.10				<1 mm fines	
14260	282.50				<1 mm fines	
14261	8.20				2–4 mm fines	
14262	9.10				1–2 mm fines	
14263	16.20				4–10 mm fines	
14264	117.89				rock	
14265	65.79				rock	
14266	6.95				rock chip	
14267	54.77				rock	
14268	23.12				rock	
14269	17.19				rock	
14270	25.59				rock	
14271	97.41				rock	
14272	46.63				rock	
14273	22.40				rock	
14274	15.18				rock	
14275	12.46				rock	
14276	12.75				rock	
14277	7.59				rock chip	
14278	7.60				rock chip	
14279	5.67				rock chip	
14280	6.20				rock chip	
14281	12.03				rock	
14282	1.89				rock chip	
14283	1.25				rock chip	
14284	1.47				rock chip	
14285	2.23				rock chip	
14286	4.42				rock chip	
14287	1.07				rock chip	
14288	3.44				rock chip	
14289	0.20				residue, weigh bag 1039	
14298	200.00				<1 mm fines reserve from	
14299	225.00				<1 mm fines 14259	
14300	4.06				rock chip	
14421	260.90				reserve fines from unsieved comprehensive sample	

See footnotes at end of table.

TABLE 5.—*Cross-reference of lunar samples with locations, lunar-surface photographs, status of determining sample location and orientation, megascopic sample description, and comments by the astronaut crew during sample collection*—Continued

Sample Number	Weight (g)	Lunar-surface Photographs: [1,2]	Location Status	Orientation[3]	Sample description[4]	Crew comments[5]
			EVA 1—Station: LM Area Toward ALSEP Site: Continued			
14303	898.4	With comprehensive sample. Not identified in lunar-surface photographs.	Approx.	From surface pitting only	A blocky, subrounded rock with zap pits on all but one side and having only a few poorly developed, irregular fractures. The sample is a very friable fine-grained clastic rock having less than 1 percent subrounded light-colored clasts in a medium-gray matrix.	CDR: Put your UHT [Universal Hand Tool] handles for it. LMP: I'll use this handle. Fortunately, I don't think more than a little bit fell out. CDR: Okay, we've got it packed down to only half full. *** CDR: Okay, Houston, for your information, documentary location shots of the comprehensive sample taken on [film roll] JJ and I'm now showing 40. *** CDR: And on the comprehensive sample, Houston, I feel we have about 15 rocks, and some fines. One weigh bag [No. 1039] is going in the SRC. *** LMP: Okay. We want you to be discriminating about our samples now. We have the comprehensive rocks in the left-hand storage compartment. The comprehensive fines, however, are in the SRC. CDR: Now I'll head on back a little farther, get a football-size rock. CDR: There's some pretty good-sized ones back over in here. Okay, that's too big. I'll get one that's a little smaller. ***
14304	2498.9	67–9390 XSB 67–9391 XSB	Approx.	Known	A blocky, subangular rock cut by a few poorly developed, irregular fractures. Zap pits are not prominent, and all surfaces appear immature. The rock is a coherent breccia with a moderate pércentage of angular to subrounded, blocky to slabby dark clasts in a very light gray matrix. A very small percentage of light clasts is present.	CDR: Okay, Houston, you can see the area where the football-sized rock [14304] is coming from. It's essentially two-thirds of the way back toward the LM, from the ALSEP site. The rock appears to have been ejected from the crater which Ed was describing earlier, in his 12:30 position. As a matter of fact, it's going to be a small football-sized rock—no, it turned out to be two of them.
14305	2497.5	67–9392 XSB 67–9393 XSB	Approx.	Known	A blocky, subangular rock with a poorly developed set of planar fractures. Two nearly planar faces of the rock appear to be controlled by splitting along planar fractures. Zap pits are inconspicuous, and all surfaces appear immature. The rock is a coherent breccia with a moderate proportion of subrounded dark clasts and subordinate light clasts in a very light gray matrix.	CDR: The second small football [14305] is from near the same crater. And, at first glance, appears to be fairly similar color. It's a large hand sample. It's essentially nonvesicular. Just some very small vesicles. CDR: There looks to be a fairly large crystal in that second small football rock and now starting back toward the MESA. *** LMP: The number of surface rocks, or rocks compared with the number of surface fines is very, very small, Houston. There's a few boulders lying around and there's a few blocks around some of the craters, but by and large, it's a powdery surface. *** CDR: Houston, we were unable to get all of the weigh bags in the SRC. It's full. We're putting the small samples of small rocks from the comprehensive sample in the weigh bag along with the two small football rocks. [Weigh bag 1027] *** LMP: Houston, let me tell you what we've done. Remember, Al said that we brought in the small rocks from the comprehensive sample area in one weigh bag. [1027] We couldn't get them all in the SRC. We got in the contingency sample here. And it so happens that the material cracked on the contingency sample bag, and it's leaking. So we're putting it in the weigh bag [1039] with these other rocks. And the weight of that total combination is 5 pounds. *** LMP: And, Houston, the next bag [1027] has two toy-sized football rocks in it. And they weigh 15 pounds total. *** LMP: And that's going into the left-hand storage compartment. *** LMP: Okay, Houston. Both of those rock bags [1027, 1028] are going to left-hand storage compartment. CC: Okay, Ed. That's the one with the contingency sample and the comprehensive and the football ones, right? LMP: That's affirmative. [Note: The contingency sample went into SRC–1 along with weigh bag 1039.] *** CC: Okay. Next question: on the football samples, were they documented? CDR: That's affirmative. They were documented with a stereopair before, in the case of both samples. And they were taken from the crater which is located at CR.1 and 64.6. They came from the southwest rim of that crater.

TABLE 5.—*Cross-reference of lunar samples with locations, lunar-surface photographs, status of determining sample location and orientation, megascopic sample description, and comments by the astronaut crew during sample collection*—Continued

EAV I—Station: LM Area Toward ALSEP Site: Continued

Sample Number	Weight (g)	Lunar-surface Photographs:[1,2]	Location Status	Orien-tation[3]	Sample description[4]	Crew comments[5]
		Probably in LM window photographs but not identified	Unknown	NA	Bulk sample, weigh bag 1028	CC: Roger. If you take an additional weigh bag, and put material from the immediate vicinity of the LM into it to fill up the SRC, we request that you drop a documented sample bag in it as a tag. *** CDR: Okay, where's that tin scoop? LMP: Which one, the big one? Why don't you let me help you with the—let's take the shovel, Al; it'll be faster. CDR: All right. LMP: Trenching tool. CDR: Want to hold the bag? LMP: Yes. CDR: Let's hit that little crater out there. It looks like a secondary. LMP: Okay, let's go get it. CDR: Right out here. LMP: I saw a little crater about this size out here that I'd swear had glass in the bottom of it, but I was too busy thumping to stop and make any comment on it. LMP: There's a little different-colored layer at the bottom of it there. CDR: Yes. Scoop it out. LMP: See, there's a different color there, maybe. CDR: Okay, how does that look to you? LMP: I can take another shovelful. That's good. CDR: Okay. Houston, that's in a small crater; looks like it might be a secondary impact, just hazarding a guess; it's about 2 feet in diameter, and it's between 130–50 feet, 130–40 feet from the LM. CDR: We'll put a documented sample bag in there with it, and that will be bag number 1. Here you go, Ed. LMP: Okay, put it in. CDR: One November. [Weigh Bag 1028]
14160	196.5				4–10mm fines	
14161	197.1				2–4 mm fines	
14162	288.7				1–2 mm fines	
14163	7129.8				<1 mm fines	
14422	251.0				reserve from 14163	
14425	0.79				rock chip	
14426	1.59				rock chip	
14427	4.47				rock chip	
14428	1.47				rock chip	
14429	3.03				rock chip	
14430	4.81				rock chip	
14431	1.70				rock chip	
14432	1.81				rock chip	
14433	1.23				rock chip	
14434	1.68				rock chip	
14435	0.92				rock chip	
14436	3.76				rock chip	
14437	2.65				rock chip	
14438	3.35				rock chip	
14439	1.00				rock chip	
14440	1.50				rock chip	
14441	0.23				rock chip	
14442	3.52				rock chip	
14443	2.54				rock chip	
14444	1.56				rock chip	
14445	9.22				rock chip	
14446	0.82				rock chip	
14447	0.91				rock chip	
14448	1.06				rock chip	
14449	1.70				rock chip	
14450	1.27				rock chip	
14451	2.10				rock chip	
14452	1.77				rock chip	
14453	6.03				rock chip	
14402	0.20				residue from EVA 1 ALSRC [Apollo Lunar Sample Return Container]	

EVA 2—Station: A

Sample Number	Weight (g)	Lunar-surface Photographs:[1,2]	Location Status	Orien-tation[3]	Sample description[4]	Crew comments[5]
14211	39.5	64–9046 XSD	Known	NA	Double drive tube (upper)	CDR: Fred, the surface, here is textured. It is, of course, a very fine grain dusty regolith, much the same as we have in the vicinity of the LM. But, there seems to be more small pebbles here on the surface than we had back around the LM area. And the population of larger rocks, perhaps small boulder size, is more prevalent here. Okay, this is probably pretty good [for Station A]. LMP: Yes, this is a good place for A and we might also comment, Fredo, that they have an appearance, here, quite often like raindrops—a very few raindrops have splattered the surface. It gives you that appearance. Obviously, they haven't; but it's that sort of texture, in places. CDR: Yes, I think that there's a relationship between the texture and these small surface pebbles. Okay, point A. LMP: Okay, at point A, we do a double core [drive tube]. *** CDR: The point where we're sampling is just about in the center of three craters of almost equal size. I would say, perhaps, 20 metres in diameter. The ones to the north are more fresh, more sharp; the one to the left is more subdued. I'm pretty sure we're just about where point A is on the map; it fits the description of it. *** CC: Okay, and Al, a word from the back room says go at least two crater diameters away from the crater you're just describing, when you get ready to take the double core. CDR: Okay, we'll try to put it in the center of the three craters to get all three, well, to get whatever stratigraphy we have here. *** CDR: Okay, all set up for the double core here. *** CDR: The bottom core tube will be number 2, no tab. [14210] Top core tube will be number 3, no tab. [14211] *** CDR: Okay, Houston. A couple of quick stereos and the locator of the core tube as it's about to be driven, and the LM is in the background. *** CDR: Okay, Houston. We got almost two complete tubes here, about one and seven-eighths tubes, I would say. ***
14210	169.7	64–9047 XSD 64–9048 LOC			(lower)	

TABLE 5.—*Cross-reference of lunar samples with locations, lunar-surface photographs, status of determining sample location and orientation, megascopic sample description, and comments by the astronaut crew during sample collection*—Continued

EVA 2—Station: A—Continued

Sample Number	Weight (g)	Lunar-surface Photographs:[1,2]	Location Status	Orien-tation[3]	Sample description[4]	Crew comments[5]
14411	5.5				Core bit, double drive tube	CDR: And the core bit [14411] just for the fun of it, is going in bag 2 November. If we can get it back. CC: And Al, they'd like a description of the surface where you drove the core tube.
14041 14042 14043	166.27 103.19 5.94	68-9409 DSB 68-9410 XSB 68-9411 XSB 68-9412 XSA 68-9413 LOC	Known	Unknown	A blocky, angular rock with a small percentage of its surface coated by vesicular glass. The rock is cut by widely spaced, irregular fractures intersecting at high angles, the rock breaks readily along these fractures. Some surfaces are lightly covered by glass-lined zap pits. The rock is mostly a friable, fine-grained clastic rock with less than 5 percent of subrounded light-colored clasts in a medium gray matrix. A piece of this rock (14043) has a considerably higher proportion of clasts, but is otherwise similar.	CDR: Okay, Fred. Nothing, but it's the same textured pattern of which we spoke coming up in this traverse. *** CDR: Continuing our description of the surface, it appears to be a scattered population of very small blocks, some of which Ed is going to photograph here, and his documented sample. I believe they came from the crater to the north of the sampling site. Other than that, the pebble core *** sample site is not unique to the traverse, so far. The first core went in fairly easily. I had some difficulty with the last core.
14044	4.68				Residue from bag 3N	
14045	65.24	Same as for 14041–14044			A blocky, subangular rock with a rough, hackly surface. Glass-lined zap pits occur on all but one surface. There are very poorly developed irregular internal fractures, but one face of the sample has broad, parallel steps suggestive of fracture control. The sample is a friable fine-grained clastic rock with very sparse subangular light-colored clasts in a medium-gray matrix.	LMP: And, Houston, the rock I'm sampling seems to be a fairly typical one of this multiple crater that we're working around right now near A, and it's going into the bag 3 November. LMP: It's breaking apart on me as I pick it up. I'll try to get most of the pieces. *** LMP: Houston, I can't get all of this sample in 3-N. That's going to be able to go in 3-N [14041–14044] and the next one [4-N, 14045–14046]. It looked like it was fractured, and when I picked it up, it fractured into about four pieces.
14046	1.21				Residue from bag 4N	

EVA 2—Station: B

Sample Number	Weight (g)	Lunar-surface Photographs:[1,2]	Location Status	Orien-tation[3]	Sample description[4]	Crew comments[5]
						CC: Al and Ed, I don't think you have to worry too much about the exact position of site B. If it appears you're getting close to the general area, that should be good enough on B. LMP: Okay. I think we're very close to it. I think this crater we just went by is probably it, but it's very hard to tell, Fredo. I don't see anything else that might be it, unless it's the next crater up. Al, I've spotted it. That next crater up is this one right here. *** CDR: Where do you think B is? LMP: I think B's the one we just passed, back there where we were talking. CDR: All right. LMP: And here's the little double crater right beside it. Look here [On the map]. See, there's the little double crater; it's right there in front of you. CDR: Okay, let's grab sample B. ***
14047	242.01	64-9073 XSB 64-9074 XSB	Known	Known	A blocky, subangular rock with about 10 percent of its surface coated by vesicular glass. Irregular, slightly rounded surfaces are lightly covered by glass-lined zap pits. One nearly planar bounding face of the rock has well-developed slickensides. Multiple sets of irregular fractures occur at one end of the specimen. The sample is a friable fine-grained clastic rock having a small percentage of subangular light clasts in a medium-gray matrix.	CDR: I'll get a pan, Ed. LMP: Okay. And while Al takes the pan, I'll go ahead and give you a site description. The area here is in an area with considerably more boulders, a larger boulder field, more numerous boulders than we've seen in the past. We've just come into it as we approach B from A. Now there are boulders to the north of us; we previously talked of boulders to the north, and doggone it, they may turn out to be a ray pattern. It looks suspiciously like one. However, where we are now, we're about on the edge of a general boulder population lining the flank of Cone Crater. Now they're not too numerous at this point. They're somewhat patchy. There's a lot of them buried, half-buried, a few of the smaller ones sitting on the surface. These boulders are filleted, and we'll have to sample that filleting later. The surface texture—the fine is very much the same as what we've been walking on all along. And about the only difference we could see is probably a larger number of smaller craters. I say probably; they're so numerous that unless you really make a population count, you can't tell. I'm guessing a larger number of craters, probably secondaries from Cone perhaps—and certainly a larger number of boulders lying around. Now, most of these boulders are rounded; there are a few angular ones but by and large, you can see edges that have been chipped off indicating the beginning of a smoothing process. And some of them are far beyond the beginning of smoothing. They're worn down pretty well. And most of the rough edges are where they have fractured and perhaps turned over. Most of them appear to be along fractures of where other rocks are sitting near them that might have once been a part of that boulder.
14048	10.17				Residue from bag 5N	

TABLE 5.—*Cross-reference of lunar samples with locations, lunar-surface photographs, status of determining sample location and orientation, megascopic sample description, and comments by the astronaut crew during sample collection*—Continued

Sample Number	Weight (g)	Lunar-surface Photographs:[1,2]	Location Status	Orien-tation[3]	Sample description[4]	Crew comments[5]
					EVA 2—Station: B—Continued	
						CC: Roger, Ed. And has Al got the grab sample completed and up? CDR: I'm grabbing it now. CDR: We're going to give you a quick stereo of it [64–9073, 9074]. CDR: Okay. Grab sample from the west rim of Bravo Crater, bag 5 November [14047, 14048].
					EVA 2—Station: Bg	
						LMP: Fredo, I'm trying to find something distinctive to say about some of these craters we're going by, and it's very hard to do so. They're all smooth-walled except the very freshest one; and we're coming by a very fresh one now, which has some pretty good chunks of rubble on the insides. This is about the freshest crater this size we've seen, Al.
14049	200.13	No photographs	Approx.	Unknown	A blocky, subrounded rock lacking zap pits and having only a few very poorly developed, irregular fractures. The sample is a very friable fine-grained clastic rock having less than 1 percent of subrounded light-colored clasts in a medium-gray matrix.	CDR: That's correct. This is a very fresh crater. It's about opposite to the crater at stop E. It's a crater about 20 metres in diameter and about 2 metres deep, and I'll get a quick rock from the side. LMP: Al just dropped down on a knee to pick up a rock, and he went in 3 or 4 inches. ***
14050	6.91				Residue from bag 6N	CDR: That's just a quick hand sample from the side of that crater. *** LMP: We're starting uphill now. Climb's fairly gentle at this point but it's definitely uphill. CDR: Okay, that sample from the west rim, of the crater, which we described as blocky, is in bag 6.
					EVA 2—Station: C′ (Prime)	
						CDR: Okay Houston. We are in the middle of a fairly large boulder field. It covers perhaps as much as a square mile. And, as the pan will show, I don't believe we have quite reached the rim [of Cone Crater] yet. However, we can't be too far away and I think certainly we'll find that these samples are pretty far down in Cone Crater. *** CDR: I would say, Houston, that most of the boulders are the same brownish gray that we've found. But we see one that is definitely almost white in color. Very definite difference in color, which we'll document. We noticed that beneath this dark-brown regolith, there is a very light-brown layer. And I think we'll get a core tube right here to show that. As a matter of fact, I think I'll do that right now.
14051	191.31	68–9443 XSB 68–9444 XSB 68–9445 DSB 68–9446 XSA 68–9447 LOC	Known	Known	A blocky, subrounded rock with all surfaces lightly covered by zap pits with or without glass linings. Spall-like fractures occur locally. Irregular to rounded cavities 1–3 mm across may be clast molds. The sample is a friable, fine-grained clastic rock having a small percentage of subrounded light and subordinate dark clasts in a medium-gray matrix.	LMP: This area that we're sampling in is a pretty darn rugged boulder-strewn area. One of the smaller rocks I've sampled is going into 7–N [14051–14052]. *** CDR: Okay. The core tube sample turned out to only be about three-quarters of a tube. The area is apparently very rocky, but I did get down into the second layer of the underlying layer of the regolith, which was white as opposed to being dark brown.
14052	2.89				Residue from bag 7N	*** CDR: On second thought, forget that core tube. It's too granular and most of the material came out of the tube. *** CDR: Hand me the shovel, please, Ed.
14068 14069 14070 14071 14072	35.47 24.87 36.56 2.16 45.06	64–9125 XSB 64–9126 XSB 64–9127 XSA	Known	Tentative for rocks	All rocks are blocky, angular to subrounded with very rough surfaces. 14068 appears to be shattered on one side, but otherwise the rocks are unfractured. All lack zap pits, but irregular vugs are moderately developed. The samples are fine-grained crystalline rocks with sparsely scattered large (to 1 mm) white grains.	CDR: Right now I'm sampling a layer that is sort of a light gray just under the regolith. That went in bag number 9 [14140–14143] and bag number 10 [14068–14072, 14144] was a sample of some of the surface rocks that were right around that area. It looks like a secondary impact that has disrupted the surface regolith and gone on down into the gray area. ***
14140 14141 14142 14143 14144	12.57 28.50 5.35 6.73 4.77				4–10 mm fines <1 mm fines 1–2 mm fines 2–4 mm fines unsorted fines	CDR: The first thing that we ought to do, if we want to drag the MET with us, is—see that white boulder down there. LMP: Yes. I saw it. Let's grab a— CDR: We can sample both types of boulders right down in that area, so let's go on down there. *** CDR: Okay. I guess we just run down there this way, huh?

TABLE 5.—*Cross-reference of lunar samples with locations, lunar-surface photographs, status of determining sample location and orientation, megascopic sample description, and comments by the astronaut crew during sample collection*—Continued

Sample Number	Weight (g)	Lunar-surface Photographs:[1,2]	Location Status	Orientation[3]	Sample description[4]	Crew comments[5]
					EVA 2—Station: C′ (Prime)—Continued	
						LMP: Yes. CDR: Okay. One of these boulders, Fredo, is broken open. They're really brown boulders on the outside, and the interface that's broken is white, and then another one that most of it is white. They are right in the same area. CC: Okay, Ed. I assume you're going to sample some of those. LMP: That's where we're headed right now. It's about 50 yards away. CDR: Why don't you go on down and start, and let me bring the MET down. LMP: All right. Yes. It's further than it looks.
					EVA 2—Station: C1	
						LMP: Okay, Fredo. I'm right in the midst of a whole pile of very large boulders here. (I'll) see what I can do to grab a meaningful sample. First of all, let me start photographing this whole area. LMP: They're awful darn big, but there's hardly anything that I can find. Let's see if I can chip one. ***
14082	62.63	68–9452 XSA 68–9453 XSA (After chipping but before bagging? Rock may be seen on fillet in 68–9452.)	Known	From surface pitting only	A blocky to slightly slabby, angular rock with a very rough surface. Glass-lined zap pits are very sparsely distributed over one surface. There are no fractures. The sample is a very friable, fine-grained clastic rock with a few percent of subrounded dark clasts in a very light gray matrix. Clasts are locally concentrated in a thin layer at one end of the specimen (14083).	LMP: I've chipped off one of the white rocks I put it in bag 13–N. [14082–14084]. I'll photograph it. There doesn't seem to be any samples of the white rocks lying around that are small enough for me to sample and be sure they're what I'm looking for.
14084	0.83				Residue from bag 13N	
14063 14064	135.45 107.53	No photographs	Approx.	Unknown	Blocky, subangular to subrounded rocks with a light to moderate density of glass-lined zap pits. Irregular fractures are poorly developed. A number of subrounded clast molds occur in both rocks. The samples are friable breccias having about 40 percent of subangular to subrounded clasts in a very light-gray fine-grained matrix. Dark clasts are subordinate to light clasts.	CDR: (I am) just going around picking up hand-size grab samples from the immediate vicinity of where Ed is operating. I have a couple that are going in bag 16 [14063–14065].
14065	7.72				Residue from bag 16N	
14321	8998.0	64–9128 XSB 64–9129 XSB	Approx.	Known	A blocky, subrounded rock with a moderately dense covering of glass-lined zap pits on all surfaces. Multiple irregular fractures are well developed along one edge of the sample. The rock is a coherent breccia with about 40 percent of blocky, angular to well-rounded clasts of which the great majority are dark. The matrix is very light gray.	CDR: There's a football-size rock, Houston, coming out of this area, which will not be bagged. It appears to be the prevalent rock of the boulders of the area. *** CDR: Put it right in here. LMP: I don't think it'll go. CDR: Yes. Core tube's out of the way. *** CDR: These boulders in this field appear to be very weathered, obviously not by atmosphere but eroded by some process, because they all show cracks. They show evidences of being broken up either by impact or subsequently. And it looks to me as though these rocks are really pretty old.
					EVA 2—Station: C2	
14053	251.32	64–9130 XSB 64–9131 XSB 64–9132 XSB 64–9133 XSB (Sample not identified)	Known	From surface pitting only	A blocky, subrounded rock with glass-lined zap pits on only one side. Vugs lined with a light colored mineral are present. The sample is an equigranular, fine-grained crystalline rock.	CDR: Okay. We're now out of the boulder field, Houston. And proceeding on down the flank. And, I believe—just get a shot—let's get a sample of that baby right there. Let's grab some from that one. LMP: Okay.
14054	0.52				Residue from bag 14N	CDR: We're just going to get a quick grab here of a rock. I'll photograph it because it's got some tremendous fillets on it. Don't hit the fillets until I photograph it, and let me get a quick shot there. Okay, and a quick pan across there. That looks like—Yes, we ought to get a piece of that baby. LMP: No, man; that's hard, hard, hard! Look at that *** in it. CDR: Yes. Okay, here's a piece of it. Bag? LMP: *** crystals here, don't lose it. LMP: Houston, the rock we're taking is in 14–N [14053–14054]. LMP: *** large filleted rock that Al photographed. Okay, let's go on.

TABLE 5.—*Cross-reference of lunar samples with locations, lunar-surface photographs, status of determining sample location and orientation, megascopic sample description, and comments by the astronaut crew during sample collection*—Continued

Sample Number	Weight (g)	Lunar-surface Photographs: [1,2]	Location Status	Orien-tation[3]	Sample description[4]	Crew comments[5]
					EVA 2—Station: Dg	
14311	3204.4	No photographs	Approx.	From surface pitting only	A blocky, subrounded rock broken into four pieces along irregular fractures. Irregular vugs are sparsely distributed through the rock. The sample is a coherent clastic rock with a few percent of subangular clasts, mostly light-colored, in a fine-grained crystalline groundmass.	CDR: Okay. I hate to make a grab here that's not from this crater. It looks like that cuts fairly deep, though. [Flank crater?] LMP: Yes. Here's a whole batch of them right down here, Al. Let's grab those. CDR: Which way, left or right? LMP: Off to the left ahead, around that little crater. They're all from this same area. CDR: Houston. Unable to see any stratigraphy in any of these craters. The slumping has been such that it's pretty much destroyed. LMP: I'll grab this one right here [14311?] *** LMP: As a matter of fact, I think this is Flank right here. CDR: Get it on board? LMP: Yes, I've got the rock on board [14311?].
					EVA 2—Station: E	
14055 14056 14057 14058 14059 14060 14061	110.99 6.38 5.51 4.53 8.68 2.50 3.11	No photographs	Approx.	Unknown, or from surface pitting only	14055, 14058 are blocky, subangular to subrounded rocks lightly covered with glass-lined zap pits. A few poorly developed irregular fractures occur. 14055 has about 15 to 20 percent of its surface coated by vesicular glass. The samples are friable, fine-grained clastic rocks with 5 to 15 percent of subrounded light-colored clasts in a medium-gray matrix. 14056, 14057, 14059, 14060, 14061 are blocky, subrounded rocks mostly lacking zap pits and fractures. The samples are very friable, fine-grained clastic rocks with less than 5 percent subrounded light-colored clasts in a medium gray to brownish-gray matrix.	LMP: This is a big crater. It's 40, 50 metres across. It has a fairly sharp crater in the south edge of it, which is— CC: Okay, that looks like it may be the one by E. LMP: —20, 30 feet across. Yes, I think that's it, Fredo. And it's—no, it's at least 50 or 60 feet deep. CDR: Why don't we just grab a couple from right here. LMP: Yes. Okay. CDR: That baby came apart. Very soft. LMP: Yes, it's falling apart as you pick it up; very crumbly, isn't it? CDR: Very, very soft rock—rim of that crater, plus another one very close to us with crystal in it, now going into bag—
14062	27.50				Residue from bag 15N	LMP: 15-N.
					EVA 2—Station: F	
14066	509.8	64–9137 Pan B may include sample	Approx.	Unknown	A blocky, subrounded rock whose rounded faces are heavily covered by glass-lined zap pits. The rock is very hackly at one end and has a few other irregular fractures. The sample is a moderately friable breccia having 15 to 20 percent of subangular dark clasts and a few light clasts in a fine-grained light-gray matrix.	LMP: Okay, I think this is Weird [crater] to our right here—forward, Al. See that fresh one right there? I think that's the fresh one of the Weird pattern. *** CDR: It looks too small, I believe. Well anyway, yes, we're in the area, Houston. We've got a minute to find it.
14067	7.66				Residue from bag 17N	CC: Okay, Al, I think the pan will fill us in as to the exact position. CDR: Okay, panning's underway, now. *** CDR: Did you get a grab sample, Ed? LMP: I just got some right up here, Al. LMP: This is in bag 17, Fred.
					EVA 2—Station: G	
						LMP: I think we're seeing the rim of the Triplet series right ahead of us, aren't we, Al? CDR: I would say so, yes. We can say that's the rim of the North [Triplet] right there. LMP: Yes. It's got boulders on it, and that's the only thing big enough to have boulders. We're probably about one diameter out right now. CDR: I'd say we are. Right here. *** CC: The number one item is the triple core [drive tube]. CDR: Okay. *** CDR: The three tabbed ones, we haven't used yet. Let me get them, Ed. *** CDR: Yes, I think that's the best way to go. Let's make them 1, 2, 3 for simplicity's sake.
14220	80.70	68–9454 XSD	Approx.	NA	First attempt at triple drive tube. Recovery only in the bottom section.	CDR: The bottom one will be number 1 tube with a tab [14220], Fredo, the other one will be number 2 with a tab. And the top one will be number 3 with a tab.
14414	5.50				Core bit.	*** LMP: Fredo, I've tried to push in the triple core tube. I get maybe 3 to 4 inches of pushing in by hand.

TABLE 5.—*Cross-reference of lunar samples with locations, lunar-surface photographs, status of determining sample location and orientation, megascopic sample description, and comments by the astronaut crew during sample collection*—Continued

EVA 2—Station: G—Continued

Sample Number	Weight (g)	Lunar-surface Photographs:[1,2]	Location Status	Orien-tation[3]	Sample description[4]	Crew comments[5]
						And it's just surface stuff; a very soft—it will not support the weight of the core tubes. Now, I've got it balanced, and I can take a picture of it, perhaps. LMP: Okay. We'll try to drive it. *** CC: And do I understand correctly, Ed; you're taking care of the triple core on your own there? LMP: That's affirm. Al's digging his trench. I'll go over and help him photograph it in a while. And it's not going in easy, Fred. LMP: I'll try driving it a bit more, but I think I'm on solid rock; and, I'm about one core tube down. *** CC: Okay. The recommendation, Ed, is to pull it up and move over a bit and try it again. LMP: The way this one feels, it'll be the same thing. CC: Okay. Ed; and when you pull it out, they'd like to save the bottom core [14220], and replace it with another one there before you try again. *** LMP: Core tube cap on that sample is in 18–N [14414]. *** LMP: Okay, and I have taken the bottom core of that one, which was core 1 flag; and it's now by itself [14220] as a single core tube; and I'm going to replace that with number 1 unflagged, which is the one Al started to use earlier but didn't get anywhere with it. CC: Okay. Number 1, unflagged, on the bottom. *** CC: Are you having any better luck on the triple core this time? LMP: I've got it in about half a tube. But I'm getting ready to take a picture of it so you can locate it; and then, we'll go ahead and drive it the rest of the way in. LMP: Okay, Fredo. There's three frames here probably 69, 70, 71, that are core tubes. The first one's the aborted one that I couldn't get in. The second picture is this new attempt, and a 15-foot shot that I raised up and took a locator shot on the horizon of it. I think it might go.
14230	76.7	68–9455 XSD 68–9456 XSD 68–9457 XSD 68–9458 XSD	Approx.	NA	Second attempt at triple drive tube. Recovery only in the bottom section.	LMP: Okay, I'm getting down low enough; I'm going to have to have an extension handle to finish driving it, I think. CDR: Okay, I'll give it back to you. I'm really kind of through with this trench *** LMP: And, Houston, I'm over 40 feet, 50 feet from where Al is; and on the east side of these craters, I have the triple core in about a tube and a quarter; and it's tightening up again. I just don't think it's going to go the rest of the way. I'm maybe driving a millimetre a stroke. I'll hit it a few more licks, and I'll see if we can break through or move it a little more. No, that's as far as it is going, Houston; one and a quarter. [14230]. CC: Okay, Ed. We'll just take your judgment on that; when you don't think you can get it in any further, you can stop there. *** LMP: I'll take a final picture of it, to show you how far we got with it. *** LMP: Okay, Fredo, the bottom bit on this was 23? Isn't it, Al? That's the one you did. CDR: Twenty-three [Not returned]. *** LMP: And, Fredo, the triple core tube, the second core didn't have anything in it. As soon as I opened it up, a little bit fell out, and the second core tube is empty. *** LMP: Even though it drove in about 3 inches it didn't get anything.
14145 14146 14147 14148	0.92 2.82 1.67 71.65	64–9158 XSB 64–9159 XSB 64–9160 XSA 64–9161 XSA 64–9162 XSA 64–9163 XSA 64–9164 XSA 64–9165 XSA 64–9166 DSA	Known	NA	4–10 mm fines, top of trench. 1–2 mm fines, top of trench. 2–4 mm fines, top of trench. <1 mm fines, top of trench.	CDR: I've got a trench here. I'ts going easily, but I need the extension handle to get it deeper. I'm cutting into the rim of a crater which is approximately 6 metres in diameter, has a depth of about three-quarters of a metre. And we're back in about one diameter away from the north—Triplet. The trench is going through at least three layers that I can see. The fine-grain surface, dark browns; then, a layer of what appears to be quite a bit of black; and then, a third layer of some very light material. And, we should be able to sample all three of these. *** CDR: We did not mention this white layer down in this area before that was so obvious to us just below the surface up near the flank of Cone. But it appears as though it is relatively deep, as far as visual observation is concerned. And

TABLE 5.—*Cross-reference of lunar samples with locations, lunar-surface photographs, status of determining sample location and orientation, megascopic sample description, and comments by the astronaut crew during sample collection*—Continued

Sample Number	Weight (g)	Lunar-surface Photographs:[1,2]	Location Status	Orien-tation[3]	Sample description[4]	Crew comments[5]
EVA 2—Station: G—Continued						
						certainly not any would be picked up by footprints, or tracks or the like. But there appears to be some of that here in this trench. *** CDR: You know what's happening in this trench; surface fines are so loose that they're just falling down covering the layering that we want to get. I'll tell you, we're not going to get a classic vertical wall here, Houston, on this trench. *** CDR: Okay, Fred. Bag 19 for the sample of the fine—that is, from the surface layer of the trench. [14145–14148] ***
14080 14081	1.94 0.84				Rock chips from middle of trench; extremely irregular, angular rocks with very sparse zap pits. The rocks are not fractured, but some surfaces have slickensides. The samples are composed of fragments of fine-grained clastic rocks with sparse light-colored clasts loosely bonded by highly vesicular glass.	CDR: I am unable to take from the walls of the trench the blocky type of material that I could see when I was digging; so, I'll just get a bag full of that, and we'll mix the surface with the second layer. CC: Roger, Al. How deep did you finally end up getting down? CDR: Well, the trench is about a foot and a half deep. I gave up actually not because it was hard digging, but because the walls kept falling in on it; and it was covering all the evidence of stratigraphy.
14153 14154 14155 14156	3.91 5.49 3.69 137.98				2–4 mm fines, middle of trench. 1–2 mm fines, middle of trench. 4–10 mm fines, middle of trench. <1 mm fines, middle of trench.	CDR: *** and bag 21 [14080–14081; 14153–14156] is kind of a collection of the combination of the top two layers. Second layer is a thin layer of small glassy-like pebbles. I was unable to separate them by the trench method, so I gave it to you mixed up in that bag; and the last bag will be pebbles from the bottom layer. CC: Okay, Al. What's the thickness of the intermediate layer there? CDR: Well, it's really ephemeral*** it's very thin. I would say no more than a quarter of an inch thick, and I just noticed it because of the difference of the grain structure as I was digging the trench. *** CDR: And in bag 20, we'll fill a sample of the bottom material; also, mixed up with some of the surface material (that) has fallen down in on top of it. And that's about 18 inches below surface. [14073–14079; 14149–14152].
14073 14074 14075 14076 14077 14078 14079	10.35 5.16 4.66 2.00 2.77 8.30 3.17				Bottom/trench 14073, 14074, 14078, 14079. Blocky, subangular to subrounded rocks lacking fractures and pits. The samples are light gray, equigranular fine-grained crystalline rocks. 14076. A blocky subangular, smooth-surfaced rock lacking zap pits. One set of fractures cuts the rock parallel to its long axis. The sample is a coherent heterogeneous clastic rock, one end being a gray matrix, and the other end is a fine-grained clastic rock with sparse dark clasts in a light gray matrix. The contact between the two lithologies is sharp but irregular. 14077. A blocky, subrounded rock with a moderately rough surface. Fractures or zap pits occur. Irregular vugs are sparsely distributed over the surface. The sample is a light gray, fine-grained inequigranular crystalline rock with sparse large white grains.	
14149 14150 14151 14152	88.15 11.08 11.70 11.39				<1 mm fines, bottom of trench. 4–10 mm fines, bottom of trench. 1–2 mm fines, bottom of trench. 2–4 mm fines, bottom of trench.	
14240 (SESC)	168.0	Trench Documentation 64–9158 XSB 64–9159 XSB 64–9160 XSA 64–9161 XSA 64–9162 XSA 64–9163 XSA 64–9164 XSA 64–9165 XSA 64–9166 DSA	Known	NA	Fines from bottom of trench.	CC: Okay. And, Al, one question, did you get the SESC [Special Environmental Sample Container] sample out of the bottom of the trench? CDR: Well, I told you the trench was kind a miserable thing, because the walls kept falling down. And I could get a sample from the bottom, but it wouldn't be the bottom, I'm afraid. *** CC: I guess we'd still like the SESC sample from the bottom of the trench, even though it probably isn't the bottom. CDR: Well, I'll tell you, I'll go back and whack at it a little bit. See what I can do. *** CDR: We're digging the bottom of the trench for you, Fredo. CDR: I'm redigging the trench. *** CDR: I can't believe it. LMP: What's the matter, Al? CDR: Oh, that [vacuum] seal came off that thing. ***
14310	3439.0	No photographs	Approx.	From surface pitting only	A blocky rock with two rounded surfaces heavily covered by zap pits and the remaining faces free of zap pits and joining along sharply angular edges. Irregular vugs are sparsely distributed through the rock. The sample is a fine-grained, medium gray equigranular crystalline rock.	CDR: And a very interesting looking rock with really fine-grain crystals in it. It's a grab sample, Houston, from that same crater in which I'm digging. It's too large for a bag; it's dark brown; dark part is fractured. Its fracture face is very light gray with very small crystals. [14310] LMP: Okay. Documented samples coming up. CDR: These white rocks on the rim here? LMP: Yes. Document some of that. Here's a rock right here. CC: Okay, has Al moved over by the rim of North Crater now? LMP: Oh, no, we're still at the same place [station G]. That's pretty well disturbed, Al; I'll grab it without much documentation. ***

TABLE 5.—*Cross-reference of lunar samples with locations, lunar-surface photographs, status of determining sample location and orientation, megascopic sample description, and comments by the astronaut crew during sample collection*—Continued

Sample Number	Weight (g)	Lunar-surface Photographs:[1,2]	Location Status	Orien-tation[3]	Sample description[4]	Crew comments[5]
			EVA 2—Station: G —Continued			
14307	155.0	No photographs	Approx.	From surface pitting only	A blocky, slightly slabby, angular rock cut by multiple irregular fractures. The sample is a moderately coherent breccia with about 20 percent of subangular to subrounded light clasts in a fine-grained medium gray matrix. Seriate size distribution of light clasts is apparent. There appears to be a weak foliation of clasts approximately parallel to the flat side of the rock.	LMP: I'm picking up one of the so-called whiter rocks, Fredo, near the area where Al is digging. Since it's already disturbed, I'm not going to waste time on much documentation [14307]. *** LMP: It's going into 25 Nancy.
14306	584.5	68–9459 DSB 68–9460 XSB 68–9461 XSB 68–9462 XSA 68–9463 XSA 68–9464 LOC	Known	Known	A blocky, subangular rock with one flat face lightly covered by glass-lined zap pits and remaining rounded faces more densely covered by pits. A prominent planar fracture, lined by vesicular glass, makes an angle of about 20 degrees with the long axis of the sample. The rock split along this fracture exposing part of the fracture surface and its glass coating. A poorly developed set of planar fractures at an angle of 65 degrees to the prominent fracture. The rock is a coherent breccia having 25 or more percent of irregular, blocky to slabby, angular to subrounded light clasts in a medium gray matrix. The glass-lined fracture appears to cut matrix and clasts alike.	LMP: One more documented sample. CC: Okay, there is a special request. Rather than grab samples at the North Crater rim there, they'd like to get a documented sample of a partially buried rock. LMP: Okay. I was going to try to get you one of those right here, but it looks pretty big. I think maybe I can get it anyhow. *** LMP: This documented sample that I got of the buried rock, it's too big for regular weigh bags. See what I can do with it. A regular sample bag—I'm sticking one over it, but it'll never close. Okay, it's going in it. And will probably stay, but it won't close. *** LMP: It's bag 26–N [14306].
			EVA 2—Station: G1			
						CC: Ed and Al, we're going to have to be departing Triplet [Station G] here with that one brief stop at the North rim to pick up one documented sample [Station G1]. *** LMP: We're approaching Triplet from the east, that's North Triplet from the east. There's a little rock field down here—a small boulder field, Al. Want to get a documented sample from it? CDR: Okay. LMP: Looks good. Yes, looks like they might have come from there. *** CDR: Man, that pile of rocks right to your left. Oh, just the right size. LMP: Okay. LMP: Are these the ones over here? *** LMP: Gnomon is in place. LMP: I'm on this side; I'll get the stereo. LMP: Get the locator. *** CDR: Okay. CDR: All covered with—
14301	1360.6	64–9188 DSLOC,B 68–9466 XSB 68–9467 XSA	Known	Known	A blocky, subrounded rock with a moderately dense cover of glass-lined zap pits. Several irregular fractures cut the rock and spalling along two intersecting fractures left a V-shaped protuberance on one side of the rock. The sample is a coherent medium gray clastic rock with sparse subangular light clasts and less abundant dark clasts in a fine-grained matrix.	LMP: Yes. It's bigger than we thought. Al, we'll grab sample that one [14301]; I'll get you another one here. CDR: Okay. Listen, just put it in that thing. And let's press—because we don't have the time. LMP: All right. I'll grab it, and let me take an extra picture here.
14313	144.0	64–9188 DSLOC,B 68–9465 XSB 68–9466 XSB 68–9467 XSA	Known	Known	A blocky, subangular rock with a prominent notch produced by spalling along two sets of fractures intersecting at an angle of 105 degrees. All surfaces have a light to moderate density of glass-lined zap pits. The rock is a coherent brecia having about 10 percent of well-rounded to subangular clasts in a medium gray matrix. Both light and dark clasts occur, but there are fewer dark clasts.	CDR: All right. I'll grab one right here in the foreground [14313]. *** CDR: Okay, bag 27 Nancy. LMP: And another documented sample *** larger documented sample than we thought we were getting here, Fredo. Again, it was a buried rock; and it's too big for the sample bag; so, it'll go into the weigh bag [14301]. *** LMP: It has a very definite shape; I think you'll be able to sort it out [14313]. CC: Okay, Al and Ed. I guess we can skip the rim of North Crater and proceed right on back to the LM area. LMP: Okay. That's where we are. We're at the rim of North Crater.
			EVA 2—Station: H			
						CDR: Okay, we're approaching the LM now. Coming in at Fra Mauro Base. CC: Roger, Al, and I guess from here, we can split up; and Ed can take the MET and proceed to the cluster of boulders he had reported earlier

TABLE 5.—*Cross-reference of lunar samples with locations, lunar-surface photographs, status of determining sample location and orientation, megascopic sample description, and comments by the astronaut crew during sample collection*—Continued

EVA 2—Station: H—Continued

Sample Number	Weight (g)	Lunar-surface Photographs:[1,2]	Location Status	Orientation[3]	Sample description[4]	Crew comments[5]
						to the north of the LM; and you can proceed out to the ALSEP. *** LMP: I'll just take a couple of rock bags, put on my tongs and camera, and go. *** LMP: As a matter of fact, Fredo, I'm just going to take a weigh bag [1038] and no sample bag; that way I can get more. The size of these rocks—the sample bags are too small, anyhow. ***
14312	299.0	68–9472 XSB 68–9473 XSB 68–9474 XSB 68–9475 XSB 68–9476 XSA 68–9478 Pan A 68–9479 Pan A	Known	Known	(Eastern rock from top of Turtle Rock) A blocky, angular rock cut by irregular fractures parallel to the long axis of the rock. Glass-lined zap pits are moderately dense on all surfaces. The rock is a coherent breccia with a moderate percentage of angular dark clasts which tend to blend with the light gray matrix. A very few light clasts are present.	LMP: Okay, Fredo, my plan: I'm out in the area of the boulder field; I'm going to photograph many of the boulders, the rocks, the broken ones, the big ones, what have you, and then, grab as many of the different fragments as I can around these piles of broken boulders. Now that I'm here, I see a large number of inclusions. I can't tell whether they're crystals or not. I think that they are. And I'll grab as many of these—and give you before and after shots—as I can of a whole weigh bag full of rocks. ***
14314	115.7	68–9472 XSB 68–9473 XSB 68–9474 XSB 68–9475 XSB 68–9476 XSA	Tentative	Unknown	(Rock taken from fillet below Turtle Rock) A slabby, angular rock with no apparent zap pits. All surfaces appear immature. Several irregular fractures are parallel to the flat surface of the slab. The slabby shape of the rock appears to be controlled by fractures. The rock is a coherent breccia with a medium gray matrix and a moderate percentage of light and dark clasts. Light clasts appear to be predominate.	LMP: Okay, Fredo, I'm heading back from the boulder field. I've sampled two of the larger boulders in the area. Rocks broken from them and lying on them; and I've taken a pan; and I have maybe a third of a weigh bag full of small rocks from these boulders.
14315	115.0	68–9468 XSB 68–9469 XSB 68–9470 XSA 68–9471 XSA	Known	Tentative from lab model	A domical, blocky rock with one nearly flat non-pitted side and the rest rounded and heavily pitted. A set of closely spaced fractures makes angles of 10 to 15 degrees with the flat surface of the rock. The rock is a coherent breccia in which light clasts are dominant. The estimated percentage of clasts is 40 percent. The matrix is medium gray.	
14316	38.2	Not identified in North Boulder field photographs	Tentative	Unknown	A subslabby, subangular rock with one flat surface free of pits and the rest rounded and irregular with numerous glass-lined pits. Planar to subplanar glass-lined fractures are parallel to the flat surface of the rock and the rock has broken along one of these. The rock is a coherent breccia with an estimated 20 percent of blocky subangular to rounded clasts in a medium gray matrix. The clasts are dominantly light. One medium gray clast itself contains white clasts, probably clastic feldspar. One light clast contains lighter clasts.	
14317	16.1	Not identified in North Boulder field photographs	Tentative	Unknown	A slabby, angular rock with no apparent zap pits. All surfaces appear immature. A few irregular fractures are parallel to the flat surface of the slab. The rock is a coherent breccia with a small percentage of light clasts up to 3 mm across. The matrix is fine-grained and gray.	
14318	600.2	68–9468 XSB 68–9469 XSB 68–9470 XSA 68–9471 XSA	Known	Known	A blocky, angular rock, heavily pitted on all sides. A series of well developed, parallel fractures is parallel to one surface of the rock and the long axis. The rock has broken along one of these fractures and no pits are present on the broken vesicular glass. The glass-lined fractures appear to cut clasts and matrix alike. The rock is a tightly coherent breccia with an estimated 50 percent clasts. Of these 60 percent are judged to be light and 40 percent dark or mesocratic. One light clast has a dark clast within it and several dark clasts contain light clasts.	
14319	211.6	68–9472 XSB 68–9473 XSB 68–9474 XSB 68–9475 XSB 68–9476 XSA 68–9478 Pan A 68–9479 Pan A	Known	Known	(Western rock from top of Turtle Rock) A blocky, angular rock with a highly irregular surface. There is a low density of glass-lined zap pits on 3 faces of the rock which are somewhat rounded. The rest of the surface has no pits. One face is extremely fresh. Several irregular fractures cut the rock at a variety of angles. The rock is a coherent breccia that is broken apart along fractures. Clasts make up 30 percent of the rock and dark clasts are by far the dominant type. Some of these have white clasts within them.	
14320	64.9	Not identified in North Boulder Field photographs	Tentative	Unknown	A slabby, angular rock. One side appears fresher than the rest but sides have about the same high density of glass-lined pits. Several irregular fractures occur at odd angles to the long axis. The rock is a coherent breccia with a moderate percentage of clasts. Most of the clasts are dark;	

TABLE 5.—*Cross-reference of lunar samples with locations, lunar-surface photographs, status of determining sample location and orientation, megascopic sample description, and comments by the astronaut crew during sample collection*—Continued

Sample Number	Weight (g)	Lunar-surface Photographs:[1,2]	Location Status	Orientation[3]	Sample description[4]	Crew comments[5]
EVA 2—Station: H—Continued						
					only a few percent are light. The matrix is light gray.	
14290–14297					Residue from weigh bag 1038; probably material collected with or broken from rock samples collected at Station H, the North Boulder Field.	
14290	23.63				<1 mm fines	
14291	2.12				1–2 mm fines	
14292	3.53				2–4 mm fines	
14293	5.20				4–10 mm fines	
14294	3.43				rock chip	
14295	1.24				rock chip	
14296	2.26				rock chip	
14297	1.73				rock chip	
EVA 2—Station: Unknown						
14309	42.40	No photographs	Unknown	Unknown	A slabby subrounded rock cut by a few irregular fractures. Only a few zap pits are present. One face is irregular and may be a freshly broken surface. The rock is a moderately coherent breccia with a moderate percentage of subrounded dark clasts in a light gray matrix. A few feldspar clasts (up to 3 mm long) are present. (Location unknown: returned in weigh bag 1031 with other grab samples from EVA 2)	
14190–14204		No photographs	Unknown	Unknown	Residue from weigh bag 1031, used on the EVA 2 traverse.	
14190	34.85				<1 mm fines	
14191	5.92				1–2 mm fines	
14192	8.06				2–4 mm fines	
14193	11.15				4–10 mm fines	
14194	4.28				rock chip	
14195	2.77				rock chip	
14196	3.93				rock chip	
14197	1.63				rock chip	
14198	1.63				rock chip	
14199	1.88				rock chip	
14200	1.24				rock chip	
14201	1.56				rock chip	
14202	0.05				residue, weigh bag 1031	
14204	21.60				residue, weigh bag 1031	

[1]NASA photograph numbers include the magazine and frame numbers, but to save space the normal prefix, AS14–, has been omitted.

[2]The type of photograph refers most commonly to the viewing direction of the photograph with respect to the sun (DS, XS, US; down sun, cross sun, and up sun), and indicating whether the photograph was taken before, during, or after collecting the sample (B, D, A). Some sample documentation is included in individual frames within panoramas. Locator (LOC) photographs are those which show the horizon and some distinctive feature to show the setting of the sample site.

[3]Rock orientation at the time of sampling is considered to be known only if the sample can be recognized in a presampling documentary photograph, from which a reconstruction of the lighting and shadow characteristics can be nearly duplicated using oblique lighting in the laboratory. Surface characteristics such as rounding and pitting, coatings of dust or glass, and fresh fracturing record the exposure history of a fragment at the lunar surface, although these are not reliable indicators to define the exact orientation at the time of collection.

[4]Rocks only are described. Soils, drive tubes, small rock chips, and residues are identified without description. Rock descriptions are by H. G. Wilshire, based primarily on interpretation from LRL mugshot photographs (see also Warner and Duke, 1971).

[5]Excerpts are from the Apollo 14 air-to-ground voice transcription. The sequence of comments is in the order of events during the mission, except where later statements may clarify the documentation of certain samples. Three asterisks (***) indicate omitted dialogue.

Probable origin: Possibly ejected from one of the Triplet craters
Comments: Possibly represents smooth Fra Mauro unit from as deep as 20–25 m. Glass fills one prominent fracture

14312, 14319 (FIGS. 70, 71, 72, 73)

Station: H (Turtle Rock, North Boulder Field)
Location: 80 m NW of LM
Rock type: Coherent clastic breccia

SAMPLE AREA CHARACTERISTICS

Slopes: Flat level regolith surface
Fragment population:
Distribution and size range: Fairly abundant, from limit of resolution to 1.5 m
Color: Medium gray with lighter and darker gray clasts up to 10 cm in size
Shapes: Subangular to subrounded
Fillets: Moderate on smaller fragments on regolith; well-developed on Turtle Rock
Apparent burial: ¼–½
Dust cover: Moderate to heavy
Fines:
Color: Light to medium gray
Compaction: Moderately high
Craters:
Distribution and size range: Abundant from 0.1 to 1.3 m
Shape: Subdued to fresh
Ejecta: Debris associated with 1.3 m crater 1 m north of Turtle Rock and other boulders in area probably ejected from Cone crater

SAMPLE CHARACTERISTICS

Sample 14312
Size: 9×6×4 cm; 299 g
Color: Medium gray with brownish tint
Shape: Blocky, subrounded
Fillet: None
Apparent burial: None
Dust cover: Slight
Comparison with other rocks in area: Appears similar to Turtle Rock and smaller rocks in area

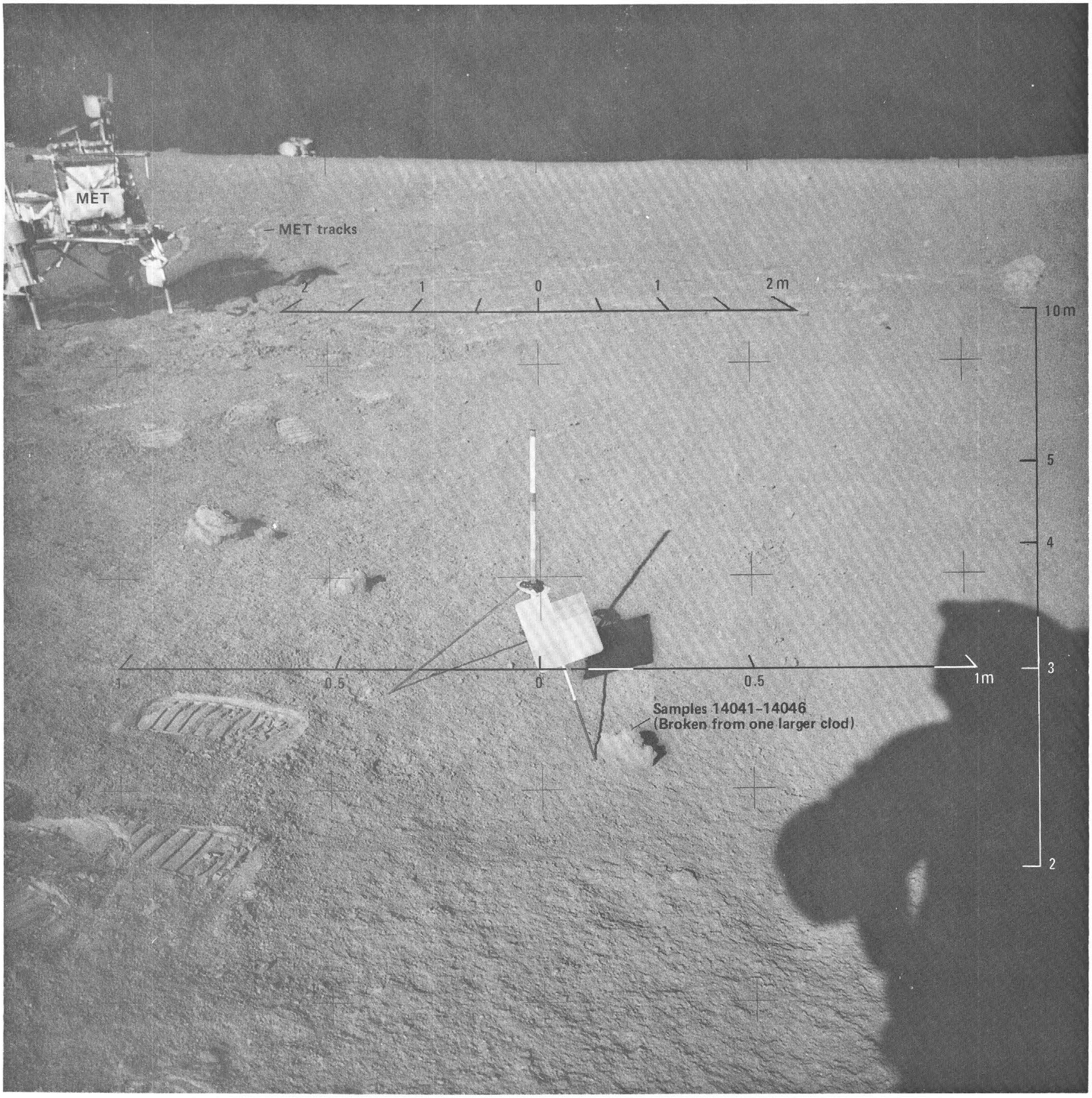

FIGURE 49.—Samples 14041–14046, originally one unbroken, poorly consolidated breccia clod at station A. The clod broke up during collection. Location photograph looking west showing the LM on the horizon. (NASA photograph AS14–68–9409.)

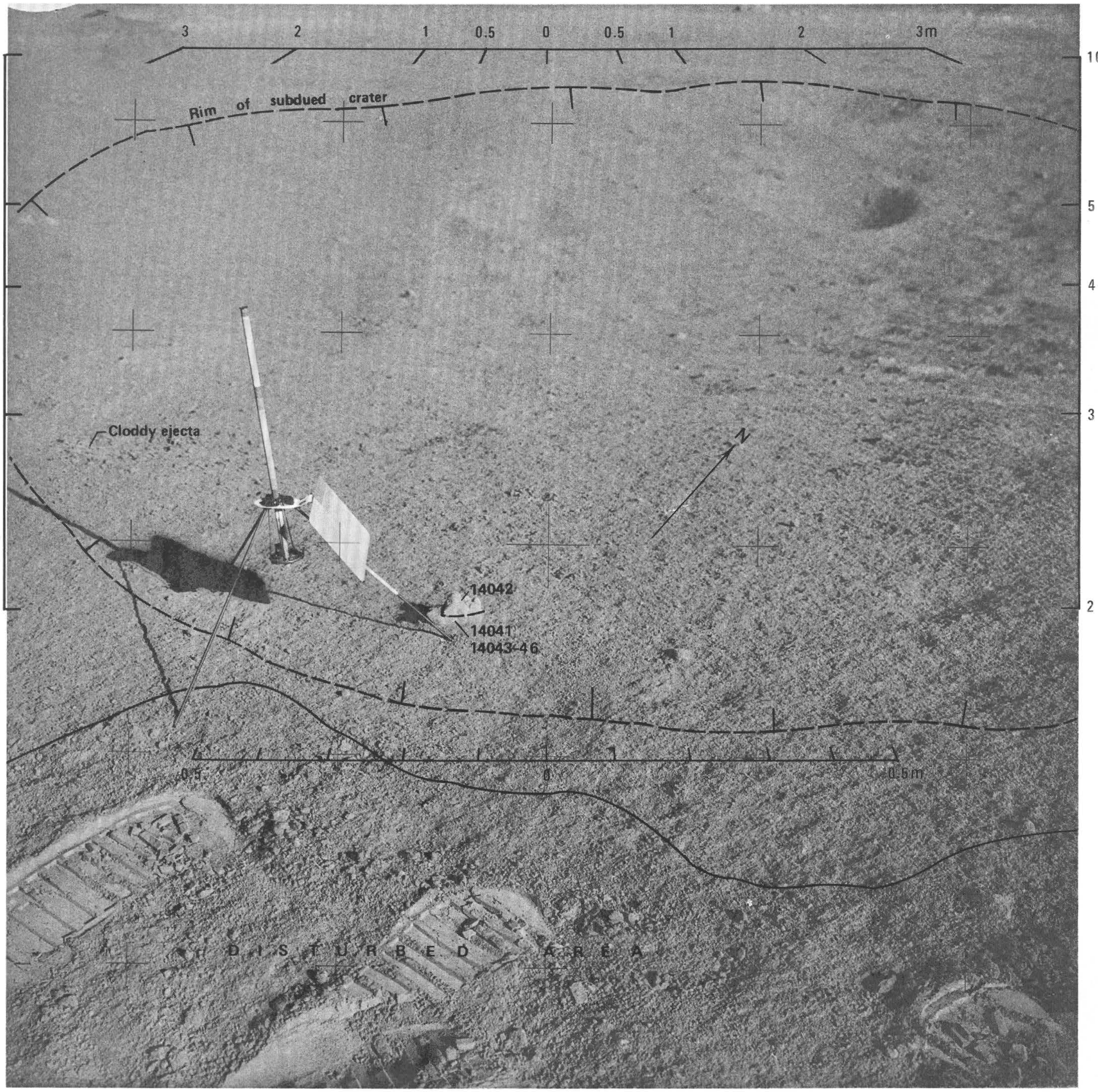

FIGURE 50.—Samples 14041–14046 in their reconstructed approximate position in the poorly consolidated breccia clod from which they broke during collection. Photograph taken before sampling; view northwest, oblique to sun. (NASA photograph AS14–68–9411.)

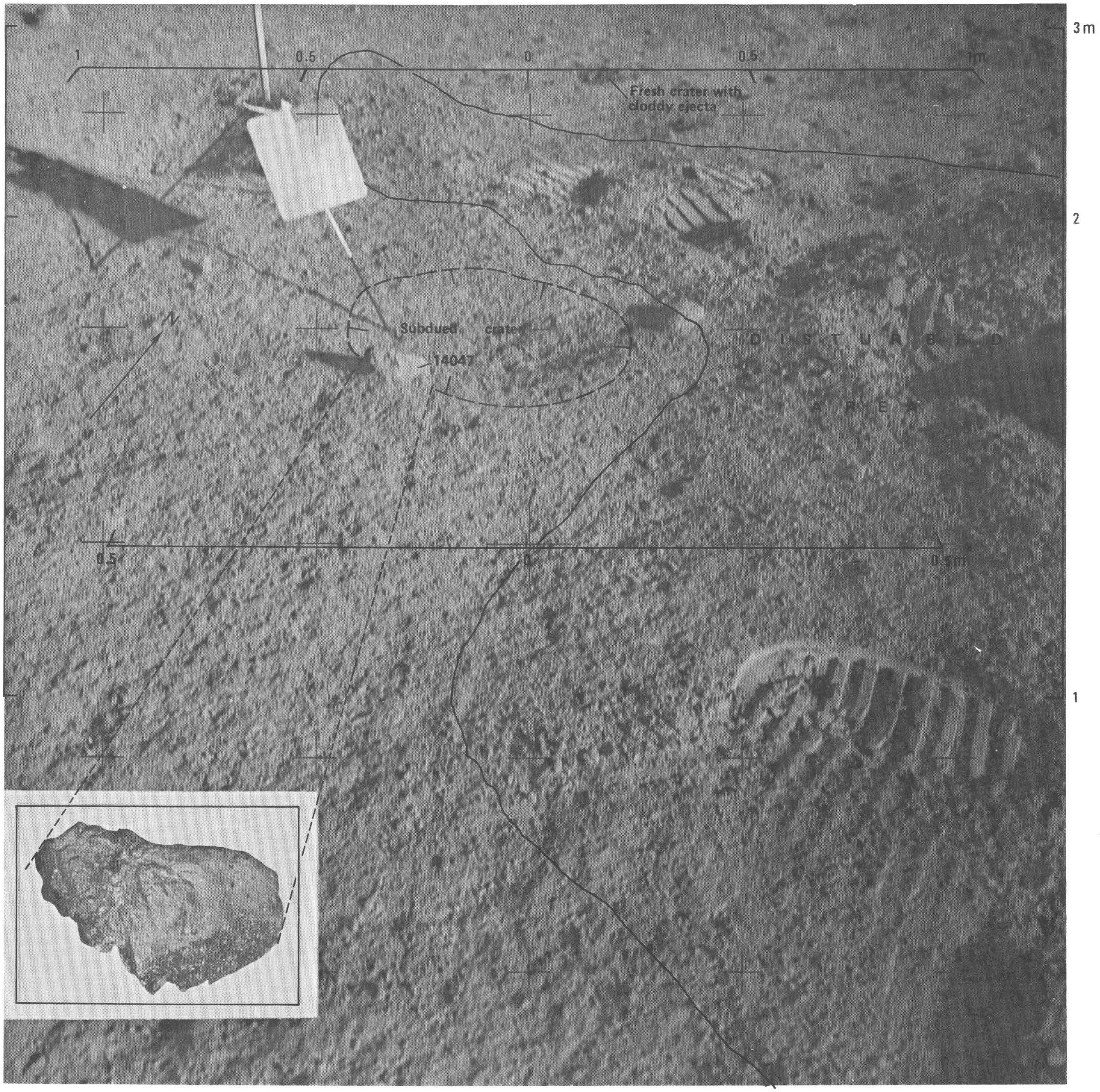

FIGURE 51.—Sample 14047 and vicinity before sampling. View northwest. (NASA photograph AS14–64–9073.) Inset shows approximate lunar orientation using LRL photograph S–71–20769.

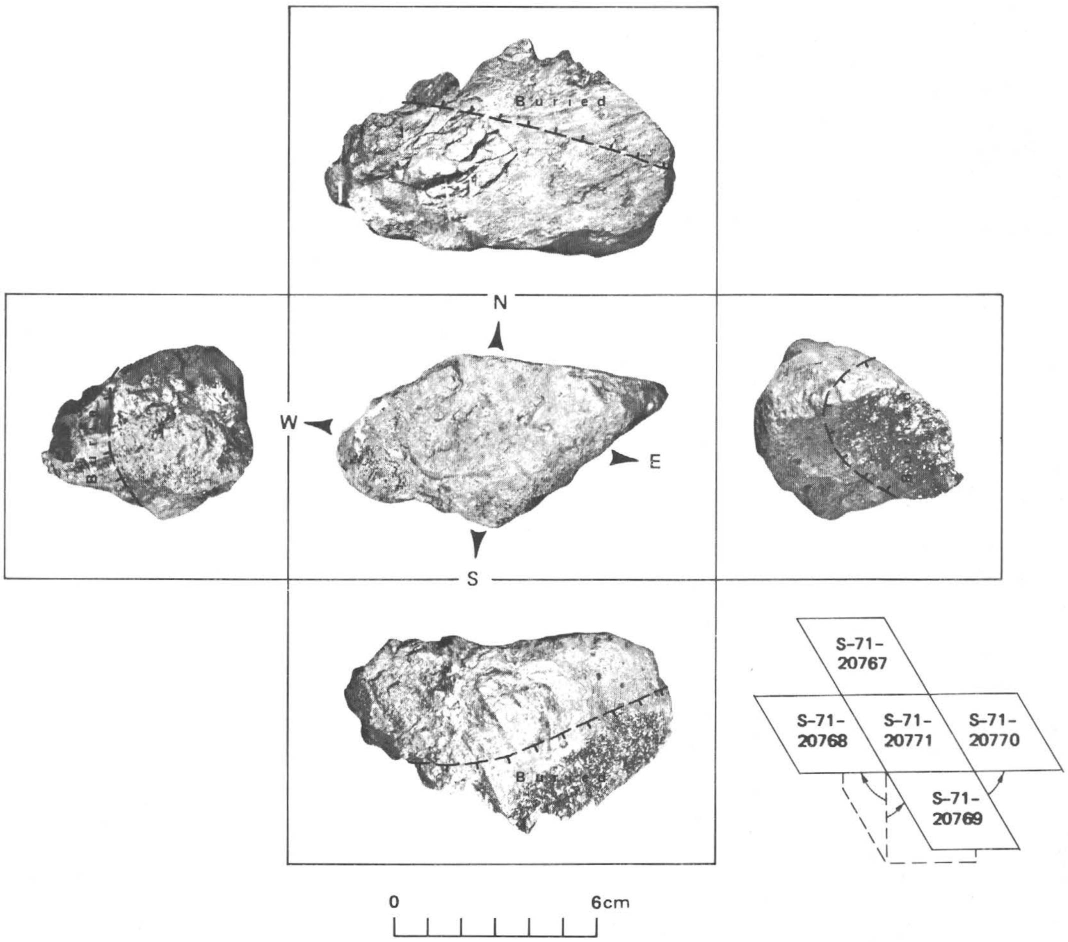

FIGURE 52.—Orthogonal views of sample 14047, shown in approximate lunar orientation. NASA photograph numbers are shown in the schematic diagram. The glass-covered surface of the rock was buried at the time of sample collection.

Probable origin: Ejected from Cone crater
Comments: Zap pits on all sides indicate that if spalled from Turtle Rock, 14312 was turned over later or else fell onto Turtle Rock from elsewhere

TABLE 6.—*Usage of film on the lunar surface during the Apollo 14 mission*

EVA	Mag	Film	Frames	EVA total
pre-EVA	KK	BW	14	14
1	II	Color	88	
1	JJ	Color	33	121
1–2	II	Color	16	16
2	LL	BW	156	
2	MM	BW	99	255
post-EVA	II	Color	11	11

Total color	148
Total black and white	269
Total	417

Sample 14319
Size: 8×5.5×3.9 cm; 211.6 g
Color: Light medium gray on fresh surface
Shape: Rounded on all but one side which is flat
Fillet: None
Apparent burial: None
Dust cover: Slight
Comparison with other rocks in area: Appears similar to Turtle Rock and other fragments in area
Probable origin: Cone crater; may be spalled from Turtle Rock by impact; vein glass on flat underside may be same as resistant ledge under sample (Fig. 71)

14314, AND UNIDENTIFIED SAMPLE (FIGS. 70, 71)

Station: H (Turtle Rock, North Boulder Field)
Location: 80 m NW of LM
Rock type: Coherent clastic breccia

SAMPLE AREA CHARACTERISTICS

(Turtle Rock fillet)

Slopes: 2–3° SE-sloping fillet on flat regolith
Fragment population: (on fillet)

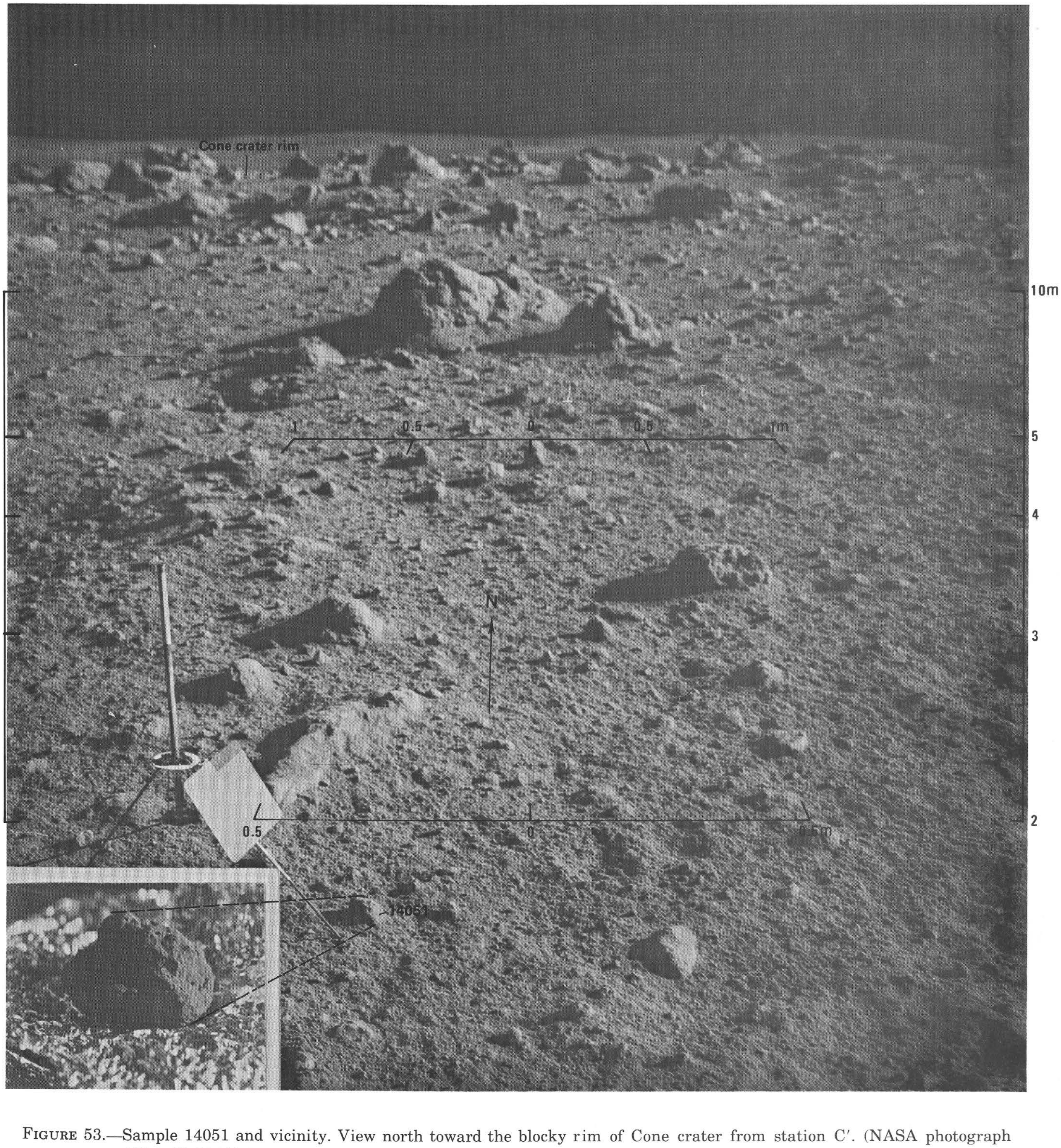

FIGURE 53.—Sample 14051 and vicinity. View north toward the blocky rim of Cone crater from station C′. (NASA photograph AS14–68–9444.) Inset shows approximate lunar orientation reconstructed in the LRL using oblique lighting.

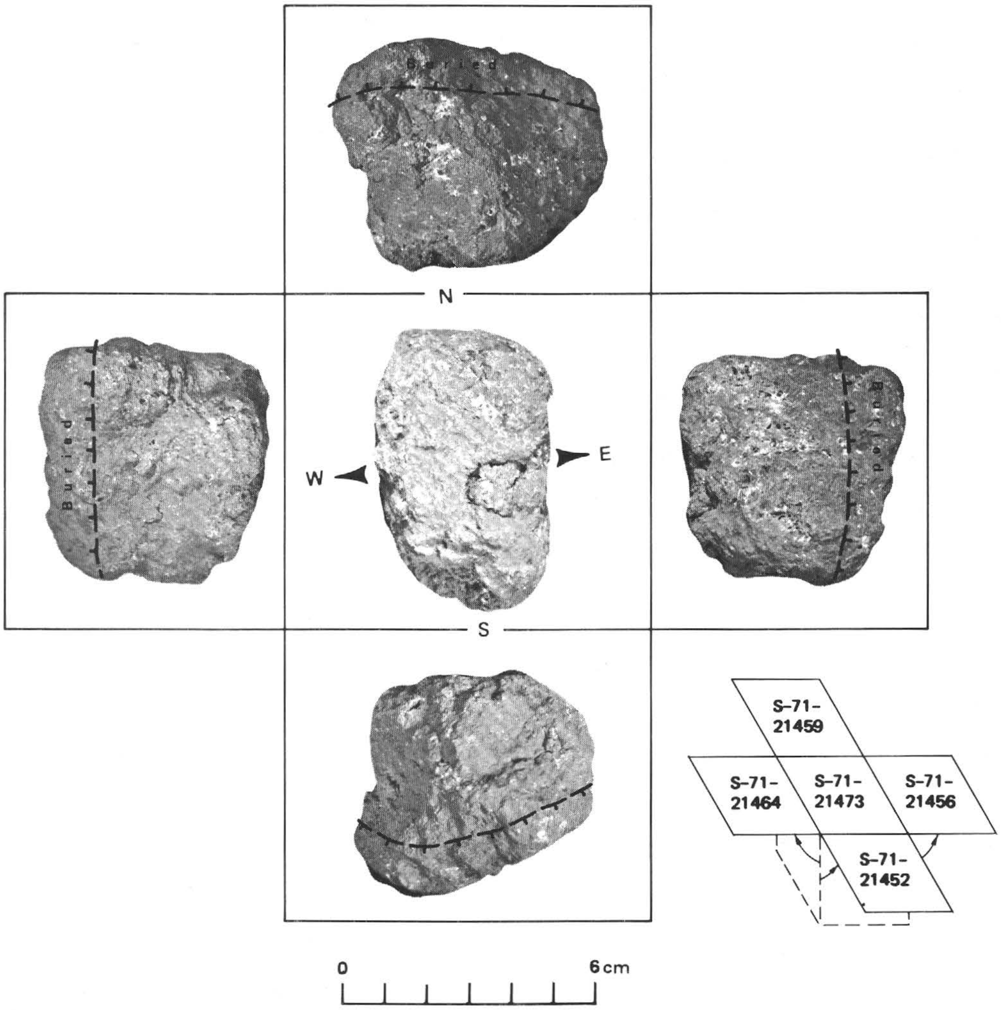

FIGURE 54.—Orthogonal views of sample 14051, shown in approximate lunar orientation. NASA photograph numbers are shown in the schematic diagram.

Distribution and size range: Abundant from limit of resolution to 30 cm
Color: Light medium gray with lighter and darker clasts
Shapes: Subrounded; irregular
Fillets: Poorly to moderately developed
Apparent burial: ¼–¾
Dust cover: Moderately high
Fines: (on fillet)
Color: Light to medium gray
Compaction: Moderately firm
Craters: (on fillet)
Distribution and size range: Very few, mostly less than 5 cm
Shape: Not discernible
Ejecta: Not discernible

SAMPLE CHARACTERISTICS

Sample 14314
Size: 7×5×3 cm; 115.7 g
Color: Fresh surface; medium to light gray; pitted surface, dark brownish gray
Shape: Irregular, slabby, rounded; fractured
Fillet: Moderately well developed
Apparent burial: ¼–⅓
Dust cover: Moderately heavy
Comparison with other rocks in area: Appears similar
Probable origin: Cone crater
Comments: May represent upper stratigraphic layer in Fra Mauro formation from the ridge impacted by the cone crater event. Unidentified sample which also may be from Turtle Rock probably 14316, 14317, or 14320

FIGURE 55.—Boulder at traverse station C2 from which sample 14053 was collected. The sample was reported to have been collected from the sunlit part of the boulder, approximately halfway up from the base. Note the light-colored clasts in the shadowed part of the boulder. Sample 14053, a crystalline rock, is thought to be a clast from this fragmental rock. The sample has not been recognized in this presampling photograph (NASA photograph AS14–64–9133.)

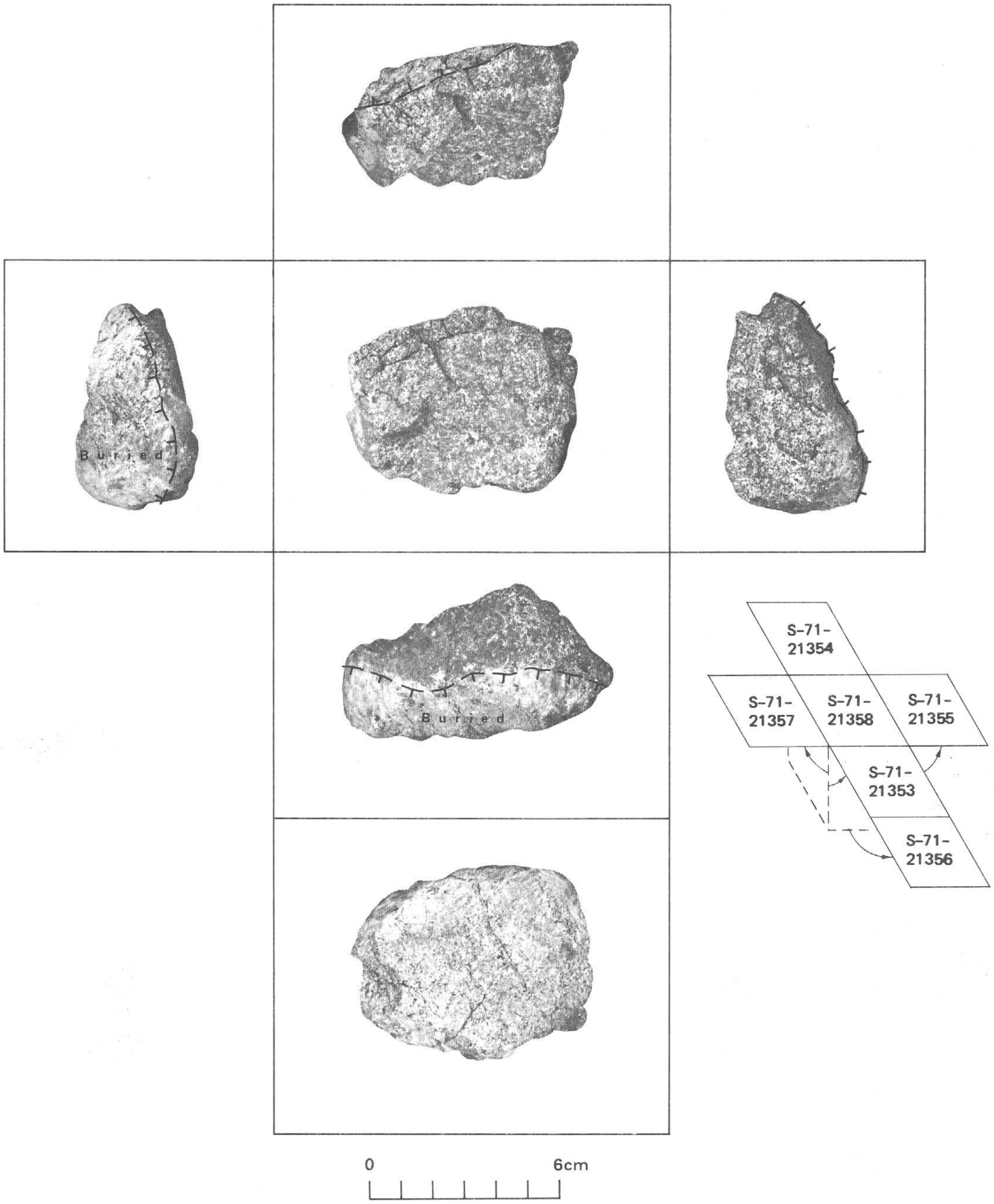

FIGURE 56.—Orthogonal views of sample 14053. The lunar orientation of the rock is not known, but weathered and unweathered parts of the rock suggest a burial line. NASA photograph numbers are shown in the schematic diagram.

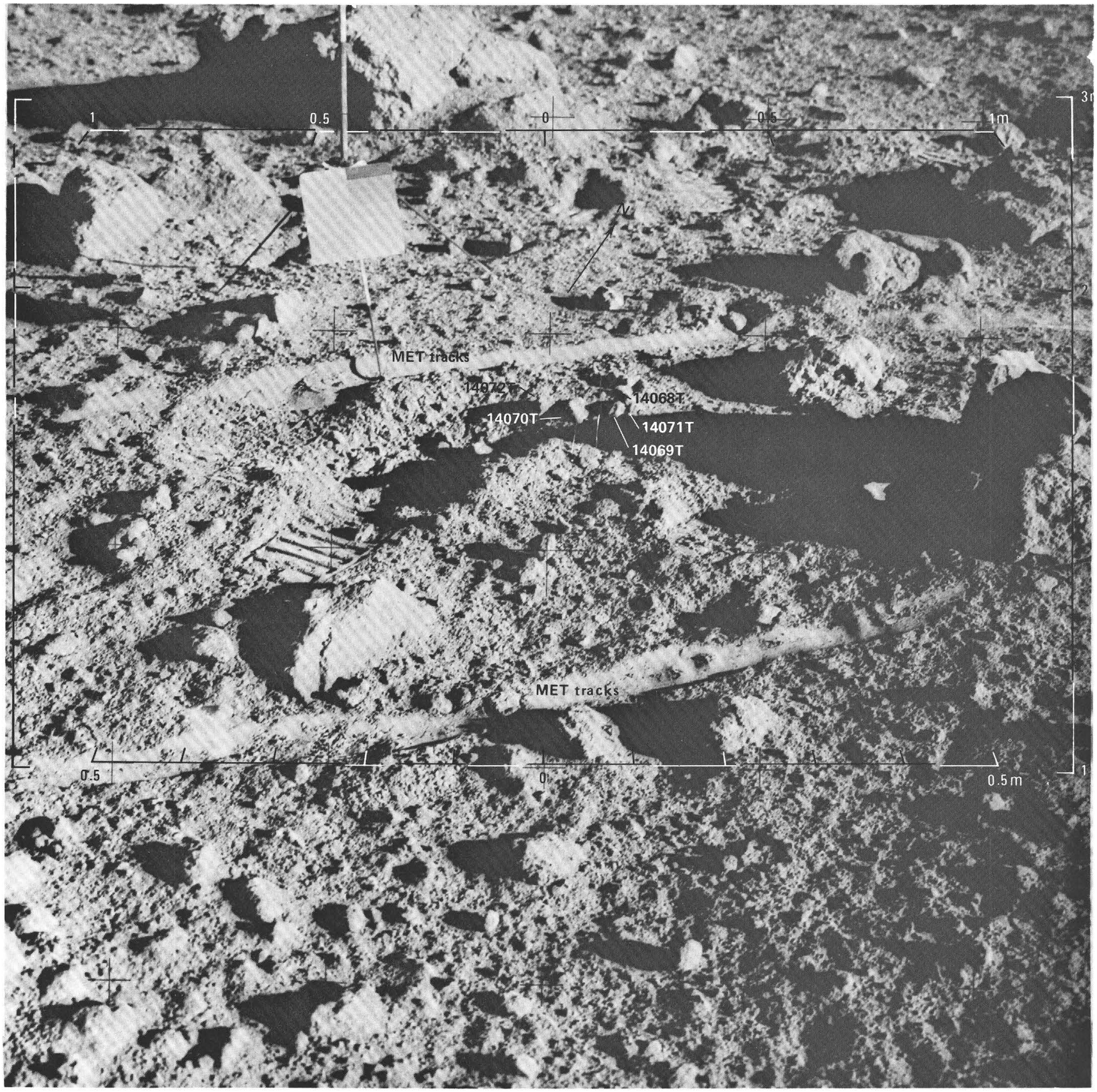

FIGURE 57.—Samples 14068–14072, small crystalline rocks collected from the blocky ejecta of Cone crater at station C′. View north. (NASA photograph AS14–64–9125.)

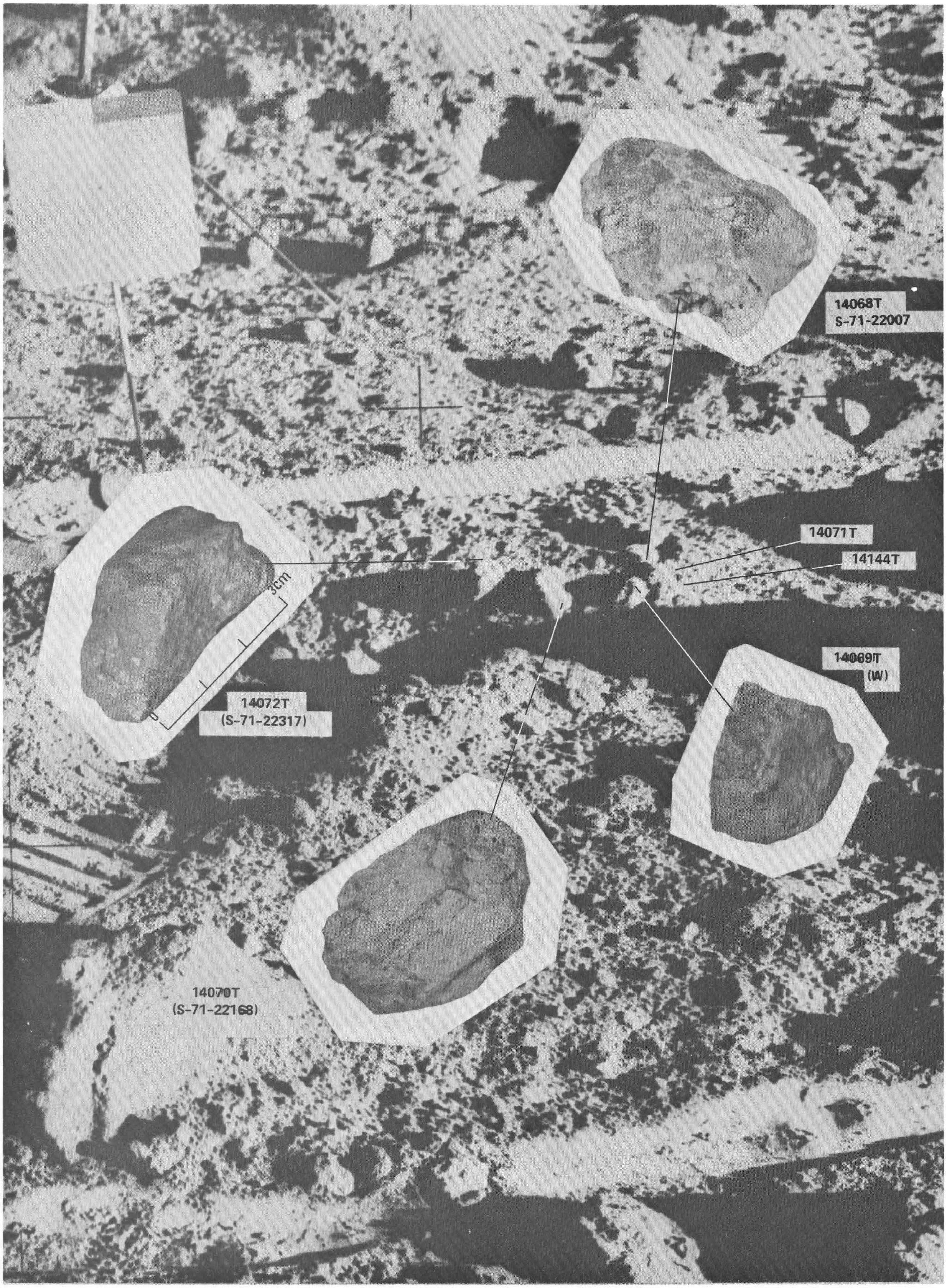

FIGURE 58.—Samples 14068–14072 photographed before collection. Inset photographs show correlations between the four largest fragments and LRL photographs of the samples. Insets are superimposed on a part of NASA photograph AS14–64–9126).

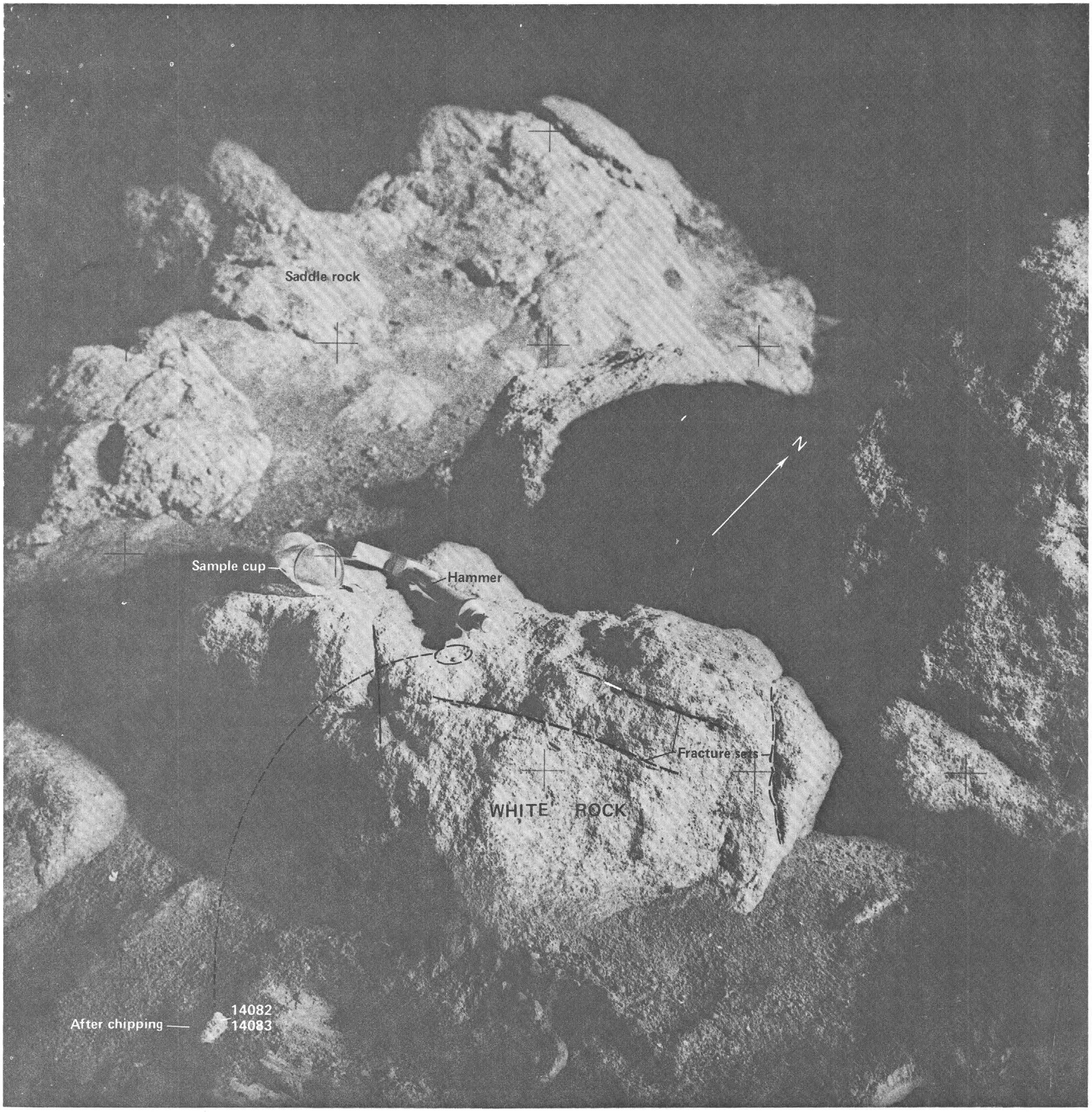

FIGURE 59.—Samples 14082 and 14083 (pieces of the same fragment) were chipped from a 1.5-m boulder in the White rocks group at station C1. The sample is shown on the fillet at the base of the boulder after chipping. Looking northwest. (NASA photograph AS14–68–7452.)

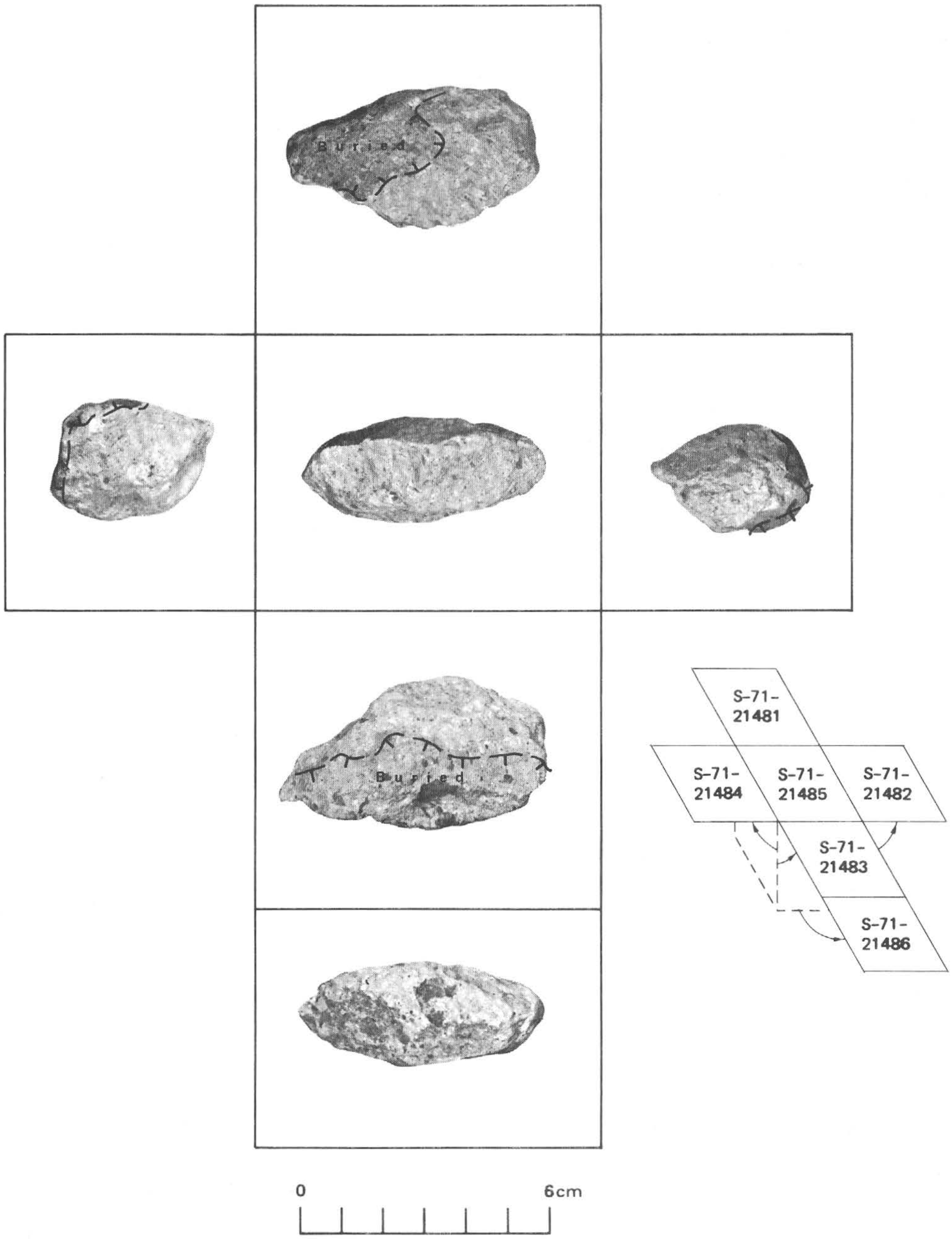

FIGURE 60.—Orthogonal views of sample 14082. The lunar orientation of the rock is not known, but weathered and unweathered portions of the rock suggest a burial line where it was chipped from the boulder. NASA photograph numbers are shown in the schematic diagram.

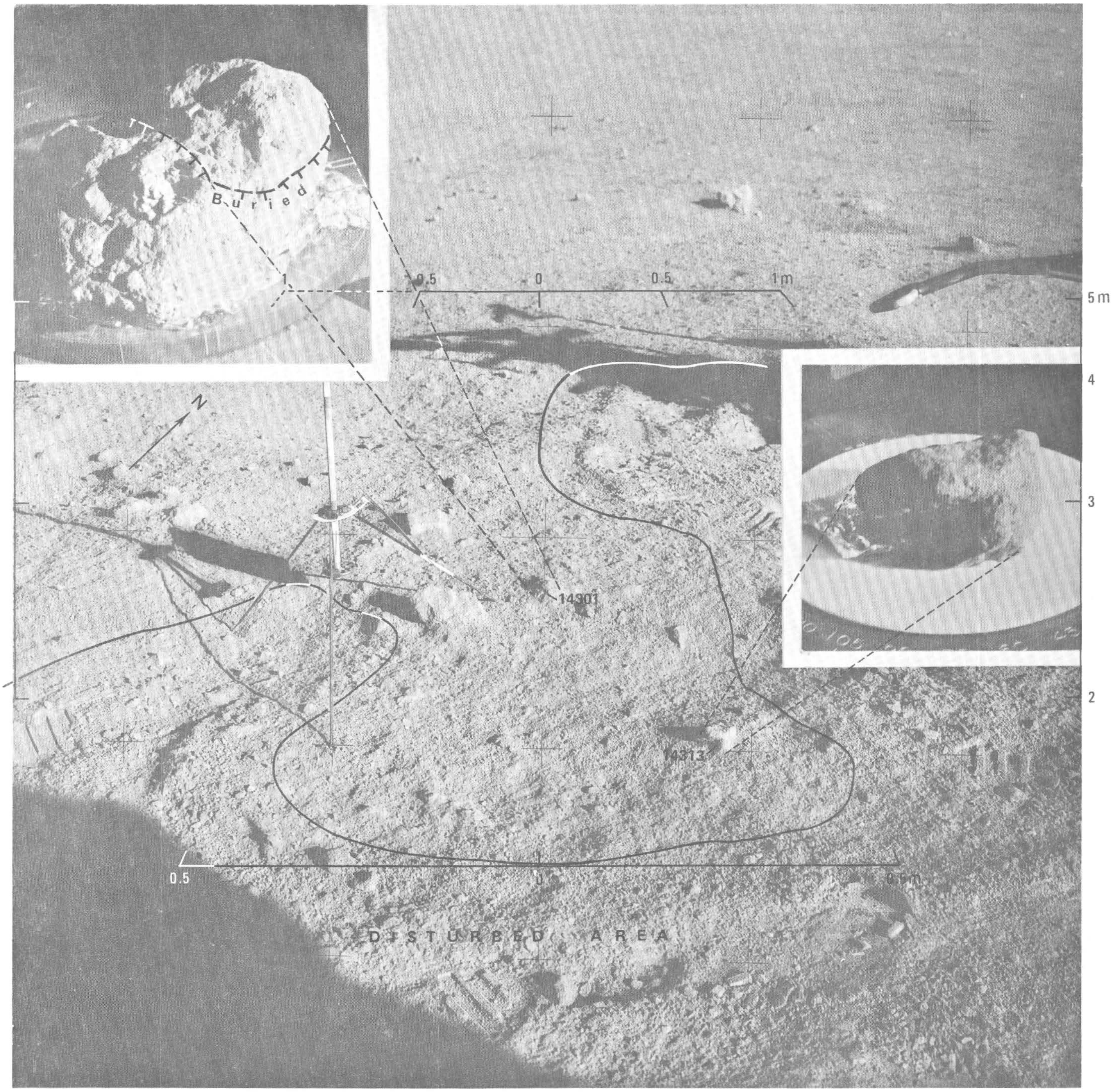

FIGURE 61.—Samples 14301 and 14313 on lunar surface. View northwest from station G1. Insets show approximate lunar orientations reconstructed in the LRL using oblique lighting. (NASA photograph AS14-68-9466).

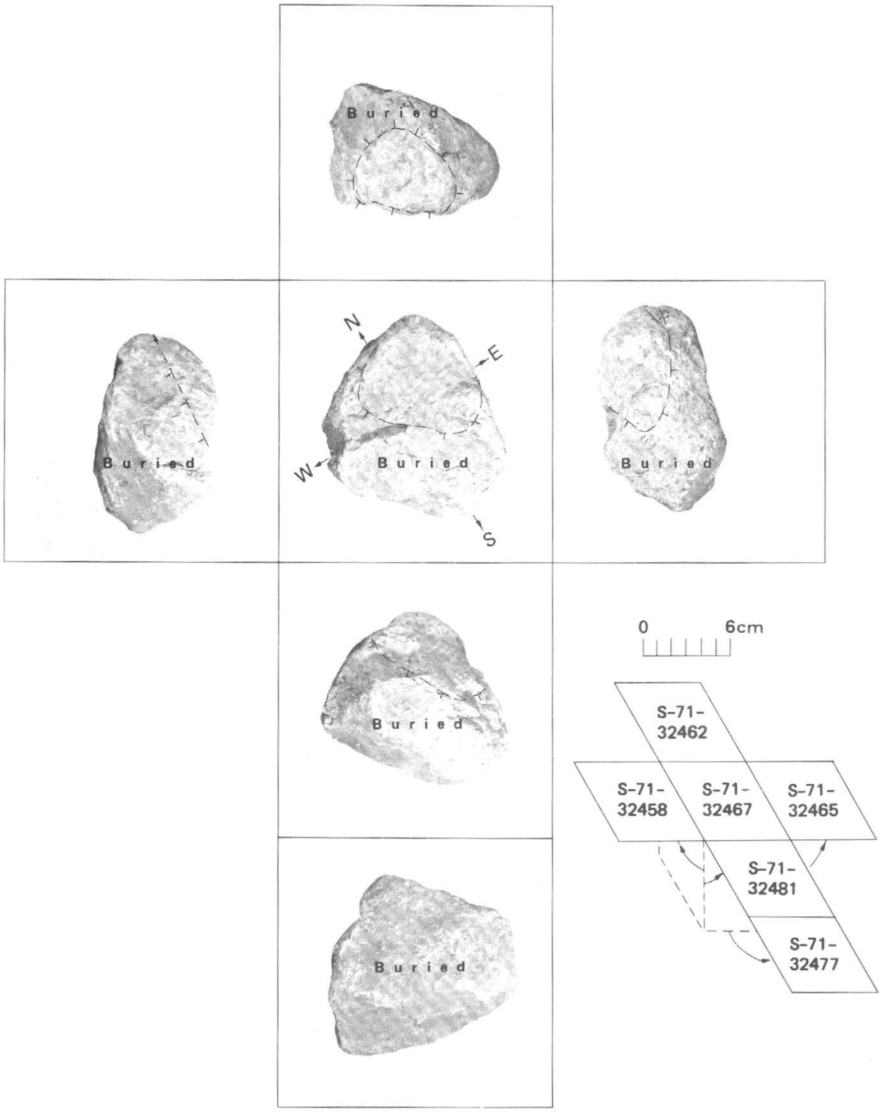

FIGURE 62.—Orthogonal views of sample 14301, shown in approximate lunar orientation. NASA photograph numbers are shown in the schematic diagram.

14315, 14318, 14320? (FIGS. 70, 71, 74, 75, 76) AND ONE SAMPLE STILL UNIDENTIFIED

Station: H (North Boulder Field)
Location: 15 m SE of Turtle Rock and 70 m NW of LM
Rock type: Coherent breccia

SAMPLE AREA CHARACTERISTICS

Slopes: Level

Fragment population:
Distribution and size range: Moderately abundant from limit of resolution to about 1 m. Samples from a cluster of about 20 fragments in a 3×3 m area
Color: Light to medium gray with white clasts
Shapes: Subangular to rounded
Fillets: Moderately to well developed
Apparent burial: ¼–⅓
Dust cover: Moderate

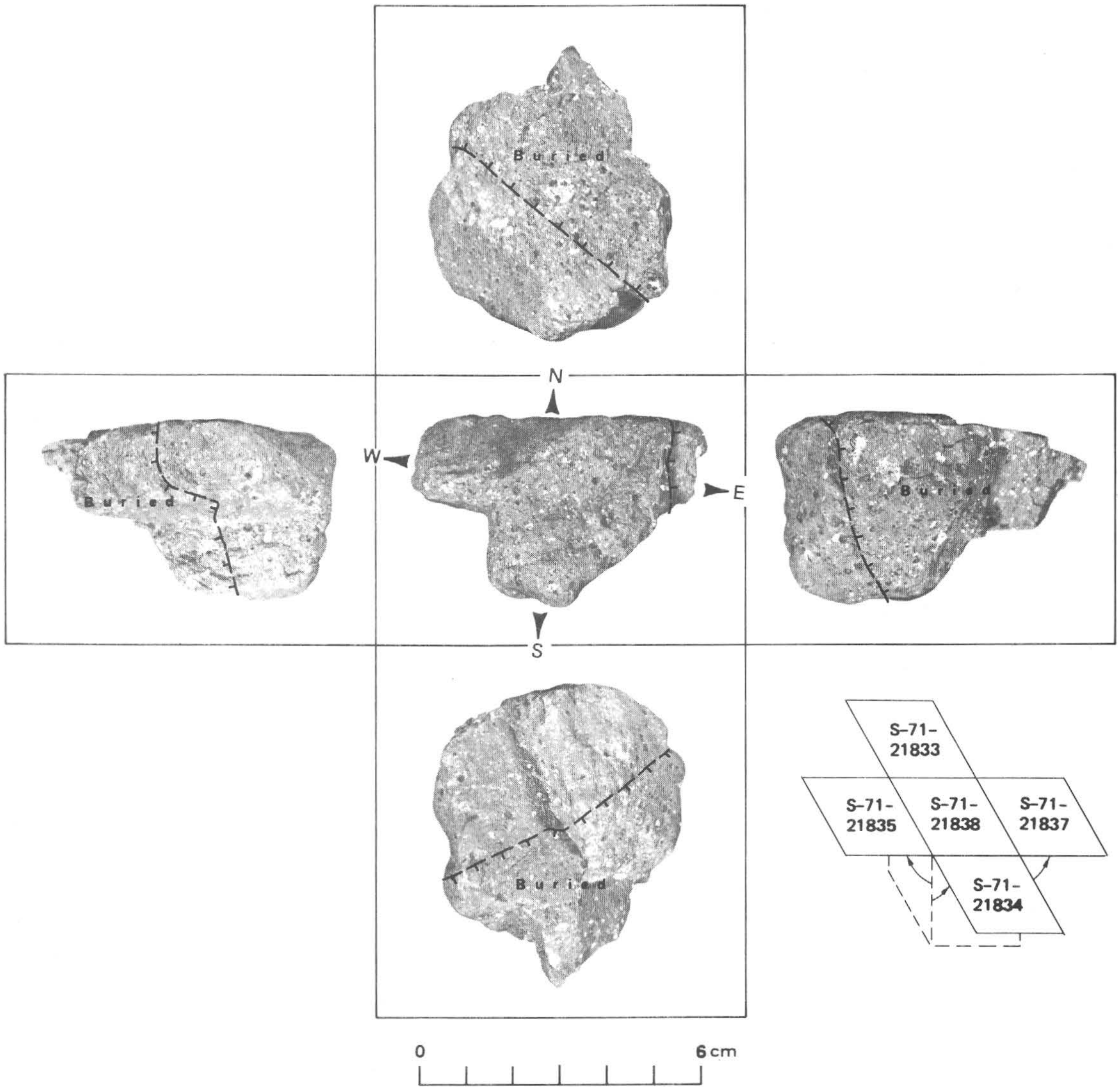

FIGURE 63.—Orthogonal views of sample 14313, shown in approximate lunar orientation. NASA photograph numbers are shown in the schematic diagram.

Fines:
Color: Medium gray; appears lighter than most of traverse area
Compaction: Moderately high
Craters:
Distribution and size range: 10–50 cm craters common; five small craters in sample vicinity; samples from fragments around a subdued 35-cm crater
Shape: Moderately subdued to subdued; 50-cm crater SE of sample site has one straight side
Ejecta: Fragments appear to be associated with several craters in the photograph. Abundant fragments up to 15 cm in size around the 35-cm crater between samples

SAMPLE CHARACTERISTICS

Sample 14315
Size: 3×6×6 cm; 115 g
Color: Medium gray matrix with white clasts
Shape: Rounded on exposed surface; angular on buried surface
Fillet: Poorly developed
Apparent burial: ⅓
Dust cover: Moderate
Comparison with other rocks in area: Appears typical of fragments in cluster
Probable origin: From blocky ray of Cone crater. Possibly reejected from 35-cm crater
Comments: Angular underside and numerous pits on the rounded surface suggest a simple tumbling history

Sample 14318
Size: 11.4×7.8×5.3 cm; 600.2 g
Color: Medium gray matrix with light gray clasts
Shape: Rounded on exposed surface; irregular and sub-rounded on buried surface
Fillet: Poorly developed
Apparent burial: ⅓
Dust cover: Moderate
Comparison with other rocks in area: Appears similar to other rocks in cluster
Probable origin: From blocky ray of Cone crater. Possibly reejected from 35-cm crater

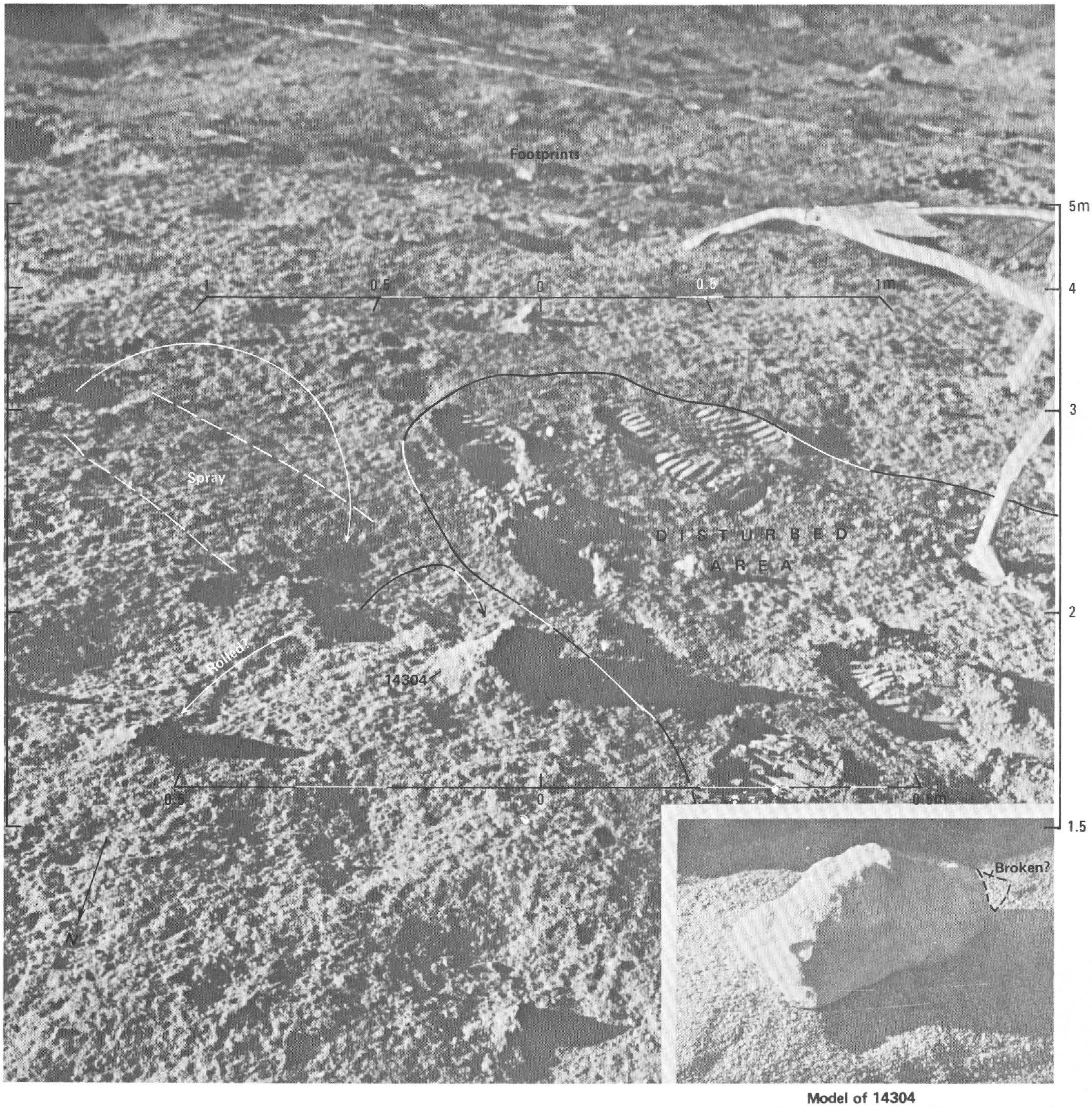

FIGURE 64.—Sample 14304 and vicinity; view south. (NASA photograph AS14–67–9390.) Inset shows approximate lunar orientation reconstructed using a plaster model and oblique lighting. Note that the pointed right end of the rock on the lunar surface is absent from the model, indicating that the sample was broken during transport.

Comments: Dense pitting on all sides suggests a complex tumbling history. Glass-lined fractures present

Sample 14320?

Size: 5.5×5×2.5 cm; 64.9 g

Color: Medium gray

Shape: Slabby; rounded; one surface convex and rounded and opposite surface is roughly planar

Fillet: Poorly developed

Apparent burial: ⅓–½

Dust cover: Moderate

Comparison with other rocks in area: Appears similar to other rocks in cluster

Probable origin: From blocky ray of Cone crater. Possibly reejected from 35-cm crater

Comments: All surfaces equally pitted at saturation density suggesting a long and complex tumbling history

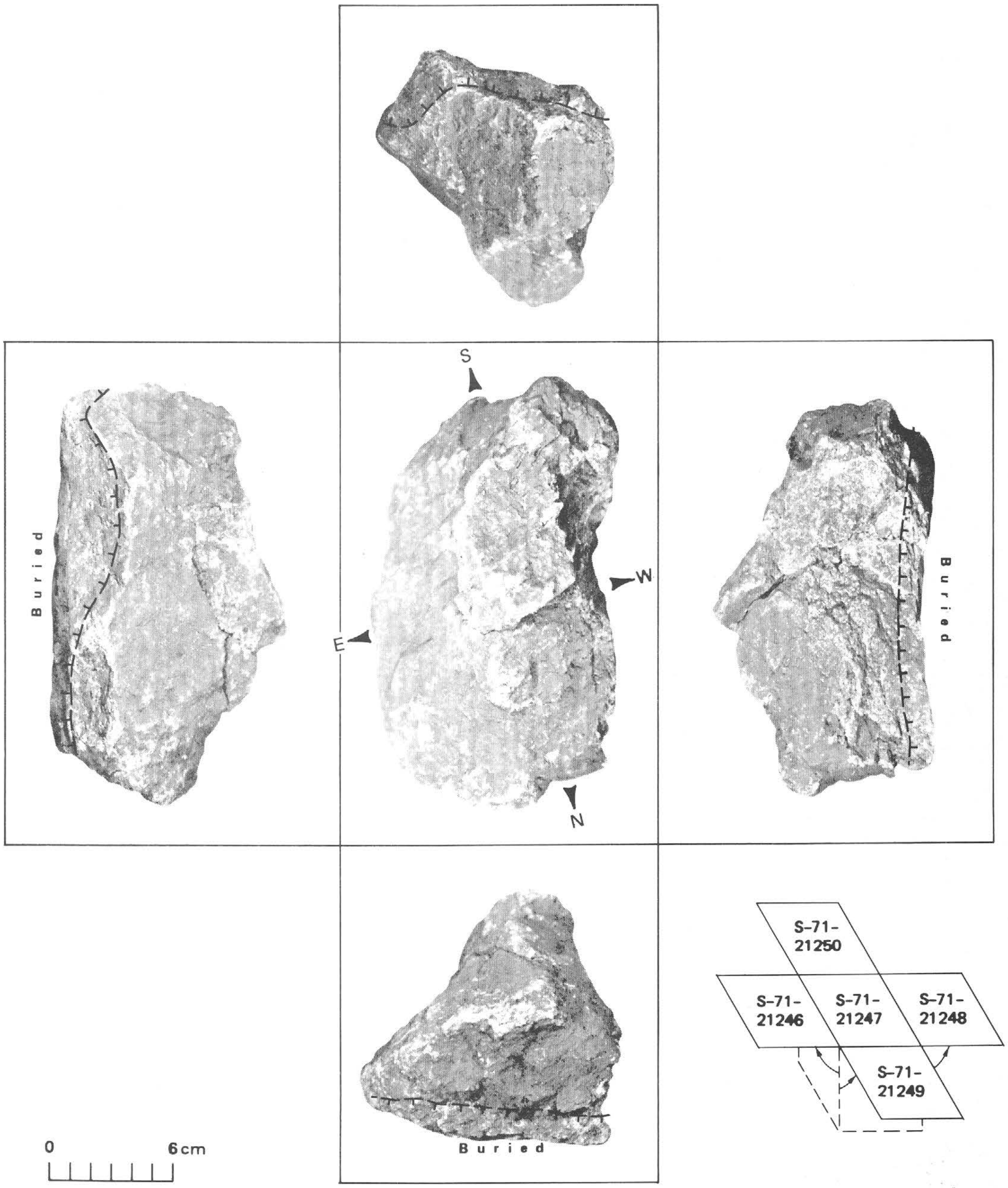

FIGURE 65.—Orthogonal views of sample 14304, shown in approximate lunar orientation. NASA photograph numbers are shown in the schematic diagram.

14321 (FIGS. 77, 78)

Station: C1
Location: 1.25 km NE of LM and about 30 m SE of Cone crater rim
Rock type: Moderately friable clastic breccia

SAMPLE AREA CHARACTERISTICS

Slopes: Gentle slope to south
Fragment population:
  Distribution and size range: Very abundant from limit of resolution to 1.5 m
  Color: Light to dark gray
  Shapes: Subrounded to rounded; irregular
  Fillets: Mostly well developed; a few poorly developed
  Apparent burial: ⅛–½
  Dust cover: Moderate to high
Fines:
  Color: Light gray to tan; almost white in places
  Compaction: Firm
Craters:
  Distribution and size range: A few subdued 0.2- to 1.5-m craters
  Shape: Subdued
  Ejecta: Station is on continuous ejecta deposit from Cone crater

SAMPLE CHARACTERISTICS

Sample 14321

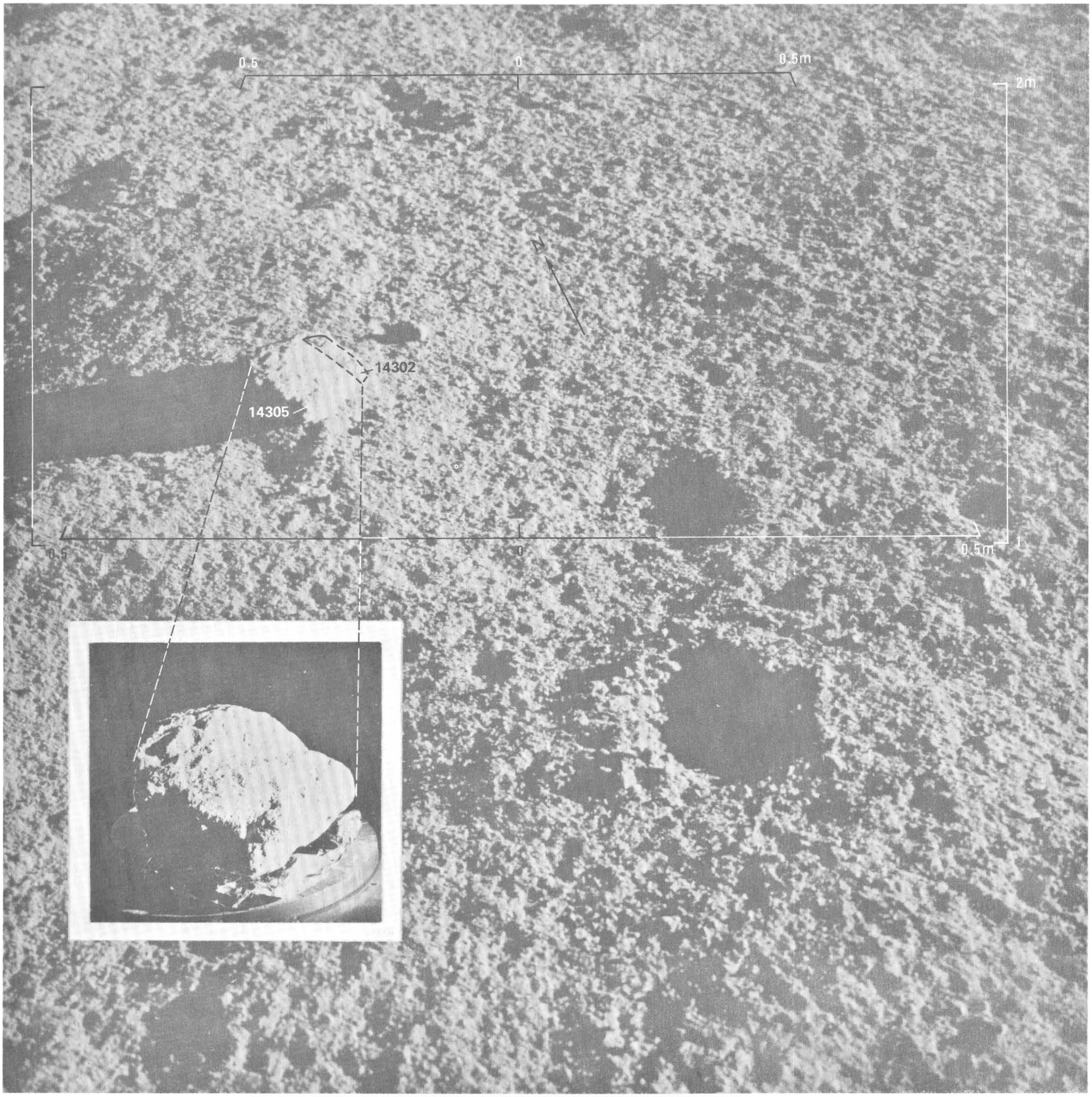

FIGURE 66.—Sample 14305, from which the end (sample 14302) was broken during transport. View north. (NASA photograph AS14-67-9393.) Inset shows approximate lunar orientation reconstructed (without the broken end) in the LRL using oblique lighting.

Size: 23×23×17 cm; 8998 g
Color: Grayish to black to white
Shape: Blocky, subround on exposed surface, with some irregular surfaces
Fillet: Well developed
Apparent burial: ¼
Dust cover: Moderate
Comparison with other rocks in area: Appears similar in color, texture, and shape to other rocks
Probable origin: Cone crater
Comments: Probably represents material excavated from as deep as 60–80 m

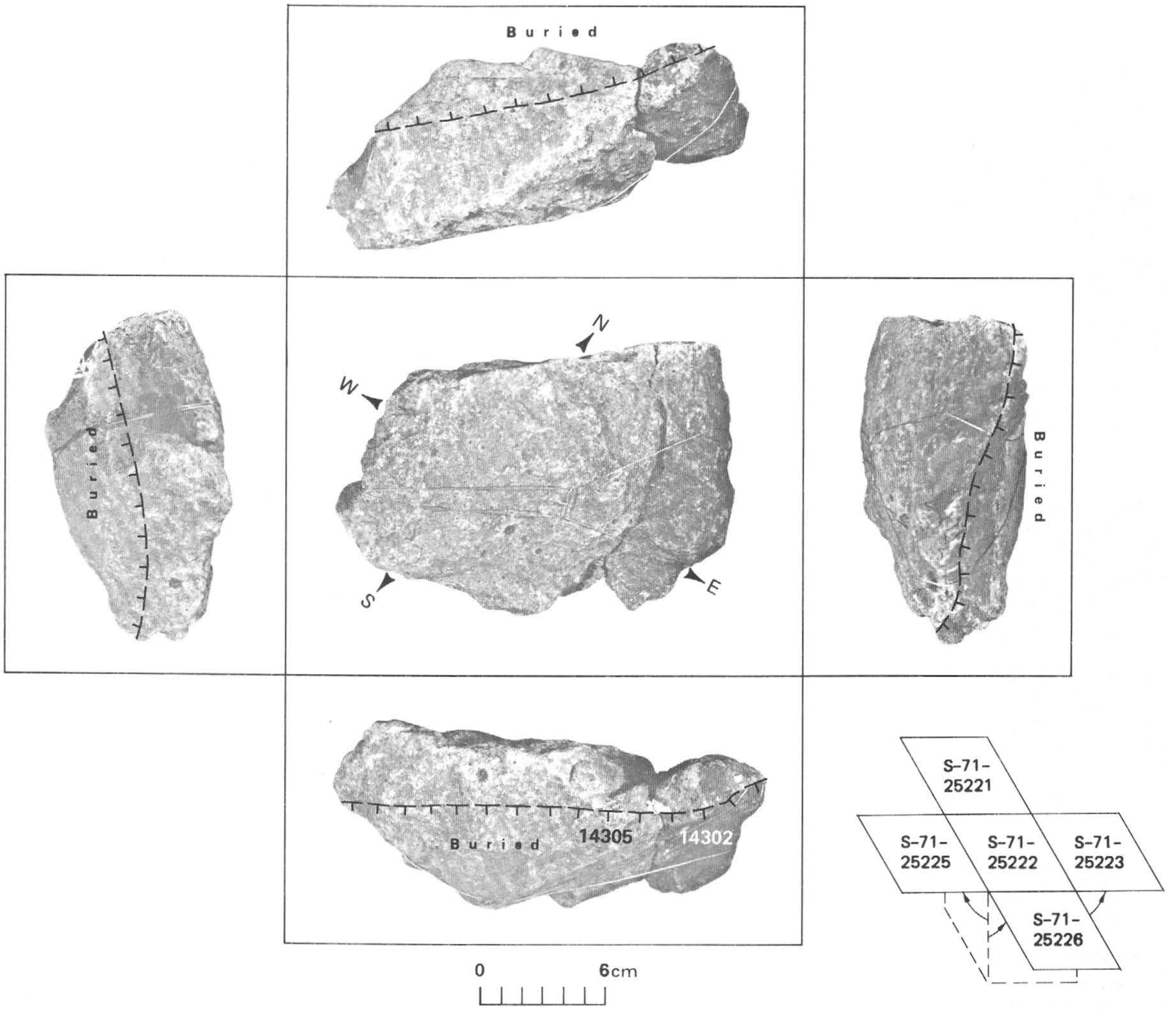

FIGURE 67.—Orthogonal views of samples 14305 and 14302 wired together, shown in approximate lunar orientation. NASA photograph numbers are shown in the schematic diagram.

CATALOG OF 70-MM PHOTOGRAPHS TAKEN ON THE LUNAR SURFACE DURING THE APOLLO 14 MISSION

This log of photographs taken by the Apollo 14 crew was designed as an aid and reference for interpreting data gathered during the EVA's. Data on 16-mm motion picture film or on photographs taken with the Apollo Lunar Stereo Closeup Camera during the lunar stay are not included.

The photographic surveys taken during the Apollo 14 lunar stay were designed for several specific purposes:

1.—Locating and illustrating the gross topographic features at each major geologic station.

2.—Photographic documentation of geologic targets of opportunity.

3.—Recording the in situ surface characteristics of sample areas, correlating returned samples with these areas, and determining the orientation and location on the lunar surface of the samples at the time they were collected.

Nongeologic photographic surveys were taken to document the deployment of the ALSEP, the interaction between the LM and the lunar surface during landing and other soil mechanics experiments, miscel-

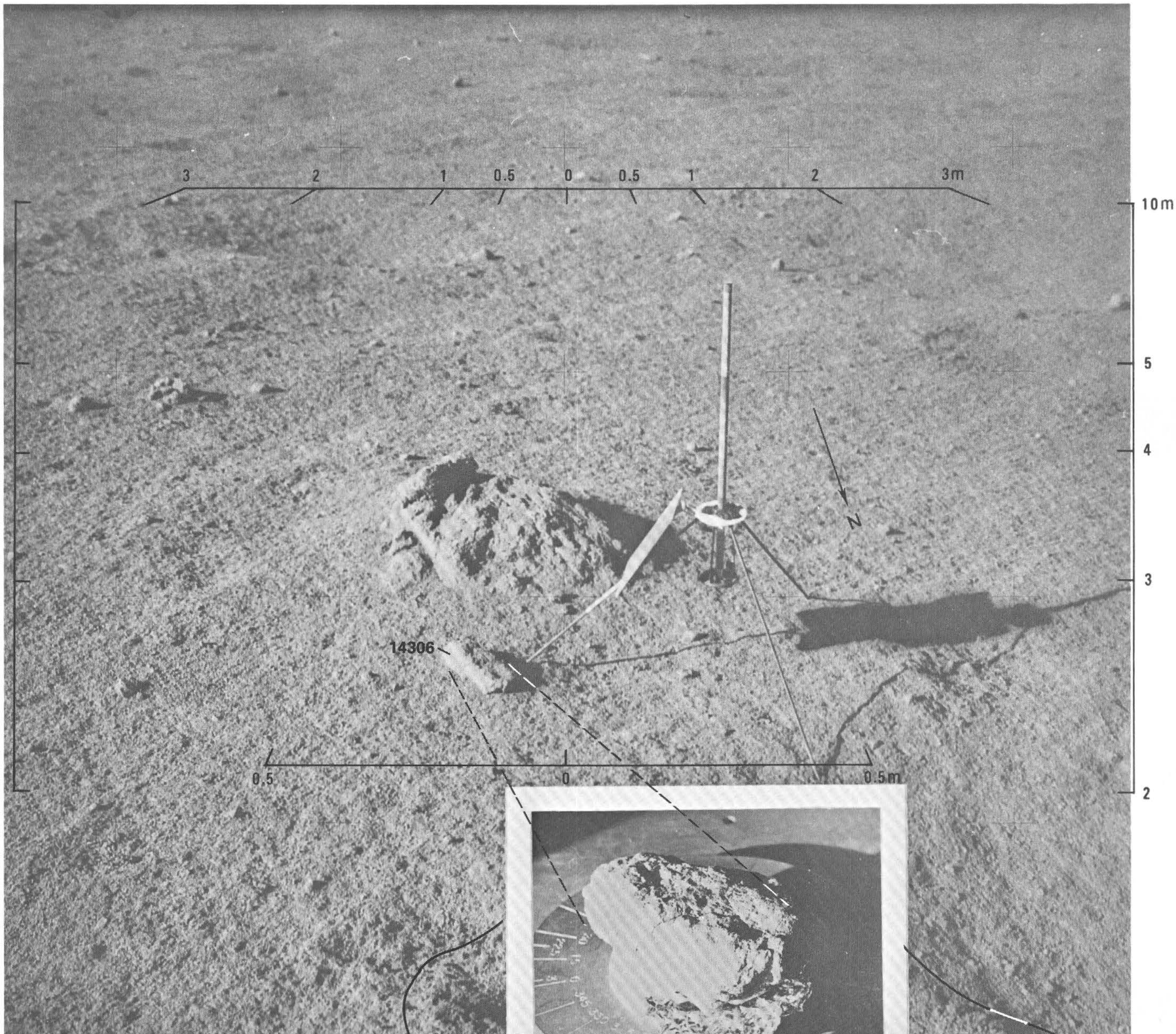

FIGURE 68.—Sample 14306 and vicinity at station G; view south. (NASA photograph AS14–68–9460.) Inset shows approximate lunar orientation reconstructed in the LRL using oblique lighting.

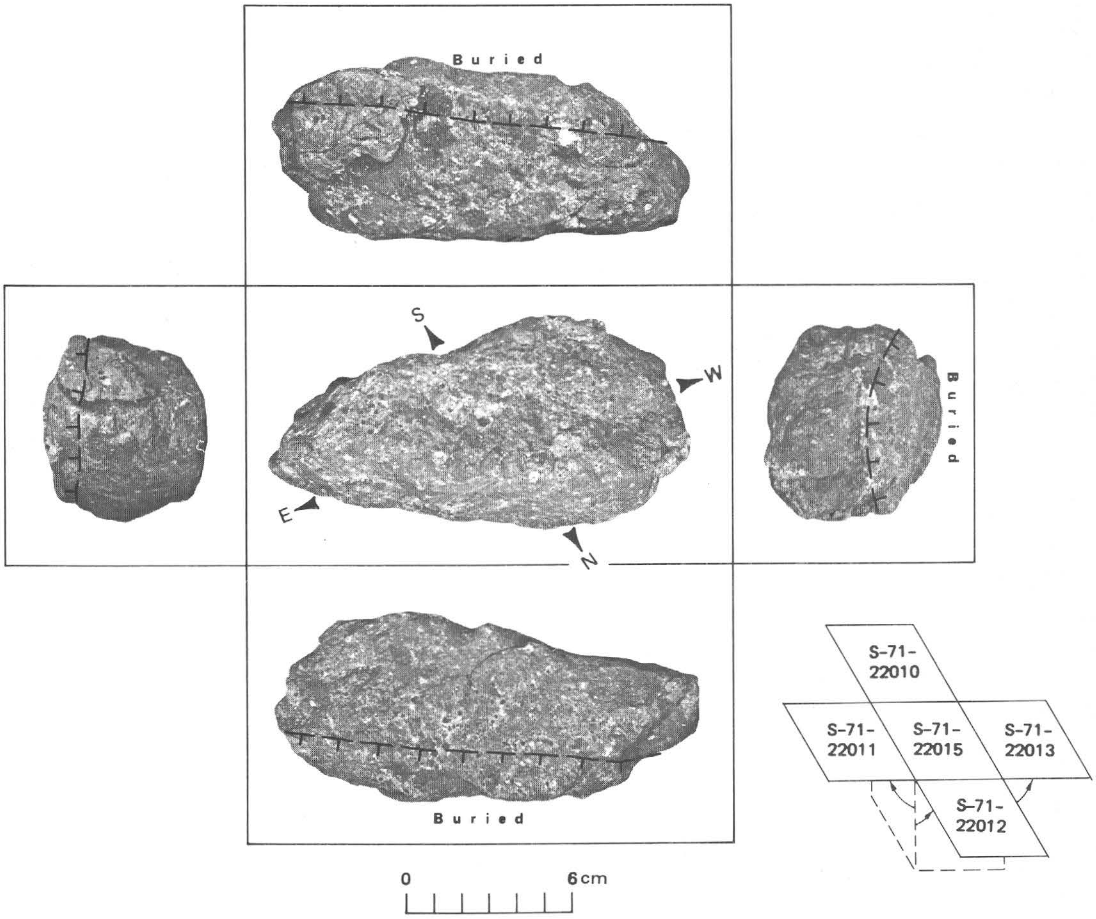

FIGURE 69.—Orthogonal views of sample 14306, shown in approximate lunar orientation. NASA photograph numbers are shown in the schematic diagram.

laneous astronaut activity, and targets of opportunity. Because these pictures were interspersed throughout the five film magazines used for geologic documentation, they are also included.

A total of 417 pictures was taken on the lunar surface with the Hasselblad cameras during the Apollo 14 mission. Fifteen panoramas, consisting of 275 photographs, were taken for major station location and general geologic documentation, 49 pictures were taken for sample documentation, and 27 pictures were taken to document ALSEP deployment. The remaining 66 pictures were taken of miscellaneous targets of opportunity. Color film was used during the first EVA in magazines II and JJ. The other three magazines were loaded with black-and-white film.

The general location on a rectified copy of Lunar Orbiter III frame H–133 of major geologic stations was determined by examining transcripts of oral reports and by talking with the crew. Gross features appearing on 70-mm lunar surface panoramas and on the rectified Orbiter picture were then identified, and the panorama station was located by resection. Final locations for the panorama stations were determined by a second stage of resection on small nearby features appearing on the panoramas, on the unrectified version of the Lunar Orbiter picture, and on the shaded relief map (pl. 2).

After the major geologic stations had been located, the approximate placement relative to the panorama stations of individual pictures was determined by their sequence within the traverse relative to the panoramic surveys, and by resection on identifiable features. Most

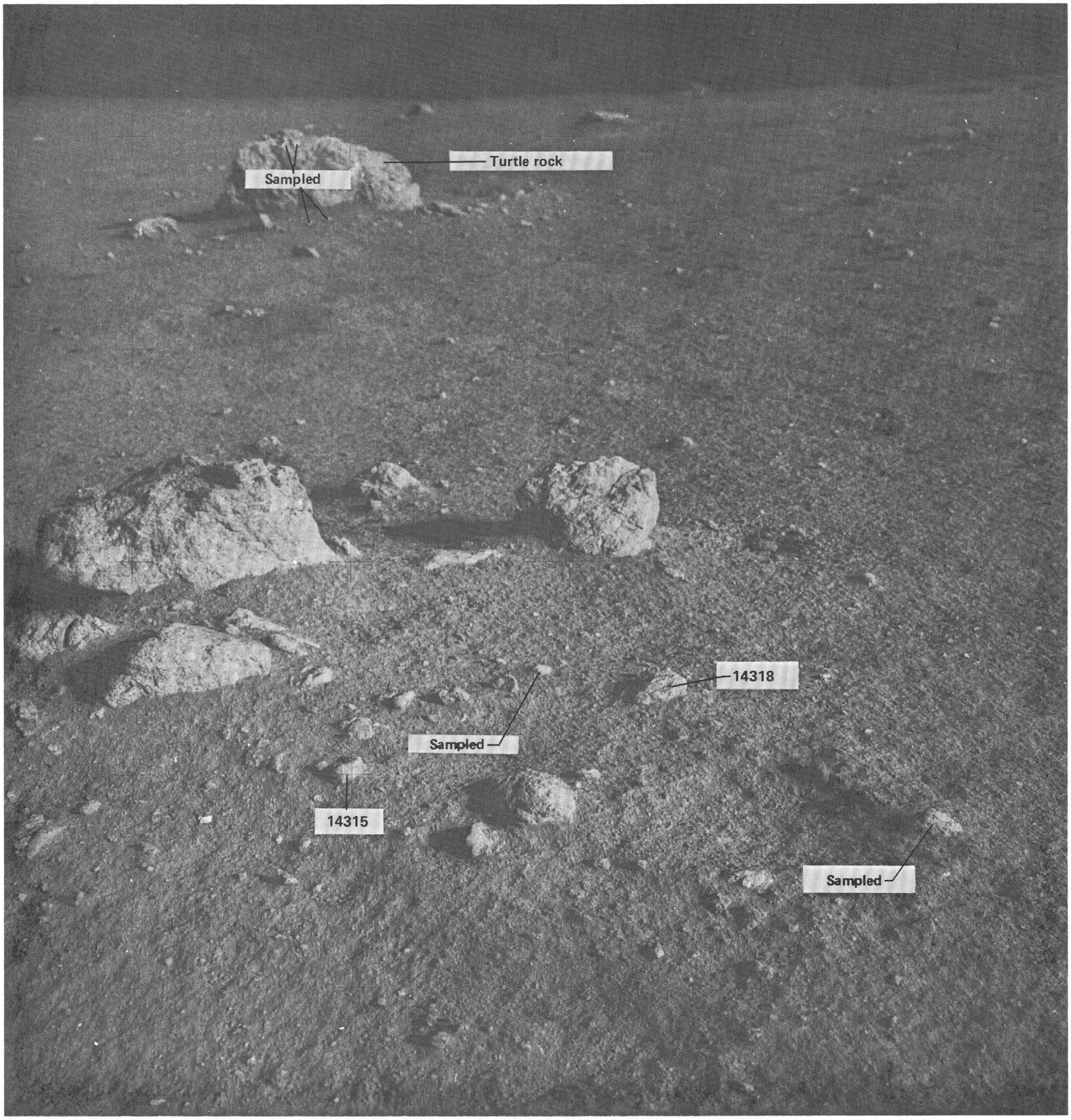

FIGURE 70.—North Boulder Field cluster (station H) sample area. View north. (NASA photograph AS14–68–9469.)

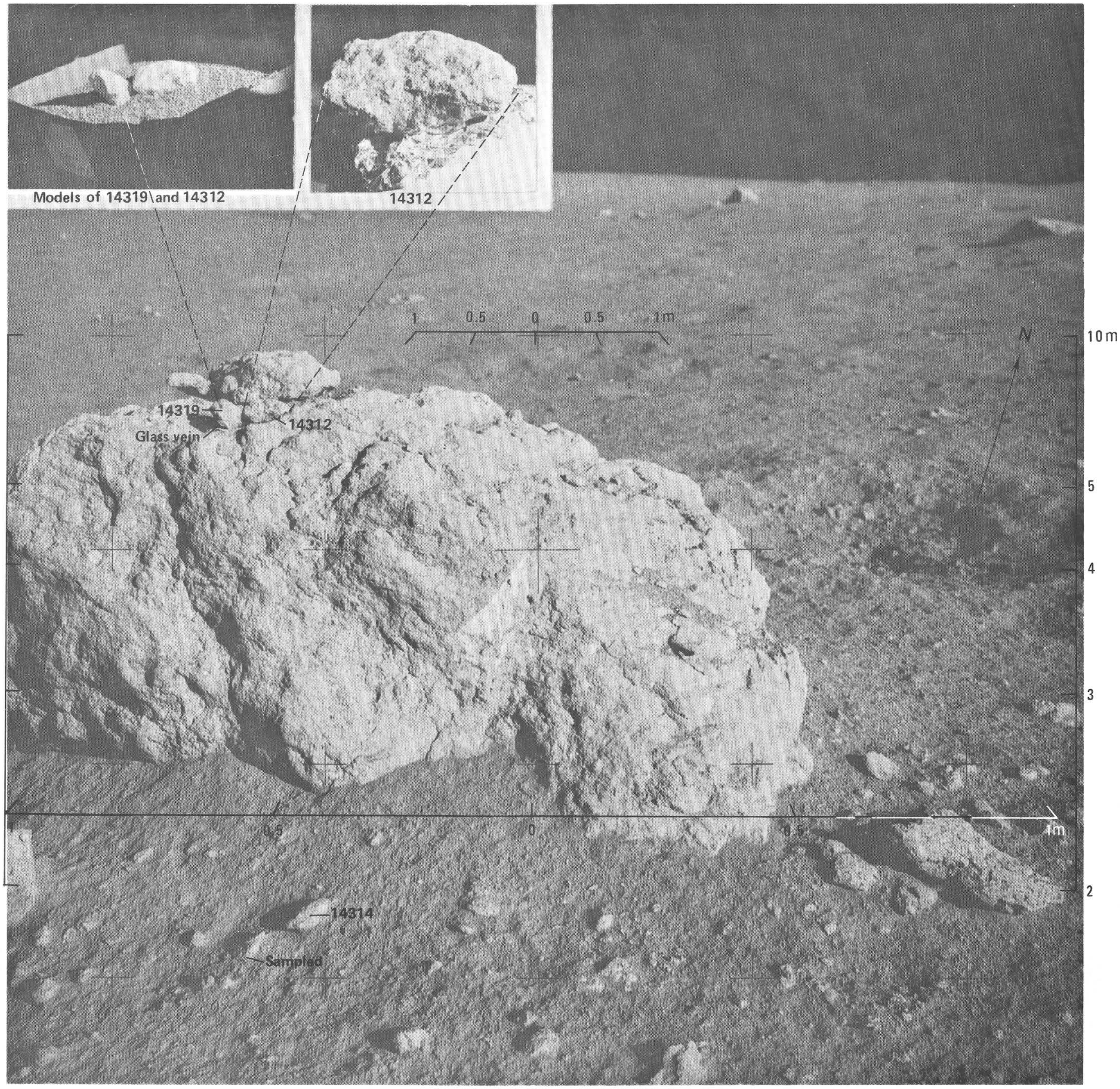

FIGURE 71.—Turtle rock samples at station H. View north. (NASA photograph AS14-68-9474.) Samples 14312 and 14319 were picked from the top of the 1.7-m boulder. Sample 14314 and one unidentified fragment were taken from the fillet at the base of Turtle rock. Left-hand inset shows approximate lunar orientations reconstructed using plaster models photographed under oblique lighting. Right-hand inset is a reconstruction using the actual sample 14312.

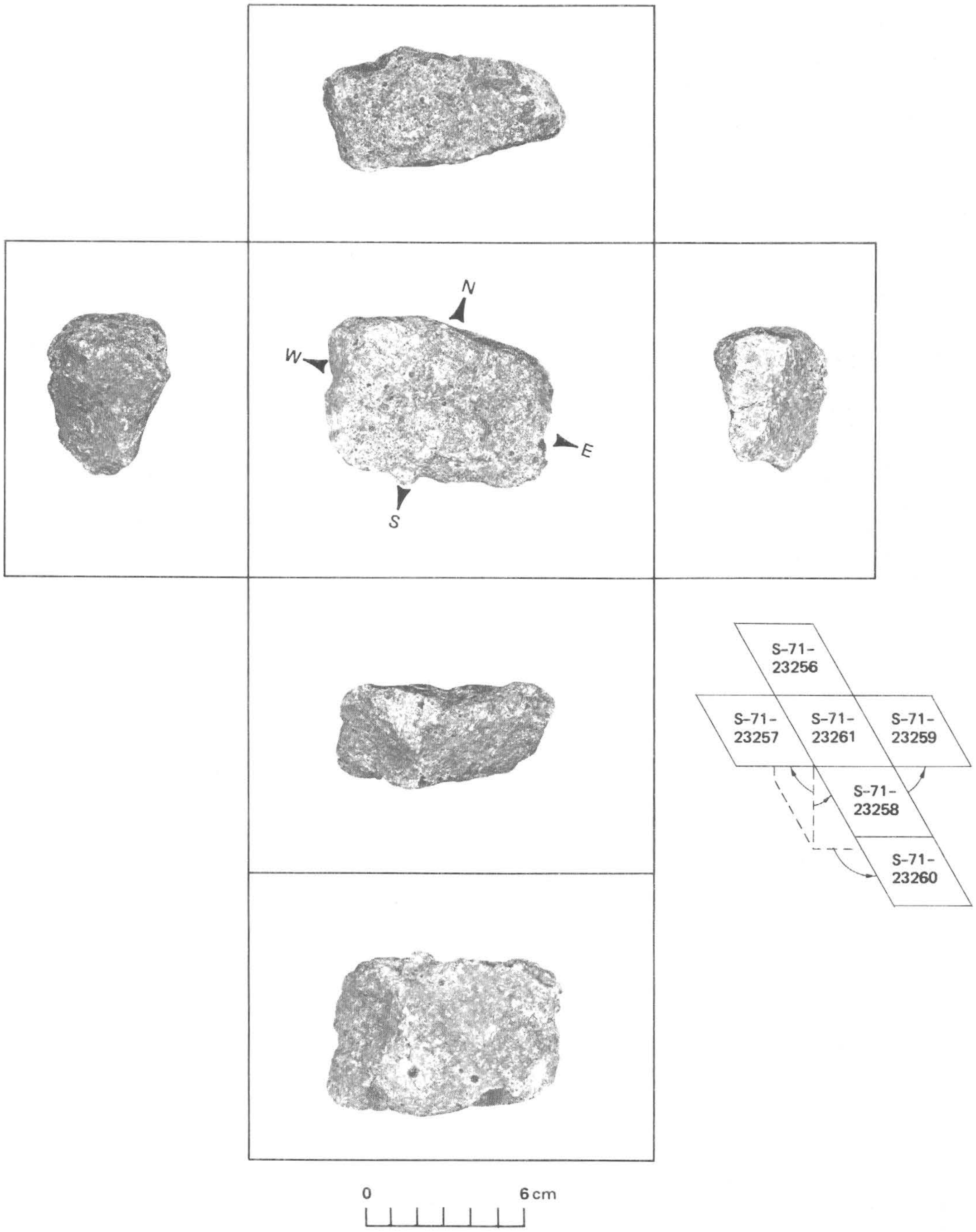

FIGURE 72.—Orthogonal views of sample 14312, shown in approximate lunar orientation. NASA photograph numbers are shown in the schematic diagram.

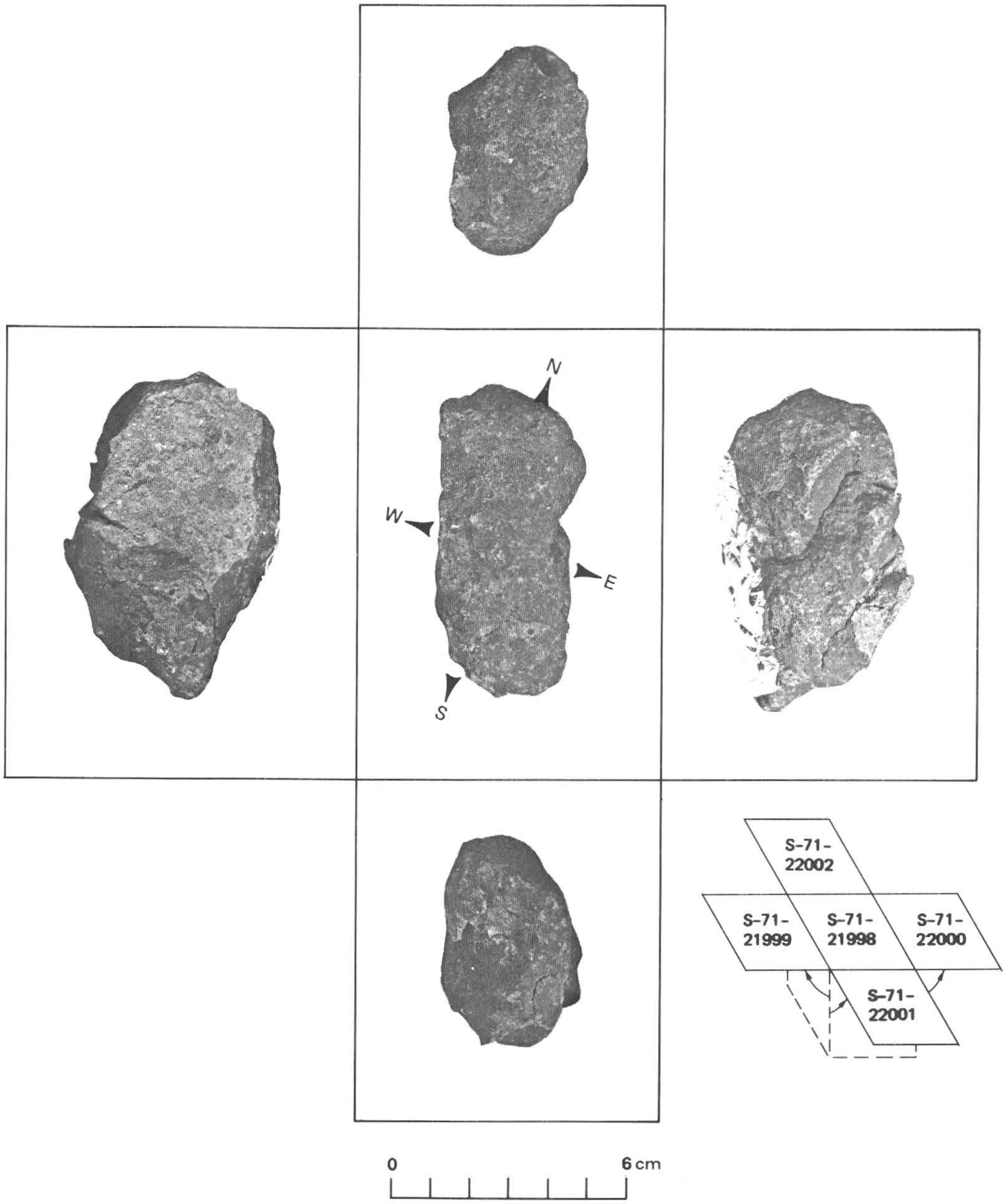

FIGURE 73.—Orthogonal views of sample 14319, shown in approximate lunar orientation. NASA photograph numbers are shown in the schematic diagram.

of the photographic station location information is shown on plate 2. The subject matter in the photographs and the approximate picture sequence were then determined by detailed examination of the pictures and transcripts of oral reports and by talking with the crew.

Several tabulations of the photographic data are shown here to facilitate topical study. Table 6 (p. 65) is a summary of film usage. Table 7 is a complete set of photographic data in chronological sequence. The picture numbers in this table are not necessarily sequential. Table 8 is a chronological listing of pictures in each magazine. Table 9 lists film usage by camera number.

The tabulations were designed to aid in the following specific tasks:

1. Given a particular location or activity within the sequence of lunar surface activity, find the pictures taken at that time, and their subject matter (table 7).
2. Given the number of a particular frame, find its location in the sequence of lunar surface activity, the station from which it was taken, and the subject matter of the picture (table 8).

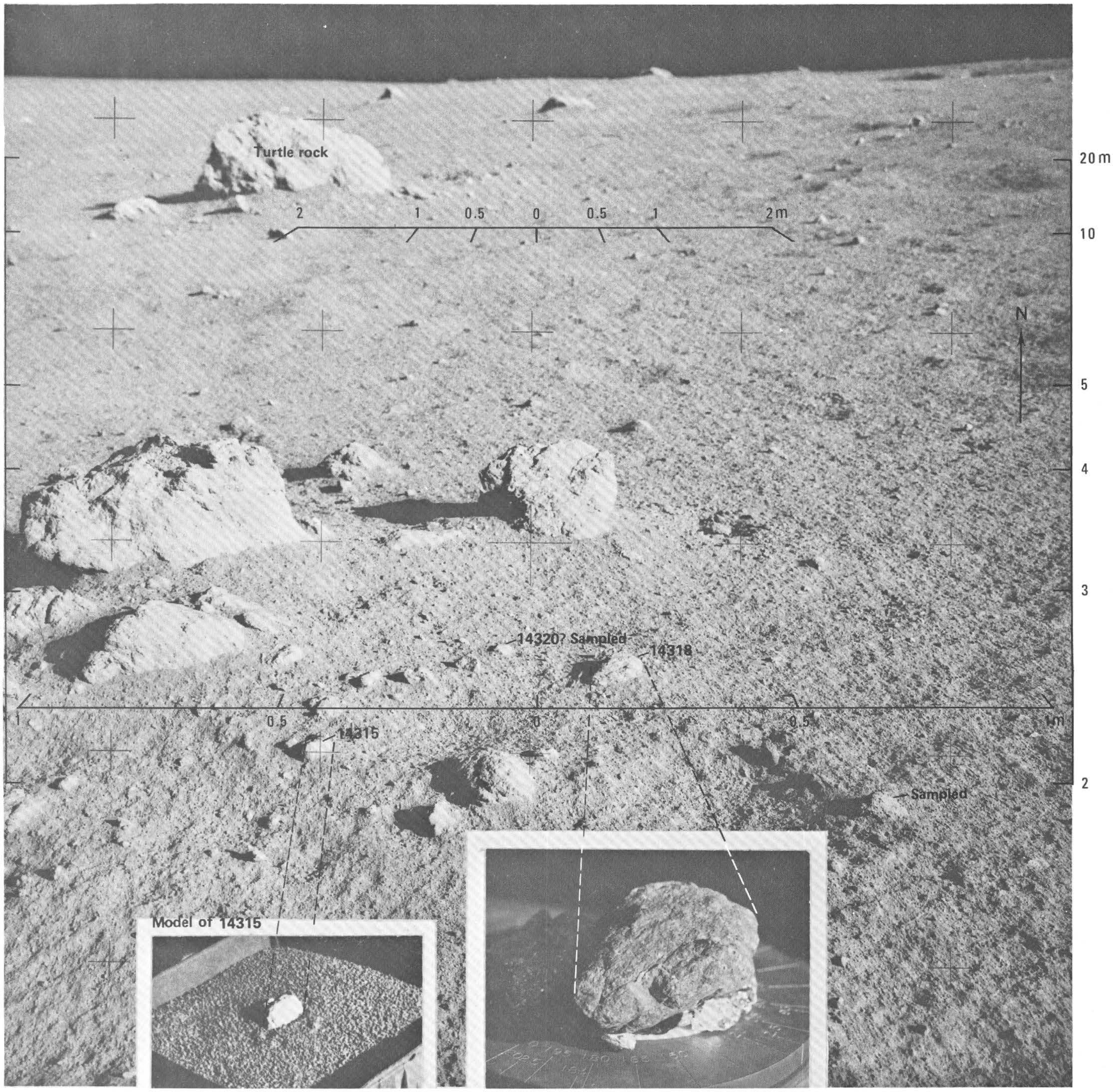

FIGURE 74.—Samples 14315, 14318, 14320?, and one unidentified sample from the North Boulder Field cluster, station H. View north. (NASA photograph AS14-68-9469.) Left-hand inset shows approximate lunar orientation of sample 14315 reconstructed using a plaster model under oblique lighting. Right-hand inset is a reconstruction using the actual sample 14318.

3. Given a specific frame number, find the serial number of the camera with which it was taken (table 9).

THE APOLLO 14 BASE MAP

Part of Lunar Orbiter III frame H-133 was used to map the Apollo 14 landing site. This frame had the highest resolution of any photographic coverage of the area, resolving craters as small as 2 m, and boulders as small as 1 m. The camera, however, was tilted approximately 33° when the picture was taken. This, plus the fact that there is nearly 100 m vertical relief at the

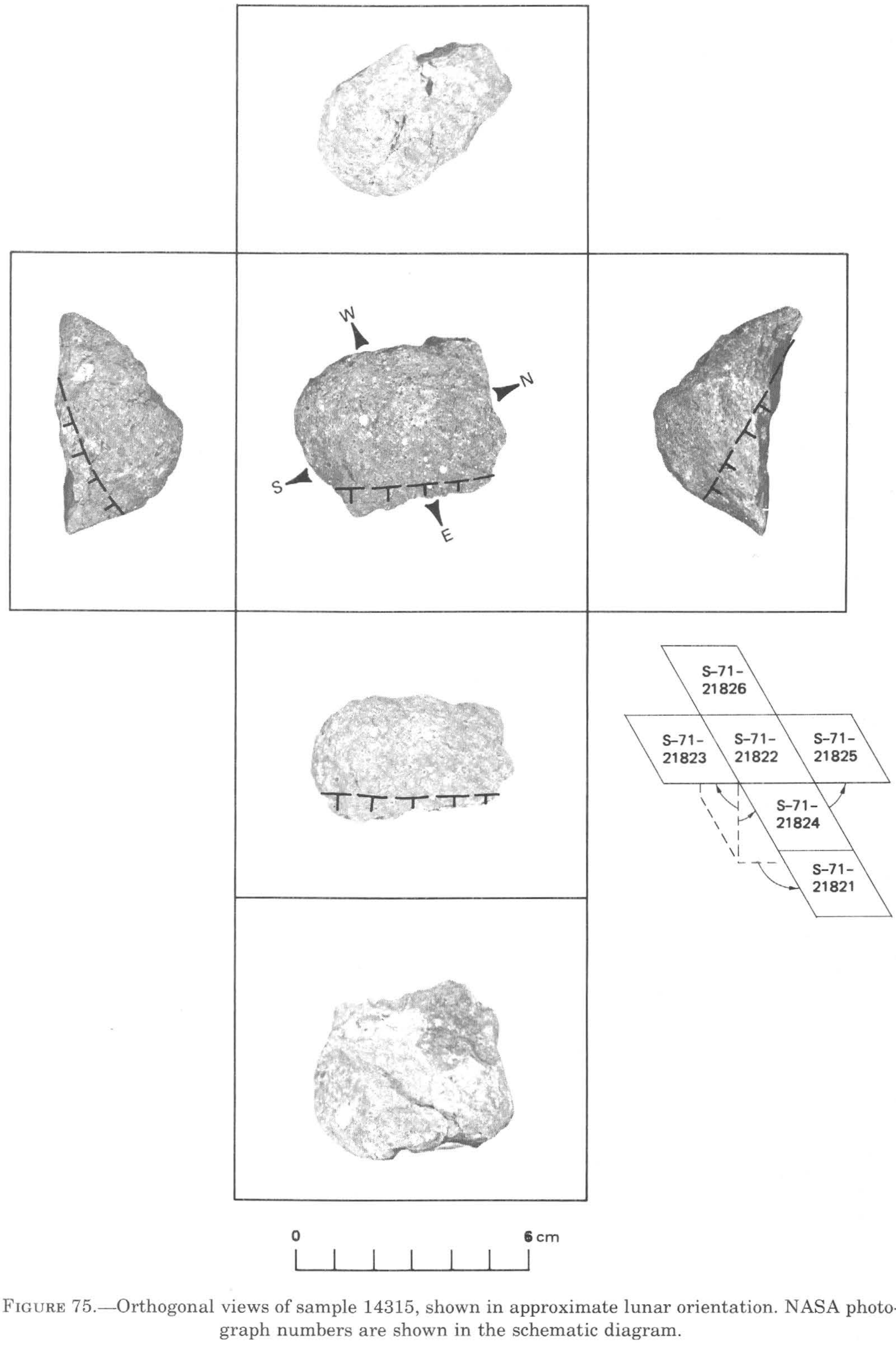

FIGURE 75.—Orthogonal views of sample 14315, shown in approximate lunar orientation. NASA photograph numbers are shown in the schematic diagram.

landing site, produced variable distortion in the picture that could not be removed by optical rectification. The geometry of this condition is illustrated in figure 79. Feature P appears at point P_p on the untransformed picture. If the picture is projected onto a plane differing from that of the original image by angle t, P appears at point P_r. This point is displaced from the correct map location by distance ΔG_n because of the effect of topographic relief h_n.

Even if the geometric distortion is neglected, all at-

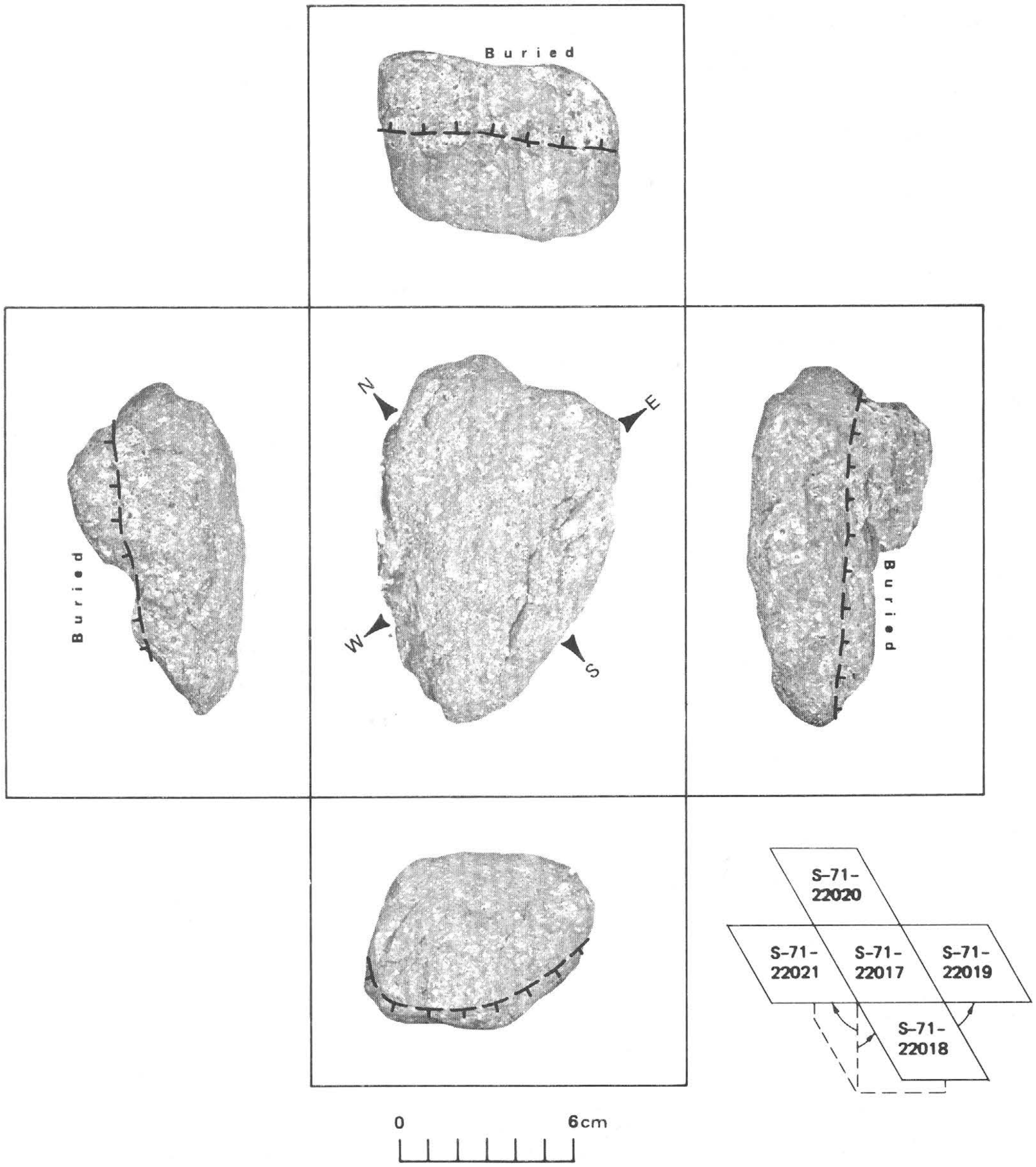

FIGURE 76.—Orthogonal views of sample 14318, shown in approximate lunar orientation. NASA photograph numbers are shown in the schematic diagram.

tempts to rectify the picture have degraded its resolution by at least a factor of two. This degradation obliterated many of the blocks and craters on the rectified photograph, severely reducing its usefulness for scientific evaluation and measurement of traverse data.

A shaded relief map was therefore compiled with an airbrush. The map has as much resolution as the original Lunar Orbiter photograph and is differentially rectified to remove, insofar as practical, the effects of tilt and relief. This was done by superimposing a grid of 50 m squares, deformed to match the distortions in the Lunar Orbiter photograph, on that photograph. Details were then transferred manually from the deformed grid to an undeformed one, and enhanced with the airbrush to produce the finished map. Because the angle subtended by the landing site was only about 2°, for simplicity the lines of sight from the camera are considered to be parallel (fig. 79). The deformed grid overlay for the unrectified Lunar Orbiter photograph was constructed by solving for X_n at even intervals of G along evenly spaced lines parallel to the direction of tilt:

$$\Delta G_n = h_n \tan t$$
$$X_n = (\Delta G_n + nG) \cos t$$
$$X_n = h_n \sin t + G_n \cos t, \qquad (1)$$

where G is the grid interval, h is the relative topographic elevation, t is the camera tilt with respect to the

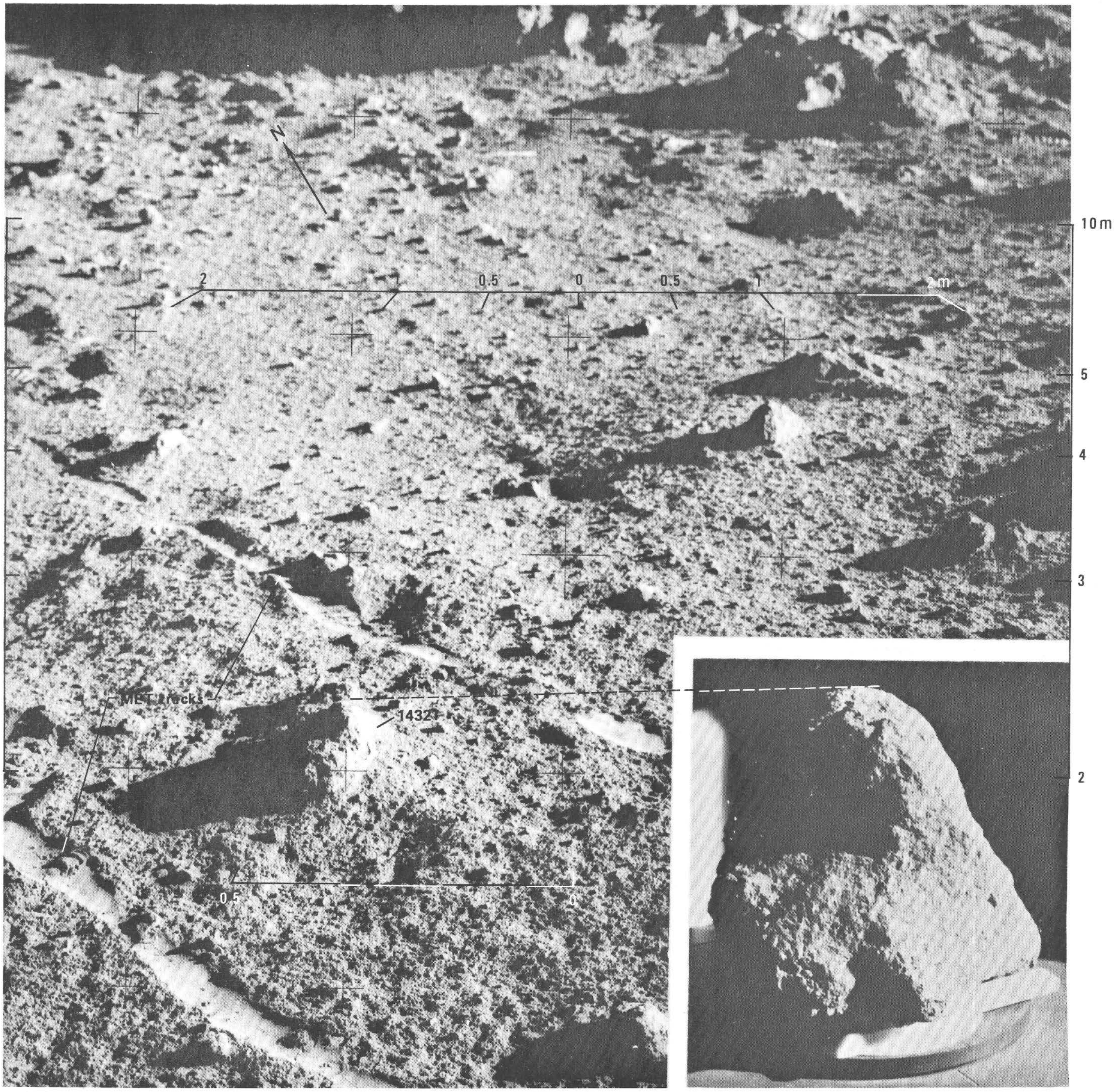

FIGURE 77.—Sample 14321 and vicinity at station C1. View northeast toward the blocky rim of Cone crater. (NASA photograph AS14–64–9128.) Inset shows approximate lunar orientation reconstructed in the LRL using oblique lighting.

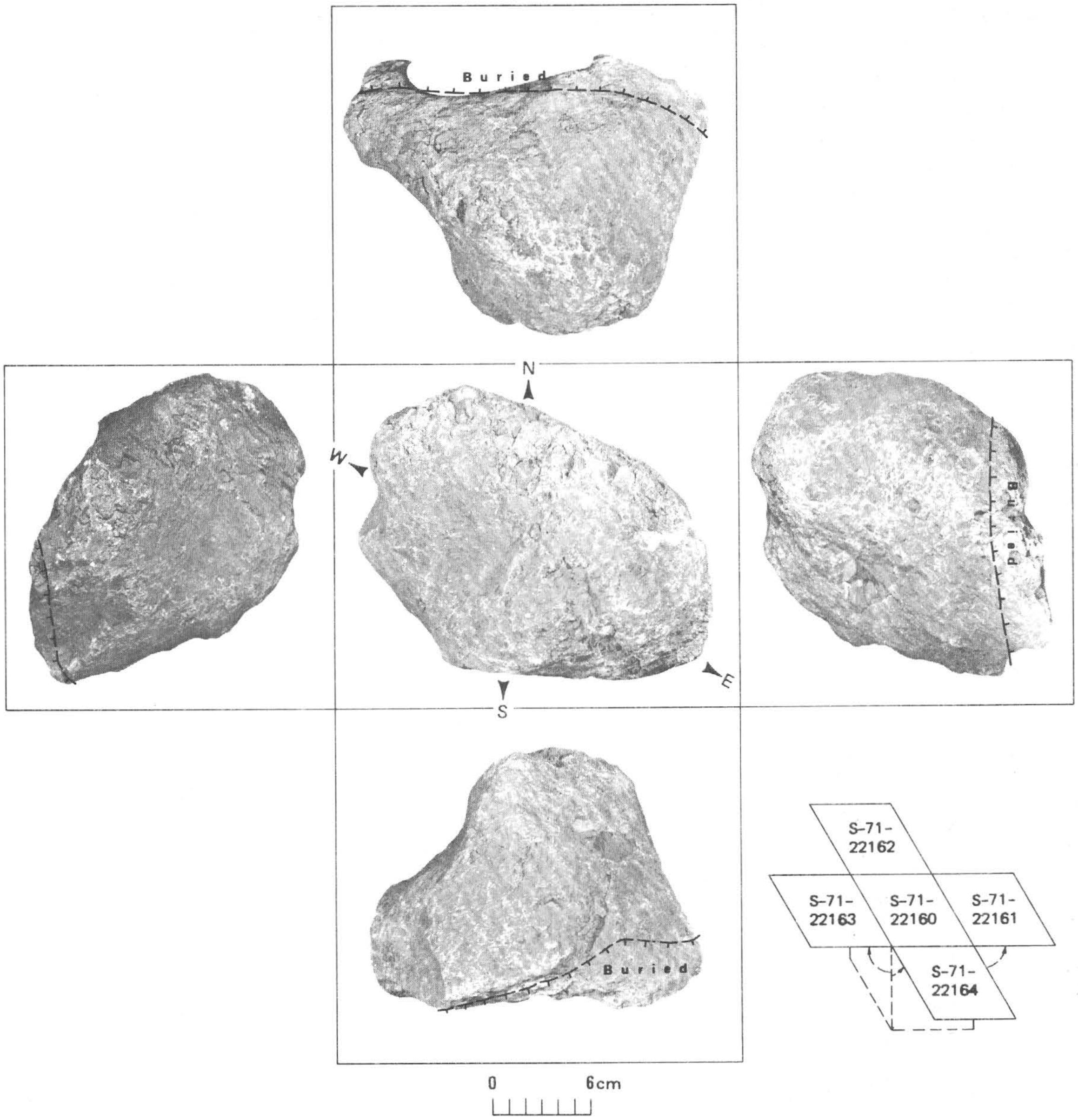

FIGURE 78.—Orthogonal views of sample 14321, shown in approximate lunar orientation. NASA photograph numbers are shown in the schematic diagram.

lunar gravity vector (assumed to be vertical) and X_n is the distance along an unrectified picture corresponding to nG on the map.

The topographic elevation h was determined from a contour map made with Apollo 12 Hasselblad pictures taken from lunar orbit (unpublished map by Mapping Sciences Laboratory, Johnson Space Center, 1970). Since this value is not precisely known, error is introduced into the computation. Assuming that h is the sole source of error and differentiating X_n with respect to h_n in (1):

$$dX_n = dh_n \sin t. \tag{2}$$

Since $\sin t \sim 0.5$, the error in X_n is equal to roughly half the error in the assumed elevation. For example, if the assumed h_n is in error by 10 m (probably a reasonable worst case), the horizontal error dX_n will be about 5 m. This is well within required tolerances for the geologic base map and is smaller than errors introduced by the visual interpolation method of plotting map details.

TABLE 7.—*Sequential listing within each magazine of 60mm Apollo 14 lunar surface pictures*

Magazine LL—black and white

Photo	Seq	EVA	Sta	Az	Remarks
64–9046	165	2	A		Core spls 210, 211 XSD
64–9047	166	2	A		Core spls 210, 211 XSD
64–9048	167	2	A		Core spls 210, 211 LOC, LM
64–9049	188	2	B	269	Pan 7
64–9050	189	2	B	286	Pan 7
64–9051	190	2	B	297	Pan 7
64–9052	191	2	B	317	Pan 7
64–9053	192	2	B	337	Pan 7
64–9054	193	2	B	355	Pan 7
64–9055	194	2	B	8	Pan 7
64–9056	195	2	B	25	Pan 7
64–9057	196	2	B	36	Pan 7
64–9058	197	2	B	41	Pan 7
64–9059	198	2	B	53	Pan 7
64–9060	199	2	B	53	Pan 7
64–9061	200	2	B	70	Pan 7
64–9062	201	2	B	86	Pan 7
64–9063	202	2	B	96	Pan 7
64–9064	203	2	B	108	Pan 7
64–9065	204	2	B	136	Pan 7
64–9066	205	2	B	153	Pan 7
64–9067	206	2	B	171	Pan 7
64–9068	207	2	B	189	Pan 7
64–9069	208	2	B	202	Pan 7
64–9070	209	2	B	222	Pan 7
64–9071	210	2	B	240	Pan 7
64–9072	211	2	B	251	Pan 7
64–9073	212	2	B		Spls 047, 048 XSB
64–9074	213	2	B		Spls 047, 048 XSB
64–9075	214	2	B1	274	Pan 8
64–9076	215	2	B1	276	Pan 8
64–9077	216	2	B1	294	Pan 8
64–9078	217	2	B1	314	Pan 8
64–9079	218	2	B1	327	Pan 8
64–9080	219	2	B1	344	Pan 8
64–9081	220	2	B1	358	Pan 8
64–9082	221	2	B1	11	Pan 8
64–9083	222	2	B1	28	Pan 8
64–9084	223	2	B1	40	Pan 8
64–9085	224	2	B1	66	Pan 8
64–9086	225	2	B1	90	Pan 8
64–9087	226	2	B1	104	Pan 8
64–9088	227	2	B1	121	Pan 8
64–9089	228	2	B1	137	Pan 8
64–9090	229	2	B1	153	Pan 8
64–9091	230	2	B1	167	Pan 8
64–9092	231	2	B1	184	Pan 8
64–9093	232	2	B1	199	Pan 8
64–9094	233	2	B1	224	Pan 8
64–9095	234	2	B1	231	Pan 8
64–9096	235	2	B1	258	Pan 8
64–9097	236	2	B1	261	Pan 8
64–9098	266	2	C′	274	Pan 11
64–9099	267	2	C′	286	Pan 11
64–9100	268	2	C′	302	Pan 11
64–9101	269	2	C′	314	Pan 11
64–9102	270	2	C′	323	Pan 11
64–9103	271	2	C′	337	Pan 11
64–9104	272	2	C′	354	Pan 11
64–9105	273	2	C′	6	Pan 11
64–9106	274	2	C′	20	Pan 11
64–9107	275	2	C′	36	Pan 11
64–9108	276	2	C′	44	Pan 11
64–9109	277	2	C′	63	Pan 11
64–9110	278	2	C′	80	Pan 11
64–9111	279	2	C′	90	Pan 11
64–9112	280	2	C′	104	Pan 11
64–9113	281	2	C′	119	Pan 11
64–9114	282	2	C′	139	Pan 11
64–9115	283	2	C′	157	Pan 11
64–9116	284	2	C′	172	Pan 11
64–9117	285	2	C′	184	Pan 11
64–9118	286	2	C′	206	Pan 11
64–9119	287	2	C′	223	Pan 11
64–9120	288	2	C′	247	Pan 11
64–9121	289	2	C′	243	Pan 11
64–9122	290	2	C′	265	Pan 11
64–9123	291	2	C′		CT 1XS, no recovery; used at Sta G
64–9124	292	2	C′		CT 1XS, no recovery; used at Sta G
64–9125	298	2	C′		Spls 140–144, 068–072 XSB
64–9126	299	2	C′		Spls 140–144, 068–072 XSB
64–9127	300	2	C′		Spls 140–144, 068–072 XSA
64–9128	307	2	C1		Spl 321 XSB, 'Big Bertha'
64–9129	308	2	C1		Spl 321 XSB, 'Big Bertha'
64–9130	309	2	C2		Spl 053 XSB, Fillet
64–9131	310	2	C2		Spl 053 XSB, Fillet
64–9132	311	2	C2		Spl 053 XSB, Fillet
64–9133	312	2	C2		Spl 053 XSB, Fillet
64–9134	313	2	C2–F		Rock E of Weird
64–9135	314	2	C2–F		Rock E of Weird
64–9136	315	2	C2–F		Rock E of Weird
64–9137	316	2	F	274	Pan 12, may include SPL 066
64–9138	317	2	F	293	Pan 12
64–9139	318	2	F	273	Pan 12
64–9140	319	2	F	291	Pan 12
64–9141	320	2	F	313	Pan 12
64–9142	321	2	F	334	Pan 12
64–9143	322	2	F	350	Pan 12
64–9144	323	2	F	6	Pan 12

TABLE 7.—*Sequential listing within each magazine of 60 mm Apollo 14 lunar surface pictures*—Continued

Magazine LL′—black and white—Continued

Photo	Seq.	EVA	Sta.	Az.	Remarks
64–9145	324	2	F	24	Pan 12
64–9146	325	2	F	41	Pan 12
64–9147	326	2	F	57	Pan 12
64–9148	327	2	F	81	Pan 12
64–9149	328	2	F	99	Pan 12
64–9150	329	2	F	118	Pan 12
64–9151	330	2	F	141	Pan 12
64–9152	331	2	F	154	Pan 12
64–9153	332	2	F	171	Pan 12
64–9154	333	2	F	188	Pan 12
64–9155	334	2	F	210	Pan 12
64–9156	335	2	F	231	Pan 12
64–9157	336	2	F	251	Pan 12
64–9158	342	2	G		Trench XSB Spls 145–148 (top)
64–9159	343	2	G		Trench XSB Spls 080, 081, 153–156 (middle)
64–9160	344	2	G		Trench XSA Spls 073–089, 149–152 (bottom)
64–9161	345	2	G		Trench XSA Spl 240, SESC (bottom)
64–9162	346	2	G		Trench XSA
64–9163	347	2	G		Trench XSA
64–9164	348	2	G		Trench XSA
64–9165	349	2	G		Trench XSA
64–9166	350	2	G		Trench DSA
64–9167	351	2	G	272	Pan 13
64–9168	352	2	G	294	Pan 13
64–9169	353	2	G	312	Pan 13
64–9170	354	2	G	331	Pan 13
64–9171	355	2	G	354	Pan 13
64–9172	356	2	G	11	Pan 13
64–9173	357	2	G	34	Pan 13
64–9174	358	2	G	52	Pan 13
64–9175	359	2	G	66	Pan 13
64–9176	360	2	G	83	Pan 13, core spl 230 loc
64–9177	361	2	G	98	Pan 13, core spl 230 loc
64–9178	362	2	G	115	Pan 13
64–9179	363	2	G	122	Pan 13
64–9180	364	2	G	135	Pan 13
64–9181	365	2	G	150	Pan 13
64–9182	366	2	G	168	Pan 13
64–9183	367	2	G	185	Pan 13
64–9184	368	2	G	208	Pan 13
64–9185	369	2	G	229	Pan 13
64–9186	370	2	G	251	Pan 13
64–9187	371	2	G	265	Pan 13
64–9188	378	2	G1		Spls 313, 301 DS, loc
64–9189	407	2	LM		LM, Earth
64–9190	408	2	LM		LM, Earth
64–9191	409	2	LM		LM, Earth
64–9192	410	2	LM		LM, Earth
64–9193	411	2	LM		LM, Earth
64–9194	412	2	LM		LM, Earth
64–9195	413	2	LM		LM, Earth
64–9196	414	2	LM		LM, Earth
64–9197	415	2	LM		LM, Earth
64–9198	416	2	LM		SWC
64–9199	417	2	LM		SWC
64–9200	418	2	LM		SWC
64–9201	419	2	LM		SWC

Magazine KK—black and white

Photo	Seq.	EVA	Sta.	Az.	Remarks
65–9202	014	Pre	LM	321	LM Window Pan 1
65–9203	015	Pre	LM	346	LM Window Pan 1
65–9204	016	Pre	LM	306	LM Window Pan 1
65–9205	017	Pre	LM	335	LM Window Pan 1
65–9206	018	Pre	LM	311	LM Window Pan 1
65–9207	019	Pre	LM	291	LM Window Pan 1
65–9208	020	Pre	LM	346	LM Window Pan 1
65–9209	021	Pre	LM	236	LM Window Pan 1
65–9210	022	Pre	LM	226	LM Window Pan 1
65–9211	023	Pre	LM	249	LM Window Pan 1
65–9212	024	Pre	LM	283	LM Window Pan 1
65–9213	025	Pre	LM	279	LM Window Pan 1
65–9214	026	Pre	LM	247	LM Window Pan 1
65–9215	027	Pre	LM	270	LM Window Pan 1

Magazine II—color

Photo	Seq.	EVA	Sta.	Az.	Remarks
66–9216	001				Orbit
66–9217	002				Orbit
66–9218	003				Orbit
66–9219	004				Orbit
66–9220	005				Orbit
66–9221	006				Orbit
66–9222	007				Orbit
66–9223	008				Orbit
66–9224	009				Orbit
66–9225	010				Orbit
66–9226	011				Orbit
66–9227	012				Orbit
66–9228	013				Orbit
66–9229	028	1	LM		Cdr
66–9230	029	1	LM		Cdr
66–9231	030	1	LM		Flag
66–9232	031	1	LM		Flag
66–9233	032	1	LM		Flag
66–9234	033	1	LM		Footpad

TABLE 7.—*Sequential listing within each magazine of 60 mm Apollo 14 lunar surface pictures*—Continued

Photo	Seq.	EVA	Sta.	Az.	Remarks
Magazine II—color—Continued					
66-9235	034	1	LM		Footpad
66-9236	035	1	LM	272	Pan 2, NE of LM
66-9237	036	1	LM	284	Pan 2, NE of LM
66-9238	037	1	LM	292	Pan 2, NE of LM
66-9239	038	1	LM	308	Pan 2, NE of LM
66-9240	039	1	LM	325	Pan 2, NE of LM
66-9241	040	1	LM	339	Pan 2, NE of LM
66-9242	041	1	LM	353	Pan 2, NE of LM
66-9243	042	1	LM	13	Pan 2, NE of LM
66-9244	043	1	LM	30	Pan 2, NE of LM
66-9245	044	1	LM	40	Pan 2, NE of LM
66-9246	045	1	LM	58	Pan 2, NE of LM
66-9247	046	1	LM	82	Pan 2, NE of LM
66-9248	047	1	LM	106	Pan 2, NE of LM
66-9249	048	1	LM	130	Pan 2, NE of LM
66-9250	049	1	LM	146	Pan 2, NE of LM
66-9251	050	1	LM	159	Pan 2, NE of LM
66-9252	051	1	LM	174	Pan 2, NE of LM
66-9253	052	1	LM	192	Pan 2, NE of LM
66-9254	053	1	LM	207	Pan 2, NE of LM
66-9255	054	1	LM	229	Pan 2, NE of LM
66-9256	055	1	LM	242	Pan 2, NE of LM
66-9257	056	1	LM	260	Pan 2, NE of LM
66-9258	057	1	LM		LM Misc
66-9259	058	1	LM		LM Misc
66-9260	059	1	LM		LM Misc
66-9261	060	1	LM		DPS
66-9262	061	1	LM		DPS
66-9263	062	1	LM		DPS
66-9264	063	1	LM		Footpad
66-9265	064	1	LM		Footpad
66-9266	065	1	LM		DPS
66-9267	066	1	LM		DPS
66-9268	067	1	LM		DPS
66-9269	068	1	LM		Footpad
66-9270	069	1	LM		Footpad
66-9271	070	1	LM	270	Pan 3, S of LM
66-9272	071	1	LM	283	Pan 3, S of LM
66-9273	072	1	LM	294	Pan 3, S of LM
66-9274	073	1	LM	308	Pan 3, S of LM
66-9275	074	1	LM	320	Pan 3, S of LM
66-9276	075	1	LM	338	Pan 3, S of LM
66-9277	076	1	LM	358	Pan 3, S of LM
66-9278	077	1	LM	15	Pan 3, S of LM
66-9279	078	1	LM	33	Pan 3, S of LM
66-9280	079	1	LM	49	Pan 3, S of LM
66-9281	080	1	LM	67	Pan 3, S of LM
66-9282	081	1	LM	85	Pan 3, S of LM
66-9283	082	1	LM	101	Pan 3, S of LM
66-9284	083	1	LM	115	Pan 3, S of LM
66-9285	084	1	LM	133	Pan 3, S of LM
66-9286	085	1	LM	148	Pan 3, S of LM
66-9287	086	1	LM	165	Pan 3, S of LM
66-9288	087	1	LM	181	Pan 3, S of LM
66-9289	088	1	LM	196	Pan 3, S of LM
66-9290	089	1	LM	210	Pan 3, S of LM
66-9291	090	1	LM	223	Pan 3, S of LM
66-9292	091	1	LM	237	Pan 3, S of LM
66-9293	092	1	LM	260	Pan 3, S of LM
66-9294	093	1	LM	286	Pan 4, W of LM
66-9295	094	1	LM	297	Pan 4, W of LM
66-9296	095	1	LM	311	Pan 4, W of LM
66-9297	096	1	LM	327	Pan 4, W of LM
66-9298	097	1	LM	341	Pan 4, W of LM
66-9299	098	1	LM	0	Pan 4, W of LM
66-9300	099	1	LM	15	Pan 4, W of LM
66-9301	100	1	LM	32	Pan 4, W of LM
66-9302	101	1	LM	45	Pan 4, W of LM
66-9303	102	1	LM	60	Pan 4, W of LM
66-9304	103	1	LM	77	Pan 4, W of LM
66-9305	104	1	LM	90	Pan 4, W of LM
66-9306	105	1	LM	105	Pan 4, W of LM
66-9307	106	1	LM	120	Pan 4, W of LM
66-9308	107	1	LM	136	Pan 4, W of LM
66-9309	108	1	LM	151	Pan 4, W of LM
66-9310	109	1	LM	169	Pan 4, W of LM
66-9311	110	1	LM	181	Pan 4, W of LM
66-9312	111	1	LM	199	Pan 4, W of LM
66-9313	112	1	LM	215	Pan 4, W of LM
66-9314	113	1	LM	232	Pan 4, W of LM
66-9315	114	1	LM	254	Pan 4, W of LM
66-9316	115	1	LM	272	Pan 4, W of LM
66-9317	149	1–2	LM	287	LM Window Pan 5
66-9318	150	1–2	LM	285	LM Window Pan 5
66-9319	151	1–2	LM	275	LM Window Pan 5
66-9320	152	1–2	LM	254	LM Window Pan 5
66-9321	153	1–2	LM	261	LM Window Pan 5
66-9322	154	1–2	LM	222	LM Window Pan 5
66-9323	155	1–2	LM	6	LM Window Pan 5
66-9324	156	1–2	LM	308	LM Window Pan 5
66-9325	157	1–2	LM	310	LM Window Pan 5
66-9326	158	1–2	LM	354	LM Window Pan 5
66-9327	159	1–2	LM		Earth
66-9328	160	1–2	LM		Earth
66-9329	161	1–2	LM		Earth
66-9330	162	1–2	LM		Earth
66-9331	163	1–2	LM		Earth
66-9332	164	1–2	LM		Earth
66-9333	420	Post	LM	282	LM Window Pan 15

TABLE 7.—*Sequential listing within each magazine of 60 mm Apollo 14 lunar surface pictures*—Continued

Photo	Seq.	EVA	Sta.	Az.	Remarks
Magazine II—color—Continued					
66-9334	421	Post	LM	289	LM Window Pan 15
66-9335	422	Post	LM	285	LM Window Pan 15
66-9336	423	Post	LM	288	LM Window Pan 15
66-9337	424	Post	LM	328	LM Window Pan 15
66-9338	425	Post	LM	298	LM Window Pan 15
66-9339	426	Post	LM	309	LM Window Pan 15
66-9340	427	Post	LM	332	LM Window Pan 15
66-9341	428	Post	LM	353	LM Window Pan 15
66-9342	429	Post	LM	330	LM Window Pan 15
66-9343	430	Post	LM	322	LM Window Pan 15
66-9344	431				Command Module
66-9345	432				Command Module
66-9346	433				Command Module
66-9347	434				Command Module
66-9348	435				Command Module
66-9349	436				Command Module
66-9350	437				Command Module
66-9351	438				Command Module
66-9352	439				Command Module
66-9353	440				Command Module
66-9354	441				Command Module
66-9355	442				Command Module
66-9356	443				Command Module
66-9357	444				Command Module
66-9358	445				Command Module
66-9359	446				Command Module
66-9360	447				Command Module
Magazine JJ—color					
67-9361	116	1	ALSEP		C/S, MET
67-9362	117	1	ALSEP		PSE
67-9363	118	1	ALSEP		C/S, PSE
67-9364	119	1	ALSEP		CPLEE
67-9365	120	1	ALSEP		C/S, CPLEE
67-9366	121	1	ALSEP		C/S, RTG
67-9367	122	1	ALSEP		ALSEP LOC, MET tracks, LM
67-9368	123	1	ALSEP		ALSEP LOC, MET tracks, LM
67-9369	124	1	ALSEP		Side
67-9370	125	1	ALSEP		Side
67-9371	126	1	ALSEP		Side
67-9372	127	1	ALSEP		C/S, Side
67-9373	128	1	ALSEP		Side
67-9374	129	1	ALSEP		Geophone Line, LMP
67-9375	130	1	ALSEP		C/S, RTG
67-9376	131	1	ALSEP		C/S
67-9377	132	1	ALSEP		C/S
67-9378	133	1	ALSEP		C/S
67-9379	134	1	ALSEP		C/S
67-9380	135	1	ALSEP		C/S
67-9381	136	1	ALSEP		C/S
67-9382	137	1	ALSEP		C/S
67-9383	138	1	ALSEP		C/S
67-9384	139	1	ALSEP		C/S, PSE
67-9385	140	1	ALSEP		LRRR
67-9386	141	1	ALSEP		LRRR
67-9387	142	1	ALSEP		LRRR, LOC, LM
67-9388	143	1	ALSEP		LOC to LM for comprehensive SPL
67-9389	144	1	ALSEP		LOC to ALSEP for comprehensive SPL
67-9390	145	1	ALSEP		SPL 304 XSB, FSR
67-9391	146	1	ALSEP		SPL 304 XSB, FSR
67-9392	147	1	ALSEP		SPL 305, XSB, FSR
67-9393	148	1	ALSEP		SPL 305 XSB, FSR
Magazine MM—black and white					
68-9394	168	2	A	271	Pan 6
68-9395	169	2	A	269	Pan 6
68-9396	170	2	A	285	Pan 6
68-9397	171	2	A	312	Pan 6
68-9398	172	2	A	335	Pan 6
68-9399	173	2	A	359	Pan 6
68-9400	174	2	A	23	Pan 6
68-9401	175	2	A	58	Pan 6
68-9402	176	2	A	82	Pan 6
68-9403	177	2	A	116	Pan 6
68-9404	178	2	A	141	Pan 6
68-9405	179	2	A	160	Pan 6
68-9406	180	2	A	193	Pan 6
68-9407	181	2	A	210	Pan 6
68-9408	182	2	A	232	Pan 6
68-9409	183	2	A		Spls 041–046 DSB
68-9410	184	2	A		Spls 041–046 XSB
68-9411	185	2	A		Spls 041–046 XSB
68-9412	186	2	A		Spls 041–046 XSA
68-9413	187	2	A		Spls 041–046 LOC
68-9414	237	2	B2		Large rock above flank
68-9415	238	2	B2	263	Pan 9
68-9416	239	2	B2	284	Pan 9
68-9417	240	2	B2	316	Pan 9
68-9418	241	2	B2	345	Pan 9
68-9419	242	2	B2	9	Pan 9
68-9420	243	2	B2	33	Pan 9
68-9421	244	2	B2	57	Pan 9
68-9422	245	2	B2	92	Pan 9
68-9423	246	2	B2	120	Pan 9
68-9424	247	2	B2	148	Pan 9

TABLE 7.—*Sequential listing within each magazine of 60 mm Apollo 14 lunar surface pictures*—Continued

Photo	Seq.	EVA	Sta.	Az.	Remarks
Magazine MM——black and white—Continued					
68-9425	248	2	B2	165	Pan 9
68-9426	249	2	B2	184	Pan 9
68-9427	250	2	B2	200	Pan 9
68-9428	251	2	B2	223	Pan 9
68-9429	252	2	B2	241	Pan 9
68-9430	253	2	B3	267	Pan 10
68-9431	254	2	B3	304	Pan 10
68-9432	255	2	B3	323	Pan 10
68-9433	256	2	B3	350	Pan 10
68-9434	257	2	B3	7	Pan 10
68-9435	258	2	B3	33	Pan 10
68-9436	259	2	B3	72	Pan 10
68-9437	260	2	B3	99	Pan 10
68-9438	261	2	B3	123	Pan 10
68-9439	262	2	B3	149	Pan 10
68-9440	263	2	B3	176	Pan 10
68-9441	264	2	B3	200	Pan 10
68-9442	265	2	B3	238	Pan 10
68-9443	293	2	C'		Spls 051, 052 XSB
68-9444	294	2	C'		Spls 051, 052 XSB
68-9445	295	2	C'		Spls 051, 052 DSB, includes rocks in 9448–9453
68-9446	296	2	C'		Spls 051, 052 XSA
68-9447	297	2	C'		Spls 051, 052 LOC
68-9448	301	2	C1		White rocks
68-9449	302	2	C1		White rocks
68-9450	303	2	C1		White rocks
68-9451	304	2	C1		White rocks
68-9452	305	2	C1		White rocks, spl 082 XSA
68-9453	306	2	C1		White rocks, spl 082 XSA
68-9454	337	2	G		Core spl 220
68-9455	338	2	G		Core spl 230
68-9456	339	2	G		Core spl 230
68-9457	340	2	G		Core spl 230
68-9458	341	2	G		Core spl 230
68-9459	372	2	G		Spl 306 DSB
68-9460	373	2	G		Spl 306 XSB
68-9461	374	2	G		Spl 306 XSB
68-9462	375	2	G		Spl 306 XSA
68-9463	376	2	G		Spl 306 XSA
68-9464	377	2	G		Spl 306 LOC
68-9465	379	2	G1		Spls 313, 301 XSB, may include some loose rock
68-9466	380	2	G1		Spls 313, 301 XSB
68-9467	381	2	G1		Spls 313, 301 XSA
68-9468	382	2	H		Grab spl, 4 rocks, XSB
68-9469	383	2	H		Grab spl, 4 rocks, XSB
68-9470	384	2	H		Grab spl, 4 rocks, XSA
68-9471	385	2	H		Grab spl, 4 rocks, XSA
68-9472	386	2	H		2 spl rocks off turtle rock, 2 rocks on fillet, XSB
68-9473	387	2	H		2 spl rocks off turtle rock, 2 rocks on fillet, XSB
68-9474	388	2	H		2 spl rocks off turtle rock, 2 rocks on fillet, XSB
68-9475	389	2	H		2 spl rocks off turtle rock, 2 rocks on fillet, XSB
68-9476	390	2	H		2 spl rocks off turtle rock, 2 rocks on fillet, XSA
68-9477	391	2	H	264	Pan 14
68-9478	392	2	H	297	Pan 14
68-9479	393	2	H	319	Pan 14
68-9480	394	2	H	345	Pan 14
68-9481	395	2	H	8	Pan 14
68-9482	396	2	H	27	Pan 14
68-9483	397	2	H	57	Pan 14
68-9484	398	2	H	83	Pan 14
68-9485	399	2	H	113	Pan 14
68-9486	400	2	H	136	Pan 14
68-9487	401	2	H	147	Pan 14
68-9488	402	2	H	177	Pan 14
68-9489	403	2	H	203	Pan 14
68-9490	404	2	H	225	Pan 14
68-9491	405	2	H	242	Pan 14
68-9492	406	2	LM		S-band antenna, accidental

TABLE 8.—*Chronologic listing of 60 mm Apollo 14 lunar surface pictures*

Photo	Seq.	EVA	Sta.	Az.	Remarks
66-9216	001				Orbit
66-9217	002				Orbit
66-9218	003				Orbit
66-9219	004				Orbit
66-9220	005				Orbit
66-9221	006				Orbit
66-9222	007				Orbit
66-9223	008				Orbit
66-9224	009				Orbit
66-9225	010				Orbit
66-9226	011				Orbit
66-9227	012				Orbit
66-9228	013				Orbit
65-9202	014	Pre	LM	321	LM Window Pan 1
65-9203	015	Pre	LM	346	LM Window Pan 1
65-9204	016	Pre	LM	306	LM Window Pan 1
65-9205	017	Pre	LM	335	LM Window Pan 1

TABLE 8.—*Chronologic listing of 60 mm Apollo 14 lunar surface pictures*—Continued

Photo	Seq.	Eva	Sta.	Az.	Remarks
65-9206	018	Pre	LM	311	LM Window Pan 1
65-9207	019	Pre	LM	291	LM Window Pan 1
65-9208	020	Pre	LM	346	LM Window Pan 1
65-9209	021	Pre	LM	236	LM Window Pan 1
65-9210	022	Pre	LM	226	LM Window Pan 1
65-9211	023	Pre	LM	249	LM Window Pan 1
65-9212	024	Pre	LM	283	LM Window Pan 1
65-9213	025	Pre	LM	279	LM Window Pan 1
65-9214	026	Pre	LM	247	LM Window Pan 1
65-9215	027	Pre	LM	270	LM Window Pan 1
66-9229	028	1	LM		Cdr
66-9230	029	1	LM		Cdr
66-9231	030	1	LM		Flag
66-9232	031	1	LM		Flag
66-9233	032	1	LM		Flag
66-9234	033	1	LM		Footpad
66-9235	034	1	LM		Footpad
66-9236	035	1	LM	272	Pan 2, NE of LM
66-9237	036	1	LM	284	Pan 2, NE of LM
66-9238	037	1	LM	292	Pan 2, NE of LM
66-9239	038	1	LM	308	Pan 2, NE of LM
66-9240	039	1	LM	325	Pan 2, NE of LM
66-9241	040	1	LM	339	Pan 2, NE of LM
66-9242	041	1	LM	353	Pan 2, NE of LM
66-9243	042	1	LM	13	Pan 2, NE of LM
66-9244	043	1	LM	30	Pan 2, NE of LM
66-9245	044	1	LM	40	Pan 2, NE of LM
66-9246	045	1	LM	58	Pan 2, NE of LM
66-9247	046	1	LM	82	Pan 2, NE of LM
66-9248	047	1	LM	106	Pan 2, NE of LM
66-9249	048	1	LM	130	Pan 2, NE of LM
66-9250	049	1	LM	146	Pan 2, NE of LM
66-9251	050	1	LM	159	Pan 2, NE of LM
66-9252	051	1	LM	174	Pan 2, NE of LM
66-9253	052	1	LM	192	Pan 2, NE of LM
66-9254	053	1	LM	207	Pan 2, NE of LM
66-0255	054	1	LM	229	Pan 2, NE of LM
66-9256	055	1	LM	242	Pan 2, NE of LM
66-9257	056	1	LM	260	Pan 2, NE of LM
66-9258	057	1	LM		LM misc
66-9259	058	1	LM		LM misc
66-9260	059	1	LM		LM misc
66-9261	060	1	LM		
66-9262	061	1	LM		DPS
66-9263	062	1	LM		DPS
66-9264	063	1	LM		Footpad
66-9265	064	1	LM		Footpad
66-9266	065	1	LM		DPS
66-9267	066	1	LM		DPS
66-9268	067	1	LM		DPS
66-9269	068	1	LM		Footpad
66-9270	069	1	LM		Footpad
66-9271	070	1	LM	270	Pan 3, S of LM
66-9272	071	1	LM	283	Pan 3, S of LM
66-9273	072	1	LM	294	Pan 3, S of LM
66-9274	073	1	LM	308	Pan 3, S of LM
66-9275	074	1	LM	320	Pan 3, S of LM
66-9276	075	1	LM	338	Pan 3, S of LM
66-9277	076	1	LM	358	Pan 3, S of LM
66-9278	077	1	LM	15	Pan 3, S of LM
66-9279	078	1	LM	33	Pan 3, S of LM
66-9280	079	1	LM	49	Pan 3, S of LM
66-9281	080	1	LM	67	Pan 3, S of LM
66-9282	081	1	LM	85	Pan 3, S of LM
66-9283	082	1	LM	101	Pan 3, S of LM
66-9284	083	1	LM	115	Pan 3, S of LM
66-9285	084	1	LM	133	Pan 3, S of LM
66-9286	085	1	LM	148	Pan 3, S of LM
66-9287	086	1	LM	165	Pan 3, S of LM
66-9288	087	1	LM	181	Pan 3, S of LM
66-9289	088	1	LM	196	Pan 3, S of LM
66-9290	089	1	LM	210	Pan 3, S of LM
66-9291	090	1	LM	223	Pan 3, S of LM
66-9292	091	1	LM	237	Pan 3, S of LM
66-9293	092	1	LM	260	Pan 3, S of LM
66-9294	093	1	LM	286	Pan 4, W of LM
66-9295	094	1	LM	297	Pan 4, W of LM
66-9296	095	1	LM	311	Pan 4, W of LM
66-9297	096	1	LM	327	Pan 4, W of LM
66-9298	097	1	LM	341	Pan 4, W of LM
66-9299	098	1	LM	0	Pan 4, W of LM
66-9300	099	1	LM	15	Pan 4, W of LM
66-9301	100	1	LM	32	Pan 4, W of LM
66-9302	101	1	LM	45	Pan 4, W of LM
66-9303	102	1	LM	60	Pan 4, W of LM
66-9304	103	1	LM	77	Pan 4, W of LM
66-9305	104	1	LM	90	Pan 4, W of LM
66-9306	105	1	LM	105	Pan 4, W of LM
66-9307	106	1	LM	120	Pan 4, W of LM
66-9308	107	1	LM	136	Pan 4, W of LM
66-9309	108	1	LM	151	Pan 4, W of LM
66-9310	109	1	LM	169	Pan 4, W of LM
66-9311	110	1	LM	181	Pan 4, W of LM
66-9312	111	1	LM	199	Pan 4, W of LM
66-9313	112	1	LM	215	Pan 4, W of LM
66-9314	113	1	LM	232	Pan 4, W of LM
66-9315	114	1	LM	254	Pan 4, W of LM
66-9316	115	1	LM	272	Pan 4, W of LM
67-9361	116	1	ALSEP		C/S, MET
67-9362	117	1	ALSEP		PSE
67-9363	118	1	ALSEP		C/S, PSE
67-9364	119	1	ALSEP		CPLEE

TABLE 8.—*Chronologic listing of 60 mm Apollo 14 lunar surface pictures*—Continued

Photo	Seq.	EVA	Sta	Az.	Remarks
67–9365	120	1	ALSEP		C/S, CPLEE
67–9366	121	1	ALSEP		C/S, RTG
67–9367	122	1	ALSEP		ALSEP LOC, MET tracks, LM
67–9368	123	1	ALSEP		ALSEP LOC, MET tracks, LM
67–9369	124	1	ALSEP		Side
67–9370	125	1	ALSEP		Side
67–9371	126	1	ALSEP		Side
67–9372	127	1	ALSEP		C/S, Side
67–9373	128	1	ALSEP		Side
67–9374	129	1	ALSEP		Geophone line, LMP
67–9375	130	1	ALSEP		C/S, RTG
67–9376	131	1	ALSEP		C/S
67–9377	132	1	ALSEP		C/S
67–9378	133	1	ALSEP		C/S
67–9379	134	1	ALSEP		C/S
67–9380	135	1	ALSEP		C/S
67–9381	136	1	ALSEP		C/S
67–9382	137	1	ALSEP		C/S
67–9383	138	1	ALSEP		C/S
67–9384	139	1	ALSEP		C/S, PSE
67–9385	140	1	ALSEP		LRRR
67–9386	141	1	ALSEP		LRRR
67–9387	142	1	ALSEP		LRRR, LOC, LM
67–9388	143	1	ALSEP		LOC to LM for comprehensive spl
67–9389	144	1	ALSEP		LOC to ALSEP for comprehensive spl
67–9390	145	1	ALSEP		Spl 304 XSB, FSR
67–9391	146	1	ALSEP		Spl 304 XSB, FSR
67–9392	147	1	ALSEP		Spl 305 XSB, FSR
67–9393	148	1	ALSEP		Spl 305 XSB, FSR
66–9317	149	1–2	LM	287	LM Window Pan 5
66–9318	150	1–2	LM	285	LM Window Pan 5
66–9319	151	1–2	LM	275	LM Window Pan 5
66–9320	152	1–2	LM	254	LM Window Pan 5
66–9321	153	1–2	LM	261	LM Window Pan 5
66–9322	154	1–2	LM	222	LM Window Pan 5
66–9323	155	1–2	LM	6	LM Window Pan 5
66–9324	156	1–2	LM	308	LM Window Pan 5
66–9325	157	1–2	LM	310	LM Window Pan 5
66–9326	158	1–2	LM	354	LM Window Pan 5
66–9327	159	1–2	LM		Earth
66–9328	160	1–2	LM		Earth
66–9329	161	1–2	LM		Earth
66–9330	162	1–2	LM		Earth
66–9331	163	1–2	LM		Earth
66–9332	164	1–2	LM		Earth
64–9046	165	2	A		Core spls 210, 211 XSD
64–9047	166	2	A		Core spls 210, 211 XSD
64–9048	167	2	A		Core spls 210, 211 LOC, LM
68–9394	168	2	A	271	Pan 6
68–9395	169	2	A	269	Pan 6
68–9396	170	2	A	285	Pan 6
68–9397	171	2	A	312	Pan 6
68–9398	172	2	A	335	Pan 6
68–9399	173	2	A	359	Pan 6
68–9400	174	2	A	23	Pan 6
68–9401	175	2	A	58	Pan 6
68–9402	176	2	A	82	Pan 6
68–9403	177	2	A	116	Pan 6
68–9404	178	2	A	141	Pan 6
68–9405	179	2	A	160	Pan 6
68–9406	180	2	A	193	Pan 6
68–9407	181	2	A	210	Pan 6
68–9408	182	2	A	232	Pan 6
68–9409	183	2	A		Spls 041-046 DSB
68–9410	184	2	A		Spls 041-046 XSB
68–9411	185	2	A		Spls 041-046 XSB
68–9412	186	2	A		Spls 041-046 XSA
68–9413	187	2	A		Spls 041-046 LOC
64–9049	188	2	B	269	Pan 7
64–9050	189	2	B	286	Pan 7
64–9051	190	2	B	297	Pan 7
64–9052	191	2	B	317	Pan 7
64–9053	192	2	B	337	Pan 7
64–9054	193	2	B	355	Pan 7
64–9055	194	2	B	8	Pan 7
64–9056	195	2	B	25	Pan 7
64–9057	196	2	B	36	Pan 7
64–9058	197	2	B	41	Pan 7
64–9059	198	2	B	53	Pan 7
64–9060	199	2	B	53	Pan 7
64–9061	200	2	B	70	Pan 7
64–9062	201	2	B	86	Pan 7
64–9063	202	2	B	96	Pan 7
64–9064	203	2	B	108	Pan 7
64–9065	204	2	B	136	Pan 7
64–9066	205	2	B	153	Pan 7
64–9067	206	2	B	171	Pan 7
64–9068	207	2	B	189	Pan 7
64–9069	208	2	B	202	Pan 7
64–9070	209	2	B	222	Pan 7
64–9071	210	2	B	240	Pan 7
64–9072	211	2	B	251	Pan 7
64–9073	212	2	B		Spls 047, 048 XSB
64–9074	213	2	B		Spls 047, 048 XSB
64–9075	214	2	B1	274	Pan 8
64–9076	215	2	B1	276	Pan 8
64–9077	216	2	B1	294	Pan 8
64–9078	217	2	B1	314	Pan 8
64–9079	218	2	B1	327	Pan 8
64–9080	219	2	B1	344	Pan 8
64–9081	220	2	B1	358	Pan 8
64–9082	221	2	B1	11	Pan 8
64–9083	222	2	B1	28	Pan 8
64–9084	223	2	B1	40	Pan 8
64–9085	224	2	B1	66	Pan 8
64–9086	225	2	B1	90	Pan 8
64–9087	226	2	B1	104	Pan 8
64–9088	227	2	B1	121	Pan 8
64–9089	228	2	B1	137	Pan 8
64–9090	229	2	B1	153	Pan 8
64–9091	230	2	B1	167	Pan 8
64–9092	231	2	B1	184	Pan 8
64–9093	232	2	B1	199	Pan 8
64–9094	233	2	B1	224	Pan 8
64–9095	234	2	B1	231	Pan 8
64–9096	235	2	B1	258	Pan 8
64–9097	236	2	B1	261	Pan 8
68–9414	237	2	B2		Large rock above Flank
68–9415	238	2	B2	263	Pan 9
68–9416	239	2	B2	284	Pan 9
68–9417	240	2	B2	316	Pan 9
68–9418	241	2	B2	345	Pan 9
68–9419	242	2	B2	9	Pan 9
68–9420	243	2	B2	33	Pan 9
68–9421	244	2	B2	57	Pan 9
68–9422	245	2	B2	92	Pan 9
68–9423	246	2	B2	120	Pan 9
68–9424	247	2	B2	148	Pan 9
68–9425	248	2	B2	165	Pan 9
68–9426	249	2	B2	184	Pan 9
68–9427	250	2	B2	200	Pan 9
68–9428	251	2	B2	223	Pan 9
68–9429	252	2	B2	241	Pan 9
68–9430	253	2	B3	267	Pan 10
68–9431	254	2	B3	304	Pan 10
68–9432	255	2	B3	323	Pan 10
68–9433	256	2	B3	350	Pan 10
68–9434	257	2	B3	7	Pan 10
68–9435	258	2	B3	33	Pan 10
68–9436	259	2	B3	72	Pan 10
68–9437	260	2	B3	99	Pan 10
68–9438	261	2	B3	123	Pan 10
68–9439	262	2	B3	149	Pan 10
68–9440	263	2	B3	176	Pan 10
68–9441	264	2	B3	200	Pan 10
68–9442	265	2	B3	238	Pan 10
64–9098	266	2	C′	274	Pan 11
64–9099	267	2	C′	286	Pan 11
64–9100	268	2	C′	302	Pan 11
64–9101	269	2	C′	314	Pan 11
64–9102	270	2	C′	323	Pan 11
64–9103	271	2	C′	337	Pan 11
64–9104	272	2	C′	354	Pan 11
64–9105	273	2	C′	6	Pan 11
64–9106	274	2	C′	20	Pan 11
64–9107	275	2	C′	36	Pan 11
64–9108	276	2	C′	44	Pan 11
64–9109	277	2	C′	63	Pan 11
64–9110	278	2	C′	80	Pan 11
64–9111	279	2	C′	90	Pan 11
64–9112	280	2	C′	104	Pan 11
64–9113	281	2	C′	119	Pan 11
64–9114	282	2	C′	139	Pan 11
64–9115	283	2	C′	157	Pan 11
64–9116	284	2	C′	172	Pan 11
64–9117	285	2	C′	184	Pan 11
64–9118	286	2	C′	206	Pan 11
64–9119	287	2	C′	223	Pan 11
64–9120	288	2	C′	247	Pan 11
64–9121	289	2	C′	243	Pan 11
64–9122	290	2	C′	265	Pan 11
64–9123	291	2	C′		CT 1 XS, no recovery; used at Sta G
64–9124	292	2	C′		CT 1 XS, no recovery; used at Sta G
68–9443	293	2	C′		Spls 051, 052 XSB
68–9444	294	2	C′		Spls 051, 052 XSB
68–9445	295	2	C′		Spls 051, 052 DSB, includes rocks in 9448–9453
68–9446	296	2	C′		Spls 051, 052 XSA
68–9447	297	2	C′		Spls 051, 052 LOC
64–9125	298	2	C′		Spls 140–144, 068–072 XSB
64–9126	299	2	C′		Spls 140–144, 068–072 XSB
64–9127	300	2	C′		Spls 140–144, 068–072 XSA
68–9448	301	2	C1		White rocks
68–9449	302	2	C1		White rocks
68–9450	303	2	C1		White rocks
68–9451	304	2	C1		White rocks
68–9452	305	2	C1		White rocks, Spl 082 XSA
68–9453	306	2	C1		White rocks, Spl 082 XSA
64–9128	307	2	C1		Spl 321 XSB, 'Big Bertha'
64–9129	308	2	C1		Spl 321 XSB, 'Big Bertha'
64–9130	309	2	C2		Spl 053 XSB, fillet
64–9131	310	2	C2		Spl 053 XSB, fillet
64–9132	311	2	C2		Spl 053 XSB, fillet
64–9133	312	2	C2		Spl 053 XSB, fillet
64–9134	313	2	C2–F		Rock E of Weird
64–9135	314	2	C2–F		Rock E of Weird
64–9136	315	2	C2–F		Rock E of Weird
64–9137	316	2	F	274	Pan 12, may include spl 066
64–9138	317	2	F	293	Pan 12
64–9139	318	2	F	273	Pan 12
64–9140	319	2	F	291	Pan 12
64–9141	320	2	F	313	Pan 12
64–9142	321	2	F	334	Pan 12
64–9143	322	2	F	350	Pan 12

TABLE 8.—*Chronologic listing of 60 mm Apollo 14 lunar surface pictures*—Continued

Photo	Seq.	EVA	Sta.	Az.	Remarks
64-9144	323	2	F	6	Pan 12
64-9145	324	2	F	24	Pan 12
64-9146	325	2	F	41	Pan 12
64-9147	326	2	F	57	Pan 12
64-9148	327	2	F	81	Pan 12
64-9149	328	2	F	99	Pan 12
64-9150	329	2	F	118	Pan 12
64-9151	330	2	F	141	Pan 12
64-9152	331	2	F	154	Pan 12
64-9153	332	2	F	171	Pan 12
64-9154	333	2	F	188	Pan 12
64-9155	334	2	F	210	Pan 12
64-9156	335	2	F	231	Pan 12
64-9157	336	2	F	251	Pan 12
68-9454	337	2	G		Core spl 220
68-9455	338	2	G		Core spl 230
68-9456	339	2	G		Core spl 230
68-9457	340	2	G		Core spl 230
68-9458	341	2	G		Core spl 230
64-9158	342	2	G		Trench XSB spls 145–148 (top)
64-9159	343	2	G		Trench XSB spls 080–081, 153–156 (middle)
64-9160	344	2	G		Trench XSA spls 073–089, 149–152 (bottom)
64-9161	345	2	G		Trench XSA spl 240, SESC (bottom)
64-9162	346	2	G		Trench XSA
64-9163	347	2	G		Trench XSA
64-9164	348	2	G		Trench XSA
64-9165	349	2	G		Trench XSA
64-9166	350	2	G		Trench DSA
64-9167	351	2	G	272	Pan 13
64-9168	352	2	G	294	Pan 13
64-9169	353	2	G	312	Pan 13
64-9170	354	2	G	331	Pan 13
64-9171	355	2	G	354	Pan 13
64-9172	356	2	G	11	Pan 13
64-9173	357	2	G	34	Pan 13
64-9174	358	2	G	52	Pan 13
64-9175	359	2	G	66	Pan 13
64-9176	360	2	G	83	Pan 13, core spl 230 LOC
64-9177	361	2	G	98	Pan 13, core spl 230 LOC
64-9178	362	2	G	115	Pan 13
64-9179	363	2	G	122	Pan 13
64-9180	364	2	G	135	Pan 13
64-9181	365	2	G	150	Pan 13
64-9182	366	2	G	168	Pan 13
64-9183	367	2	G	185	Pan 13
64-9184	368	2	G	208	Pan 13
64-9185	369	2	G	229	Pan 13
64-9186	370	2	G	251	Pan 13
64-9187	371	2	G	265	Pan 13
68-9459	372	2	G		Spl 306 DSB
68-9460	373	2	G		Spl 306 XSB
68-9461	374	2	G		Spl 306 XSB
68-9462	375	2	G		Spl 306 XSA
68-9463	376	2	G		Spl 306 XSA
68-9464	377	2	G		Spl 306 LOC
64-9188	378	2	G1		Spls 313, 301 DS, LOC
68-9465	379	2	G1		Spls 313, 301 XSB, may include loose rock
68-9466	380	2	G1		Spls 313, 301 XSB
68-9467	381	2	G1		Spls 313, 301 XSA
68-9468	382	2	H		Grab spl, 4 rocks, XSB
68-9469	383	2	H		Grab spl, 4 rocks, XSB
68-9470	384	2	H		Grab spl, 4 rocks, XSA
68-9471	385	2	H		Grab spl, 4 rocks, XSA
68-9472	386	2	H		2 spl rocks off Turtle Rock, 2 rocks on fillet, XSB
68-9473	387	2	H		2 spl rocks off Turtle Rock, 2 rocks on fillet, XSB
68-9474	388	2	H		2 spl rocks off Turtle Rock, 2 rocks on fillet, XSB
68-9475	389	2	H		2 spl rocks off Turtle Rock, 2 rocks on fillet, XSB
68-9476	390	2	H		2 spl rocks off Turtle Rock, 2 rocks on fillet, XSA
68-9477	391	2	H	264	Pan 14
68-9478	392	2	H	297	Pan 14
68-9479	393	2	H	319	Pan 14
68-9480	394	2	H	345	Pan 14
68-9481	395	2	H	8	Pan 14
68-9482	396	2	H	27	Pan 14
68-9483	397	2	H	57	Pan 14
68-9484	398	2	H	83	Pan 14
68-9485	399	2	H	113	Pan 14
68-9486	400	2	H	136	Pan 14
68-9487	401	2	H	147	Pan 14
68-9488	402	2	H	177	Pan 14
68-9489	403	2	H	203	Pan 14
68-9490	404	2	H	225	Pan 14
68-9491	405	2	H	242	Pan 14
68-9492	406	2	LM		S-band antenna, accidental
64-9189	407	2	LM		LM, Earth
64-9190	408	2	LM		LM, Earth
64-9191	409	2	LM		LM, Earth
64-9192	410	2	LM		LM, Earth
64-9193	411	2	LM		LM, Earth
64-9194	412	2	LM		LM, Earth
64-9195	413	2	LM		LM, Earth
64-9196	414	2	LM		LM, Earth
64-9197	415	2	LM		LM, Earth
64-9198	416	2	LM		SWC
64-9199	417	2	LM		SWC
64-9200	418	2	LM		SWC

TABLE 8.—*Chronologic listing of 60 mm Apollo 14 lunar surface pictures*—Continued

Photo	Seq.	EVA	Sta.	Az.	Remarks
64-9201	419	2	LM		SWC
66-9333	420	Post	LM	282	LM Window Pan 15
66-9334	421	Post	LM	289	LM Window Pan 15
66-9335	422	Post	LM	285	LM Window Pan 15
66-9336	423	Post	LM	288	LM Window Pan 15
66-9337	424	Post	LM	328	LM Window Pan 15
66-9338	425	Post	LM	298	LM Window Pan 15
66-9339	426	Post	LM	309	LM Window Pan 15
66-9340	427	Post	LM	332	LM Window Pan 15
66-9341	428	Post	LM	353	LM Window Pan 15
66-9342	429	Post	LM	330	LM Window Pan 15
66-9343	430	Post	LM	322	LM Window Pan 15
66-9344	431				Command Module
66-9345	432				Command Module
66-9346	433				Command Module
66-9347	434				Command Module
66-9348	435				Command Module
66-9349	436				Command Module
66-9350	437				Command Module
66-9351	438				Command Module
66-9352	439				Command Module
66-9353	440				Command Module
66-9354	441				Command Module
66-9355	442				Command Module
66-9356	443				Command Module
66-9357	444				Command Module
66-9358	445				Command Module
66-9359	446				Command Module
66-9360	447				Command Module

Furthermore, dX_n is independent of nG and is therefore a local random error rather than one that becomes systematically larger with distance between points.

After the shaded-relief map was made, spot elevations were computed by a method called "photographic trigonometry," or, more coloquially, "phototrig" (Batson, 1969). Briefly this method consists of the following steps:

1. The point on the surface from which each photographic panorama was taken is located by resection. As many points as possible are used in the resection to reduce errors caused by local map distortions. Where nearby features are identifiable on the map and on surface panoramas, the station is located with respect to those features rather than with respect to distant ones. In general, the resection data on the Apollo 14 map resulted in panorama station locations that are consistent within approximately 5 m horizontally.
2. Vertical angles from an assumed horizon to features visible on panoramas and on the map are measured on the pictures in the panoramic mosaic.
3. Horizontal distances between the camera station and the features are measured on the map.

TABLE 9.—*Apollo 14 lunar surface 70 mm film usage by camera number*

Camera serial number 1027 (Shepard)
65-9202 through 9215 (Magazine KK)
67-9361 through 9393 (Magazine JJ)
64-9046 through 9201 (Magazine LL)
Camera serial number 1020 (Mitchell)
66-9216 through 9360* (Magazine II)
68-9394 through 9492 (Magazine MM)

*Includes 30 pictures taken from lunar orbit.

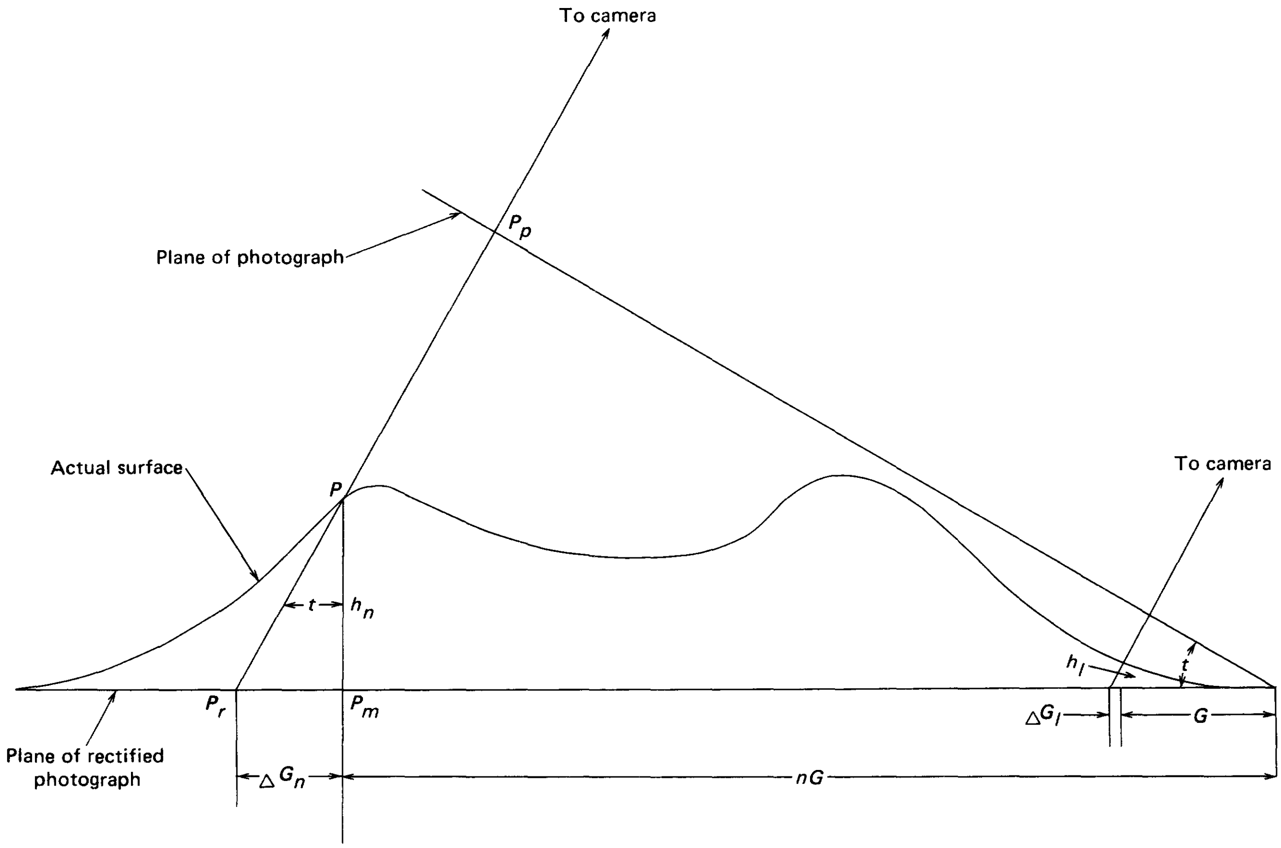

FIGURE 79.—Geometry of a tilted Lunar Orbiter photograph.

4. Relative topographic elevations are computed from the measurements made in 2 and 3 above.
5. Each set of elevations computed at each of the panorama stations is adjusted as a block for best agreement with other elevation sets when intervisible points are measured from different stations. After the adjustment, these spot elevations on the Apollo 14 map were consistent within about 1 metre (table 10).
6. Contour lines are compiled, controlled by the set of spot elevations and by interpretation of images on the base map.

The contour lines on the map of the Apollo 14 landing site are generalized and do not reflect the intricate surface structure visible on the shaded-relief base map. To draw fine details in the contour lines would be misleading because of wide variation in their accuracy. Where control points were not available, the lines were simply transferred from the NASA map, and are accurate to within 10 m. In the immediate vicinity of traverse stations, however, relative accuracies are of the order of tenths of a metre.

The identity of features on the map and on the surface panoramas is not intuitively obvious. As an aid in understanding the geology of the site as it appears in map view and from the surface, plate 2 identifies features that are identified on the surface panoramas on plates 3 through 6. Table 10 shows the computed elevations of the features, including standard deviations where more than one measurement was made. Table 11 shows the derived camera heights at each panorama station.

GLOSSARY

Active Seismic Experiment (ASE): Consisted of three geophones in a line, along which 15 explosive squibs were fired to supply seismic energy. The impacts on the Moon of the Saturn S IV–B rocket stage and the Lunar Module after it was abandoned in lunar orbit were also used as seismic energy sources.

Apollo Lunar-Surface Closeup Camera (ALSCC): A 35-mm stereo camera for taking detailed photographs of the textures of materials at the lunar surface.

Apollo Lunar Surface Experiments Package (ALSEP): A group of instruments attached to a central transmitting station, all of which were left behind for long-term monitoring of lunar events and processes. The ALSEP flown on Apollo 14 included a charged-particle detector, a passive and an active seismometer, a suprathermal ion detector, and a cold cathode gauge. (Other in-

TABLE 10.—*Elevations of points identified on plates 3 through 6 which are correlated with points on plate 2*

Point	Identified on panorama no.	Elevation	Mean elevation	δ
C/S	1 14	570.6 569.3	570.0	.92
111	1	570.4		
201	1	568.3		
401	1	569.0		
402	1	568.4		
403	1	568.5		
404	1	568.5		
405	1 14	569.8 569.8	569.8	.00
406	1	569.4		
410	4	569.7		
605	6	563.2		
606	6	564.2		
607	6	567.1		
608	6	566.5		
609	6	569.3		
610	6	570.7		
612	6	569.0		
613	6	566.6		
614	6	558.4		
616	6	554.2		
618	6	568.6		
619	6	566.3		
620	6	570.2		
623	6	570.1		
624	6	568.6		
625	6	568.0		
626	6	566.7		
630	6	564.6		
701	6 7 13	573.4 574.1 573.5	573.7	.38
702	6 7 8 13	575.0 576.6 578.8 574.7	576.3	1.88
703	6 7 13 14	597.1 596.4 597.6 594.9	596.5	1.17
704	6 7 12	616.9 615.1 616.3	616.1	0.92
705	13 7 8	572.4 573.9 574.6	573.6	1.12
706	6 7 13	578.8 579.6 579.4	579.3	.42
707	6 7 13	583.4 582.8 582.6	582.9	.42
708	6 7 13	571.6 572.3 573.0	572.3	.70
709	6 7 13	600.6 602.1 604.2	602.3	1.81
710	9	601.0		
711	6 7 12 13	633.6 633.1 634.6 635.9	634.3	1.24
712	6 7 13	610.1 606.9 611.2	609.4	2.23
713	6 7	611.6 613.3	612.4	1.20
720	6 7	567.8 566.4	567.1	0.99
740	7	568.0		
750	13 7	570.3 572.0	571.1	1.20
760	7 13	571.9 570.3	571.1	1.13
803	6 7 8 9 12	593.0 590. 591.4 591.1 591.9	591.6	.86
804	6 7 8 12 13	594.8 593.3 592.3 595.0 594.3	593.9	1.13
806	8	589.6		
807	8	589.5		
809	8	589.1		
812	13 12 6 7	582.2 582.2 582.9 582.9	582.6	.40
905	9	602.9		
908	9	603.2		
911	9	600.4		
914	9	604.4		
915	9	597.2		
918	9	601.9		
919	9	606.8		
920	9	598.6		
924	9	596.5		
927	9	577.5		
1001	10 11	642.6 640.2	641.4	1.70
1002	10	641.7		
1003	10	642.4		
1004	10	642.6		
1005	10	642.8		
1006	10	644.6		
1007	10	644.4		
1008	10	647.0		
1009	10	644.3		
1010	10 11	653.7 654.7	654.2	.71
1011	10	647.3		
1012	10	647.3		
1013	10	643.4		
1014	10	629.7		
1015	10	642.3		
1016	10	639.2		
1017	10	640.4		
1021	10	608.9		
1022	10	581.0		
1023	10	647.2		
1031	10	634.4		
1033	10	638.7		
1102	11	665.2		
1103	11	663.0		
1104	11	662.8		
1106	11 10	657.3 655.8	656.6	1.06
1107	11	657.0		
1108	11	665.0		
1109	11	665.5		
1110	11	664.0		
1111	11	665.4		
1112	11	665.3		
1115	11 10	661.5 656.1	658.8	3.82
1117	11	665.2		
1118	11	664.0		
1119	11	663.8		
1202	12	577.6		
1203	12	579.6		
1204	7 8 9	575.7 576.0 573.4	575.6	1.62

TABLE 10.—*Elevations of points identified on plates 3 through 6 which are correlated with points on plate 2*—Continued

Point	Identified on panorama no.	Elevation	Mean elevation	δ
	12	577.3		
1205	12	579.9		
1206	12	579.8		
1207	12	578.3		
1208	12	579.2		
1209	12	579.2		
1210	12	575.7		
1211	12	578.3		
1212	12	579.0		
1213	12	581.9		
1214	12	577.1		
1215	12	578.4		
1308	13	575.5		
1401	1 14	571.4 572.3	571.8	.64
1402	1 14	572.2 572.8	572.5	.42
1403	1 14	573.2 573.3	573.2	.07
1404	14	573.3		
1405	1 14	573.2 573.2	573.2	.00
1407	1 14	570.3 571.7	571.0	.99
1408	14	572.0		
1412	14	567.8		
1413	14	568.2		
1414	14	568.3		
1415	1 14	570.0 569.6	569.8	0.28
1417	14	570.1		
1418	14	570.8		
1419	14	571.1		
1420	14	569.9		
1421	14	571.0		
1501	1	570.0		
1502	1	569.6		
1503	1	568.8		
		Mean standard deviation		1.01

struments, not a part of ALSEP, included a lunar portable magnetometer, a laser ranging retroreflector, and a solar wind composition experiment.)

Apollo orbital photographs: The Command Module, which remains in lunar orbit while the LM is on the moon, is equipped to take photographs of the lunar surface with different resolutions using several types of cameras.

Bulk sample: A large amount of material scooped at random into a container for the sake of filling the sample containers when there is not sufficient time to take selected and well-documented samples. Commonly referred to as the "desperation sample."

Capsule communicator (Capcom): An astronaut assigned to the Mission Control Center, who relays all information to the astronaut crew during a mission. The Capcom is normally the only person who talks directly to the crew. (CC in table 5.)

Command Module (CM): That part of the spacecraft system that remains in lunar orbit with one astronaut aboard while the LM is on the lunar surface. After the LM returns into lunar orbit, the astronauts transfer to the CM along with items to be returned to Earth.

TABLE 11.—*Elevation of camera at panorama stations*

Panorama	Station	Camera elevation (m)
1	LM window	573.2
6	A	571.6
7	B	572.3
8	B1	590.3
9	B2	603.6
10	B3	645.7
11	C′	666.7
12	F	581.1
13	G	575.5
14	NBF	573.8

Comprehensive sample: A random collection of many fragments a centimetre or two across plus about a kilogram of soil, taken from a small area. The purpose is to get a representative sample of the many lunar rock types present at the landing site.

Documented sample bags: Prenumbered Teflon sample bags, approximately 10×12 cm, which can be identified by correlation with the astronauts' voice transcript.

Drive tube: An aluminum cylinder approximately 2.5 cm in diameter and 38 cm long, driven into the ground to take cores of regolith. The tubes can be attached end-to-end and are then generally referred to as "double cores." Six single-core tubes were carried by Apollo 14.

Extravehicular activity (EVA): Tasks performed by the crew outside the spacecraft, whether orbiting the Earth or Moon, between the Earth and the Moon, or on the lunar surface.

Football-size rock: Rocks that are too large to put into the prenumbered sample bags. (Many of the football-size rocks collected by Apollo missions are much smaller than an NFL-approved football.)

Gardening: Repeated turnover of the lunar regolith by meteorite bombardment.

Gnomon: Generally, a shadow-casting device such as the style on a sundial, or a shaft erected perpendicular to the horizon with its shadow length indicating time of day. The gnomon used on the Apollo missions is a weighted staff on a two-axis gimbal supported by a tripod. From the staff and its shadow, local vertical, camera-pointing azimuth, and scale can be determined for photogrammetric control.

Hasselblad Electric Data Camera (HEDC; referred to as the Hasselblad camera in this report): A 60-mm focal length, 70-mm format camera, with an automatic film advance. The camera is attached to the front of the astronaut's pressure suit. These cameras are calibrated both photogrammetrically and photometrically before each mission.

Lunar Module (LM): That part of the spacecraft system that lands on the Moon. The LM consists of two parts: the descent stage, which is left on the lunar surface, and the ascent stage, which returns to lunar orbit.

Lunar Orbiter: An unmanned probe designed primarily to photograph the lunar surface by means of electronic scanning of photographic film exposed, advanced, and developed aboard the spacecraft. Five Lunar Orbiter missions were flown, all successfully, during the period 1966 to 1967, and nearly all of the lunar surface was photographed.

Lunar Receiving Laboratory (*LRL*): The facility at the Johnson Space Center, Houston, Tex., where the lunar rocks from Apollo missions 11–17 were processed. On the basis of an initial examination in the LRL, parts of lunar rocks were selected for distribution to various investigators.

Modularized Equipment Transporter (MET): A small two-wheeled cart designed to carry equipment and samples during the lunar surface EVA's. The MET represented an intermediate stage between a hand-held equipment carrier that was flown on Apollos 12 and 13, and the lunar rover, which was used on the later missions.

Phase angle: The angle between the incident ray from a light source (the sun) and the reflected ray to a light sensor (a camera).

Photometric angles:

1. Phase angle: defined above
2. Azimuth angle: the angle between the sun's azimuth and the azimuth of the reflected ray measured in the horizontal plane.
3. Elevation angle: The angle between the sun and the projection of the reflected ray to the vertical plane through the sun, measured vertically.
4. Alpha: the angle between the reflected ray and projection of the surface normal, measured in the plane of the phase angle.

Photometric chart: An aluminum plate approximately 15×15 cm that is attached to a leg of the gnomon. It is painted with the three primary colors and a gray scale. The color chart is placed in the field of view of some of the Hasselblad photographs for calibration purposes.

Pre-mission mapping: The earliest lunar geologic maps were compiled from telescopic observation and photography, and these maps formed much of the general rationale for lunar exploration. Later maps of specific landing sites were compiled from Lunar Orbiter and Apollo orbital photographs; in the case of Apollo 14, the site maps were compiled at scales up to 1:5,000 from Lunar Orbiter and Apollo 12 photographs. The large-scale detailed maps were used to pick the landing spot, to preplan the traverses for each EVA, and to brief the astronaut crew.

Raindrop pattern or depressions: The Apollo 12 crew applied this term to the pattern produced by craterlets a fraction of a centimetre to a few centimetres in diameter formed by the impact of micrometeorites. (This is the same process that causes zap pits on the rock surfaces.)

Ranger: Unmanned space and lunar probes, launched during the period 1961–65. Rangers 3 through 9 were lunar probes, but only 7 through 9 were successful. These probes transmitted pictures back to Earth during the last minutes before crashing on the Moon, thereby providing the first closeup views of the lunar surface.

Science Operations Room (SOR): A room in the Mission Control Center at Johnson Space Center, Houston, Texas, where an advisory team of scientists re-establishes mission science priorities in light of contingencies and scientific findings that arise during the mission. This team was responsible for changing preplanned traverse routes, sampling priorities and procedures, and instrument deployments as the need arose; these changes had to be made within strict constraints called "mission rules" that deal with such things as the maximum distance the crew can be from the LM at any given time.

Soil breccia: Soft, incoherent clods to highly annealed rocks that are formed by induration of the lunar regolith by meteorite impact.

Soil mechanics experiment: The determination of the mechanical properties of lunar regolith materials by studying the action of such things as boots and pieces of equipment on the regolith, the walls of dug trenches and the angle of repose of excavated materials, and soil samples.

Surveyor: An unmanned lunar probe that soft-landed on the lunar surface. It carried a high-resolution vidicon imaging system and other equipment for scientific experiments. Apollo 12 landed near Surveyor 3 in Oceanus Procellarum. Seven Surveyor spacecraft were flown from 1966 to 1968, and five landed successfully.

Target materials: The materials excavated or strongly shocked by a meteorite impact; the term refers to these materials as they existed before the impact.

Targets of opportunity: Commonly applies to photographic targets, but sometimes used in reference to features described or sampled, that are not specifically included in the mission, but that are recognized by the astronauts as being of special interest or significance. The importance of recognizing targets of opportunity was a primary reason for training the astronauts in the geosciences.

Weigh bag: A bag approximately $20 \times 30 \times 45$ cm used to hold samples for weighing prior to return to Earth, to insure that the limit on sample weight is not exceeded. Rocks too large to place in the documented sample bags are commonly returned to Earth in the weigh bags, along with samples left over after filling the metal Sample Return Containers.

Zap pits: This term was coined during the preliminary examination of Apollo 11 samples in the Lunar Receiving Laboratory. The pits are caused by micrometeorite bombardment. They are commonly glass-lined, show concentric and radial fracture patterns, and in some cases have raised rims.

SELECTED REFERENCES

Adams, J. B., and McCord, T. B., 1971, Alterations of lunar optical properties—Age and composition effects: Science, v. 171, p. 567–571.

Andersen, C. A., and Hinthorne, J. R., 1973, $^{207}Pb/^{206}Pb$ ages and REE abundances in returned lunar material by ion microprobe mass analysis, *in* Chamberlain, J. W. and Watkins, Carolyn, eds., Lunar science IV, Abs. of papers presented at the Fourth Lunar Sci. Conf., Houston: Lunar Sci. Inst. Contr., p. 37–39.

Apollo Field Geology Investigation Team, 1973, Geologic exploration of Taurus-Littrow: Apollo 17 landing site: Science, v. 182, p. 672–690.

Baldwin, R. B., 1963, The Measure of the Moon: Chicago, Univ. Chicago Press.

Batson, R. M., 1969, Photogrammetry with surface-based images: Applied Optics, v. 8, p. 1315–1322.

Bence, A. E., and Papike, J. J., 1972, Pyroxenes as recorders of lunar basalt petrogenesis—Chemical trends due to crystal-liquid interaction, *in* King, E. A., Jr., ed., Mineralogy and petrology, v. 1, Third Lunar Sci. Conf., Houston, Proc.: Geochem. et Cosmochim. Acta, Supp. 3, p. 431–469.

Berdot, J. L., Chetrit, G. C., Lorin, J. C., Pellas, P. and Poupeau, 1972, Track studies of Apollo 14 rocks, and Apollo 14, Apollo 15, and Luna 16 soils, *in* Criswell, D. R., ed., Physical properties, v. 3, Third Lunar Sci. Conf., Houston, Proc.: Geochim. et Cosmochim. Acta, Supp. 3, p. 2867–2881.

Carr, M. H., 1966, Interpretation of the Ranger records, *in* Rangers VIII and IX, pt. 2, Experimenters' analysis and interpretations: Jet Propulsion Lab. Tech. Rept. 32–800, p. 249–338.

Chao, E. C. T., Minkin, J. A., and Best, J. B., 1972, Apollo 14 breccias—General characteristics and classification, *in* King, E. A., Jr., ed., Mineralogy and petrology, v. 1, Third Lunar Sci. Conf., Houston, Proc.: Geochim. et Cosmochim. Acta, Supp. 3., p. 645–659.

Compston, W., Chappell, B. W., Arriens, P. A., and Vernon, M. J., 1970, The chemistry and age of Apollo 11 lunar material, *in* Levinson, A. A., Chemical and isotope analyses, v. 2, Apollo 11 Lunar Sci. Conf., Houston, Proc.: Geochim. et Cosmochim. Acta, Supp. 1, p. 1007–1027.

Compston, W., Vernon, M. J., Berry, H., Rudowski, R., Gray, C. M., and Ware, N., 1972a, Apollo 14 mineral ages and the thermal history of the Fra Mauro formation, *in* Heymann, Dieter, ed., Chemical and isotope analyses/organic chemistry, v. 2, Third Lunar Sci. Conf., Houston, Proc.: Geochim. et Cosmochim. Acta, Supp. 3, p. 1487–1501.

———1972b, Age and petrogenesis of Apollo 14 basalts, *in* Watkins, Carolyn, ed., Lunar science III, Rev. Abs., Houston: Lunar Sci. Inst. Contr. 88, p. 151–153.

Crozaz, G., Drozd, R., Hohenberg, C. M., Hoyt, H. P., Ragan, D., Walker, R. M., and Yuhas, D., 1972, Solar flare and galactic cosmic ray studies of Apollo 14 and 15 samples, *in* Criswell, D. R., ed., Physical properties, v. 3, Third Lunar Sci. Conf., Houston, Proc.: Geochim. et Cosmochim. Acta, Supp. 3, p. 2917–2931.

Dollfus, Audouin, 1962, The polarization of moonlight, *in* Kopal, Ždenek, ed., Physics and astronomy of the Moon, ch. 5: New York, Academic Press, p. 131–159.

Dollfus, Audouin, Geake, J. E., and Titulaer, 1971, Polarimetric properties of the lunar surface and its interpretation, pt. 3—Apollo 11 and Apollo 12 lunar samples, *in* Levinson, A. A., ed., Physical properties, v. 3, Second Lunar Sci. Conf., Houston, Proc.: Geochim. et Cosmochim. Acta, Supp. 3, p. 2285–2300.

Eggleton, R. E., 1964, Preliminary geology of the Riphaeus quadrangle of the Moon and definition of the Fra Mauro Formation, *in* Astrogeol. Studies Ann. Prog. Rept., Aug. 25, 1962 to July 1, 1963, pt. A: U.S. Geol. Survey open-file rept., p. 46–63.

Eggleton, R. E., and Offield, T. W., 1970, Geologic maps of the Fra Mauro region of the Moon, Apollo 14 pre-mission maps: U.S. Geol. Survey Misc. Geol. Inv. Map I–708.

Eggleton, R. E., and Schaber, G. G., 1973, Cayley Formation interpreted as basin ejecta, *in* Apollo 16 Prelim. Sci. Rept, pt. B,: Natl. Aeronautics and Space Adm. Spec. Pub. SP–315, p. 29–7 to 29–16.

Eldridge, J. S., O'Kelley, G. D., and Northcutt, K. J., 1972, Abundances of primordial and cosmogenic radionuclides in Apollo 14 rocks and fines, *in* Heymann, Dieter, ed., Chemical and isotope analyses/organic chemistry, v. 2, Third Lunar Sci. Conf., Houston, Proc.: Geochim. et Cosmochim. Acta, Supp. 3, p. 1651–1658.

Englehardt, W. von, Arndt, J., Stoffler, D., and Schneider, H., 1972, Apollo 14 regolith and fragmental rocks, their compositions and origin by impacts, *in* King, E. A., Jr., ed., Mineralogy and petrology, v. 1, Third Lunar Sci. Conf., Houston, Proc.: Geochim. et Cosmochim. Acta, Supp. 3, 753–770.

Elston, W. E., Laughlin, W. A., and Bower, J. A., 1971, Lunar near side tectonic patterns from Orbiter 4 photographs: Jour. Geophys. Research, v. 76, no. 23, p. 5670–5674.

Floran, R. J., Cameron, K. L., Bence, A. E., and Papike, J. J., 1972, Apollo 14 breccia 14313—A mineralogic and petrologic report, *in* King, E. A., Jr., ed., Mineralogy and petrology, v. 1, Third Lunar Sci. Conf., Houston, Proc.: Geochim. et Cosmochim. Acta, Supp. 3, p. 661–671.

Gault, D., Collins, R., Gold, T., Green, J., Kuiper, G. P., Masursky, H., O'Keefe, J., Phinney, R., and Shoemaker, E. M., 1967, Lunar theory and processes, *in* Surveyor III mission rept., pt. II, Scientific results: Jet Propulsion Lab. Tech. Rept. 32–1177, p. 195–213.

Gilbert, G. K., 1893, The Moon's face—A study of the origin of its features: Philos. Soc. Washington Bull., v. 12, p. 241–292.

Helz, R. T., 1972, Rock 14068—An unusual lunar breccia, *in* King, E. A., Jr., ed., Mineralogy and petrology, v. 1, Third Lunar Sci. Conf., Houston, Proc.: Geochim. et Cosmochim. Acta, Supp. 3, p. 865–886.

Hörz, Friedrick, Morrison, D. A., and Hartung, J. B., 1972, The surface orientations of some Apollo 14 rocks: Modern Geology, v. 3, p. 93–104.

Howard, K. A., and Larsen, B. R., 1972, Lineaments that are artifacts of lighting, *in* Apollo 15 Prelim. Sci. Rept.: Natl. Aeronautics and Space Adm. Spec. Pub. SP–289, p. 25–58 to 25–62.

Husain, L., and Schaeffer, O. A., 1973, $^{40}Ar-^{39}Ar$ crystallizations ages and $^{38}Ar-^{37}Ar$ cosmic ray exposure ages of samples from the vicinity of the Apollo 16 landing site, *in* Chamberlain, J. W., and Watkins, Carolyn, Lunar Science IV, Abs. of papers presented at the Fourth Lunar Sci. Conf., Houston, p. 406–408.

Juan, V. C., Chen, J. C., Huang, C. K., Chen, P. Y., and Wang Lee, C. M., 1972, Petrology and chemistry of some Apollo 14 samples, *in* King, E. A., Jr., Mineralogy and Petrology, v. 1: Third Lunar Sci. Conf., Houston, Proc., Geochim. et Cosmochim. Acta, Supp. 3, p. 687–705.

Kirsten, T., Horn, P., and Kiko, J., 1973, $Ar^{40}-AR^{39}$ dating of Apollo 16 and Apollo 15 rocks and rare gas analysis of apollo 16 soils, *in* Chamberlain, J. W., and Watkins, Carolyn, eds., Lunar Science IV, Abs of papers presented at the Fourth Lunar Sci. Conf.,l Houston, The Lunar Science Institute, p. 438–440.

Kovach, R. L., and Watkins, J. S., 1972, The near-surface velocity structure of the moon, *in* Watkins, Carolyn, ed., Lunar Science III, Rev. Abs., Houston: Lunar Sci. Inst. Contr. 88, p. 461–462.

Kovach, R. L., Watkins, J. S., and Landers, Tom, 1971, Active seismic experiment, *in* Apollo 14 Prelim. Sci. Rept.: Natl. Aeronautics and Space Adm. Spec. Pub. SP–272 p. 163–174.

Kushiro, I., Ikeda, Y., and Nakamura, Y., 1972, Petrology of Apollo 14 high-alumina basalt, *in* King, E. A., Jr., ed., Mineralogy and petrology, v. 1, Third Lunar Sci. Conf., Houston, Proc.: Geochim. et Cosmochim. Acta, Supp. 3, p. 115–129.

Longhi, J., Walkder, D., and Hays, J. F., 1972, Petrography and crystallization history of basalts 14310 and 14072, *in* King, E. A., Jr., ed., Mineralogy and petrology, v. 1, Third Lunar Sci. Conf., Houston, Proc.: Geochim. et Cosmochim. Acta, Supp. 3, p. 131–139.

Lovering, J. F., Wark, D. A., Gleadow, A. J. W., and Sewell, D. K. B., 1972, Uranium and potassium fractionation in pre-Imbrian lunar crustal rocks, *in* King, E. A., Jr., ed., Mineralogy and Petrology, v. 1, Third Lunar Sci. Conf., Houston, Proc.: Geochim. et Cosmochim. Acta, Supp. 3, p. 281–294.

Lunar Sample Preliminary Examination Team, 1971, Preliminary examination of lunar samples from Apollo 14: Science, v. 173, p. 681–693.

McCauley, J. F., 1967a, Geologic map of the Hevelius region of the Moon: U.S. Geol. Survey Misc. Geol. Inv. Map I–491 (LAC–56).

———1967b, The nature of the lunar surface as determined by systematic geologic mapping, *in* Runcorn, S. K., ed., Mantles of the Earth and terrestrial planets: New York, Interscience Publishers, p. 431–460.

———1968, Geologic results from the lunar precursor probes: AIAA Journal, v. 6, no. 10, p. 1991–1996.

McCauley, J. F., and Masursky, Harold, 1969, The bedded white sands at Meteor Crater, Arizona: Meteorites, v. 4, no. 3, p. 196–197.

McKay, D. S., Heiken, G. H., Taylor, R. M., Clanton, U. S., Morrison, D. A., and Ladle, G. H., 1972, Apollo 14 soils: Size distribution and particle types, *in* King, E. A., Jr., ed., Mineralogy and Petrology, v. 1, Third Lunar Sci. Conf., Houston, Proc.: Geochim. et Cosmochim. Acta, Supp. 3, p. 983–994.

Mitchell, J. K., Bromwell, L. G., Carrier, W. D., III, Costes, N. C., and Scott, R. F., 1971, Soil mechanics experiment, *in* Apollo 14 Prelim. Sci. Rept.: Natl. Aeronautics and Space Adm. Spec. Pub. SP–272, p. 87–108.

Morris, E. C., and Shoemaker, E. M., 1968, Television observations from Surveyor, *in* Surveyor Project Final Rept., pt. 2, Science Results: Jet Propulsion Laboratory Tech. Rept. 32–1265, p. 65–69.

Morris, E. C., and Wilhelms, D. E., 1967, Geologic map of the Julius Caesar quadrangle of the Moon: U.S. Geol. Survey Misc. Geol. Inv. Map I–510.

Muehlberger, W. R., and Field Geology Team. 1972, Preliminary geologic investigations of the Apollo 16 landing site, *in* Apollo 16 Prelim. Sci. Rept.: Natl. Aeronautics and Space Adm. Spec. Pub. SP–315, p. 6-1 to 6-81.

Murthy, V. R., Evensen, N. M., and Coscio, M. R. Jr., 1973, Episodic lunacy IV—ages, trace elements and delphic speculations, *in* Chamberlain, J. W., and Watkins, Carolyn eds., Lunar science IV, Abs of papers presented at the Fourth Lunar Sci. Conf., Houston: The Lunar Science Institute, p. 549–551.

Nelen, J., Noonan, A., and Fredriksson, K., 1972, Lunar glasses, breccias, and chondrules, *in* King, E. A., Jr., ed., Mineralogy and petrology, v. 1, Third Lunar Sci. Conf., Houston, Proc.: Geochim. et Cosmochim. Acta, Supp. 3, p. 723–737.

Nyquist, L. E., Hubbard, N. J., Gast, P. W., Church, S. E., Bansal, B. M., and Wiesmann, H., 1972, Rb-Sr systematics for chemically defined Apollo 14 breccias, *in* Heymann, Dieter, ed., Chemical and isotope analyses/organic chemistry, v. 2, Third Lunar Sci. Conf., Houston, Proc.: Geochim. et Cosmochim. Acta, Supp. 3, p. 1515–1530.

Papanastassiou, D. A., and Wasserburg, G. J., 1970, Rb-Sr ages from the Ocean of Storms: Earth and Planetary Sci. Letters, v. 8, p. 269–278.

———1971a, Lunar chronology and evolution from Rb-Sr studies of Apollo 11 and 12 samples: Earth and Planetary Sci. Letters, v. 11, p. 37.

———1971b, Rb-Sr ages of igneous rocks from the Apollo 14 mission and the age of the Fra Mauro Formation: Earth and Planetary Sci. Letters, v. 12, p. 36.

———1972, Rb-Sr systematics of Luna 20 and Apollo 16 samples: Earth and Planetary Sci. Letters, v. 17, p. 52–63.

Pohn, H. A., and Wildey, R. L., 1970, A photoelectric-photographic study of the normal albedo of the Moon: U.S. Geol. Survey Prof. Paper 599–E.

Quaide, W. L., and Oberbeck, V. R., 1968, Thickness determinations of the lunar surface layer from lunar impact craters: Jour. Geophys. Research, v. 73, no. 16, p. 5247–5270.

Quaide, W. L., and Wrigley, Robert, 1972, Mineralogy and origin of Fra Mauro fines and breccias, *in* King, E. A., ed., Mineralogy and petrology, v. 1, Third Lunar Sci. Conf., Houston, Proc.: Geochim. et Cosmochim, Acta, Supp. 3, p. 771–784.

Schaber, G. G., and Swann, G. A., 1971, Surface lineaments at the Apollo and Apollo 12 landing sites, *in* Levinson, A. A., ed., Mineralogy and petrology, v. 1, Second Lunar Sci. Conf., Houston, Proc.: Geochim. et Cosmochim. Acta, Supp. 2, p. 27–38.

Schürmann, K., and Hafner, S. S., 1972, Distinct subsolidus cooling histories of Apollo 14 basalts, *in* King, E. A., Jr., ed., Mineralogy and petrology, v. 1, Third Lunar Sci. Conf., Houston, Proc.: Geochim. et Cosmochim. Acta, Supp. 3, p. 493–506.

Scott, D. H., Lucchitta, B. K., and Carr, M. H., 1972, Geologic maps of the Taurus-Littrow region of the Moon: U.S. Geol. Survey Misc. Geol. Inv. Map I–800.

Shoemaker, E. M., 1960, Penetration mechanics of high-velocity meteorites, illustrated by Meteor Crater, Arizona: Internat. Geol. Cong., 21st., Copenhagen 1960, Rept., pt. 18, p. 418–434.

———1971, Origin of fragmental debris on the lunar surface and history of bombardment of the Moon: Inst. de Investigaciones Geol. de la Diputacion Provincial, v. XXV, Universidad de Barcelona, p. 27–56.

———1972, Cratering history and early evolution of the Moon, *in* Third Lunar Sci. Conf., Houston, Texas, January 1972: Lunar Sci. Inst. Contr. 88, p. 696–698.

Shoemaker, E. M., Batson, R. M., Holt, H. E., Morris, E. C., Rennilson, J. J., and Whitaker, E. A., 1969, Observations of the lunar regolith and the Earth from the television camera on Surveyor 7: Jour. Geophys. Research, v. 74, p. 6081.

Shoemaker, E. M., Hait, M. H., Swann, G. A., Schleicher, D. L., Schaber, G. G., Sutton, R. L., Dahlem, D. H., Goddard, E. N., and Waters, A. C., 1969, Origin of the regolith at Tranquillity Base, *in* Levinson, A. A., ed., Physical properties, v. 3, Apollo 11 Lunar Sci. Conf., Houston, Proc.: Geochim. et Cosmochim. Acta, Supp. 1, p. 2399–2412.

Shoemaker, E. M., Hait, M. H., Swann, G. A., Schleicher, D. L., Dahlem, D. H., Schaber, G. G., and Sutton, R. L., 1970, Lunar regolith at Tranquillity Base: Science, v. 167, p. 452.

Shoemaker, E. M., Morris, E. C., Batson, R. M., Holt, H. E., Larson,

K. B., Montgomery, D. R., Rennilson, J. J., and Whitaker, E. A., 1968, Television observations from Surveyor *in* Surveyor project final report, pt. II, Science results: NASA Tech. Rept. 32–1265, p. 21–137.

Silver, Leon T., 1971, U-Th-Pb isotopic systems in Apollo 11 and Apollo 12 regolithic materials and a possible age for the Copernicus event [abs.]: Am. Geophys. Union Trans., v. 52, no. 7, p. 534.

Soderblom, L. A., 1970, A model for small-impact erosion applied to the lunar surface: Jour. Geophys. Research, v. 75, p. 2655.

Soderblom, L. A., and Lebofsky, L. A., 1972, Technique for rapid determination of relative ages of lunar areas from orbital photography: Jour. Geophys. Research, v. 77, no. 2, p. 279–296.

Steele, I. M., and Smith, J. V., 1972, Compositions and mineralogy of lithic fragments in 1–2 mm soil samples 14002, 7 and 14258, 33, *in* King, E. A., Jr., ed., Mineralogy and petrology, v. 1, Third Lunar Sci. Conf., Houston, Proc.: Geochim. et Cosmochim. Acta, Supp. 3, p. 971–981.

Strom, R. G., 1964, Analysis of lunar lineaments I, tectonic maps of the Moon: Univ. Ariz. Lunar and Planetary Lab. Commun., v. 2, no. 39, p. 205–216.

Swann, G. A., Bailey, N. G., Batson, R. M., Eggleton, R. E., Hait, M. H., Holt, H. E., Larson, K. B., McEwen, M. C., Mitchell, E. D., Schaber, G. G., Shafer, J. P., Shepard, A. B., Sutton, R. L., Trask, N. J., Ulrich, G. E., Wilshire, H. G., and Wolfe, E. W., 1971, Preliminary geologic investigations of the Apollo 14 landing site, *in* Apollo 14 Prelim. Sci. Rept.: Natl. Aeronautics and Space Adm. Spec. Pub. SP–272, p. 39–86.

Swann, G. A., Bailey, N. G., Batson, R. M., Freeman, V. L., Hait, M. H., Head, J. W., Holt, H. E., Howard, K. A., Irwin, J. B., Larson, K. B., Muehlberger, W. R., Reed, V. S., Rennilson, J. J., Schaber, G. G., Scott, D. R., Silver, L. T., Sutton, R. L., Ulrich, G. E., Wilshire, H. G., and Wolfe, E. W., 1972, Preliminary geologic investigation of the Apollo 15 landing site, *in* Apollo 15 Prelim. Sci. Rept.: Natl. Aeronautics and Space Adm. Spec. Pub. SP–289, p. 5-1 to 5-112.

Tatsumoto, M., 1970, Age of the Moon—an isotopic study of U-Th-Pb systematics of Apollo 11 lunar samples—II, *in* Levinson, A. A., ed., Chemical and isotope analyses, v. 2, Apollo 11 Lunar Sci. Conf., Houston, Proc.: Geochim. et Cosmochim. Acta, Supp. 1, p. 1595–1612.

Tatsumoto, M., Hedge, C. E., Doe, B. R., and Unruh, D. M., 1972, U-Th-Pb and Rb-Sr measurements on some Apollo 14 lunar samples, *in* Heymann, Dieter, ed., Chemical and isotope analyses/organic chemistry, v. 2, Third Lunar Sci. Conf., Houston, Proc.: Geochim. et Cosmochim. Acta, Supp. 3, p. 1531–1555.

Trask, N. J., 1966a, Maximum polarization of some lunar geologic units, *in* Astrogeol. Studies Ann. Prog. Rept, July 1, 1965 to July 1, 1966, pt. A, Lunar and planetary investigations: U.S. Geol. Survey open-file rept., p. 163–168.

———1966b, Size and spatial distribution of craters estimated from Ranger photographs, *in* Rangers VIII and IX, pt. 2, Experimenters' analysis and interpretations: Jet Propulsion Lab. Tech. Rept. 32–800, p. 249–338.

Turner, Grenville, Huneke, J. C., Podosek, F. A., and Wasserburg, G. J., 1971, $^{40}Ar-^{39}Ar$ ages and cosmic ray exposure ages of Apollo 14 samples: Earth and Planetary Sci. Letters, v. 12, no. 1, p. 19–35.

Warner, J. L., 1972, Metamorphism of Apollo 14 breccias, *in* King, E. A., Jr., ed., Mineralogy and petrology, v. 1, Third Lunar Sci. Conf., Houston, Proc.: Geochim. et Cosmochim. Acta, Supp. 3, p. 623–643.

Warner, J. L., and Duke, M. B., 1971, Apollo 14 lunar sample information catalog: Natl. Aeronautics and Space Adm. Tech. Memo. TM X–58062, 114 p.

Wasserburg, G. J., and Papanastassiou, D. A., 1972, Age of an Apollo 15 mare basalt, lunar crust and mantle evolution: Earth and Planetary Sci. Letters, v. 13, p. 97–104.

Watkins, J. W., and Kovach, R. L., 1972, Apollo 14 active seismic experiment: Science, v. 175, p. 1244–1245.

Wilhelms, D. E., 1970, Summary of lunar stratigraphy—Telescopic observations: U.S. Geol. Survey Prof. Paper 599–F, p. F1–F47.

Wilhelms, D. E., and McCauley, J. F., 1971, Geologic map of the near side of the Moon: U.S. Geol. Survey Misc. Geol. Inv. Map I–703.

Wilhelms, D. E., and Trask, N. J., 1965, Polarization properties of some lunar geologic units, *in* Astrogeol. Stud. Ann. Prog. Rept., July 1, 1964–July 1, 1965, pt. A, Lunar and planetary investigations: U.S. Geol. Survey open-file report, p. 63–80.

Willingham, D., 1964, The lunar reflectivity model AD–264070 for Ranger Block III analysis: Jet Propulsion Lab. Tech. Rept. 32–664.

Wilshire, H. G., and Jackson, E. D., 1972, Petrology and stratigraphy of the Fra Mauro Formation at the Apollo 14 site: U.S. Geol. Survey Prof. Paper 785, 26 p.

Wolfe, E. W., and Bailey, N. G., 1972, Lineaments of the Apennine front—Apollo 15 landing site, *in* King, E. A., Jr., ed., Mineralogy and petrology, v. 1, Third Lunar Sci. Conf., Houston, Proc.: Geochim. et Cosmochim. Acta, Supp. 3, p. 15–25.

Wright, F. E., Wright, F. H., and Wright H., 1963, The lunar surface introduction, *in* Middlehurst, B. M., and Kuiper, G. P., eds., The Moon, meteorites, and comets, ch. 5: Univ. Chicago Press, p. 1–47.

York, D., Kenyon, W. J., and Doyle, R. J., 1972, $^{40}Ar-^{39}Ar$ ages of Apollo 14 and 15 samples, *in* Heymann, Dieter, ed., Chemical and isotope analyses/organic chemistry, v. 2, Third Lunar Sci. Conf., Houston, Proc.: Geochim. et Cosmochim. Acta, Supp. 3, p. 1613–1622.

☆U.S. GOVERNMENT PRINTING OFFICE: 1976 - 789-025/12